Investigating the responses of Brassica oilseed crops to real-world ozone levels

Hattie Rose Roberts

BSc Plant Biology,
MRes Biosciences,
Prifysgol Aberystwyth

This thesis is submitted for the degree of Doctor of Philosophy
May 2023

Lancaster Environment Centre
Faculty of Science and Technology
Lancaster University

Declaration

This thesis has not been submitted in support of an application for another degree at this or any other university. It is the result of my own work and includes nothing that is the outcome of work done in collaboration except where specifically indicated, including figures and graphics. The ideas in this thesis were the product of discussion with my supervisors Dr Kirsti Ashworth, Prof Ian Dodd, and Dr Felicity Hayes.

Excerpts of this thesis have been published in the following academic journals:

Chronic tropospheric ozone exposure reduces seed yield and quality in spring and winter oilseed rape. Roberts, H.R., Dodd, I.C., Hayes, F., Ashworth, K., 2022, published in *Agricultural and Forest Meteorology*, vol. 316, 108859. doi: 10.1016/j.agrformet.2022.108859

Abstract

Oilseed rape (hereafter OSR) contributes a fifth of calories consumed by humans from oilseeds annually. The composition and quality of their lipid-rich seeds is tightly regulated to prevent introducing toxic compounds to the food chain. As these increase in response to environmental stresses such as the phytotoxic pollutant tropospheric ozone, understanding the effects of ozone on, and potential tolerance mechanisms in, this lucrative crop is necessary to maintain crop quality and yield. Firstly, I investigated the impact of 'real-world' ozone levels (20 - 110 ppbv over 12 days to 5 months) on the seed and oil yield of one shorter-lived spring OSR cultivar and one longer-lived winter cultivar to realistic ozone levels over a growing season. High ozone levels caused differences in seed yield and quality losses, but the winter cultivar's yield losses were more substantial. I postulated that winter OSR diverted more photosynthate to antioxidants, which protect metabolic processes and prevent damage caused by ozone. I then focused on ascorbic acid, which directly reacts with ozone and stress-inducing products within the leaf and is associated with ozone tolerance. Despite higher concentrations of total ascorbic acid in the leaf, short-term ozone exposure decreased winter OSR physiology and productivity, and cumulative ozone uptake was a key factor in ozone tolerance. I then questioned whether canola-grade cultivars of advanced pedigree and therefore high gas exchange and low antioxidant levels were more sensitive to ozone. Surprisingly, a canola-grade cultivar with the lowest gas exchange and highest antioxidant activity (compared to two non-canola-grade cultivars) was ozone tolerant. I also developed a relative oxidative stress index incoroporating biochemical responses, which adequately predicted ozone tolerance in the four *Brassica* oilseeds, which may be applied to identify and exploit *Brassica* ozone tolerance.

Acknowledgements

I could write an accompanying thesis on the brilliant people who have supported me throughout my PhD. Firstly, I'm incredibly thankful to Dr Kirsti Ashworth, my primary supervisor and PI for this project, for her unwavering support, sage advice, and wonderful whisky. I'm also grateful to my second LEC supervisor, Prof Ian Dodd for taking me under his wing for the first 6 months at LEC and welcoming me back to the Water Stress lab group after my 18-month stint at UKCEH. I thank my UKCEH supervisor Dr Felicity Hayes, who supported me while I was located at UKCEH Bangor, and has continued to check in whilst I 'wrote up'. Special thanks to review my panel, Prof Elizabete Carmo-Silva and Dr Marjorie Lundgren for the valuable suggestions and encouragement.

I have been incredibly fortunate to be involved in many active research groups and I thank each lab member from lab SAPLING, the Water Stress group, and the ECR Ozone group, for the moral, practical, and caffeic support. Each of you are fantastic and I feel privileged to work alongside you. I am particularly grateful to Isla Young for taking the lead in building the BAI ozone fumigation system, and to Hao Zhou for his patience and support in the plant ecophysiology, and BAI/GC labs. I am also very grateful to the technical support and academic staff, with special mention to Dr Sam Taylor, Dr Tim Gregson, Dr Geoff Holroyd, Dr Dave Hughes, Dr Annette Ryan, Dr Rhiannon Page, Dr Shane Rothwell, Maureen Harrison, and David Lewis. Huge thanks to Sam Jones in LEC Stores for keeping me organised and supplied with everything I needed to make this project happen. In UKCEH Bangor, I am grateful to Aled Williams for maintaining the ozone Solardome system at Abergwynwen field site, and Dr Amanda Holder, Dr Clare Brewster, and Dr Katrina Sharps for assisting with plant care, and giving statistical/ozone/general advice.

I sincerely thank my previous supervisors, Prof John Warren, Dr Dylan Gwynn-Jones, and Dr Jim Provan for encouraging me to pursue a PhD. Jim passed away in 2022 and I will remember him as a caring and diligent supervisor with infectious enthusiasm for conservation genetics, curious plants, and fossils.

Thank you to my family, my pillars of support and sound advice. To my parents, thank you for the unwavering support, blissful visits home, and the long calls about local life. To my siblings, Ethan, Harvey, and Anabel, thank you for keeping my sense of humour in check. Thank you to Nan a.k.a. Betty Chamberlain, Grandad Dave Morgan, and Aunt Rachel and Uncle Myrdd Jones, who have been my constant cheerleaders. To my friends, for putting up with my unavailability, and for enduring my conversations about plants when I am available. I'm so grateful to each of you for the laughs and advocating a healthy work-life balance: Jem McPartlin, Katie Bithell, Emily Howard, Matthew Hawkins, Dr Louise Ridden, and Dr Sabine Reinsch. To Rosemary Bashford, who advised me to stay in science. Lastly, thank you to Max Davis, for everything.

This work was supported by the Natural Environment Research Council (NERC grant reference number NE/L002604/1), with my studentship through the Envision Doctoral Training Partnership. Thank you to Envision DTP for supporting my PhD journey.

To all of you and those I haven't named, you do not realise how brilliant you are individually and collectively. I am raising a toast to all of you. *Iechyd da!*

Contents

List of Tables

List of Figures

List of common Abbreviations and Acronyms

ABA	Abscisic acid
AIC	Akaike Information Criterion
ANCOVA	Analysis of covariance
APX	Ascorbate peroxidase
AsA	Ascorbic acid
CEO_3	Cumulative ozone exposure
CUO_3	Cumulative ozone uptake
cv.	Cultivar
DW	Dry weight
E.C.	Enzyme Commission number
FOSFA	Federation of Oils, Seeds, and Fats Association
F_v/F_m	Maximum potential quantum efficiency of Photosystem II
FW	Fresh weight
g_s	Stomatal conductance
H_2O_2	Hydrogen peroxide
$_i$WUE	Intrinsic water use efficiency
L.	Linnaeus
MDA	Malondialdehyde
NIR	Near infra-red
NPQt	Non photochemical quenching
O_3	Ozone
OSR	Oilseed rape
PAR	Photosynthetically active radiation
PCD	Programmed cell death
PI	Performance Index
P_{net}	Net photosynthetic rate
ppbv	Parts per billion by volume
ppm	Parts per million by mass
RH	Relative humidity
ROS	Reactive oxygen species
rOSI	Relative oxidative stress index
SEM	Standard error of the mean
SOD	Superoxide dismutase
TSW	Thousand seed weight
USD	United States dollars

1. Introduction

1.1 Oilseed rape: an economically important crop

In 2021, the global yield of *Brassica* oilseeds reached 68 million metric tonnes, contributing 11% of global oilseed yields, making it second only to soybean which yielded 384 million tonnes (USDA, 2021). However, despite taking up a quarter of the growing area, oilseed rape (hereafter OSR) oil produces around the same calories as soybean as its seed oil content is at least double that of soya: ≥41% compared to soya seed's 20% oil (AHDB, 2023). Crushed and pressed OSR is used primarily to produce edible oil, contributing 6.0×10^{11} kcal to the food industry in 2021, which represents ~4% of average global calorific needs annually (D'Odorico et al., 2014; Berners-Lee et al., 2018). Once the edible oil has been extracted, the remainder of the seed (39 million tonnes) is used as seed meal for livestock, the products of which account for a further 9.9×10^{9} kcal (Orlovius, 2003). The precise distribution of OSR production remains unclear as the term 'rapeseed' is ascribed to several progenitor and dominant hybrid *Brassica* species (USDA, 2023), but it is virtually ubiquitous across the Northern Hemisphere crop-producing regions.

There are six major agricultural *Brassica* species. The relationships between them are demonstrated in The Triangle of U (Figure 1.1, adapted from Xue et al., 2020).

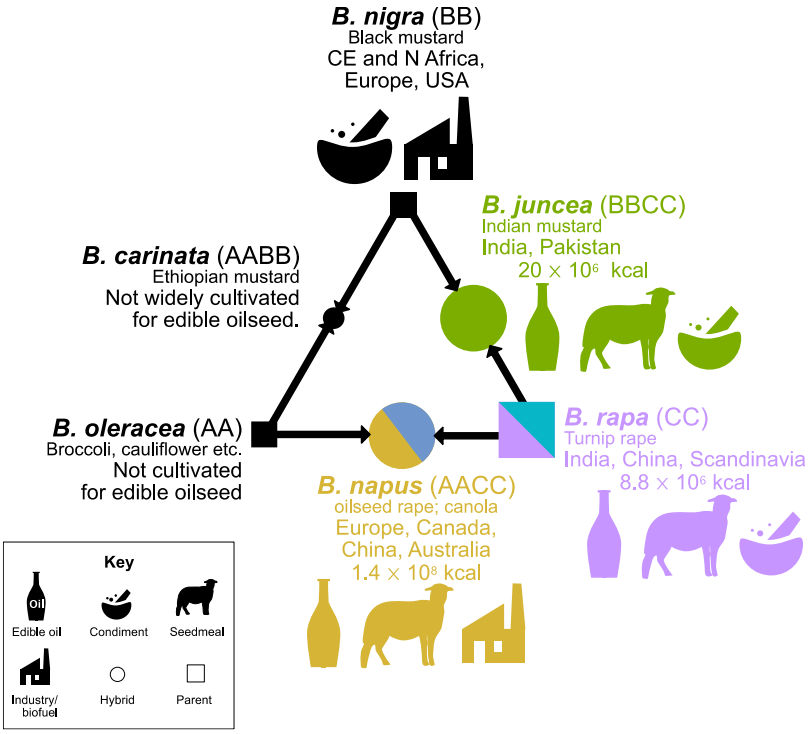

Figure 1.1. Adapted Triangle of U applied to key Brassica oilseeds, with cultivation uses, largest production locations, and annual calorific production (as pressed oil). Calorific value refers edible oil production in five highest-producing regions (China, Canada, EU, India, Japan). Calorific data from Shekhawat et al. (2012) and USDA (2023). Large symbols show three cultivars that have been bred to canola-grade tolerance in OSR (*B. napus* in yellow, *B. rapa* in purple/blue, and *B. juncea* in green). Colours codes indicated here are used throughout this thesis.

Progenitor species (*B. rapa* L., *B. oleracea* L., *B. nigra* L.,) co-occur as archaeophytes across Europe, Asia, and Africa, and as neophytes in the Americas and Australasia. The three species naturally hybridised multiple times, producing three dominant amphiploid hybrids (*B. caratina* L., *B. juncea* L., *B. napus* L.) (Allender and King, 2010).

Per capita consumption of *Brassica* oilseeds is highest in the European Union, where *B. rapa* and *B. napus* are the dominant cultivated species. Both species have been cultivated in both a winter- and spring-sown form, with their quality tightly regulated. For example, OSR lines are selected during breeding programmes based on high oleic acid levels, a desirable omega-9 fatty acid, and low erucic acid, an undesirable compound which is known to cause myo-cardiotoxicity at high levels (Knutsen et al., 2016). These cultivars are referred to as High Oleic Low Linolenic - HOLL or '00' (Fu and Gugel, 2009; Lu et al., 2019). The earliest advanced cultivar development programmes in the 1940's exploited both *B. napus* and *B. rapa*, but *B. napus* became favoured in the 1960s due to its superior herbicide tolerance (Canola Council, 2017). *B. napus* breeding intensified from then with a focus on exploiting valuable traits such as high oil content, low proportion of non-nutritive compounds, and high productivity and yield (Fu and Gugel, 2010). The name 'canola' was coined and trademarked in the late 1970s as an acronym of Canadian Oil Low Acid (Canola Council, 2017). The name could initially only be ascribed to varieties that contained <2% erucic acid and produced feed with less than 30 µl aliphatic Glucosinolates per g of dry seed (Raymer, 2002). However, as the quality of all edible *B. napus* currently traded and processed for human consumption is so tightly regulated as to inevitably meet these criteria (as in EU), the names canola and oilseed rape are now considered interchangeable (Wittkop et al., 2009).

India and China consume one-third of total global yields of *Brassica* oilseeds, with China consuming twice that of India (USDA, 2023). *Brassica* oilseed oil comprises over a quarter of total oilseed yields in India, totalling 8 million tonnes (USDA, 2021), with *B. juncea* accounting for 75-80% of Indian rapeseed production and consumption. The remainder comprises a mix of *B. rapa*, *Eruca vesicaria*, and *B. napus* (Shekhawat et al., 2012). China cultivates *B. napus* and *B. rapa*, with production of *B. napus* increasing by a third since 2006 to 14 million tonnes in 2021 and now contributing ~85% of *Brassica* oilseed production in the country (USDA, 2021). Despite this, China relies on 2.2 million tonnes imports annually, bringing their total consumption to 15 million tonnes per year (USDA, 2021). *B. carinata* and *B. nigra* seeds are also cultivated in Northern Africa, Europe, and the Middle East but the seeds contain high levels of non-nutritive compounds and erucic acid levels <40%, so cannot be used in large volumes in food and animal feed (De Zoysa et al., 2021). Hence, they are primarily used as a spice and as medicine (Nicácio et al., 2021). However, those very same qualities are desirable for industrial uses and both species are now being considered as promising biofuel feedstocks (Roslinsky et al., 2021).

This thesis primarily focuses on *B. napus* (hereafter OSR), which accounts for ~90% of total *Brassica* oilseed yields globally and which has been extensively selectively bred on four continents, primarily to increase yield and human edible oil content and quality (Wittkop et al., 2009). OSR breeding in Europe has resulted in two

seasonal cultivars: spring-sown (considered annual) cultivars and winter-sown (biennial) cultivars (AHBD, 2023; Gulden et al., 2008). In Europe, winter varieties are sown in mid-August to early September, and harvested in July to August, whereas spring varieties are sown in late March to early April, and harvested in late August to September (AHDB, 2020). Therefore, spring varieties have a shorter life cycle, and less time in which to be productive, resulting in more efficient conversion of sequestered carbon to oilseed (Felzer et al., 2007). Previous studies have suggested that varieties of crops with shorter life cycles are more susceptible to oxidative damage due to abiotic stress, such as exposure to elevated tropospheric ozone (Felzer et al., 2007; Emberson et al., 2018). This may be caused by plants with shorter life cycles failing to deploy or utilise protective mechanisms over their growing season when compared to slow-growing counterparts. Given the very low economic return for OSR (Hu et al., 2017), it is uncertain whether the winter crops with a longer life cycle would remain economically viable if yields or quality declined.

1.2 Tropospheric ozone

Ozone (O_3) is a key air pollutant in the lowest atmospheric region, the troposphere, and the third most important greenhouse gas in terms of climate forcing, at an estimated 0.28-0.43 W m^{-2} since pre-Industrial times (Zeng et al., 2008). Ozone is formed through a series of non-linear chemical reactions involving natural and anthropogenic nitrogen oxides (NO_x) and volatile organic compounds (VOC) in the presence of UV light (Hauglustaine and Brasseur, 2001; Cooper et al., 2014), as shown in Figure 1.2. Despite declines in anthropogenic emissions of these precursor compounds from industrial and urban areas in Northern Europe and North America, ozone concentrations have not decreased proportionally (Ziemke et al., 2019). Average annual background concentrations have instead generally increased by ~15% in many areas of the Northern Hemisphere since 1900 and are projected to increase by a further 5-10% by 2100 from 30 ppb to 35 ppb (Archibald et al., 2020).

Increased ozone levels have in part been driven by increasing Northern Hemisphere temperatures, which increase biogenic volatile organic compounds (BVOC) from vegetation, and increase rates of the reactions leading to ozone formation (Coates et al., 2016). Moreover, stratospheric ozone depletion increases UV radiative forcing in the troposphere and increases the rate of the initiation steps in the reaction, thereby increasing tropospheric ozone formation still further (Hegglin and Shepherd, 2009). This has resulted in the total tropospheric burden reaching ~5000 Tg yr^{-1} (Archibald et al., 2020), although there were slight declines of ozone (by 6.5 Tg yr^{-1}) in summer 2020 due to COVID-19 lockdowns inducing substantial decreases in urban and industrial NO_x of ~15% (Miyazaki et al., 2021). A significant proportion, thought to be around 10% or ~450 Tg yr^{-1}, of tropospheric ozone comes from stratospheric exchange, as shown in Figure 1.2 (Archibald et al., 2020). Ozone levels drop sharply by approxiamtely a third overnight largely due to a) dry deposition onto reactive surfaces (e.g., vegetation, soils) and b) the night time fall in precursor compounds such as NO (Fujita et al., 2003; Hu et al., 2021; Masiol et al., 2019). This creates a characteristic

diurnal profile wherein ozone is high during the day and low at night (Petetin et al., 2016). Moreover, ozone levels also have a seasonal cycle due to most importnatly increased temperaure and light, alongside BVOC emissions during the peak Northern Hemispheric growth season, i.e. between April and September (Parrish et al., 2013; 2020).

Ozone is relatively long-lived compared to other tropospheric pollutants with an average lifetime of ~20 days, approximately 10-fold longerthan that of sulphur dioxide (SO_2) and several orders of magnitude greater than that of NO_2 (Lelieveld et al., 1997; Fowler et al., 2008). This means that ozone may be transported many hundreds of miles from precursor sources, such as urban and industrial areas. Moreover, ozone is higher in rural areas due to (a) higher VOC emissions and (b) the NO titration effect, whereby extremely high concentrations of NO over cities, leads to chemical loss of ozone. Ozone is thereby often considered a rural air pollutant, with rural concentrations being a third or more higher than urban concentrations. For example, maximum ozone concentrations in northern UK cities were 70 ppb while rural areas reached 100 ppb in 2005 (Jenkin, 2008; Sicard, 2021). Once ozone is transported to rural areas, its lifetime declines to 2 days as enhanced rates of dry deposition occur (Fowler et al., 2008). Tropospheric ozone's lifetime allow transport between countries and even continents (Dueñas et al., 2004; Derwent et al., 2015; Han et al., 2018). Ozone annual cycles and distribution are largely driven by meteorology (sunlight, wind speed and direction, temperature) (Hu et al., 2021) and determine whether crops are exposed to medium-high (50-100 ppb) concentrations over weeks or months (chronic ozone exposure), or very high (up to 200 ppb) over hours or days (acute ozone exposure) (Fiala et al., 2003; Lin et al., 2020). All

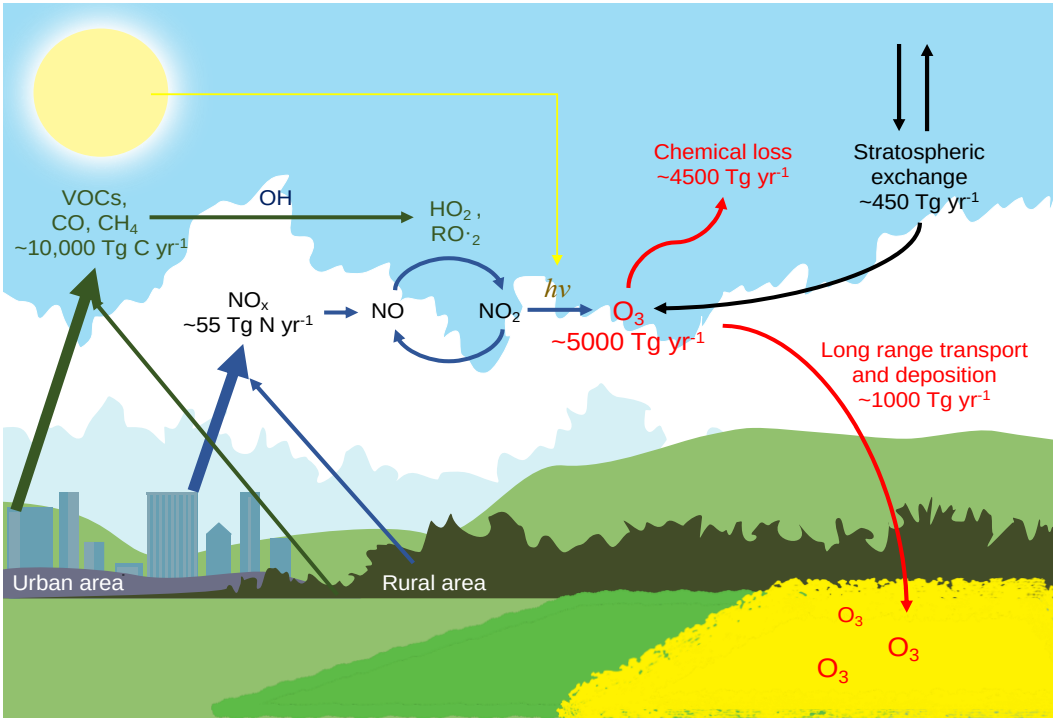

Figure 1.2. Ozone formation and occurrence adapted from Fowler et al., (2008). Ozone burden (Tg yr^{-1}) from Archibald et al., (2020) Miyazaki et al., (2021).

experiments in this thesis use a range of 'real-world' levels of ozone, from low concentrations (~20-30 ppb) representative of mid-high latitude European background levels, up to 110 ppbv, representative of typical maximum summertime levels in areas of long-term measurement, such as southern Europe, Asia and North America (Pay et al., 2019; Boleti et al., 2020).

1.3 Ozone phytotoxicity

Ozone is a well-known phytotoxin, as it is a powerful oxidant that directly damges leaf tissue. Ozone also generates highly oxidising reactive oxygen species (ROS), which disrupt metabolic pathways, damage cell membranes, and ultimately result in decreased photosynthetic rate, loss of stomatal control, accelerated senescence, and declines in plant biomass (Agathokleous et al., 2020). Elevated ozone concentrations (e.g. >30 ppbv) are considered as an abiotic stress, as they are a sub-optimal environmental condition which decreases vegetation abundance and diversity (e.g., Mills et al., 2018a), and decrease the productivity of ozone-sensitive species, significantly decreasing yields (Zhang et al., 2022).

1.3.1 Ozone in plant tissues, ROS formation, and oxidative stress

Ozone mainly enters plant tissue via the stomata and rapidly dissolves and oxidises into the apoplastic space, due to the apoplast's aqueous state which contains solubilised low-weight molecular compounds, water and vitamins (Qi et al., 2017). The apoplast consists of intercellular space, cell wall, and xylem, and is considered the primary interface of intracellular inference (Farvardin et al., 2020). The oxidation reactions triggered by ozone generate ROS species including superoxide (O^{-}_{2}•), singlet oxygen ($^{1}O_{2}$) and the hydroxyl radical (OH•), which in turn oxidise the low-weight compounds in the apoplast (Halliwell, 2006). Superoxide is dominantly produced in these apoplastic oxidation reactions but is relatively unstable with a half-life of 1 µs, compared to singlet oxygen at 3 µs (Halliwell, 2006). Superoxide either is quenched by defensive compounds (*section 1.4*) or undergoes spontaneous dismutation to hydrogen peroxide (H_2O_2), which is the most stable and therefore the longest-lived ROS at 1 ms (Sies and Chance, 1970; Phua et al., 2021). For this reason, H_2O_2 is used as a marker of oxidative stress (Shulaev and Oliver, 2006) although H_2O_2 can also diffuse through phospholipid membranes via aquaporins into cytosol and organelles, where it can either act as a signal, or further damage membranes if not reduced to water by biochemical defences (Bienert and Chaumont, 2014; Smirnoff and Arnaud, 2019). Cellular homeostasis is ultimately disrupted through damage of metabolic and photosynthetic apparatus such as thylakoid membranes, open calcium ion and potassium ion channels, and disrupt key signalling pathways such as ABA signalling to induce stomatal closure (Mills et al., 2009; McAdam et al., 2017).

ROS are also formed under non-stress conditions as a by-product of aerobic metabolism via pathways involving electron transport chains e.g., photosynthesis and respiration, which are prone to 'electron leakage' (Hajiboland, 2014). Oxygen, which

is present in high levels in plant tissues, gains these electrons and is therefore reduced to super oxygen, which has a higher energy state and is more reactive (Demidchik, 2015). Ozone, oxygen and ROS are therefore also abundant within organelles such as mitochondria, chloroplasts, and peroxisomes. Other abiotic stresses, e.g., high temperatures, similarly increase ROS formation, via increased rates of respiration/photosynthesis (Nievola et al., 2017). If ROS concentrations exceed and overwhelm defence mechanisms, the plant is under 'oxidative stress' (Phua et al., 2021). When plants undergo oxidative stress, ROS oxidise phospholipid membranes, thus causing lipid peroxidation which generates malondialdehyde (MDA), which is therefore commonly used as a marker of oxidative damage (Vaultier and Jolivet, 2015). High levels of ROS (in particular H_2O_2 which is a multi-faceted molecular signal at low levels) also trigger the upregulation of senescence-associated genes (*SAG*) initiating biochemical processes such as programmed cell death (PCD), a tightly orchestrated pathway which terminates cells and tissue (De Pinto et al., 2012).

1.3.2 Ozone decreases photosynthesis

While senescence processes largely contribute to photosynthetic declines, ozone-induced ROS, such as H_2O_2, also downregulate photosynthesis-associated genes (PAGs), and lead to catabolism of photosynthetic components such as chloroplasts. Ozone has well-known detrimental effects on crop photosynthetic rate: high ROS levels damage both the light-dependent and light-independent photosynthetic pathways in ozone-sensitive species, such as soybean (Rai and Agrawal, 2012). These include decreased Rubisco synthesis through damage to mRNA, and enzymes such as Rubisco activase and ATP synthase (Tammam et al., 2019). Proteins such as the oxygen-evolving subunit of Photosystem II are also significantly damaged, meaning that the light-dependent reaction is a key site for ozone damage (Bohler et al., 2007). Decreased carbon assimilation ultimately leads to decreased non-structural carbohydrate synthesis, therefore decreasing carbon storage and allocation to reproductive organs (Bohler et al., 2007; Tammam et al., 2019). This is reflected in decreased leaf area and reproductive output.

1.3.3 Ozone impairs stomatal functioning

Stomata are the primary entry point for ozone uptake; therefore, it is important to measure stomatal conductance (openness and density of stomata) and the effects of ozone on stomatal conductance. However, ozone level, magnitude and duration dictate the degree and type of stomatal damage that may occur. For example, chronic tropospheric ozone exposure generally decreases stomatal conductance (Ainsworth et al., 2012), and many mechanisms have been ascribed to this physiological phenomenon. For example, it is thought that a decreased photosynthetic rate and increased mitochondrial respiration rate (Lombardozzi et al., 2012) cause an increase in internal carbon dioxide concentration and therefore decrease stomatal conductance (Gandin et al., 2021). This causes an uncoupling between photosynthetic rate and stomatal conductance (Lombardozzi et al., 2012). Such an uncoupling of stomatal conductance

from environmental parameters results in higher transpiration rates, decreases intrinsic water use efficiency (iWUE), and may lead to further oxidative and physiological damage from stresses such as drought (McAinsh et al., 2002; Paoletti and Grulke, 2010).

While secondary stomatal impacts are well-documented, direct damage of stomata have been given little attention. However, high ozone levels of ~200 ppb directly decrease stomatal conductance through influx of ROS through guard cells, leading to indirect stimulation of potassium ion channels, leading to an an efflux of potassium ions, and ultimately stomatal closure (Vahisalu et al., 2010). Another proposed theory is that ABA precursors are directly oxidised by ROS, which increases localised relative ABA production, inducing stomatal closure (McAdam et al., 2017). However, signalling pathways involved in stomatal control, e.g., calcium-based signalling via changes in the calcium homeostasis of guard cells, can also be altered or interrupted by high ozone levels (>70 ppb) (McAinsh et al., 2002; Short et al., 2012). Such changes prevent full stomatal closure in response to other environmental (light, temperature) and biochemical stimuli (phytohormones such as ABA) (Ainsworth et al., 2012). This may cause "sluggish" stomatal responses, wherein stomata respond slowly to biochemical and environmental stimuli, further causing declines in productivity such as biomass accumulation.

1.3.4 Foliar injury and accelerated senescence

Injury metrics based on early disease marking indices are commonly adopted to describe ozone-induced damage (Paoletti et al., 2022). For example, tissue necrosis, resulting in foliar necrotic lesions, manifests as rust-like flecks on leaves or bronzing between leaf veins, as observed in *B. juncea* after 26 days' exposure to 100 ppbv ozone (Figure 1.3a). The proportion of leaf area covered by such lesions can be estimated and scored as a percentage with a lower foliar injury score effectively signifying relative ozone tolerance (De Temmerman et al., 2002; Paoletti et al., 2022). This type of injury is caused by a hypersensitive response, wherein a sudden increase in H_2O_2 levels ('oxidative burst') genetically upregulates biochemicals akin to a local pathogenic response, meaning that affected cells initiate rapid cell death. This highly localised response causes the characteristically irregular and isolated foliar lesions (Grulke and Heath, 2020). However, some crop species, such as *B. napus*, do not to present this classic ozone symptom under more moderate ozone levels (<110 ppb) (Ollerenshaw et al., 1999). Therefore, the only visible injury symptom may be increased foliar

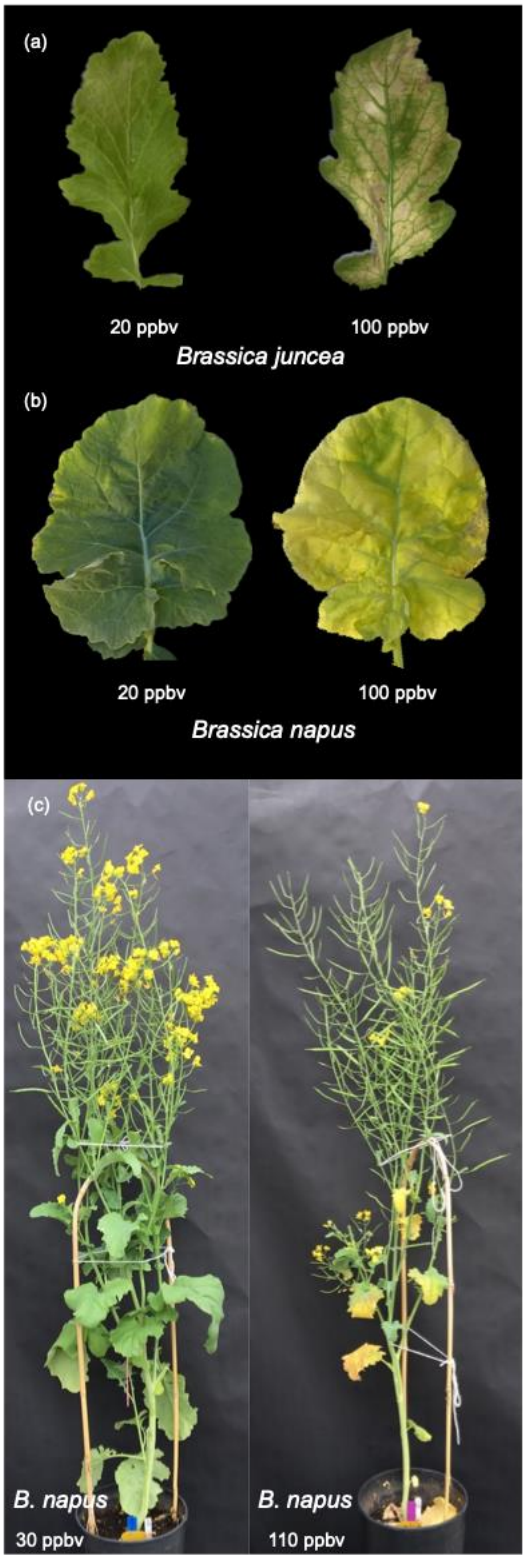

Figure 1.3. a) Necrotic lesions on *B. juncea* leaf under 100 ppbv ozone after 26 days. b) Spring *B. napus* ozone damage is manifested as accelerated senesnence at ~100 ppbv compared to ambient (20 ppbv). c) Long-term exposure to 110 ppbv ozone accelerates growth stagest in spring-sown OSR.

senescence with non-specific yellowing or browning of the leaf, as shown in Figure 1.3b (usually measured non-destructively with a chlorophyll content meter e.g., soil plant analysis development meter or 'SPAD') or foliar abscission (i.e., leaf number) in an acropetal gradient.

Tropospheric ozone damage in crops is most reliably apparent as a PCD-induced accelerated senescence response (Grulke and Heath, 2020). Senescence is a tightly regulated process that is initiated by key signalling molecules integrated to developmental and age-dependent pathways including ROS such as H_2O_2 (Dat et al., 2003; Bieker et al., 2012; Zentgraf et al., 2022). H_2O_2 upregulates senescence-associated genes (SAGs), such as SAG2 and SAG12 which metabolises enzymes involved in macromolecular catabolism and cycling, such as chloroplast breakdown (Grbić and Bleecker, 1995; Miller et al., 1999; Kusaba et al., 2013; Li et al., 2013). H_2O_2 is also known to initiate transcription of auxin phytohormones (e.g., IAA), which in turn stimulates biosynthesis of ethylene, a phytohormone well-known to induce many senescence and abscission processes in crops such as mungbean (*Vigna radiata* L.) (Song et al., 2007). This shift in primary metabolic profile and transport leads to chlorophyll degradation, hence, declines in photosynthesis. The effects of leaf ageing and ozone are considered synergistic, as ozone exposure increases the endogenous ROS pool beyond that associated with natural ageing, as well as directly oxidising photosynthetic components. While many senescence-associated pathways have been

identified, there are still challenges in describing the full biochemical senescence mechanism in plants due to its complexity and genetic regulation (Nooden, 2003; Kim et al., 2016).

During senescence, older leaves reallocate nutrients to younger leaves, therefore providing metabolic compensation, and thus increasing plant fitness when crops are under stress (Gan and Amasino, 1997; Guiboileau et al., 2010). Therefore, growers may adjust nitrogen application in-field to attempt to mitigate senescence acceleration, as increased nitrogen stimulates chlorophyll synthesis in crops under ozone exposure and may be misdiagnosed as nutrient deficiency (Pandey et al., 2018). However, whole-plant senescence is also accelerated, leading to earlier transitions between growth stages (Figure 1.3c). Such changes in phenology advance maturity and harvest dates, and therefore modify agricultural calendars. In the case of *Brassica* leafy crops and oilseeds, market value may decline due to appearance (i.e., loss of chlorophyll) or lack of seed filling (Teixeira et al., 2011). Moreover, as nutrient use efficiency declines, input costs for growers are increased, which is at odds with global efforts to improve crop resource efficiencies and land management (Fuhrer and Booker, 2003).

1.4 Biochemical defence responses to ozone

Plants have evolved a suite of constituent, systemically and locally induced biochemical compounds synthesised in response to stress. These secondary metabolic compounds include antioxidants, that ultimately prevent oxidative stress and damage (Pisoschi and Pop, 2015). Key compounds and enzymes associated with ozone exposure and defence are described in this section and presented in Figure 1.4. Optimal defence theory suggests that the shift in the secondary metabolic profile ensures that tissues closely associated with plant fitness are defended at the constitutive level, i.e., antioxidants are produced throughout the plant, and expendable tissues, such as older leaves, are more associated with oxidative damage (Strauss et al., 2004).

1.4.1 Antioxidant function and purpose

Antioxidants may have multiple roles, such as inhibition of a range of ROS species, e.g., ascorbate species (Xiao et al., 2021), or may be upregulated in response to specific stimuli in localised areas, such as via H_2O_2 signalling (Zhanassova et al., 2021). Therefore, antioxidants tend to co-occur in high concentrations at sites of high ROS concentrations: mitochondria, chloroplasts, peroxisomes, and the apoplast. Antioxidants prevent or delay cell damage by inhibiting ROS-induced oxidation reactions and by directly or indirectly quenching ROS (Larson, 1988). Apoplastic antioxidants are considered as the primary detoxicants under high ozone uptake (Castagna et al., 2005). There are two key apoplastic antioxidant groups: enzymatic and non-enzymatic antioxidants. Non-enzymatic antioxidants are generally simple low-molecular weight compounds which react directly with ROS, or regenerate enzymatic antioxidants. Enzymatic compounds are larger, structurally complex and consist of

protein subunits, and directly quench a range of ROS including H_2O_2 (Dumanović et al., 2021).

1.4.2 Non-enzymatic antioxidants and ozone tolerance

Non-enzymatic antioxidants that have been repeatedly associated with biochemical tolerance to moderate-high Northern Hemispheric levels (<110 ppb ozone treatments) and chronic ozone treatments in primary research studies are ascorbic acid (AsA) (Conklin and Barth, 2004), and glutathione (GSH) (Noctor et al., 1998). These compounds are key electron donors in the ascorbate-glutathione cycle, which is considered the dominant pathway of apoplastic antioxidant defence (Sharma and Davis, 1997). Due to the extensive literature on the response of AsA and its redox forms in a range of crop species, AsA can be used as a marker for ozone tolerance.

Ascorbic acid (AsA), a monosaccharide micronutrient (vitamin C), is the most frequently cited and longest-established antioxidant associated with ozone responses in higher plants such as white stonecrop *Sedum album* L. and wheat (*Triticum durum* L. and *T. aestivum* L.) (e.g., Castillo and Greppin, 1988; de la Torre, 2008; Fatima et al., 2019). It is a water-soluble molecule which rapidly changes redox state depending on environmental conditions, such as pH and temperature (Smirnoff, 2000; Dai et al., 2020). Ozone uptake increases AsA levels (Castillo and Greppin, 1988; Chen and Gallie, 2005), as AsA directly quenches ROS such as ozone and hydroxyl radicals, but mainly singlet oxygen (as shown in Figure 1.4), which has been observed *in vivo* in leaf extracts (Luwe et al., 1993) *in vitro* (Chou and Khan, 1983) and reproduced *in silico* in model simulations (Plöchl et al., 2000).

AsA is also a redox buffer for enzymatic scavenging of hydrogen peroxide (H_2O_2) in the glutathione-ascorbate cycle (Wu et al., 2017): Ascorbate peroxidase (APX, an enzymatic antioxidant, described in ***Section 1.4.3***) uses AsA as an electron donor, and reduces H_2O_2 to water, as shown in Figure 1.4; Smirnoff, 2000; Ishikawa and Shigeoka, 2008). Moreover, AsA is one of the most ubiquitous antioxidants and makes up a significant proportion of the apoplastic antioxidant pool in *Brassicaceae* (Das and Roychoudhury, 2014; Raseetha et al., 2013). AsA is a key modulator between growth transitions and senescence, acting as a nuclear signal to induce flowering and an antagonistic signal in senescence onset: for example, declines in AsA levels initiate senescence-associated genetic upregulation. AsA-deficient *Arabidopsis thaliana* mutants show accelerated senescence (Conklin and Barth, 2004; Kiddle et al., 2003; Pavet et al., 2005; Smirnoff, 2000).

Similarly to AsA, Glutathione (GSH) is a water-soluble redox buffer that directly quenches ROS species such as superoxide (Wefers and Sies, 1983). It is also involved in the glutathione-ascorbate cycle, where it is used as an electron donor to regenerate AsA, as shown in Figure 1.4 (Noctor et al., 1998; Pasqualini et al., 2001). In turn, GSH is regenerated by reduced nicotinamide adenine dinucleotide phosphate (NADPH)-dependent glutathione reductase, which is a key enzyme in the ascorbate-glutathione cycle (Noctor et al., 1998). It is considered a transportable form of reduced sulphur, which has been identified to initiate signal transduction in response to changes

in redox status (Alscher, 1989; Kumar et al., 2010). While its precise role in signal transduction has not been fully elucidated, ~80 ppb ozone exposure increased GSH levels in an ozone-tolerant rice cultivar, which maintained yield relative to another more ozone-sensitive cultivar (Wang et al., 2013).

Ozone exposure also increases the concentrations of a range of other foliar antioxidants, such as phenols (anthocyanins, flavanols) (Boublin et al., 2022; Pellegrini et al., 2015) and tocopherols (Guo et al., 2009; Wedow et al., 2021). However, these antioxidants did not appear to confer morphological or physiological tolerance (e.g., chlorophyll content was lost, where measured). Moreover, these studies often fumigate with more than 200 ppbv, which doesn't represent realistic Northern Hemisphere levels where *Brassica* crops majorly are grown. Plant responses under such extreme conditions may therefore not be representative of crop responses under lower (real-world) ozone levels.

1.4.3 Enzymatic antioxidants and ozone tolerance

Enzymatic antioxidants, which include polypeptide subunits (and metal ions), are synthesised in response to stress by genetic transcript accumulation (Camp et al., 1994; Raven, 2003). Multiple gene families associated with enzymatic antioxidant synthesis are known to be triggered by phytohormones and secondary metabolites such as ethylene (Agrawal et al., 2003) and ABA (Zhou and Guo, 2009).

The enzyme superoxide dismutase (SOD; E.C. 1.15. 1.1), considered the primary enzymatic antioxidant in ROS-antioxidant pathway, has long been associated with ROS quenching and therefore with abiotic stress tolerance. As shown in Figure 1.4, SOD initiates a series of reactions by reducing superoxide to H_2O_2, which in turn is quenched to water and oxygen by other enzymatic antioxidants (including peroxidases (APX) and catalase (CAT)) (Sharma et al., 2012; Gill et al., 2015). Around 20 SOD genes have been identified in Brassica species and are known to be upregulated in response to salinity, cold, waterlogging, and drought in *Brassica napus*, *B. juncea*, and *B. rapa* (Verma et al., 2019; Su et al., 2021). Importantly, increased SOD activity has been observed to reduce ozone-induced programmed cell death (PCD) (Lee & Bennett, 1982) and overexpression of a SOD gene improved salinity tolerance in *Arabidopsis* (Wang et al., 2004).

Ascorbate peroxidase (APX; E.C. 1.11. 1.11) is a Class I haem-containing peroxidase that directly quenches H_2O_2 into water (Jones et al., 1998). It is considered to be the antioxidant that functions downstream from SOD and is a major component of the apoplastic antioxidant pathway and ascorbate-glutathione cycle (Figure 1.4). APX also co-occurs with SOD in sites of high ROS: the apoplast, cytosol, mitochondria, and chloroplasts (Caverzan et al., 2019). APX is synthesised via multiple signal pathways, such as ethylene increasing caffeic acid synthesis, which in turn increases *APX* transcript accumulation, thus increasing APX synthesis and activities, and therefore decreasing H_2O_2 concentration, under abiotic stress such as exposure to ozone (Torsethaugen et al., 1997; Castagna and Ranieri, 2009). APX has long been associated with ozone responses in higher plants (Mehlhorn et al., 1987): chronic levels (60 ppbv)

over 56 days have been shown to stimulate APX activities in the apoplast in ozone-resistant white clover (*Trifolium repens* L.) (Nali et al., 2005). Moreover, three *APX* genes have been associated with APX upregulation in response to abiotic stress in *B. juncea*, while five have been identified in *B. rapa*, and *B. juncea* (Ma et al., 2022; Verma et al., 2021), suggesting APX it may be suitable for selecting for allelic variation to develop ozone-tolerant crops (Pandey et al., 2017).

While other peroxidases (POX; E.C. 1.11. 1.x) and catalase (CAT; EC 1.11.1.6) also catalyse H_2O_2 to water, APX and SOD are more closely associated with increased activity and antioxidant capacity under ozone levels representative of real-world conditions, as shown in response to <110 ppbv ozone (SOD and APX) in rice (Sarkar et al., 2015), and <110 ppbv in wheat (APX) (Wang et al., 2014). Furthermore, POX and CAT are present at comparatively lower apoplastic concentrations. CAT is mainly found in peroxisomes, and is less effective at quenching ROS than APX, as it has a lower affinity for H_2O_2 (Mizuno et al., 1998). Moreover, POX is localised mainly to vacuoles (Sharma and Davis, 1997), are a diverse superfamily (which include APX), and therefore not considered a specific enough marker for ozone tolerance due to its comparative complexity and diversity. Hence, neither CAT nor POX were a focus of this thesis.

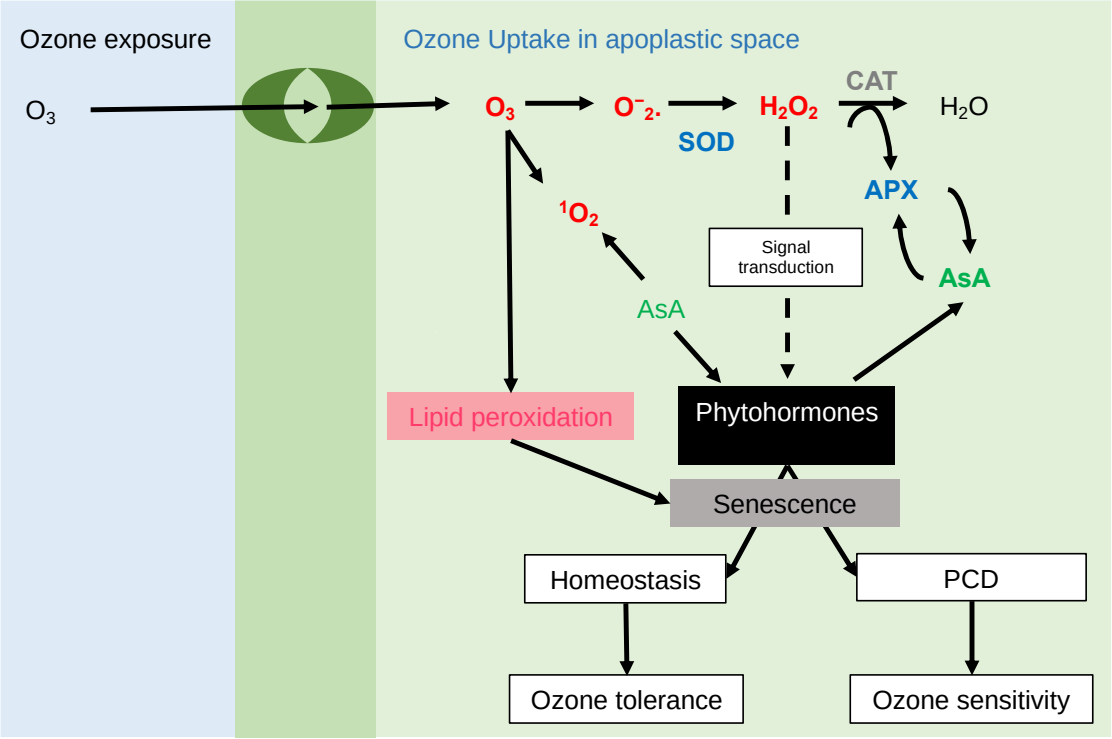

Figure 1.4. Simplified schematic of ozone uptake, ROS generation and scavenging from three key antioxidants AsA (green), SOD, APX (blue). Ozone enters the leaf via stomata, where it rapidly dissolves into the apoploastic space and oxidises to for reactive oxygen species. Key ROS are sinlget oxygen ($^1O_2$) and superoxide (O^-_2•), which are quenched by ascorbic acid (AsA) and superoxide dismutase (SOD). Hydrogen peroxide is in turn quenched by ascorbate peroxidase, which is regenerated by AsA.

1.5 Tropospheric ozone decreases *Brassica* oilseed yield and quality

B. napus is described as 'moderately sensitive' to ozone, with critical levels based on AOT40 being half the value of that for soya in a meta-analysis (Mills et al., 2006). Despite this, the European agricultural sector rarely view chronic ozone exposure as a major risk factor in OSR cultivation due to OSR yeild variation being attributed to other stresses and the likely misidentification of ozone damage (Mills et al., 2006). Furthermore, the vegetative stage (growth stage/GS15, i.e., 5 leaves fully unfolded) and early reproductive stages (GS50, i.e., inflorescence emergence) are considered the most ozone-sensitive (as in Table 1.1.) (AHBD, 2019) and these coincide with the period of highest ozone concentrations in the Northern Hemisphere (i.e., where OSR is majorly grown).

Table 1.1. Oilseed rape growth stage development index adapted from AHDB, 2023. Blue shading presents growth stages which are considered most sensitive to ozone exposure. Red shading denotes growth stages exposed to elevated ozone in each study chapter.

Growth stage (GS)	Description	Growth stages ozone-exposed in thesis chapters:		
00-09	Germination and emergence	3	4	5
00-19	Leaf development	**3**	**4**	**5**
20-29	Side-shoot formation	**3**	4	**5**
30-39	Stem elongation/extension	**3**	4	**5**
40-49	Not applicable in OSR	**3**	4	**5**
50-59	Inflorescence/flower-bud emergence	**3**	4	**5**
60-69	Flowering	**3**	4	5
70-79	Pod/seed development	**3**	4	5
80-89	Pod/seed ripening	**3**	4	5
90-99	Senescence/harvest	**3**	4	5

Fewer than six studies have investigated the effects of real-world ozone exposure on *Brassica* oilseed since 1990. In spring *B. napus*, thousand seed weight (TSW), considered a key indicator of yield, declined between 15 and 30% in OSR exposed to ozone over three months (Adaros et al., 1991; Bosac et al., 1998; De Bock et al., 2011). Total seed mass per plant also declined by ~25% (Vandermeiren et al., 2012). However, reproductive site losses (declines in seed, pod, and flower spike or 'racemes' number) were inconsistent between studies, with some cultivars losing a third of reproductive sites (Bosac et al., 1998; De Bock et al., 2011), and some gaining reproductive sites by 10% (Bosac et al., 1994). *Brassica* oilseed quality also generally declined in all studies where measured. For example, total oil content declined by a third under exposures of ~70 ppbv over a growing season (De Bock et al., 2011), which represents a risk of oil content falling to below the threshold for marketing as canola-grade. Fatty acid composition has also been reported to change, leading to a general decline in seed quality. For example, in one study, the fatty acid family including erucic acid (omega-9 fatty acid, denoted 22:1) increased by 5% in *B. rapa* seeds exposed to 70 ppbv over a growing season, increasing levels to above the limits for safe consumption.

Hence, this would require further processing to remove such compounds, incurring substantial economic penalties for growers (Tripathi and Agrawal, 2012). Glucosinolates, an equally undesirable compound to erucic acid, also increased by ~30% following exposure to 63 ppbv ozone over three months (Vandermeiren et al., 2009).

However, considerable knowledge gaps remain. Whether antioxidant responses convey physiological tolerance and whether such parameters could provide a quantitative measure of ozone-tolerance has not been established. It is also important to compare how both yield and quality parameters are affected between two seasonal varieties (spring and winter sown OSR), and between the different *Brassica* oilseed species. Changes in yield and quality would decrease economic returns of this crop for growers, and improved understanding would enable informed cultivar choice and desirable trait selection in future scenarios.

1.6 Quantifying ozone exposure/uptake

Several metrics and models for quantifying ozone exposure, the ozone concentration that the plant endures over a season, and uptake, the ozone flux inside the leaves via stomata, have been developed or proposed since 1979. Following this, the Convention on Long Range Transboundary Air Pollution (CLRTAP) was established to develop international policies from research that clearly demonstrated the damaging effects of air pollution on vegetation.

Initially, metrics merely expressed an amount of ozone to which a plant had been exposed. The first were simply the sum of the mean 7-, 12-, or 24-hourly concentrations over an entire growing season (M7, M12, M24) - estimates of the average concentration of ozone the plant was in contact with (Fuhrer et al., 1997). However, in 1995, the European LRTAP proposed a standardised measurement: AOT40, which measures the accumulated exposure to ozone concentrations above 40 ppbv during daylight hours over a 3-month period (Fuhrer et al., 1978; Chapter and Full, 2000; Pleijel et al., 1991). This was adopted because vegetation biomass losses of 5% or greater showed a very strong relationship to 3-month AOT40 in multiple studies in wheat; 40 ppb was also considered substantially removed from background concentrations to provide a policy relevant target for emission reductions (Fuhrer and Acherman, 1994; Musselman et al., 1994; Finnan et al., 1996). AOT40 marked an important step forward, as it considered that seasonal exposures to the same mean concentration, but with a greater frequency of high concentrations, had a greater impact on vegetation (Critical Loads Advisory Group, 1996). This development coincided with the adoption of critical levels, which was defined as ‘a given concentration [of a pollutant] in the atmosphere above which direct adverse effects on vegetation may occur’ (Critical Loads Advisory Group, 1996; CLRTAP, 2017). The AOT40 critical levels for agricultural crops (wheat) was established as 3000 ppb *h* over 3 months to prevent annual yield losses of 5% or more. At the time this critical level was widely

adopted, 70% of England and Wales exceeding this AOT40 level (Critical Loads Advisory Group, 1996).

However, while AOT40 calculated cumulative ozone *exposure* over a certain threshold, it failed to account for ozone *uptake* into the leaf via stomata. This led to eco-physiologists developing an alternative flux-based metric - now referred to as PODy (Phytotoxic Ozone Dose) - which quantifies the cumulative uptake of ozone through the stomata and into the apoplast, i.e. the dose that plant cells are subject to (LRTARP Convention, 2017; Pleijel et al., 2022), which better predicted crop yield responses to seasonal ozone exposure (Mills et al., 2011). However, the additional complexity of calculating stomatal flux for this approach and the need for high-resolution meteorological data and accurate means of estimating stomatal conductance have delayed its wide-spread adoption by policy bodies outside of the LRTAP region.

Several models have been developed to estimate such a flux-based metric. Of these, the most detailed is the Deposition of Ozone for Stomatal Exchange (DO_3SE) model. While DO_3SE is considered a more accurate predictor of dose received by the plant and hence impact, it relies on robust stomatal conductance modelling. While many such models have been proposed, DO_3SE is based on a multiplicative algorithm adapted from Jarvis (1976) (Emberson et al., 2000). This algorithm requires measurements of many environmental parameters that stomata respond to, such as phenology, light, temperature, vapour pressure deficit, and soil water potential (Emberson et al., 2000), but this raises practical limitations, as these measurements over a growing season are often scarce (Emberson et al., 2000; Damor et al., 2020). The DO_3SE model has since been expanded to calculate the impacts of ozone on crop photosynthesis and carbon allocation (Emberson, 2023).

As a result of the difficulties accessing the data required for the DO_3SE model, more parsimonious exposure/uptake calculations have also been proposed and widely adopted. Here, we use those developed by Lombardozzi et al. (2013), such that cumulative ozone exposure (CEO_3) is calculated as:

$$CEO_3\ (mmol\ mol^{-1}\,\mathrm{h}) = [O_3] \cdot H \cdot D \cdot 10^{-3}$$

[Equation 1]

where: $[O_3]$ is ozone concentration in mol, H is number of hours, and D number of days, and 10^{-3} is the conversion from mol to mmol.

Cumulative ozone uptake (CUO_3) is then estimated as:

$$CUO_3\ (mmol\ mol^{-1}\mathrm{h}\ leaf) = CEO_3 \cdot g_s \cdot 1.67$$

[Equation 2]

where CEO_3 is cumulative ozone exposure, g_s is stomatal conductance as a single value, and 1.67 is the ratio of leaf resistance for ozone to leaf resistance for water vapour.

1.7 Ozone exposure experimental designs

To empirically understand vegetation responses to ozone, various bespoke experiments have been developed since the 1970s. Free-air O_3 elevation interfaces are considered the most important for establishing critical levels, as they are most comparable to real-world conditions (Matyssek et al., 2007; Paoletti et al., 2017). Free-air O_3 elevation interfaces have relatively simple experimental designs: perforated tubes release controlled volumes of ozone into plots or small cropping areas to elevate ozone to the desired concentration, with environmental conditions logged in each plot. Crops are generally planted/sown directly into the ground, meaning that there is little risk of pot-based compaction or root constraint occurring which may be synergistic with ozone effects (Whitfield et al., 1996). However, while the set-up is straightforward, there are limitations such as the flow of ozone being re-directed by prevailing winds or rapid deposition, creating heterogenous ozone distribution, and therefore a non-uniform ozone response, within a plot (Watanabe et al., 2013; Paoletti et al., 2017). It may also be challenging to eliminate or moderate other stressors, such as pests and disease, which may exacerbate or mitigate the observed ozone effect.

Open top chambers (OTC) are the most frequently used experimental setups in ozone exposure studies (Calatayud et al., 2011; De Bock et al., 2012; Desotgiu et al., 2013). OTCs are a semi-enclosed system, with Perspex or Teflon chamber sides rising from ~1.6 to 4 m in ozone-exposure experiments (Pleijel et al., 1991). For example, the OTCs at the University of Antwerp, Belgium has a 3 m radius, with a frustrum placed at a 40° downward angle at the top of each chamber (De Bock, 2011). This, along with the enclosed sides, limits the risk of wind direction and speed dispersing ozone beyond cropping area and better maintains ozone homogeneity within chambers. However, the enclosed sides and materials used may increase internal air temperatures and decrease relative humidity beyond that of typical field conditions, termed ‘passive chamber warming’, which may induce stomatal closure and limit ozone uptake (Fuhrer, 1994; Frei et al., 2020). While OTCs and free air enrichment are similar, directly comparing the ozone damage or yield loss in the two experimental setups highlights discrepancies between them. For example, when comparing multiple studies, Feng et al. (2018) found that rice and wheat had a greater ozone-induced yield loss in free air experiments than those conducted in OTCs (with ozone ranging between 20 and 100 ppbv above ambient), but soybean lost more yield in OTCs than free-air plots. This suggests that OTCs may over- or under-estimate critical levels and yield losses at an interspecific level, when compared with free air experiments, with free-air experiments considered to better represent real-world conditions than OTCs (Feng et al., 2018).

Glasshouses retrofitted with ozone fumigation piping are also regularly used for ozone experiments. For example, UKCEH’s Abergwyngregyn site comprises of four heated and four unheated geodesic glasshouses (Solardomes), with monitored ozone injection lines independently elevating ozone levels in each (van Oijen et al., 2003; Hayes et al., 2006). This allows pot-based experiments over an entire growing season. Ozone levels are carefully controlled and continuously monitored. Other environmental parameters (relative humidity, temperature, light) within the Solardomes are monitored

and logged, and are statistically similar across Solardomes. Solardomes remove the risk of ozone being diverted by wind speed or direction and reduce the heterogeneity of ozone within each glasshouse using engine-driven fans to circulate ozone-elevated air. The enclosed space also limits prevalence of pests (van Oijen et al., 2003). Plant pot positions are moved within and between Solardomes to limit temperature- and shade-induced stomatal closure from edge effects and to minimise "chamber" (i.e. glasshouse) effect (Hayes et al., 2020). Four unheated Solardomes, as shown schematically in Figure 1.6a, were used for the study presented in Chapter 3 this thesis.

Laboratory experiments offer the most accurate and tightly controlled environmental conditions, e.g., light regime, temperature, and soil moisture content (Potter et al., 1996). Sealed Perspex or Teflon chambers have been frequently used to elucidate biochemical mechanisms such as phytohormone function under chronic exposures (Wilkinson and Davies, 2009), to expose plants to very high ozone levels (> 200 ppbv) (McAinsh et al., 2002; Souza and Pagliuso, 2009; Stokes et al., 1993), or to expose certain plant parts, such as flowers, to specific ozone concentrations (Black et al., 2010). While using chambers enables the researcher to remove all other sources of environmental stress and thus focus solely on the impacts of ozone exposure, there is uncertainty regarding how results translate to field conditions due to limited pot size (Poorter et al., 2012a). Experimental Chapters 4 and 5 in this thesis used sealed Perspex 1-m^3 semi-controlled chambers, refurbished in 2021 from an original fumigation system at Lancaster Environment Centre (as in Stokes et al., 1993), and are shown in Figure 1.6b. Environmental parameters (light, temperature, relative humidity) were logged throughout experiments and did not significantly differ between chambers. Pots were however rotated within each chamber to minimise edge effects.

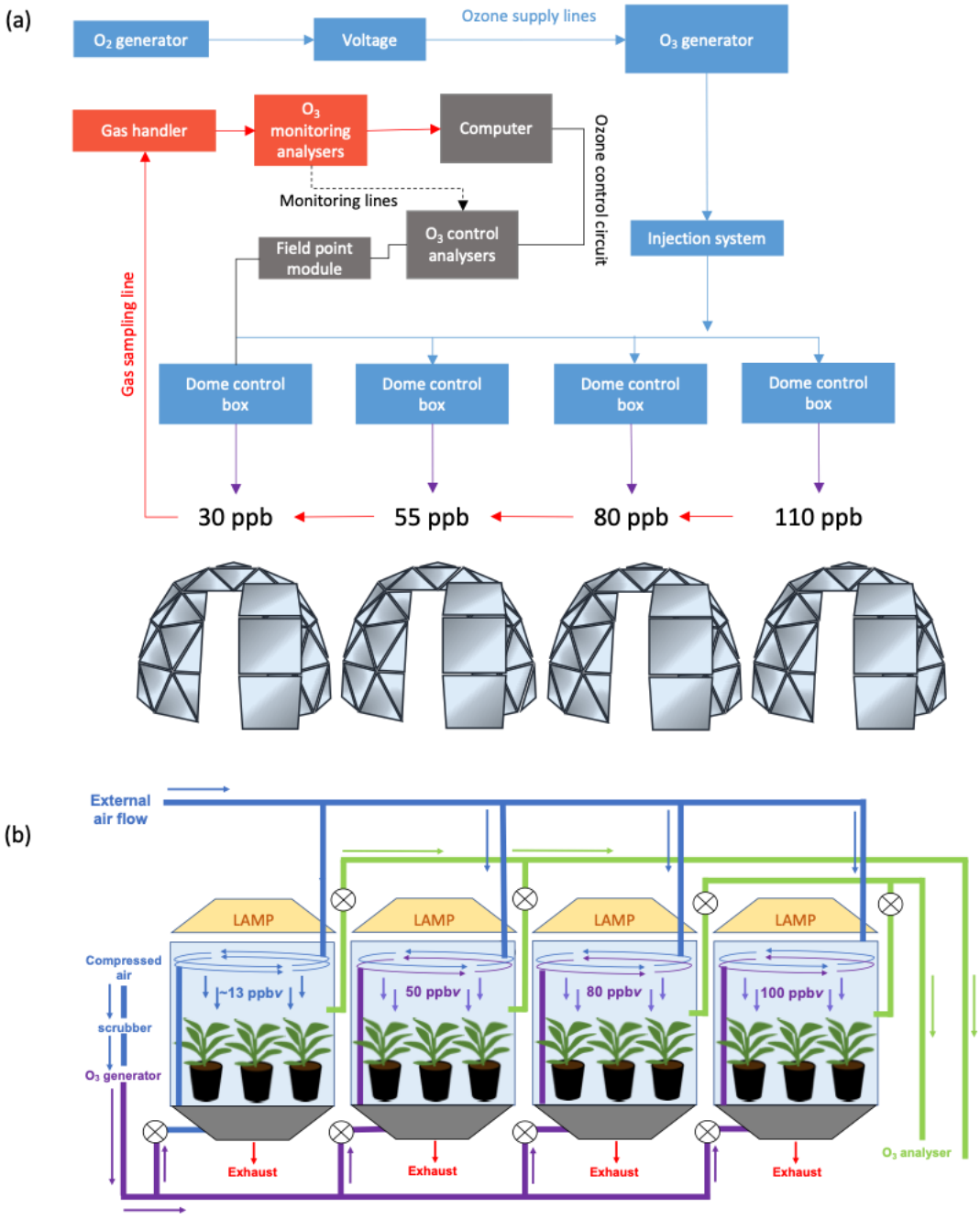

Figure 1.5. Schematic of a) Solardome experimental set-up used in UKCEH Bangor in Chapter 3, and b) laboratory experimental 1-m3 chambers at Lancaster Environment Centre used in Chapters 4 and 5.

1.8 Breeding ozone-tolerant crops

To enable agronomists to mitigate the impacts of high ozone exposure on crop yield, ozone tolerance in crops needs to be clearly identified and quantified in a standardised and reproducible way. However, there are currently multiple definitions of ozone (stress) tolerance. Moreover, *Brassica* oilseed development programmes seldom, include ozone as a stressor or risk factor in breeding trials (Wang et al., 2014; Frei,

2015), meaning the identification and exploitation of ozone tolerance traits rarely occur (Fagerstrom et al., 1987; Paul-Victor et al., 2010).

1.8.1 Defining tolerance

Ozone tolerance in crops is currently determined in several ways including measuring seedling lethality, shoot biomass changes, yield loss, and photosynthetic responses (Barnes et al., 2002; Ryan et al., 2009). Multiple studies have also focused on visible injury, with plants exhibiting smaller areas of necrotic lesions deemed more ozone tolerant (e.g., Calvo et al., 2007; Smith, 2008; Treshow, 1970). Some studies also consider germination rate under stress conditions to indicate tolerance (Zhang et al., 2015; Wu et al., 2019). While screening germinating seeds for ozone sensitivity provides a reliable and high-throughput method, it may not be representative of real-world conditions, as plants at different growth stages are known to be differently impacted by high ozone levels (Pleijel et al., 1998), as shown in Table 1.1. Furthermore, the most agronomically relevant definitions of tolerance are those associated with biomass accumulation, yield, and/or maintained mass of harvestable portion. For example, Feng et al. (2022) considered plants that maintained biomass or yield under increased exposures relative to control to be stress tolerant, and this is also the philosophy underpinning critical level set for the PODy and AOT40 metrics.

Changes in biomass accumulation and allocation are particularly important, given reported changes in the allocation of photosynthate to biomass vs. defence against ozone. For example, the optimal defence theory states that plants prioritise defensive mechanisms and divert photosynthate to antioxidants in the most 'valuable' tissues when under stress to maintain or increase plant fitness (Fagerstrom et al., 1987; McCall and Fordyce, 2010; McKey, 1974; Van Dam et al., 1996). However, antioxidant synthesis, regulation, and storage are metabolically costly, usually at the expense of growth and reproduction, and therefore may conflict with the primary aims of *Brassica* oilseed breeding programmes: to maximise relative growth rates (Wolinska and Berens, 2019). Furthermore, it is not known whether the most 'valuable' tissues are expanding leaves or reproductive tissues, as this may be species- or cultivar-dependent. For example, it may be more advantageous for slow-growing plants (perennial or biennial plants) to reallocate photosynthate to antioxidants, compared to fast-growing plants which may allocate photosynthate to reproductive sites, thus increasing plant fitness (Van Dam et al., 1996). Moreover, contrary to the optimal defence theory, antioxidant synthesis may not be detrimental to biomass allocation in response to abiotic and biotic stress in Brassicaceae species e.g., *Arabidopsis thaliana* L. (Paul-Victor et al., 2010; Züst et al., 2011) and *Boechera stricta* Graham, as antioxidants may stimulate vegetative or reproductive growth (Siemens et al., 2010).

Thus far, there is no biochemical nor physiological definition of ozone tolerance, largely due to the myriad metabolites that may be synthesised, and specialised plant tissues that may be damaged, thus causing challenges in comparing responses of cultivars or species (Chen et al., 2009; Ryan et al., 2009). Moreover, biochemical changes are commonly reported in isolation from other measurements, meaning it is

challenging to correlate biochemical responses with maintained biomass or gas exchange (Calatayud et al., 2011; Chernikova et al., 2000). However, the magnitude of ROS formation and biochemical responses are dependent on cumulative stomatal uptake, meaning that both may be required to confer tolerance (Ryan et al., 2009). For example, Massman et al (2004) proposed an 'effective ozone dose' which accounted for both stomatal uptake and ozone quenching via antioxidants similar to 'y' in the POD_y metric. To date, however, there have been no investigations of how common biomarkers, such as antioxidant activity (AsA, APX, SOD), oxidative stress (H_2O_2) and damage (MDA), relate to changes in yield/biomass and quality parameters. Identifying and quantifying such relationships would allow simple meaningful comparisons of tolerance between species and cultivars.

1.8.2 Current OSR breeding strategies and exploiting stress tolerance

Breeding programmes target different desirable traits which optimise seed yield and quality. European recommended lists (lists of high yielding cultivars by country) today consist of mostly conventional OSR cultivars, which are bred by crossing individuals, with progeny selected based on visual assessment of desirable traits (uniformity, high yield, pest resistance, and disease tolerance) (AHDB, 2020). However, a conventional breeding programme may take up to ten years to release a new cultivar due to more rigorous screening being required for genetic uniformity (Mitrousia, pers. comm.), which is at odds with improving or maintaining OSR yield and quality under future climate scenarios. "Restored" OSR hybrids, which exploit cytoplasmic male sterility to combine desirable traits from a single line, offer an opportunity to contract breeding programme timelines: hybrids may be developed in six years (Kessel et al., 2012). Restored hybrids were introduced to recommended lists in the 1990s and are increasingly popular amongst European and Canadian growers, primarily due to increased yields per hectare, as seen in mainland Europe (AHDB, 2020).

There are many methods for improving stress tolerance in *Brassica* oilseeds, including both conventional and hybrid breeding strategies. For example, herbicide resistant OSR cultivars were developed by identifying desirable traits using restored hybrid breeding methods (Senior and Dale, 2002). However, further identification of tolerance traits is required to enable improvement in advanced cultivars. Indeed, stress tolerance (and genes that confer tolerance) are progressively being identified by combining high-throughput biochemical assays and genotyping on the same leaf tissue sample (Conesa and Beck, 2019). Moreover, genetic modification offers an additional opportunity to improve drought tolerance by inserting such genes (e.g., antioxidant genes) into OSR genome and has been used in the USA (Lawlor, 2013; Wan et al., 2009). However, commercial GM technologies are not currently applicable to UK and European Union agriculture (Zilberman et al., 2013; DEFRA, 2022). Another avenue to exploit stress tolerance is introgression, supported with molecular techniques such as the identification of quantitative trait loci associated with desirable traits, wherein different *Brassica* oilseed crop species are hybridised to introduce desirable traits from

one line into another. A classic example of this is increasing seed oil content in *B. rapa* and *B. juncea* (Panjabi et al., 2019; Snowdon and Friedt, 2004).

1.9 Motivation and rationale

This thesis focuses on the effects of elevated tropospheric ozone on *Brassica* oilseed crops, and principally *B. napus*. *B. napus*, used for food, fodder, and fuel production, was the second-most important oilseed crop worldwide in 2020 after soya. Background levels of ozone have increased by up to a third in key OSR cultivation areas such as South-East Asia and Canada since 1996 (Xu et al., 2019), and are projected to increase by a further 20% by 2100 in areas of agricultural importance in the Northern Hemisphere according to RCP8.5 scenario (Archibald et al., 2020). Production areas of OSR already overlap with areas receiving potentially damaging levels of ozone (Figure 1.6, and this could cause increased damage over the full growing season (chronic exposure) and/or the short-term e.g., episodes over hours or days (acute exposure) (Grantz et al., 2003; Lin et al., 2020).

Previous studies of the impact of ozone on crop productivity have suggested significant declines in yield and crop quality under the levels of ozone projected in most world regions leading to concerns over future harvests of key crops such as *Brassica* oilseeds in the future (Fowler et al., 2009; Mills et al., 2018b). However, challenges in understanding the impact of ozone on crops have resulted in large uncertainties in projections of future harvests. Given the global socio-economic importance of *Brassica* oilseeds, the reliance on oilseed for calorie demand, and the projected increases in global population (to 9-10 billion by 2030), any loss of productivity would have severe implications for food security. It is therefore of paramount important to understand the physiological, morphological, and biochemical responses of *Brassica* oilseeds to oxidative stress caused by exposure to tropospheric ozone concentrations above current ambient levels. However, it is also essential to develop a mechanistic understanding of the role of each of antioxidants, metabolites, and gas exchange if we are to be able to project future stress-related crop losses, and potentially use mitigation strategies such as identifying and exploiting ozone tolerant OSR traits in breeding programmes and agronomic practices.

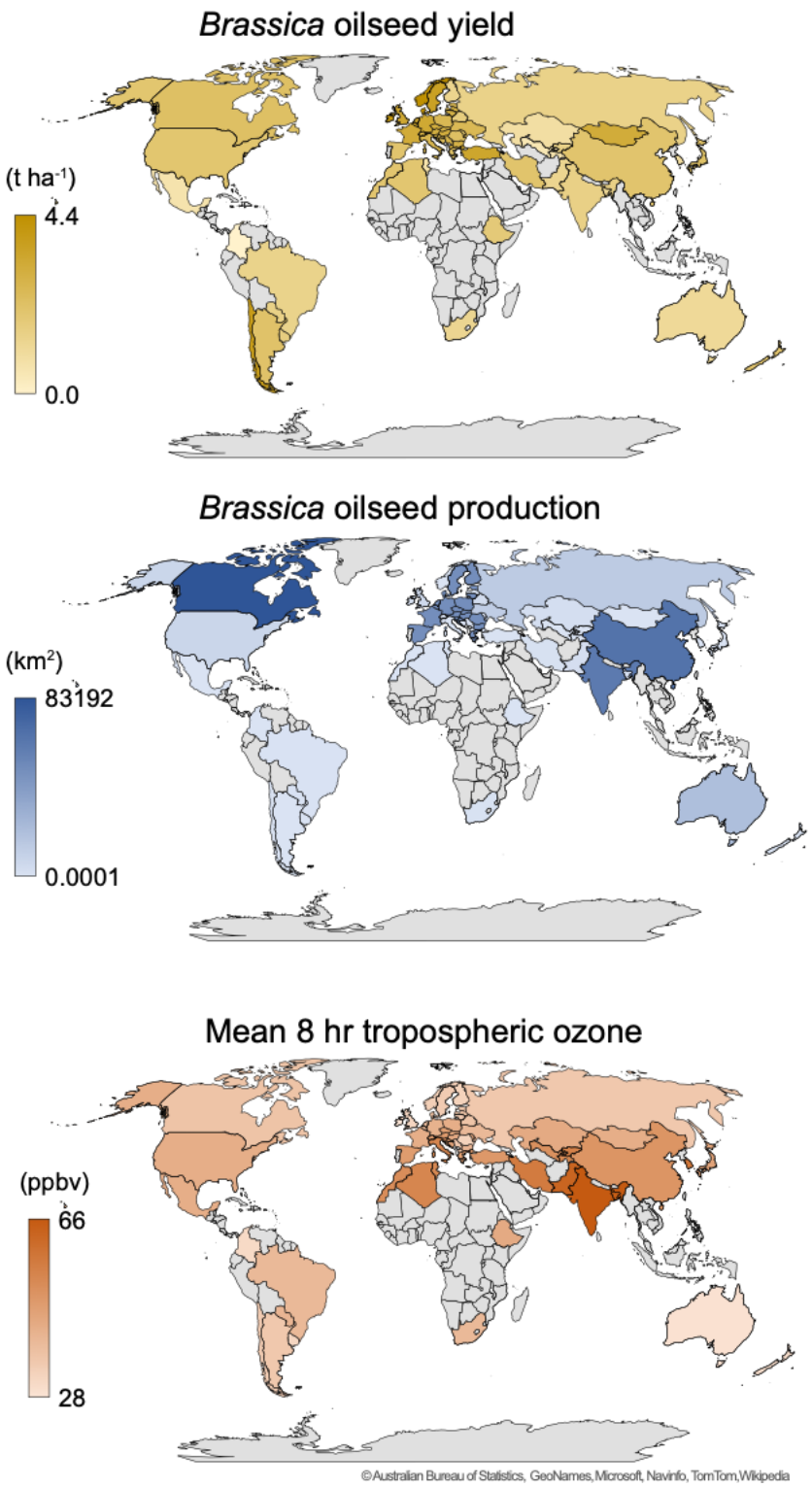

Figure 1.6. World maps of Brassica oilseeds showing a) average yield, b) areas under production, and c) population-weighted mean annual 8-hr ozone levels across major cultivation regions. Map reproduced using oilseed data from FAOSTAT (2022) and ozone data from European Environment Agency (2022).

2. Thesis aims, objectives, and structure

2.1 Thesis aims and objectives

This research aims to understand the effects of realistic tropospheric concentrations of ozone on the physiology, morphology, and biochemistry of *Brassica* oilseeds.
This thesis has three specific objectives:

1. To gain an empirical understanding of the effects of chronic and episodic ozone concentration/flux in *Brassica* oilseed morphology, physiology, antioxidants, and final yield (Chapters 3, 4, 5).
2. To determine whether ascorbic acid (AsA), a ubiquitous non-enzymatic antioxidant plays a key role in delaying ozone-induced foliar senescence and could therefore provide an indicator of ozone tolerance (Chapter 4).
3. To explore how key compounds indicative of oxidative stress, oxidative damage and enzymatic antioxidant activity may be used as biochemical markers of ozone response and whether such markers may be used to quantify ozone tolerance (Chapter 5).

2.2 Thesis structure

Chapter 1: Introduction

This chapter explores current understanding of the morphological, physiological, and biochemical effects of tropospheric ozone on *Brassica* oilseed crops. I explain the importance of different *Brassica* oilseed species to food security, and the challenges associated with ensuring seed quality and yield despite increasing environmental stressors. Following this, I describe the risks posed by one often-overlooked stress: tropospheric ozone, a phytotoxic air pollutant, levels of which are projected to continue to rise under future global change. I detail how ozone may impede physiology, stomatal functioning and accelerate senescence, thus decreasing final yield and quality of the oilseed. Subsequently, I explain the underlying biochemical effects and processes, such as oxidative stress and damage, and defence mechanisms such as antioxidants. I compare current experimental methodologies for quantifying and comparing the ozone sensitivity of different species. I conclude by describing the findings of previous studies specifically investigating the response of OSR and *Brassica* oilseeds to ozone exposure and explain the motivation and rationale of this thesis.

Chapter 2: Thesis aims, objectives, and structure (current chapter).

Chapter 3: Chronic tropospheric ozone exposure reduces seed yield and quality in spring and winter oilseed rape. Roberts, H.R., Dodd, I.C., Hayes, F., Ashworth, K., 2022, published in *Agricultural and Forest Meteorology*, vol. 316, 108859. doi: 10.1016/j.agrformet.2022.108859

This chapter addresses the first objective: to gain an empirical understanding of the effects of chronic and episodic ozone on *Brassica* oilseed yield, morphology, and physiology. Having identified a key knowledge gap: understanding the changes in physiology, biochemistry, yield, and quality in both spring and winter OSR across a range of real-world chronic ozone levels, I compared the responses of two *B. napus* cultivars with differing lifespans to ozone levels representative of realistic European growing season conditions. I hypothesised that faster-growing oilseed rape cultivars would be more sensitive to ozone due to higher leaf gas exchange rates over their (shorter) life cycle, resulting in higher ozone uptake and therefore greater cumulative exposure to this abiotic stress. I postulated that, given the tight seed quality regulations in oilseed markets and previously reported stress-induced declines in seed yield and quality in other *Brassica* oilseed species, short-lived spring OSR may become less economically viable than a slower-growing winter OSR. Hence, I exposed two currently recommended OSR cultivars - one spring variety, 'Click', and one winter variety, 'Phoenix' - to four levels of ozone, representative of real-world conditions (20, 55, 80, and 110 ppbv), over an entire growing season in a semi-controlled Solardome environment. This experiment reproduced the chronic ozone exposure typically experienced by OSR crops in different growing regions of Europe.

Analysis of physiological and morphological data collected during vegetative and reproductive growth stages showed a marked decline in photosynthesis, particularly in the spring cultivar, while accelerated senescence was observed in both varieties. Although Phoenix maintained physiology and vegetative growth despite the higher cumulative ozone exposure that resulted from its longer growth cycle, Thousand Seed Weight (TSW), an important measure of final yield, decreased by 40% in Phoenix compared with 20% in Click. However, seed quality, measured here as total oil content, declined by 9% in Click, but remained unchanged in Phoenix. As higher quality enhances financial premiums for growers, reduction in seed quality confers an economic penalty in the same way as loss of yield. Given the very low profit margins of OSR as a crop, these losses (of seed quantity in Phoenix and quality in Click) suggest that the economic viability of both OSR cultivars, vital for food and fodder production, in Europe in the future may be under threat by ozone pollution.

Chapter 4: Cultivar and leaf-specific biochemical responses to short-term ozone exposure in winter and spring oilseed rape. Roberts, H.R., Dodd, I.C., Hayes, F., Ashworth, K., in preparation for submission to *Journal of Experimental Botany*, April 2023.

This chapter addresses the second objective: to determine whether a key non-enzymatic antioxidant (ascorbic acid, AsA) may delay ozone-induced foliar senescence and could provide a marker and measure of ozone tolerance. Based on my previous findings that the gas exchange and chlorophyll content of Phoenix was maintained under high ozone levels despite substantial yield reductions, I postulated that winter OSR diverts more of the carbon assimilated during photosynthesis to protective products and mechanisms and maintains seed filling at the cost of vegetative growth (or longevity), in line with the 'optimal defence theory'. These experiments focused on ascorbic acid (AsA), as it

is known to be a primary regulator of plant responses to oxidative stress and the most ubiquitous non-enzymatic antioxidant. High concentrations of endogenous foliar AsA are a key regulator of senescence and have also previously been shown to be correlated with increased ozone tolerance in crops. I measured leaf gas exchange alongside AsA and markers of oxidative stress (H_2O_2) and damage (MDA) across an acropetal gradient of leaf ages in OSR cv. Click and cv. Phoenix under ozone. Plants were exposed to ambient (~20 ppbv) and high (100 ppbv) levels of ozone in two 1-m^3 semi-controlled environment chambers in a laboratory. This allowed me to determine whether cultivar differences in the previous experiment were correlated with differences in endogenous AsA content. The suite of measurements also enabled me to disentangle the effects of differences in cumulative ozone uptake and leaf age on ozone-induced oxidative stress and injury, and to determine the potential antioxidative role of AsA in the response of OSR to ozone. I found that total AsA content was significantly higher in Phoenix than Click, which according to the optimal defence theory would suggest that Phoenix was more ozone tolerant. However, while Phoenix better maintained stomatal conductance, chlorophyll content, and the performance of Photosystem II, leaf area and total plant mass declined after only 12 days of high ozone exposure. By contrast, the stomatal conductance, chlorophyll content at lowest leaves, and performance of Photosystem II in Click declined more than Phoenix, but leaf area and total plant mass were better maintained. Stomatal uptake dictated tolerance in Click, even over such a short period of exposure. Thus, while Click closed its stomata under high ozone conditions and therefore avoided high ozone uptake, Phoenix instead diverted photosynthate into defence against oxidative stress. Click was therefore able to maintain leaf area and biomass under stress conditions, suggesting its final yield would be relatively maintained.

Chapter 5: Canola-grade Brassica oilseed species are more ozone tolerant than non-canola counterparts Roberts, H.R., Hayes, F., Dodd, I.C., & Ashworth, K., Under Review at *Plant, Cell & Environment*, April 2023.

This chapter addresses the third objective: to determine the key biochemical factors that confer ozone tolerance in spring-sown *Brassica* oilseeds of different breeding pedigrees. Based on my previous findings that AsA did not convey tolerance in OSR despite higher levels being measured in Phoenix, I postulated that a related enzymatic antioxidant, ascorbate peroxidase (APX), and a second enzymatic antioxidant, superoxide dismutase (SOD) which functions up-stream of APX, may be more suitable markers of tolerance. Moreover, as advanced *Brassica* oilseed cultivars are selected for high productivity/yield and thus high gas exchange, I also hypothesised that more selectively bred cultivars would therefore uptake more ozone and sustain greater oxidative damage, i.e. would be more sensitive to ozone than traditional landraces. I selected two canola-grade cultivars from Canada and Europe, and two non-canola-grade landraces from Pakistan (*B. juncea* cv. 15127 and *B. rapa* cv. 07224). Each was exposed to four ozone levels spanning typical conditions during the main growing season in the Northern Hemisphere (20 ppbv, 50 ppbv, 75 ppbv, and 100 ppbv) for 24 days during the vegetative growth stages that have previously been demonstrated to be particularly

vulnerable to oxidative stress. The non-canola-grade landrace *B. rapa* cv. 07224 had the highest gas exchange and lowest antioxidant activities of the four lines and suffered the greatest damage in terms of biomass accumulation. By contrast, its canola-grade counterpart, *Brassica rapa* cv. Candle, had the lowest ozone uptake and the highest enzymatic antioxidant activities and appeared to be stimulated by ozone concentration resulting in an increase in biomass with increasing exposure.

Using the differences in key biochemical compounds I observed between the lines as a basis, I developed a relative stress index to quantify ozone tolerance, which has previously only been subjectively described and compared (Chaudhary, and Rathore, 2021; Melhorn et al., 1991; Paoletti et al., 2022; Reich, 1987). This index incorporates both the average antioxidant activity and oxidative damage, and I demonstrated that it strongly correlated with both cumulative ozone exposure and shoot plant biomass and was therefore an excellent descriptor and predictor of ozone tolerance in these oilseed species. *B. rapa* cv. Candle, qualitatively the most tolerant cultivar, returned a negative relative stress index while *B. rapa* cv. 07224, the most sensitive, a high positive index. The other two cultivars exhibited some qualitative signs of oxidative stress and damage and had slightly positive relative stress indices. I therefore concluded this study by suggesting that calculating relative stress indices based on biochemical markers and applying them during the breeding process may aid in speeding up breeding programmes when selecting for stress-tolerant crops.

The three primary research studies combine morphological, physiological, and biochemical measurements to gain a better understanding of *Brassica* oilseed response to ozone. The studies also identify opportunities for determining and exploiting ozone tolerance in OSR cultivars.

Chapter 6: General discussion and conclusions

In this chapter, I reflect on the findings from chapters 3, 4, and 5, and pose scientific questions that these have provoked. I also briefly summarise remaining gaps in knowledge and present avenues of further research to address these.

3. Chronic tropospheric ozone exposure reduces seed quantity and quality in spring and winter oilseed rape.

Author contributions

Hattie R. Roberts: Initiated experimental design, carried out plant propagation and care, carried out practical experimental work, prepared seed samples for analyses, compiled and analysed data, visualised data, participated in interpretation of results, prepared manuscript, and submitted manuscript.

Ian C. Dodd: Advised experimental planning and design, participated in interpretation of results, manuscript preparation.

Felicity Hayes: Participated in plant care, advised experimental planning and design, ensured that experimental facilities were maintained, participated in interpretation of results, participated in manuscript preparation.

Kirsti Ashworth: Principal Investigator. Experimental planning and design, participated in interpretation of results, participated in manuscript preparation.

Submission to journal

Chronic tropospheric ozone exposure reduces seed yield and quality in spring and winter oilseed rape. Roberts, H.R., Dodd, I.C., Hayes, F., Ashworth, K., 2022, published in *Agricultural and Forest Meteorology*, vol. 316, 108859. Doi: 10.1016/j.agrformet.2022.108859

A summary of this chapter can be found in section 2.2

Graphical Abstract

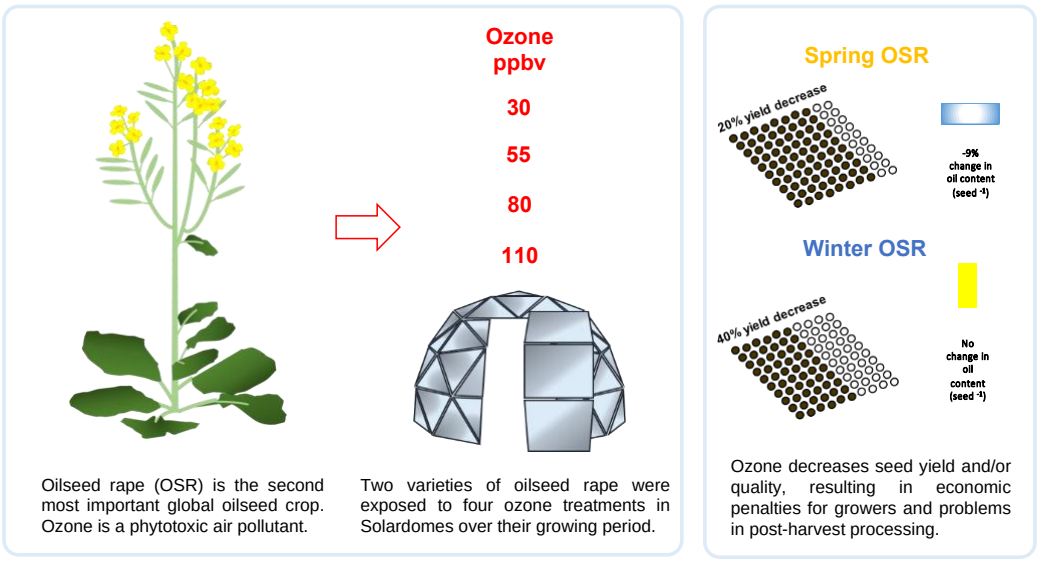

3.1 Abstract

Oilseed rape (*Brassica napus* L.) is cultivated worldwide, producing 11.5% of global oilseeds at an economic value of 38 billion USD in 2020. It is sensitive to phytotoxic damage from exposure to tropospheric ozone (O_3), a major air pollutant, which disrupts plant physiological processes and thus decreases biomass accumulation. As background ozone concentrations continue to increase globally, we investigated the impact of ozone exposure on seed and oil yield of a shorter-lived spring (cv. Click) and a longer-lived winter (cv. Phoenix) oilseed rape cultivar to ozone levels (treatments with peaks of 30, 55, 80, 110 ppbv) representative of typical European conditions where these cultivars are common. Thousand Seed Weight (TSW), an important measure of final yield, decreased more in Phoenix (40%) than Click (20%) with increasing ozone exposure. Click produced more racemes and many small seeds while Phoenix produced fewer racemes and larger seeds. However, seed quality declined more substantially in Click than Phoenix. The oil content in Click's seed significantly decreased with increased ozone exposure, while less desirable components (moisture, chlorophyll, ash) increased. Scaled to field-level, our findings imply substantial economic penalties for growers, with potential losses of 175 to 325 USD ha^{-1} in Click and 500 to 665 USD ha^{-1} in Phoenix under ozone concentrations typical of spring and summer periods in Europe. Decreased total yield would likely outweigh the benefits of any improvement in animal oilseed cake quality (increased protein and key micronutrients for livestock feed). Neither cultivar sustained visible injury at earlier growth stages, and Phoenix sustained photosynthesis even under high exposure, thereby making ozone an invisible threat. Our findings of reduced oilseed quantity and quality threaten oilseed rape production, but differences between the cultivars may also offer an opportunity for breeders and agronomists to identify and exploit variation in ozone tolerance in oilseed rape.

3.2 Introduction

Canola or oilseed rape (hereafter OSR) is the second-most economically important oilseed crop on the planet after soya, and the most important in Europe, where over 16.8 million tonnes were produced in 2020, representing 60% of total oilseed yields (European Commission, 2020). Global production of rapeseed oil exceeded 27.7 million metric tonnes in 2020, with a market worth ~24 billion USD, while soya's market produced 60.3 million tonnes of oil worth ~55 billion USD (USDA, 2021). Moreover, the oilseed cake or protein meal, left once OSR is crushed to remove edible oil, is produced as a valuable global animal feedstock. In 2020, worldwide OSR-derived animal feed totalled 39.2 million tonnes, at a market value of ~14 billion USD, with Europe generating a third of both global OSR oil and protein meal (USDA, 2021).

Understanding the effects of changes in environmental conditions on key crops such as oilseed rape has become of significant interest for agronomists, crop breeders and policy makers to reduce crop losses and risks to food security. One important but often overlooked environmental stress is tropospheric ozone. Average global ozone concentrations have increased by ~20% since 1900 and are projected to increase by a further 18% by 2100 (Young et al., 2013; Archibald et al., 2020). Increased emissions of ozone precursors, along with rises in global temperature, have resulted in average European background concentrations exceeding 30 ppb annually (Archibald et al., 2020; Boleti et al., 2020). Daytime concentrations between 50-80 ppb in Northern Europe and >100 ppb in Central and Southern Europe have been recorded in rural areas over spring-summer periods (Pay et al., 2019; Boleti et al., 2020), which coincide with key growing dates in the agricultural calendar (Mills et al., 2018a). While episodic high-ozone events (acute exposure) have long been recognised to trigger phytotoxic damage to vegetation (e.g. Heggestad & Middleton, 1959), there is increasing awareness of the impacts of cumulative, chronic exposure to lower levels of ozone (Chen et al., 2009; Mishra & Agrawal, 2015). Under current atmospheric conditions in Europe, OSR crops are exposed to levels of ozone over days, weeks, or entire growing seasons likely to be sufficiently high to reduce yields (Lei et al., 2012; Lin et al., 2020; Mills et al., 2007; Mills et al., 2018c).

Tropospheric ozone has well-documented detrimental effects on crop physiology, due to its highly oxidising properties. Ozone enters leaves (mostly) via the stomata, resulting in cellular damage and disruption of photosynthetic pathways in ozone-sensitive species, decreasing net photosynthetic rate (P_{net}) (Bohler et al., 2007). Oxidation of cellular and organelle membranes also occurs, resulting in foliar chlorosis, and accelerated senescence (Tammam et al., 2019; Sharps et al., 2021). Direct damage of stomata and guard cells can also occur, leading to loss of stomatal regulation during periods of water stress at chronic exposures of more than 40 ppbv above ambient (Mills et al., 2009), potentially exacerbating the impact. Consequently, overall productivity, and crop yields decrease in ozone-sensitive species.

Previous studies using open top chambers, free air systems, and field trials have shown OSR to be a moderately ozone-sensitive species (Mills et al., 2007), with ozone concentrations higher than 60 ppb decreasing seed yield by 15-38% and oil content by

5% (Ollerenshaw et al., 1999; Clausen et al., 2011; Namazkar et al., 2016). Experiments at both plot- and field-scale observed decreased thousand seed weight (TSW), and decreased oil content (Black et al., 2000; De Bock et al., 2011; Frenck et al., 2011; Vandermeiren et al., 2012), suggesting that ozone exposure affects crop quality as well as yield. Seed content of valuable compounds, primarily oil (for food and industrial processing) and protein (for fodder in the form of oilseed cake) may decrease by >18% in response to ozone stress as observed in OSR relatives (Singh et al., 2013). Fatty acid proportions may also be affected, with increases observed in erucic acid content (Tripathi et al., 2012), which is tightly regulated to less than 2% to avoid cardio myotoxicity in both livestock and humans (EFSA Panel on Contaminants in the Food, 2016). Furthermore, exposure to ozone may exacerbate unfavourable properties in the extracted oil, including increased moisture (>10%), chlorophyll (>20%), and Glucosinolates (>3mg/g), affecting shelf life, appearance, or palatability of edible oil (Wittkop et al., 2009). Micronutrient contents in seed cake maintain optimum livestock health, and key elements such as zinc, manganese, and iron have been observed to decrease under other abiotic stresses such as drought (Etienne et al., 2018), but have not been reported in response to ozone stress.

In Europe, OSR comprises two seasonal groupings: spring (over an area of 14,000 ha in the UK in 2020, which has tripled compared to previous four years) and winter-sown varieties (331,000 ha in the UK in 2020) (Butruille et al., 1999; DEFRA, 2020). Winter varieties are sown in mid-August to early September, harvested in July to August, and are the primary type grown in Europe. Spring varieties are sown in late March to early April, harvested in late August to September, and grown throughout Europe and Canada (AHDB, 2020). Spring varieties are faster-growing and have shorter lifespans compared to their winter counterparts. Previous studies on other species suggest those with shorter life cycles are more susceptible to ozone damage (Franzaring et al., 2000). It is postulated that short-lived plants that are bred for rapid growth have higher rates of leaf gas exchange over their life cycle, and therefore may be exposed to greater abiotic stress such as higher ozone uptake (Felzer et al., 2007), resulting in greater sensitivity to ozone (as in Osborne et al., 2016). Fast-growing spring OSR could therefore become economically unviable if exposure to high ozone levels substantially reduces yield or quality. In this study, we compare two modern cultivars of spring and winter OSR, to examine whether their physiological, morphological, and agronomic responses to ozone exposure differ over their full life cycles, and test three specific hypotheses:

i. Seed yield and quality will decrease in both cultivars as ozone exposure increases.
ii. Seed yield and quality declines will be a reflection of decreased physiology and biomass accumulation.
iii. Decreases will be more pronounced in the spring cultivar and will occur at lower exposures.

Here we used semi-controlled environments in geodesic glasshouses and a bespoke ozone injection system to expose OSR to four different concentrations of ozone

over a full growing season. This is the first study to directly compare the responses of spring and winter varieties of OSR to chronic ozone exposure over a growing season at realistic levels of ozone experienced in Europe, providing valuable information to growers on OSR yield and quality.

3.3 Methodology

3.3.1 Plant material and care

Spring (cv. Click) and winter (cv. Phoenix) *Brassica napus* cultivars (supplied by DSV United Kingdom Ltd., Top Dawkins Barn, Wardington, Banbury, UK) were vernalised for 4°C; for 14 days at 65% RH prior to being transplanted in bedding packs in John Innes no. 2 soil on 5th May 2019 in a glasshouse at the UK CEH Bangor experimental Henfaes Farm, Abergwyngregyn. Seedlings were transferred after three weeks into individual 6.5 L (28 cm H, 21 cm D) pots in John Innes no. 2 compost. Two weeks later, when plants had six fully unfolded leaves (growth stage 16), the middle 40 plants by size per cultivar were selected and divided between the 4 treatments using stratified randomisation. Plants were watered daily during late afternoon, and fertiliser (Phostrogen All Purpose Plant Food) and pesticide (Provanto systemic fruit and vegetable bug killer) applied as a soil drench 21, 35, 49 days after sowing to both varieties according to manufacturer's instructions, with an additional treatment at 70 days to Phoenix.

3.3.2 Experimental site and Solardome system

Ten plants per cultivar were placed in four ozone fumigation treatments conducted within separate geodesic glasshouses (dimensions 3m D × 2.1m H; Solardome Industries Ltd, Unit 4, Yeomans Ind Park, Nursling, UK) at Abergwyngregyn (53.23°N, -4.02°W). The computer-controlled injection system (Lab VIEW, version 8.6, National Instruments, Austin, Texas, USA) mixed a regulated flow of ozone from an ozone generator (Dryden Aqua G11, Edinburgh, UK) attached to an oxygen concentrator (Sequal 10, Pure O_2, Manchester, UK) with carbon-filtered air. An external fan circulated ozone-enriched air into the domes at a total flow rate of two changes per minute (m^3 min^{-1}) and ozone concentrations in each dome were recorded every 30 minutes using two ozone analysers with matched calibration (EnviroTech API 400A, St Albans, UK). Other environmental conditions in the domes were otherwise uncontrolled; temperature, PAR, and relative humidity were automatically measured and logged every five minutes.

3.3.3 Ozone treatments

Ozone was injected into each dome between ~9 am and 7 pm 5 days per week, to achieve a stepped diurnal profile of 20-30 ppbv elevated to the specified concentration during day (see Figure 8.1). Daytime levels of ozone in each of the Solardomes were chosen

to represent realistic European ozone levels, as shown in Table 3.1. Exposure commenced on 7th June 2019 (growth stage 16) and continued until harvest: 90 days for Click, and 125 days for Phoenix.

Cumulative ozone exposure (CEO_3) for each treatment was calculated following Lombardozzi et al. (2013), such that:

$$CEO_3 \text{ (mmol mol}^{-1}\ h) = [O_3] \times H \times D \times 10^{-3}$$

where $[O_3]$ is ozone concentration in mol, H is number of hours, and D number of days.

Table 3.1. Ozone treatments used to represent spring/ summer ozone concentrations by region

30 ppbv	55 ppbv	80 ppbv	110 ppbv
Background; N. Europe[1]	Background; S. Europe[1]	Elevated; N. Europe[2]	Elevated; S. Europe[2]

Background (daytime average) and elevated (daytime average) chronic tropospheric ozone concentrations used in the present study. As in [1] Boleti et al., 2020; [2] Pay et al., 2019. N. Europe = Northern Europe; S. Europe = Southern Europe.

3.3.4 Physiological and environmental sampling

Physiological and environmental measurements were carried out three times over the growing season for Click and four times for Phoenix using four randomly selected plants (with the same plants used for seed quality analyses). Each time, net photosynthesis rate (P_{net}), stomatal conductance (g_s), and chlorophyll content of the youngest fully expanded leaves were measured between 10am – 4pm daily (with sampling randomised over treatments), from three replicates per treatment. A handheld Soil Plant Analysis Development (SPAD) meter (CCM 200; Opti-sciences, Hudson, New Hampshire, USA) provided a relative measure of chlorophyll content. In addition to P_{net} and g_s, leaf temperature, relative humidity, and Vapour Pressure Deficit (VPD) were logged, and trace gas samples were collected over a 20-minute period using a LI-COR 6400XT (LI-COR Biosciences, Lincoln, Nebraska, USA) using a 2 cm × 3 cm LED chamber head. Experimental conditions within the chamber head were set to 400 ppm CO_2, 1000 μmol m^{-2} s^{-1} PAR, and 20°C leaf temperature at a 500 mmol sec^{-1} flow rate. A hand-held ThetaProbe (Delta-T Devices Ltd., Cambridge, UK) was used to measure soil moisture of the surface soil to 6.5 cm depth, to determine that plants were well-watered prior to measurement.

3.3.5 Seed yield measurements

Plants were harvested when siliques had completely ripened and dried, and leaves had senesced and abscised (90 days after the start of exposure in Click and 125 days in Phoenix). This maximised the number of plants that reached seed yield for subsequent analysis. Dried siliques were picked and placed into paper envelopes (one raceme per

envelope), and number of racemes per plant, number of siliques per raceme, number of seed per silique, thousand seed weight, and total seed mass per plant were recorded.

3.3.6 Seed quality

Oil, protein, chlorophyll, ash, moisture, and glucosinolate content, and fatty acid composition of the harvested seed were determined by Near Infrared (NIR) spectroscopic analysis (DA 7250, Perten Instruments AB, SE-126 09 Hägersten, Sweden) at John Innes Centre, East Anglia, UK. Micronutrient and macronutrient contents (nitrogen, phosphorus, potassium, sulphur, magnesium, N:S Ratio, copper, manganese, zinc, boron, and iron) was determined by grain suite analyses by Natural Resource Management Centre (Cawood Scientific Limited, Bracknell, Berkshire, UK).

3.3.7 Statistical analysis

Data were compiled in Microsoft Excel (Microsoft Corporation, 2018. Microsoft Excel), and interrogated in R Studio (Version 1.2.5033, Rstudio Team (2019); Rstudio: Integrated Development for R. Rstudio, Inc., Boston, MA, USA). Morphological, physiological, and seed quality parameters were tested against fixed factors of cultivar and cumulative ozone exposure. After testing for normal distribution and homogeneity of variances, curvilinear and linear models with lowest Akaike information criterion (AIC) values were used to determine effects of ozone exposure on physiology, morphology, and seed yield/ quality within cultivars. Analyses of covariance (ANCOVA) were used to explain the effects of cumulative ozone exposure and cultivar. Two-sample T-tests on quality parameters were conducted for the highest and lowest ozone treatments.

3.3.8 Economic assessment

Ozone-induced economic loss was estimated using the four-year UK average (2017-2020) yield of spring and winter OSR (2.9 and 3.3 t ha^{-1} respectively), and a yield loss derived from our TSW measurements for 80 ppbv and 110 ppbv treatments taking 30 ppbv as the zero-loss baseline. The 4-year (2017-2020) AHDB average OSR price per tonne (466.26 USD) was converted into a value per hectare. In line with industry practice, a premium of 1.5% increment above baseline selling price was assumed for every 1% oil content above 40% (Federation of Oils, Seeds and Fats Associations Ltd (FOSFA) document 26A), as presented in Table 2.

3.4 Results

3.4.1 Pre-harvest data

Net photosynthesis (P_{net}) significantly decreased with increasing ozone exposure in both varieties. However, it decreased to a greater extent (by 53%) in Click, between 30 and 110 ppbv, than in Phoenix (18% - Figure 3.1a). P_{net} dropped more substantially, by

67% in Click and 47% in Phoenix, from the commencement of flowering (Day 21 for Click corresponding to CEO_3 = 0.025 mmol mol^{-1} *h* and Day 56 for Phoenix at CEO_3 = 0.049 mmol mol^{-1} *h*) in the 110 ppbv treatment. Initial stomatal conductance (g_s) in Click was twice that of Phoenix at (0.66 and 0.32 mol m^{-2} s^{-1} respectively) as shown in Figure 3.1b. Similarly, g_s significantly decreased with increasing ozone exposure in Click, but only weakly in Phoenix. In Click, g_s decreased by 77% (from 0.66 to 0.29 mol m^{-2} s^{-1} between 30 and 110 ppbv). Again, g_s decreased more once flowering commenced under 110 ppbv, by 46% in Phoenix and 70% in Click. P_{net} and g_s decreased more significantly at a lower cumulative exposure in Click than Phoenix. Taken together, leaf gas exchange of the spring cultivar Click was more sensitive to ozone exposure than the winter cultivar Phoenix.

Decreased leaf gas exchange (P_{net} and g_s) appeared to follow decreases in leaf chlorophyll content. Both varieties presented similar linear relationships between P_{net} and chlorophyll content, and g_s and chlorophyll content with lower values in Click than Phoenix at 110 ppbv (Figure 3.2a, b). Hence, decreased chlorophyll content (indicative of increased senescence) was associated with both P_{net} and g_s.

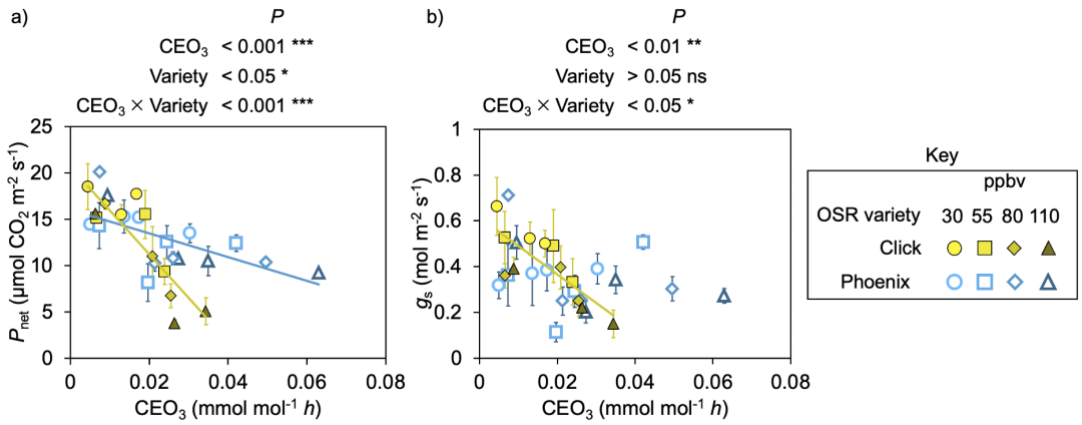

Figure 3.1. Net photosynthetic rate (a) and stomatal conductance (b) plotted against cumulative ozone exposure (CEO_3) for Click (yellow) and Phoenix (blue). P-values represent ANCOVA outputs. Asterisks indicate P <0.05 *, P <0.01 **, P <0.001 ***. Error bars indicate ± SEM, some of which are smaller than the symbols denoting ozone treatment. Regression lines are only shown for statistically significant P < 0.05) relationships; outputs in Table 8.1. Each data point represents an average of measurements logged over 20 minutes taken from youngest, fully expanded leaves across 3 replicates.

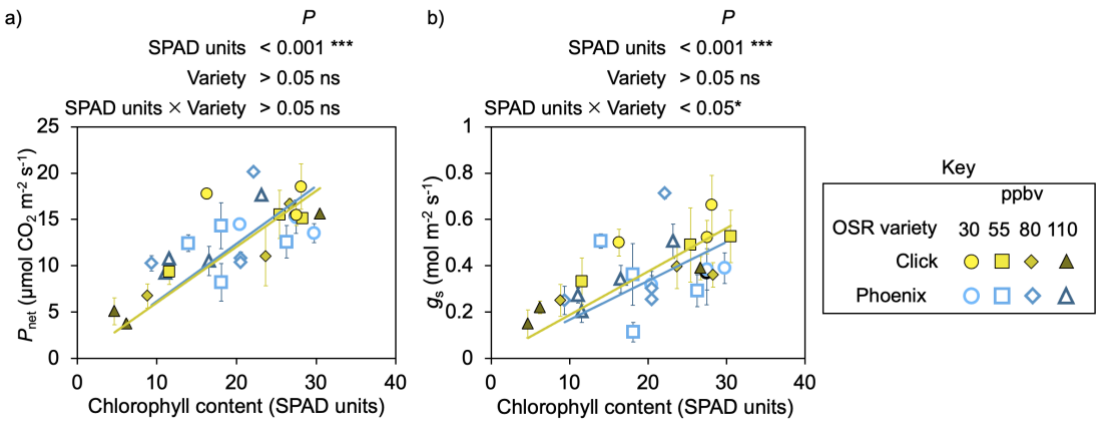

Figure 3.2. Net photosynthetic rate (a) and stomatal conductance (b) plotted against leaf chlorophyll content (SPAD units) for Click (yellow) and Phoenix (blue). P-values represent ANCOVA outputs. Asterisks indicate P <0.05 *, P <0.01 **, P <0.001 ***. Error bars indicate ± SEM, some of which are smaller than the symbols denoting ozone treatment. Regression lines are only shown for statistically significant P <0.05) relationships; outputs in Table. Each data point represents an average of measurements logged over 20 minutes taken from youngest, fully expanded leaves across 3 replicates.

3.4.2 Chlorophyll content

Chlorophyll content responded differently to ozone exposure between seeds and foliage, and between cultivars (Figure 3.3). As outlined above, leaf chlorophyll content in the youngest, fully expanded leaf significantly declined with increasing ozone exposure in both varieties, but to a greater extent in Click (83.4% between 30 and 110 ppbv) than Phoenix (40.8%). By contrast, seed chlorophyll content significantly increased with ozone exposure in Click and was 3 times higher under 110 ppbv than 30 ppbv. Although Phoenix received the highest cumulative exposure, nearly double that of Click's (CEO_3 = 0.032 mmol mol^{-1} *h* vs 0.017 mmol mol^{-1} *h* under the 110 ppbv treatment), seed chlorophyll content did not significantly differ, fluctuating between 6.7-7.9 ppm across all treatments. Taken together, seed, and foliar chlorophyll content of Click was more responsive to ozone exposure than Phoenix.

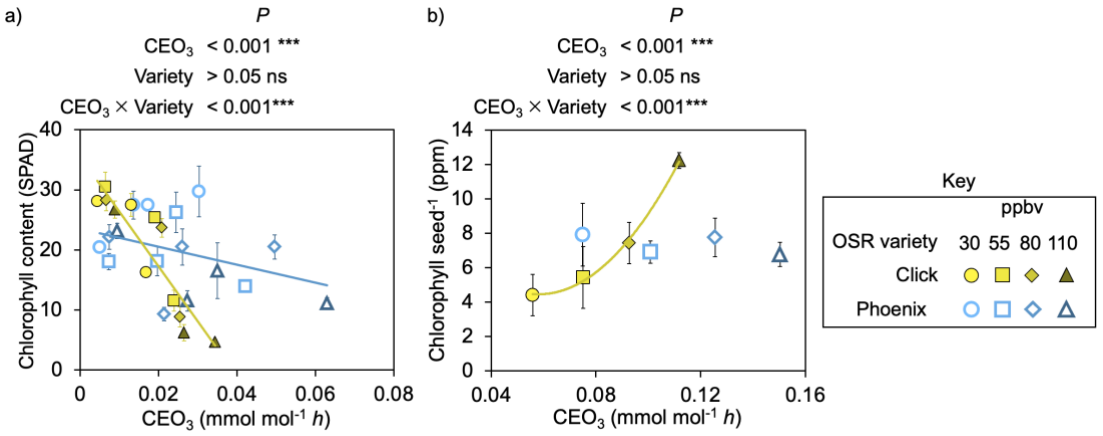

Figure 3.3. (a) Leaf chlorophyll content (SPAD units) plotted against cumulative ozone exposure (CEO_3). Each data point represents an average of measurements logged over 20 minutes taken from youngest, fully expanded leaves across 3 replicates. (b) Seed chlorophyll content (n = 4) (NIR analysis) plotted against CEO_3 for Click (yellow) and Phoenix (blue). P-values represent ANCOVA outputs. Asterisks indicate P <0.05 *, P <0.01 **, P <0.001 ***. Error bars indicate ± SEM, some of which are smaller than the symbols denoting ozone treatment. Regression lines are only shown for statistically significant P <0.05) relationships; outputs in Table 8.1.

3.4.3 Seed yield and quality

Thousand seed weight (TSW) was significantly lower in Click, the faster-growing spring cultivar, than Phoenix for all treatments (Figure 3.4a). At 30 ppbv of ozone, TSW differed by a factor of 2.5 (2.9 g (1000 seeds)$^{-1}$ vs 7.2 g (1000 seeds)$^{-1}$) whereas the smallest difference (~2.0 g (1000 seeds)$^{-1}$) between cultivars occurred under exposure to 55 ppbv of ozone. TSW significantly decreased with increasing ozone concentration in both varieties between 30 and 110 ppbv, by 40% in Phoenix and 20% in Click. TSW decreased at the same rate in both varieties between cumulative exposures of ~0.07 mmol mol^{-1} *h* and ~0.11 mmol mol^{-1} *h*. Although TSW of Phoenix was more sensitive to ozone exposure than Click, TSW remained higher for the winter cultivar under all treatments.

Total seed mass per plant did not significantly differ between cultivars (Figure 3.4b), as the significantly greater number of racemes per plant in Click (Figure 3.4c) compensated for the lower TSW. Total seed mass decreased similarly in both varieties with increasing ozone exposure, although the greater cumulative ozone exposure of Phoenix decreased seed yield by 44% from 30 ppbv to 80 ppbv. Increased raceme number between 55 ppbv and 110 ppbv in Phoenix to some extent ameliorated the impact of greater ozone exposure on total seed mass. Although the individual yield components (raceme number and TSW) showed differing sensitivity to ozone exposure between the two cultivars, total seed mass was similarly sensitive to ozone exposure.

Seed quality was much more affected by exposure to ozone in Click than Phoenix. The average proportion of oil per seed decreased from 48% to 41% as cumulative exposure increased above 0.07 mmol mol^{-1} *h* (corresponding to 55 ppbv treatment) (Figure 3.5a). Total protein content was inversely proportional to oil content, rising from ~18% under 30 ppbv and 55 ppbv to 24% at 110 ppbv (Figure 3.5b). Total ash and moisture content significantly increased by 24% and 15% with increasing ozone exposure (Figure 6). Greater ozone exposure increased concentrations of four nutrients (Figure 6): sulphur increased 46%, with more modest increases in manganese (17%), iron and zinc (both 15%). Fatty acid composition, erucic acid, and glucosinolate proportions, did not significantly change with increased ozone exposure in Click (Table 8.2). Although small changes were measured between treatments in Phoenix, proportions of key seed quality parameters (oil, protein, ash, moisture, saturated fatty acid composition, erucic acid, Glucosinolates, and micronutrients) did not significantly differ with increased ozone exposure. Total oil content fell to a minimum of 43% at 55

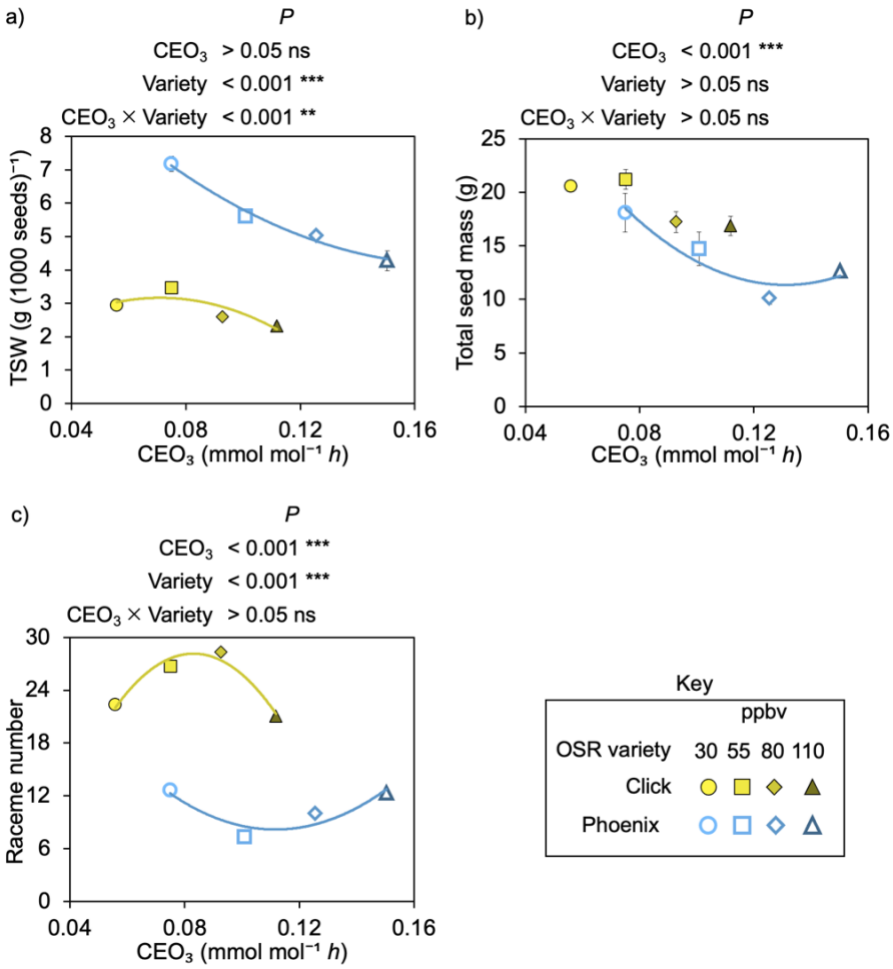

Figure 3.4 Thousand seed weight (TSW) (a), total seed mass (b), and raceme number (c) of Click (yellow) harvested at 90 days, and Phoenix (blue) harvested at 125 days against cumulative ozone exposure (CEO_3). P-values represent ANCOVA outputs. Asterisks indicate Asterisks indicate $P < 0.05$ *, $P < 0.01$ **, $P < 0.001$ ***. Error Error bars indicate ± SEM, some of which are smaller than the symbols denoting ozone treatments. Regression lines are only shown for statistically significant $P < 0.05$) relationships.

ppbv in Phoenix, with little difference between other treatments (Figure 3.5a). In contrast, average total protein content initially rose from 18% with a peak of 22% at 80 ppbv (Figure 3.5b). Overall, Click's quality parameters largely decreased, while Phoenix's remained unchanged with increasing ozone exposure.

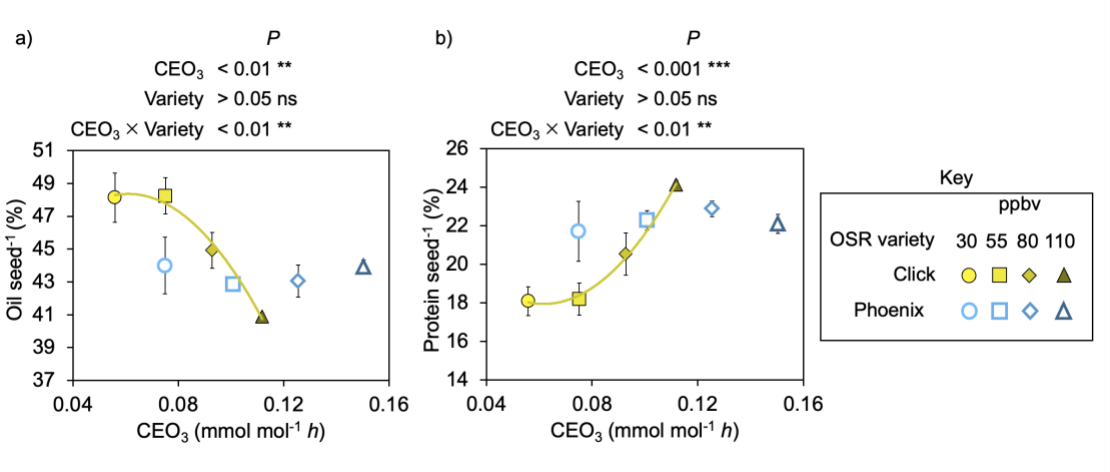

Figure 3.5. Changes in (a) seed oil content, and (b) seed protein content in Click (yellow) harvested at 90 days, and Phoenix (blue) harvested at 125 days against cumulative ozone exposure (CEO_3). Changes derived from NIR spectroscopy (John Innes Centre). P-values represent ANCOVA outputs. Asterisks indicate P <0.05 *, P <0.01 **, P <0.001 ***. Error bars indicate ± SEM, some of which are smaller than the symbols denoting ozone treatment. Regression lines are only shown for statistically significant P <0.05) relationships; outputs in Table 8.1.

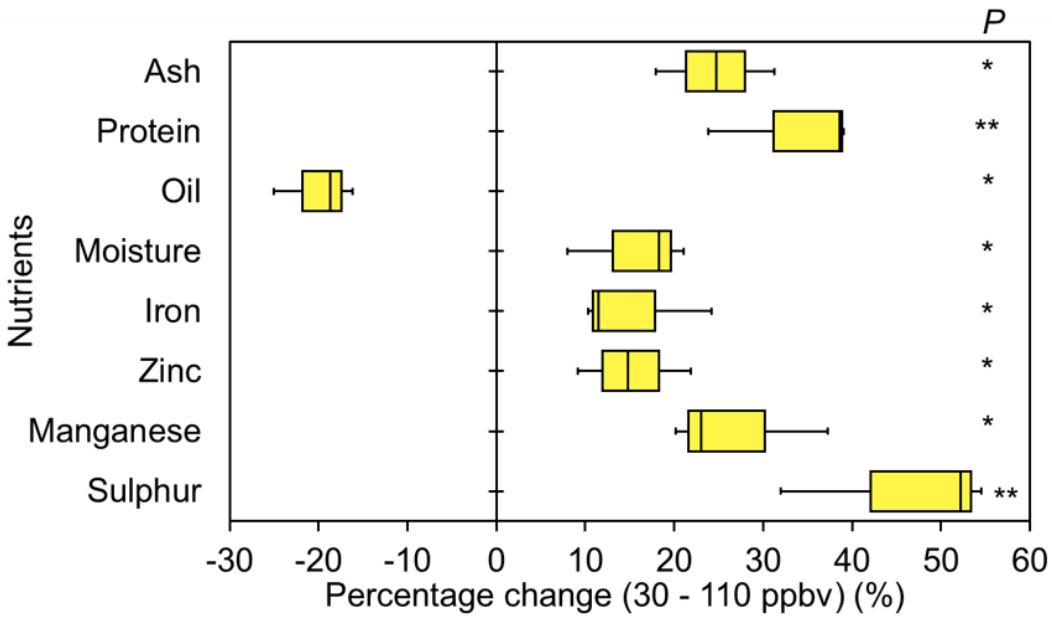

Figure 3.6. Key macro- and micronutrient changes in spring oilseed rape (cv. Click) between 30 and 110 ppb chronic ozone exposure, with the t-test significance output shown on the right. Ash, protein, oil and moisture changes derived from NIR spectroscopy (John Innes Centre), while iron, zinc, manganese, sulphur were derived from a grain suite analysis (NRM). P-values represent ANCOVA outputs. Asterisks indicate P <0.05 *, P <0.01 **, P <0.001 ***. Absolute values for quality parameters discussed in both varieties are reported in Table 8.1 and 8.2.

Table 3.2. Economic assessment outputs based on TSW, 4-year UK yields and delivered prices (2017-2020).

Cultivar	ozone treatment (ppbv)	Average UK yield (2017-2020)	TSW	TSW change (%)	Yield (pots to field scale) (t ha^{-1})	Delivered prices (USD t^{-1} 2017-2020)	Oil content (%)	FOFSA oil premium (%)	Price Increase (%)	USD ha^{-1} increase	Price + oil premium (USD t^{-1})	Total price (USD ha^{-1})	Price change from 30ppbv (USD ha^{-1})
Click (Spring)	30	2.1	2.9		2.1	466.3	48.1	8.1	12.1	1.1	522.9	1092.9	
	55		3.5	+17.7	2.5		48.2	8.2	12.3	1.1	523.6	1287.9	+195.0
	80		2.6	-12.2	1.8		44.9	4.9	7.3	1.1	500.5	918.0	-174.9
	110		2.3	-21.4	1.6		40.9	0.0	0.0	1.0	466.3	765.7	-327.2
Phoenix (Winter)	30	3.3	7.2		3.3		44.0	4.0	6.0	1.1	494.2	1643.3	
	55		5.6	-21.9	2.6		42.8	2.8	4.2	1.0	485.8	1262.2	-381.1
	80		5.1	-29.5	2.3		43.0	3.0	4.5	1.0	487.2	1141.7	-501.6
	110		4.3	-40.4	2.0		43.9	3.9	5.8	1.1	493.5	978.2	-665.1

UK average yield and delivered prices derived between 2017-2020 (AHDB, 2020). Oil premium prices calculated from industry practice in line with international guidelines (Federation of Oils, Seeds and Fats Associations Ltd. document 26A).

3.4.4 Economic Assessment

When the observed changes in TSW are scaled to field-level, Click's final yield decreased from 2.09 t ha^{-1} at 30 ppbv to 1.84 t ha^{-1} and 1.64 t ha^{-1} under 80 and 110 ppbv respectively (Table 2). Increased TSW and oil content (between 30 and 55 ppbv) are not statistically significant but represent an instability of gross profits with increased ozone exposure. More substantial final yield losses occurred in Phoenix: from 3.33 t ha^{-1} at 30 ppbv to 2.34 t ha^{-1} and 1.98 t ha^{-1} under 80 and 110 ppbv, respectively. The total oil content in both varieties was >40% across all treatments and would, therefore, still attract price premiums. However, premiums would fall under increasing exposure in both cultivars. Our findings suggest the premium would decrease from 12.5% at 30 ppbv to 7.35% under chronic exposure to 80 ppbv of ozone for Click. The premium would drop from 6% at 30 ppbv to ~4% at 55 and 80 ppbv for Phoenix. No premium would have been paid for Click seed under 110 ppbv, but Phoenix's recovered slightly to 5.8%. Overall, the combined losses in seed yield and oil content would have led to economic losses of up to 30% in Click and 40% in Phoenix between 30 and 110 ppbv, with growers' profits narrowing under increasing ozone exposure.

3.5 Discussion

This is the first study to directly compare the physiological, morphological, and seed quality responses of spring and winter oilseed rape (OSR) cultivars to chronic ozone exposure and explore the findings within the context of industry practice. Most importantly, greater ozone exposure decreased seed yield and quality in both cultivars (Figures 3.3, 3.4, 3.5), despite some

evidence of increased raceme number compensating for smaller seed (Figure 3.5c). Therefore, our first hypothesis was accepted. However, while oil content significantly decreased, and ash, moisture, protein, and micronutrients increased in the spring cultivar Click, seed quality of the winter cultivar Phoenix was largely unchanged. Furthermore, Click was more physiologically sensitive to ozone exposure than Phoenix, with net photosynthetic rate (P_{net}), stomatal conductance (g_s), relative chlorophyll content and biomass accumulation decreasing under lower cumulative exposure; thus, our second hypothesis was also partially accepted. Overall, our results support our third hypothesis and provide further evidence that shorter-lived cultivars (spring OSR) are more sensitive to chronic ozone exposure than longer-lived cultivars (winter OSR) regarding quality and physiology.

OSR is grown to provide oil for human consumption and oilcake for animal fodder. Oilseed composition is closely monitored and controlled to ensure that the oil and derived products are fit for consumption. International guidelines from the Federation of Oils, Seeds, and Fats Association (FOSFA) stipulates that seeds require a minimum of 40% total oil content and 6-10% moisture when received by a crusher (FOSFA, 2016). Seeds that fail to meet these FOSFA quality standards may be rejected. If loads are accepted, growers then receive a payment premium of 1.5% for every 1% increase in oil content above this minimum, with similar penalties as oil content falls below 40%. All seed analysed in this study passed the minimum FOSFA standards. However, the reduction in oil content in seeds from plants exposed to higher levels of ozone, particularly in Click, would result in growers forfeiting the premium payments they currently rely on to improve profit margins. For example, the decrease in oil content in Click from 48% under European background ozone concentrations of 30 ppbv to 41% following chronic exposure to 110 ppbv of ozone, typical of hot Southern European summers, represents a loss of 12% in premiums. Exposure to 80 ppbv, typical of hot Northern European summers, decreased premiums by over a third. For a crop such as OSR with very tight profit margins, this represents a high risk for growers. Although seed oil content was not affected in the Phoenix, profit from this winter cultivar would be substantially lower due to reductions in total seed mass.

Based on average UK yields and prices for OSR in 2020 (DEFRA, 2020), our results suggest that high ozone concentrations (80 and 110 ppbv) could result in a loss of between 174.87 and 327.22 USD ha^{-1} for Click and 501.61 to 665.13 USD ha^{-1} for Phoenix (Table 2), which may deter growers from planting this crop. The ozone-induced yield changes observed in this study are, therefore, sufficient to cause concern for growers in current and projected future climates. Moreover, yield instability of Click with increased ozone exposure presents a further risk to OSR growers. OSR yields in optimised field trials in UK averaged 3.3 t ha^{-1} (spring) and 5.6 t ha^{-1} (winter) between 2017 and 2020 (AHDB, 2020). However, on-farm yields were substantially lower, averaging 2.1 t ha^{-1} (spring) and 3.3 t ha^{-1} (winter) over four years (as in Table 2). UK OSR farm yield (2017-2020) has fluctuated between 1.8- 2.2 (spring), and 2.7-3.5 t ha^{-1} (winter) (Bayer Crop Science, 2020). The ozone-induced yield losses of between 0.3 and 0.5 t ha^{-1} (Click) and 1.0 and 1.3 t ha^{-1} (Phoenix) projected by this study are

therefore of real concern. In particular, the losses projected by this study surpass previously reported pest- and disease-induced yield and oil losses. For example, Turnip yellows virus and cabbage stem flea beetle decreased yields by 10-40% (Stevens et al., 2008), and 9% (Wynn et al., 2017), respectively. Furthermore, stress-induced yield losses may be additive as stresses frequently co-occur (Pullens et al., 2019).

High seed chlorophyll content is undesirable in food products. Chlorophyll oxidises oils and accelerates rancidity thereby reducing shelf life (Onyilagha et al., 2011), creates a colour that makes the product visually unappealing (Bommarco et al., 2012), and necessitates additional resources to refine (HGCA, 2003). Oil prices are reduced by up to 0.2% t^{-1} once seed chlorophyll content increases above 20 ppm (Bommarco et al., 2012). Moreover, Click and Phoenix are both hybrid cultivars, which have half the chlorophyll content of conventionally bred varieties (HGCA, 2003). Therefore, while chlorophyll content of all seeds harvested in this study were below the 20 ppm quality threshold, were the three-fold increases between lowest and highest exposures seen in this study to be replicated in older hybrids, seed chlorophyll content would cause problems for the refining chain and therefore final market with chronic ozone exposures >55 ppbv.

While ozone stress decreased yield and/or oil content, and therefore income from the human food product market, other changes may offer growers increased quality in oilseed cake. Protein and micronutrient (specifically iron, manganese, sulphur, and zinc) content all rose (Figures 3.4 and 3.5), which may be favourable for animal fodder, particularly seed cake (Arrutia et al., 2020). As global demand for animal protein is projected to double by 2050 (Westhoek et al., 2011), this may provide an unexpected bonus for growers of OSR already supplying the feedstock market or a new opportunity for others. OSR protein content currently ranges between 20-35%, and an increase of 33.4%, as in our study, would make OSR directly competitive to other high protein feedstock. For example, soya averages 45-49% and fava bean 30-36% protein (Mattila et al., 2018; Heuzé et al., 2020). However, the concomitant increase in less favourable components (moisture, ash, and chlorophyll) and substantial decreases in total seed mass may negate any benefit, as in other crops such as soya (Broberg et al., 2020).

The two cultivars differed considerably in their ozone sensitivity, which adds to a body of evidence of intraspecific differences in ozone sensitivity, such as soya (Bailey et al., 2019) and wheat (Pandey et al., 2019). Although selective breeding has favoured crops with higher rates of g_s (Lu et al., 1998; Roche, 2015) and P_{net} (Long et al., 2006; Koester et al., 2016), which is correlated with higher yields, such crops risk higher cumulative ozone exposure and ozone uptake via stomata. Both g_s and P_{net} of the fast-growing spring cultivar (Click) decreased substantially as cumulative exposure increased. Click's photosynthetic declines were correlated with significantly lower TSW and seed quality in plants grown under higher ozone concentrations. In contrast, the slower-maturing winter cultivar (Phoenix) maintained stomatal conductance and photosynthesis under increasing exposure. Hence, increased cumulative exposure over a longer growing season decreased carbon allocation, which affected Phoenix's yields, but did not affect quality. Phoenix's 40% TSW decrease indicates ozone is an invisible

threat to OSR, as leaf-level physiological measurements were not a reliable guide to seed filling. Despite increased ozone tolerance being attributed to low relative growth rates (Franzaring et al., 2000), intraspecific mechanisms are not widely discussed. Plants with longer growth cycles may divert more photosynthetic products to protective mechanisms than shorter-lived plants, which instead decrease biomass accumulation and seed filling (Zhu, 2002; Felzer et al., 2007; Kant et al., 2015). Thus, while this study presents differential ozone sensitivity between two OSR varieties, further study is warranted to identify varieties that may exhibit heritable ozone tolerance in OSR. Moreover, the effects of other environmental and phenological variables need further investigation, as this study grew plants in pots in a single soil type under glasshouse conditions for a shorter duration than in the field. Despite such uncertainties, the economic penalties presented here highlight the importance of further investigation of the effects ozone alongside other abiotic stresses, nutrient application, and different soil types.

Ozone is well-documented to accelerate leaf senescence (Miller et al., 1999; Franzaring et al., 2000; Yendrek et al., 2017). Ozone induces elicitor signalling to plant cell nuclei, which upregulates senescence-associated genes and antioxidants, and downregulates P_{net}-associated genes, which decreases rubisco and chlorophyll synthesis (Pell et al., 1997; Yendrek et al., 2015; Grulke & Heath, 2020). This contributes to re-mobilisation and re-assimilation of nutrients from leaves to seeds, hence decreasing foliar (Calatayud et al., 2004) and increasing seed chlorophyll content (Masclaux-Daubresse et al., 2010). Such nutrient remobilisation is particularly concerning, as OSR typically has a low nitrogen use efficiency, with only half of absorbed nitrogen being present in harvested seeds (Schjoerring et al., 1995). Therefore, exploiting the genotypic variation in nutrient remobilisation and delayed senescence may provide an opportunity to improve yields and selectively breed ozone tolerant OSR cultivars (Avice & Etienne, 2014; Girondé et al., 2015).

3.6 Conclusions

Our study compares the responses of two European modern OSR cultivars (one spring and one winter) to chronic exposure to realistic ozone levels over a growth season and adds to mounting evidence of intraspecific differences in yield, seed quality, and physiology. Moreover, indications of final yield differences did not manifest in classic ozone injury symptoms such as chlorosis and bronzing at earlier growth stages, indicating chronic ozone stress poses a hidden threat to the cultivation of OSR. Chronic ozone exposure reduced seed quantity and quality at relatively moderate levels of ozone (>55 ppbv), resulting in potentially large reductions (of up to 665.13 USD ha^{-1}) in selling price, threatening the commercial viability of OSR. With increased background and peak concentrations of ozone projected for the near future, our findings provide a timely warning for growers and agronomists, and a call to identify and exploit traits linked to ozone tolerance in oilseed rape.

4. Cultivar and leaf-specific biochemical responses to short-term ozone exposure in spring and winter oilseed rape

Author contributions

Hattie R. Roberts: Initiated experimental design, carried out plant propagation and care, carried out practical experimental work, ascorbic acid sample preparation, performed oxidative stress and oxidative damage assays, compiled and analysed data, visualised data, prepared manuscript, and submitted manuscript.

Felicity Hayes: Participated in interpretation of results, manuscript preparation.

Ian C. Dodd: Advised experimental planning and design, participated in interpretation of results, participated in manuscript preparation.

Kirsti Ashworth: Principal Investigator. Experimental planning and design, participated in interpretation of results, participated in manuscript preparation.

Submission to journal

This chapter was in preparation for submission to *Journal of Experimental Botany* as a primary research article in April 2023.

A summary of this chapter can be found in section 2.2

Graphical Abstract

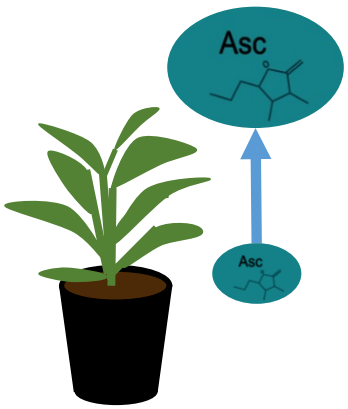

We postulated that a high levels of a key antioxidant, ascorbic acid, may provide a simple marker of ozone tolerance in oilseed rape. Ascorbic acid may be distributed in an acropetal gradient.

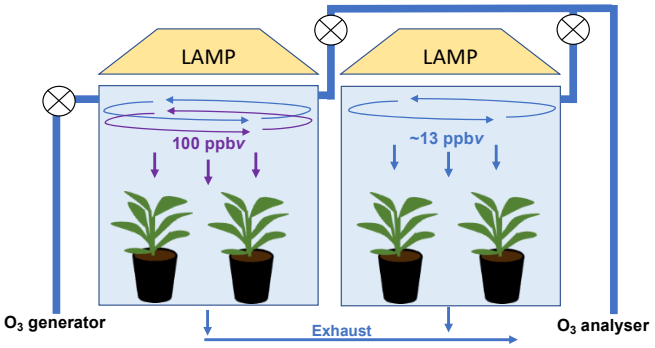

We exposed Two oilseed rape cultivars to two ozone treatments (20 and 100 ppb) in Solardomes over 12 days in laboratory conditions. We measured gas exchange, ascorbic acid, and markers of oxidative stress.

While the winter oilseed rape cultivar had higher ascorbic acid levels, the cultivar was less tolerant due to high ozone uptake via stomata. Spring OSR closed its stomata in response to ozone, meaning it maintained biomass.

4.1 Abstract

Different physiological responses to ozone exposure have previously been observed in a shorter-lived spring-sown vs. longer-lived winter-sown oilseed rape (OSR; *Brassica napus* L.) crop. It was postulated that longer-lived cultivars divert more photosynthate to biochemical protective mechanisms, such as antioxidants, and less to growth when exposed to abiotic stress, which delays senescence. This study focuses on ascorbic acid (AsA), a key antioxidant found throughout plant cells which has previously been shown to convey tolerance against ozone. Two OSR cultivars (the spring-sown cv. Click, and the winter-sown cv. Phoenix) were exposed to 12 days' fumigation at ozone levels comparable to European background and peak conditions (~20 ppbv and ~100 ppbv). Leaf gas exchange, chlorophyll content, and biochemical markers of oxidative stress and damage as well as AsA content were measured at the 2nd, 4th, and 6th nodal positions. While total AsA content was higher in Phoenix, its chlorophyll content, leaf area and mass declined, likely due to maintained stomatal conductance and therefore ozone uptake. Conversely, Click was seemingly ozone tolerant: it avoided high ozone uptake via stomatal closure, and leaf area and dry mass was maintained. This study provides further insight into whole-plant changes and intraspecific sensitivities in ozone tolerance.

4.2 Introduction

Oilseed rape (hereafter OSR) is the second-most important oilseed crop worldwide, contributing 12% of total global oilseed harvests (USDA, 2020). However, it is only narrowly economically viable due to its high nutrient demands and vulnerability to biotic and abiotic stresses relative to other crops (Avice et al., 2014). One abiotic stress of increasing interest to agronomists is tropospheric ozone, a phytotoxic air pollutant. Occurrences of high tropospheric ozone levels (>80 ppbv) during summer, i.e., main growing, months have increased in frequency in the past 50 years (Archibald et al., 2020). Tropospheric ozone concentrations above ~80 ppbv have been observed to accelerate leaf and whole plant senescence (Mills et al., 2018), the endogenous developmental process leading to cell death, and characterised by loss of chlorophyll (breakdown of chloroplasts), lipid peroxidation, and mobilisation of nutrients to younger leaves (Yendrek et al., 2017). Moreover, while developmental senescence increases with age, it is sequential and non-linear, rather than age dependent. For example, basal OSR leaves at lower nodal positions senesce and abscise along an acropetal gradient. If sequential senescence is disrupted due to stress, nutrient use efficiency declines, resulting in increased demand and cost of additional fertiliser to maintain seed yields (Bouchet et al., 2016; Tewari et al., 2013). Therefore, understanding the processes, timing, and impacts of exogenous, here ozone-induced, senescence in this crop is of global economic importance to growers and consumers.

Under natural conditions, senescence is a tightly regulated process resulting in the onset of programmed cell death (PCD). This process involves the genetically orchestrated degradation of cellular components such as chlorophyll, RNA, DNA, and lipid membranes by newly synthesised enzymes. Tropospheric ozone damage occurs when ozone enters plants, mostly via stomata, into the apoplastic space where it rapidly dissolves and oxidises to form reactive oxygen species (ROS) such as singlet oxygen, superoxide, and hydroxyl radicals (Grulke and Heath, 2020). Although exogenous, ozone-induced damage is most visibly apparent as a PCD-induced accelerated senescence response in crops. Both endogenously- and exogenously induced senescence is initiated by key signalling molecules integrated to developmental and age-dependent pathways. These include hydrogen peroxide (H_2O_2), a major component of the ROS pool (Bieker et al., 2012; Zentgraf et al., 2022). H_2O_2 is associated with the upregulation of senescence-associated pathways and downregulation of photosynthetic enzymes and metabolites (Kusaba et al., 2013). This shift in primary metabolic profile and transport leads to chlorophyll degradation and hence reduced photosynthesis (Mikkelsen et al., 1996). The effects of leaf ageing and ozone are postulated to be synergistic (Hoshika et al., 2020), as ozone exposure increases the endogenous ROS pool beyond that associated with natural ageing (Pell et al., 1997). These oxidation reactions disturb cellular homeostasis and increase the production of ROS which oxidise lipid-rich membranes, disrupt photosynthetic pathways, decrease biomass accumulation, and ultimately trigger PCD (Sharma et al., 2012). Enzymatic and non-enzymatic antioxidants are upregulated to quench ROS by acting as reducing agents or free radical scavengers to prevent oxidative damage and PCD (Gill & Tuteja, 2010).

ROS concentrations that exceed a plant's defence mechanisms are referred to as 'oxidative stress' (Pell et al., 1997).

Ascorbic acid (AsA) is the most ubiquitous non-enzymatic antioxidant and a major regulator of oxidative stress responses due to its primary location in the apoplastic space (Smirnoff, 2005; Wheeler et al., 1998). Apoplastic AsA is thought to directly quench ozone (Hove et al., 2001) and singlet oxygen (Akram et al., 2017). AsA is also a redox buffer for enzymatic scavenging of H_2O_2 in the glutathione-ascorbate cycle (Wu et al., 2017). Moreover, AsA is well-known to prevent and modulate foliar senescence, and decrease oxidative stress and PCD (Wanatabe et al., 2013; Conklin & Barth, 2004; Zhang, 2012). High concentrations of foliar AsA are generally associated with increased ozone tolerance during the vegetative stages, evident as maintained gas exchange, chlorophyll content, and biomass, and lower markers of oxidative stress and damage such as MDA and H_2O_2 (Chen & Gallie, 2006; Bellini & Tullio, 2019). For example, exogenous application of AsA has been shown to decrease lipid peroxidation by as much as 60% (Dolatabadian et al., 2008) and prevent stress-induced senescence (Barth et al., 2006). The location within organelles and bioavailability of AsA, and the ratio of AsA to its oxidised form (dehydroascorbic acid or DHA) are key to its efficacy in quenching ROS (Bellini & Tullio, 2019).

Oilseed rape is sown in two seasonal groupings, with both cultivars harvested around August to September in Europe. Spring-sown cultivars have a shorter life cycle (4-6 months) and accumulate biomass more rapidly than winter-sown cultivars (8-10 months). Responses to ozone over the growing season have previously been observed to differ between a spring-sown and winter-sown OSR, with winter-sown plants maintaining chlorophyll content and physiology over time but at the forfeit of comparatively lower seed yield (Roberts et al., 2022). It has been postulated that the maintenance of leaf physiology and homeostasis in winter OSR under ozone exposure may be due to higher levels of endogenous AsA increasing antioxidant capacity and orchestrating developmental transitions (Kotchoni et al., 2009). This may be because winter OSR conforms to the optimal defence theory, wherein photosynthate is diverted from growth to defensive compounds to protect the most 'productive' tissues (McCall & Fordyce, 2010; Herms and Mattson, 1992; McKey, 1974; Ohnmeiss and Baldwin, 2000). The aim of this study was therefore to determine the contribution of AsA to cultivar- and leaf age-specific responses to ozone exposure in a winter (cv. Phoenix) and spring (cv. Click) OSR cultivar and assess its capability as a marker of ozone tolerance in crops. Based on previous findings that winter OSR maintained physiology more effectively over increasing ozone exposure compared to spring OSR, (Roberts et al., 2022), we therefore hypothesised that:

i. Total AsA will be higher in the long-lived winter cultivar, *B. napus* Phoenix, than the shorter-lived cultivar, *B. napus* Click.
ii. OSR with higher AsA content will better maintain physiological (F_v/F_m, Performance Index) and morphological (leaf area, total mass) productivity under ozone exposure.

iii. Foliar AsA content will increase with nodal position and with increased exposure to ozone.

In this study, the two cultivars were exposed to either ambient (~20 ppbv, i.e. low background European summer concentrations) or ~100 ppbv (typical of peak summer ozone conditions in central/southern Europe) over a period of 12 days in 1-m^3 semi-controlled environment chambers. This study is novel in measuring acropetal gradients in biochemical and physiological responses of spring and winter varieties of OSR to short-term exposure 'real-world' ozone concentrations, which is key to gain a better-whole plant understanding of biochemical defences and responses to ozone.

4.3 Methodology

4.3.1 Plant cultivation and morphological measurements

After 7 days dark vernalisation at 2 ˚C, 200 spring (Click) and 200 winter (Phoenix) OSR seeds were sown on Dec 28th, 2021, in bedding packs in a 1-m^3 sealed chamber until germination. Once plants reached two true leaves (GS12), they were transplanted to 2 L pots (ø = 14 cm (top), 9.5 cm (base), d = 18.2 cm) in John Innes no. 2. Eighteen plants per cultivar were chosen for uniformity in size and leaf number at GS12 (Jan 14th, 2022) and grown on in the same semi-controlled environments. A 12-hour photoperiod (08:00 – 18:00) was applied via growth lamps (Powerstar HQI-BT, 600 W/D daylight, OSRAM, Munich, Germany) delivering 450±25 µmol photons m^{-2} s^{-1} at canopy height. Temperature, relative humidity, and PAR were monitored in each chamber and logged every 10 minutes using sensors (RH 2nl-02 Humidity Sensors; Fenwal UUA32J2 2K Thermistors; Delta T Devices Quantum Sensor, Cambridge, UK, respectively) attached to a GP2 Data logger (Delta T Devices, Cambridge, UK), and did not significantly differ between chambers used for experiment. Plants were watered daily at 16:00 by replacing the previous 24-hour evapotranspiration losses and were rotated daily within each chamber to mitigate potential edge effects. During sampling, the leaves in the 2nd (oldest nodal position sampled) 4^{th,} and 6th (youngest sampled) nodal position on the basal rosette of each plant were tagged with coloured wool and labelled to track leaf age. Morphological, physiological, and biochemical measurements began 21 days after sowing into pots i.e. on Feb 12th, 2022, when plants reached development stage GS16 i.e., with 6 fully unfolded leaves of sufficient size for gas exchange measurements.

4.3.2 Ozone fumigation

Plants of each cultivar were placed separately in two sealed 1-m^3 chambers which were fumigated with ozone to provide low (~20 ppb) and high ozone (100 ppbv) concentrations. Other environmental conditions in the chambers were maintained as described above. Ozone was generated via a bespoke fumigation system comprising a compressed air cylinder and high-voltage ozone generator (Opti Sciences, New Hampshire, USA). The flow rate of ozone into each treatment chamber was manually controlled at 200 – 300 ml min^{-1} and checked every 4 hours with in-line gas flow monitors. The ozone was mixed with carbon-filtered air, at a flow of 300 ml min^{-1}, in

ducts at the top of each chamber via a Teflon Swagelok injection system (Swagelok, Ohio, USA). Air was filtered using a scrubber containing charcoal and glass wool. The control chambers received only carbon-filtered air, and ozone concentrations fluctuated with ambient background conditions, which ranged between 13.4±6.5 ppbv over the course of the experiment. Ozone concentrations in the treatment chambers were maintained at 102.5±5.3 ppbv for 8 hours per day (09:00–17:00). Fumigation ceased overnight and ozone concentrations in the treatment chambers fell to ambient (7.9±7.1 ppbv) during this time, mirroring real-world conditions. Ozone concentrations were manually logged every 10 minutes using an Enviro 600 ozone analyser (Enviro Technology Ltd., London Road, Stroud, Gloucestershire, UK).

Cumulative ozone uptake was calculated following Lombardozzi et al., (2013), such that:

$$CUO_3\ (mmol\ mol^{-1}\mathrm{h}\ leaf) = [O_3] \cdot H \cdot D \cdot 10^{-3} \cdot \mathrm{g}_s \cdot 1.67$$

[Equation 1]

where $[O_3]$ is ozone concentration in mol, H is number of hours, and D number of days, g_s is stomatal conductance measured using LI-COR 6400 XT, and 1.67 is the ratio of leaf resistance for ozone to leaf resistance for water vapour. The flow of ozone to the treatment chambers was stopped every third day (Days 0, 3, 6, 9, 12) to allow measurements to be conducted safely.

4.3.3 Leaf gas exchange and physiological measurements

Three replicates of each leaf age for each cultivar and treatment were sampled every three days over a 12-day period. Leaf gas exchange was measured with LI-COR 6400 XT using a 2 cm x 3 cm LED chamber (LI-COR Biosciences, NE, USA). LI-COR chamber conditions were set to match growth chamber environmental conditions, i.e., 400 ppm CO_2, 400 µmol m^{-2} s^{-1} PAR, 20 °C, and 50% RH. Instantaneous net photosynthetic rate (P_{net}) and stomatal conductance (g_s) were measured following a five-minute stabilisation period. Measurements were taken from an area between the main vein and leaf edge. The chlorophyll content index (CCI) of the same leaf area was measured using an Apogee meter (Apogee, Utah, USA) and Photosystem II operating efficiency (F_v/F_m) and Performance Index (PI) were recorded using a pocket-PEA chlorophyll fluorimeter (Hansatech Instruments Ltd, King's Lynn, UK). Non-destructive morphological measurements of leaf length, width, and leaf area were made at the same time as physiological sampling to determine differences in leaf development, growth, and visible injury. Whole plant destructive harvests were carried out on days 0, 6 and 12, i.e., before, at the mid-point and at the end of ozone exposure respectively, with tissue samples taken for subsequent biochemical assays.

4.3.4 Biochemical analyses: preparation

Biochemical analysis of the harvested leaf tissue was conducted to determine foliar content of AsA, as well as H_2O_2 and MDA (malondialdehyde) which were used as

proxies for total ROS content and lipid peroxidation respectively. 300 mg fresh tissue from leaves at the 2nd, 4th and 6th nodal position were collected from each plant harvested on Days 0, 6 and 12. Three technical replicates of tissue samples were placed in pierced 2 ml Eppendorf tubes (Thermo Fisher Scientific, Oxford, UK), totalling 100 mg per tube, frozen with liquid nitrogen, and stored at -80°C until biochemical assays were carried out which took place within a month of the conclusion of the experiment. Leaf tissue AsA content was measured using High Performance Liquid Chromatography Mass Spectroscopy (HPLC-MS) as described in ***Section 4.3.5***.

4.3.5 Biochemical analyses: ascorbic acid (AsA)

Foliar AsA content was determined as described by Davey et al. (2003). In brief, 100 mg frozen leaf tissue was freeze-dried (Freeze-dryer Alpha 1-2 Ldplus, Martin Christ Gefriertrocknungsanlagen GmbH, Osterode, Germany) for 48 hours in punctured 2 ml Eppendorf tubes, and samples were ground at 30 Hz for 4 minutes to a fine powder consistency (Retsch MM400 mixer mill; Retsch, Haan, Germany). 20 mg ground leaf material was added to 5 ml 4.5% metaphosphoric acid solution (MPA) in 10 ml corning tubes. The samples were vortexed for 2 minutes (WhirliMixer, Fisons, Ipswich, UK) and centrifuged at 14000 RPM at 4 °C for 10 minutes. 2 ml of the supernatant were added to 0.2 ml 2% dithiothreitol (DTT) and samples left to stand in the dark for 2 hours. Samples were then placed in 3 ml needleless syringes and filtered into 1 ml amber glass vials using 0.45 µm syringe filters (Thermo Fisher Scientific, Massachusetts, USA). Standards were made at the same time as samples, using 10 mM AsA stock solution (Thermo Fisher Scientific, MA, USA).

The samples were analysed using a HPLC-MS (Dionex, Thermo Fisher Scientific, MA, USA). The HPLC column was a C18 150 × 4.6, 5 µm; the mobile (isocratic) phase used a 1 ml min-1 flow of 99/0.9/0.1 (by volume) solution of water/acetonitrile/formic acid. The temperatures of the column oven and auto-sampler were 20 and 10 °C, respectively. The injection volume of the samples and standards was 20 µl, the UV wavelength was 245 nm, and each sample run time was 15 minutes overall. AsA concentrations were determined from a calibration curve derived from the peak areas of the standards.

4.3.6 Biochemical analyses: H_2O_2 and MDA

A maker of oxidative stress, hydrogen peroxide (H_2O_2) and damage, malonaldehyde (MDA) content were used as measures of oxidative stress and damage respectively. Each was determined using standard protocols which are described in detail by Roberts et al. (2023). In short, H_2O_2 was determined by a potassium iodide assay, as described by Ovenston and Rees (1950) and Junglee et al. (2014). MDA was determined using a TBARS assay, as described in Du et al., 1989. A spectrophotometer (Ultrospec 2100 pro, Biochrom Ltd., Cambridge, UK), was used to determine absorbance of samples in plastic 1.5 ml cuvettes. H_2O_2 values were determined using a standard calibration curve. MDA values were determined using the below equation:

$$nmol\ MDA\ g^{-1}FW = \frac{\Delta A\ \cdot\ 3.5\ \cdot\ x\ \cdot\ 1000}{\varepsilon\ \cdot\ \beta\ \cdot\ \gamma}$$

[Equation 2]

where: ΔA represents the difference between absorptions at 532 and 600 nm (A_{532} – A_{600}), corrected by deducting ΔA of the blank; β represents length of light path (0.56 cm); ε represents TBA extinction coefficient (155 mM^{-1} cm^{-1}); 3.5 is the dilution factor from 400 µl extract + 1 ml TBA/TCA solution; x represents the volume of TCA 0.1 % used for extraction (1 ml); γ represents the frozen weight of tissue (0.1 g); 1000 is the conversion factor of µmol to nmol (as in Du et al., 1989).

4.4 Results

4.4.1 Leaf gas exchange and cumulative ozone uptake

Stomatal conductance (g_s) was similar between cultivars in control (20 ppbv), but the response of g_s to ozone significantly differed between cultivars (Figure 4.1a). g_s declined across all nodal positions in Click under ozone treatment, with the most considerable decrease (of 50%) at the 4th and 6th nodal positions. By contrast, while average g_s tended to be slightly lower under control conditions in Phoenix, g_s was better maintained in ozone-exposed plants. Similarly, there was a significant acropetal gradient, with g_s increasing in Click leaves with increased nodal position by a factor of two under control conditions, and by between 25 and 40% between the 2nd, 4th, and 6th nodal positions under 100 ppbv.

Net photosynthetic rate (P_{net}) was statistically similar between cultivars regardless of ozone treatment (Figure 4.1b). Despite declines in g_s in ozone-exposed leaves, P_{net} was maintained in Click, with only slight reductions of 15% seen at the 2nd nodal position. P_{net} was also maintained in Phoenix, with a slight increase of 13% in ozone-exposed leaves at the 6th nodal position. P_{net} displayed a significant acropetal gradient, with P_{net} increasing by 30 – 60% with increased nodal position. Overall, the two cultivars had a similar absolute P_{net} which similarly increased with ascending nodal position and was not affected by ozone.

The relationship between P_{net} and g_s (intrinsic water use efficiency, $_i$WUE) in the two cultivars were statistically similar (Figure 4.1c). P_{net} generally increased with g_s to a maximum photosynthetic rate of 15.0 µmol m^{-2} s^{-1} at ~0.8 mol m^{-2} s^{-1} in both varieties. Each leaf nodal position occupied a discrete position on the P_{net}-g_s relationship (P <0.001), irrespective of ozone treatment (P = 0.61), with P_{net} and g_s in the 2nd internodal position reaching only ~50% of the maximum. Although ozone exposed plants tended to have lower $_i$WUE at the 6th nodal position in both cultivars, regression coefficients (z-statistic) for iWUE were not significantly different between ozone-treated and control plants in either cv. Click (P = 0.07) or Phoenix (P = 0.30). In summary, while the interaction between leaf nodal position and both P_{net} and g_s is

significant, both cultivars presented a similar physiological response to ozone regarding $_{i}$WUE.

Cumulative ozone uptake (CUO_3) was significantly higher in Phoenix than in Click, particularly at the highest nodal positions, due to its maintained g_s (Figure 4.2). CUO_3 was similar between cultivars for the control group, with CUO_3 increasing with ascending nodal position. However, while CUO_3 doubled between the 2nd and 4th leaf and increased by 25% between the 4th and 6th nodal positions under ozone in Click, four-fold and two-fold increases were observed between the 2nd and 4th, and 4th and 6th leaves in Phoenix. Leaves at the 6th nodal position had the highest ozone uptake, and CUO_3 was five times higher in Phoenix than Click. Overall, Phoenix had the highest CUO_3, with both cultivars showing an acropetal gradient.

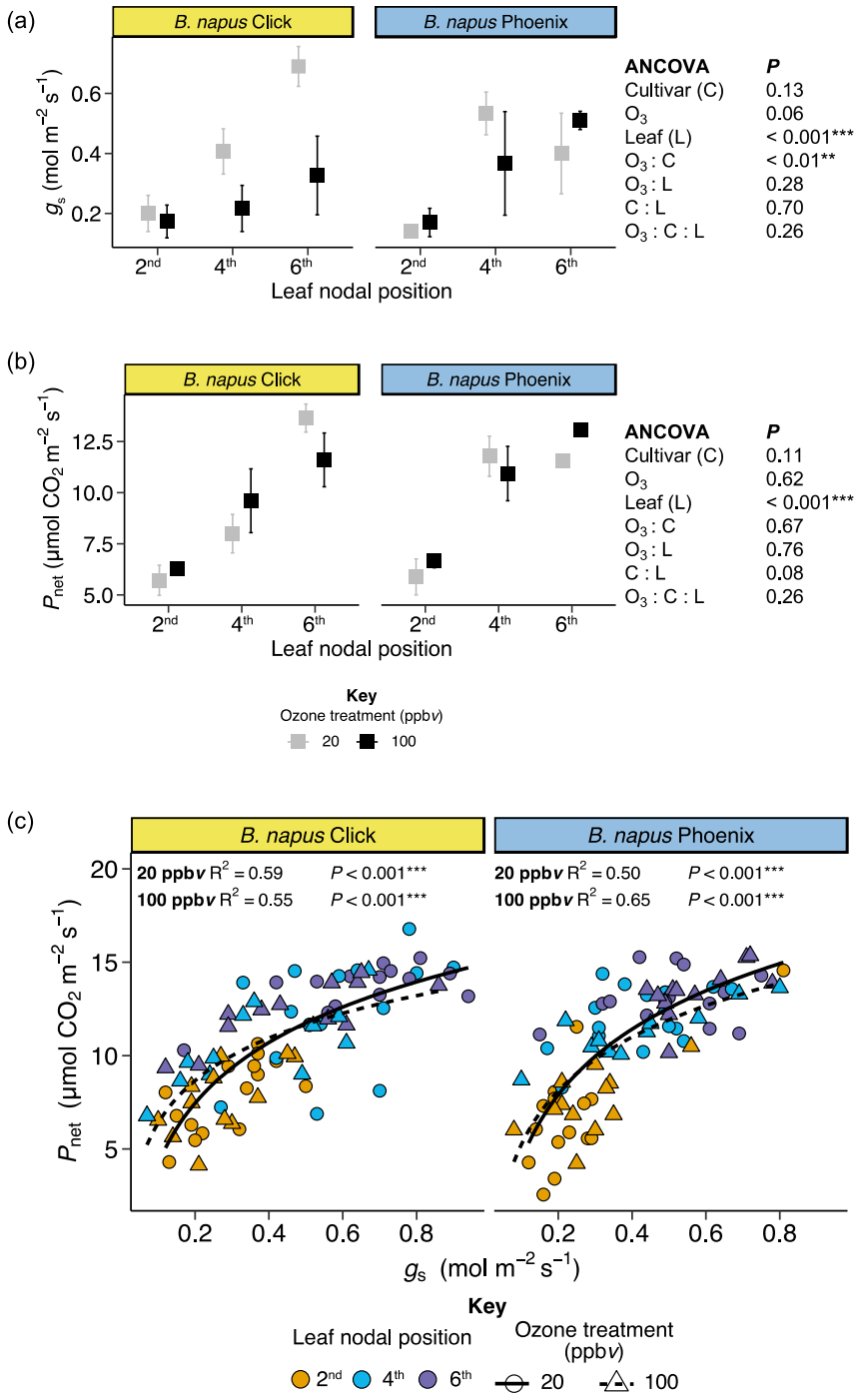

Figure 4.1. Error plots of average a) net photosynthetic rate and b) stomatal conductance in OSR cv. Click and Phoenix at three nodal positions under control conditions (ambient ozone at ~20 ppbv) and 100 ppbv ozone exposure after 12 days' treatment (n = 3); ±SEM. c) Scatter plots showing iWUE in OSR cv. Click and Phoenix at three nodal positions under control conditions (ambient ozone at ~20 ppbv, denoted by circular symbols) and 100 ppbv (triangle symbols) ozone exposure.

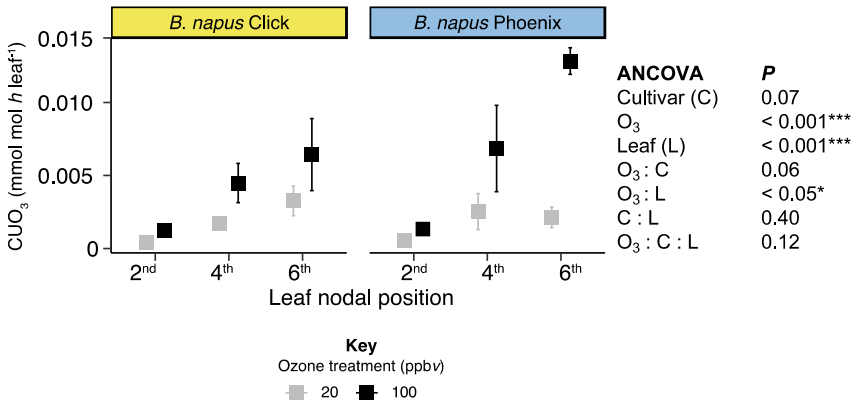

Figure 4.2. Cumulative ozone exposure in OSR cv. Click (yellow) and Phoenix (blue) at three nodal positions under control conditions (ambient ozone at ~20 ppbv) and 100 ppbv ozone exposure after 12 days' treatment (n = 3); ±SEM.

4.4.2 Chlorophyll content, F_v/F_m, PI

Chlorophyll content was higher in Click than Phoenix under control conditions and tended to increase with ascending leaf nodal position but decrease under exposure to ozone (Figure 4.3a). Average chlorophyll content was a third lower in ozone-exposed plants at the 2nd and 4th nodal positions in Click, but this was only statistically significant at the 4th nodal position. Similarly, chlorophyll content was 15% and 20% lower in the ozone-exposed treatments in the 2nd and 4th nodal positions in Phoenix. While chlorophyll content was unchanged at the 6th nodal position in Click, it was 24% higher in the ozone-exposed plants in Phoenix. The ozone effect on chlorophyll content was generally more pronounced in Phoenix, with an increasing chlorophyll gradient with ascending nodal positions.

The average maximum potential quantum efficiency of Photosystem II (F_v/F_m,) was statistically similar between cultivars and showed a similar response to ozone exposure (Figure 4.3b). F_v/F_m, was substantially (38%) higher after 12 days' exposure to ozone in Click at the 2nd nodal position compared to control leaves. F_v/F_m, was also higher (17%) in 2nd nodal leaf in Phoenix, but this was not statistically significant. The efficiency of leaves at other nodal positions was unaffected by ozone exposure in both cultivars. PSII Performance Index increased with higher nodal positions, but there were no significant differences between cultivar, nor was there a pronounced ozone effect (Figure 4.3c). Overall, ozone tended to increase Photosystem II maximum potential quantum efficiency and PI at the 2nd nodal position only.

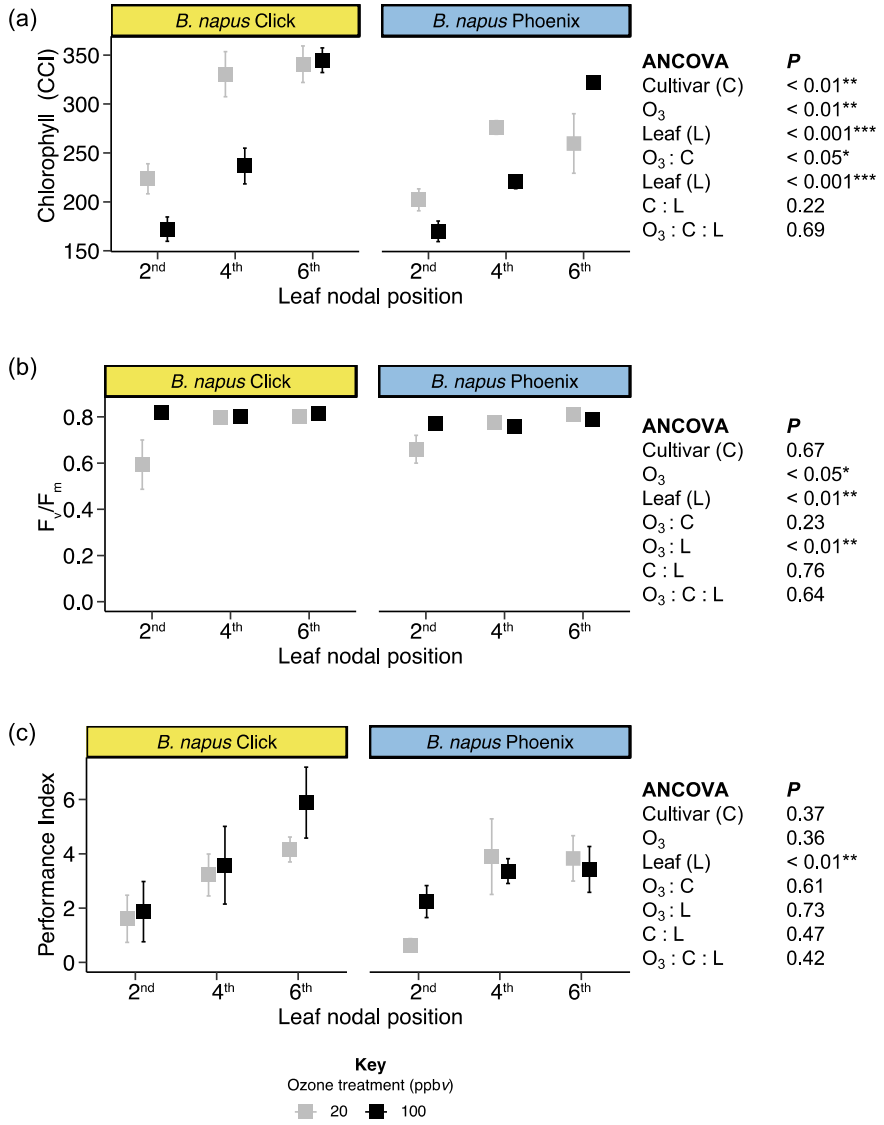

Figure 4.3 Error plots (left) showing a) F_v/F_m and b) Performance Index in OSR cv. Click (yellow) and Phoenix (blue) at three nodal positions under control conditions (ambient ozone at ~20 ppbv) and 100 ppbv ozone exposure after 12 days' treatment (n = 3); ±SEM.

4.4.3 Ascorbic acid, reactive oxygen species, lipid peroxidation

Overall, average ascorbic acid (AsA) content was significantly higher, by ~40-80% across all nodal positions in the long-lived winter OSR cultivar, cv. Phoenix, compared to the faster-growing cultivar, cv. Click (Figure 4.4a). While AsA increased between the 2nd and 6th nodal position in both cultivars, it was highest in the 4th nodal position in Phoenix in both treatment and control plants and in Click under ozone treatment. However, while average AsA tended to decline in response to ozone exposure in both varieties at all nodal positions, the differences were only significant between the 6th nodal position in ozone-exposed plants and control in Phoenix in which AsA declined by 55%.

Like AsA, hydrogen peroxide (H_2O_2), a major component of the ROS pool and used here as an indicator of oxidative stress, was higher in Phoenix than Click, with H_2O_2 content 40-60% higher at each nodal position in control plants (Figure 4.4b). Ozone treatment tended to increase H_2O_2 by ~10-30% at all nodal positions in both varieties compared to the control, but not significantly so. For example, average H_2O_2 content at the 6th nodal position in Click was a third higher in ozone-exposed leaves compared to control. H_2O_2 concentration also significantly increased with ascending leaf nodal positions in both cultivars, by ~0.2 µmol mg^{-1} FW between each nodal position.

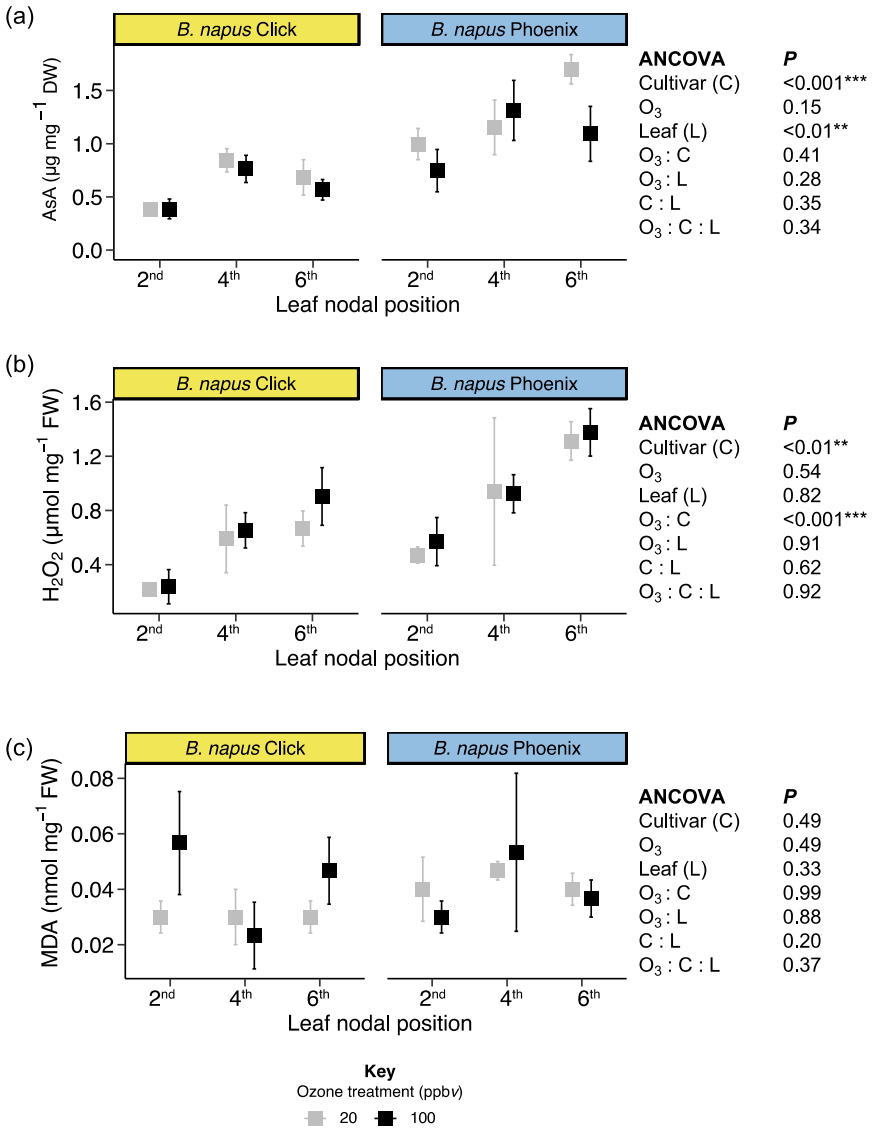

Figure 4.4. Error plots showing average a) Total endogenous ascorbic acid (AsA), b) hydrogen peroxide (H_2O_2), and c) Malonaldehyde (MDA) in OSR cv. Click (yellow) and Phoenix (blue) at three nodal positions under control conditions (ambient ozone; ~20 ppbv) and 100 ppbv ozone exposure after 12 days' treatment (n = 3); ±SEM.

Malonaldehyde (MDA), an indicator of lipid peroxidation, did not significantly differ between cultivars (Figure 4.4c). Furthermore, MDA levels did not follow H_2O_2 content, a marker of oxidative stress, nor AsA, an antioxidant, irrespective of cultivar and ozone exposure. Moreover, cultivars showed contrasting ozone responses across all nodal position, with MDA levels in Click increasing significantly at the 2nd and 6th positions but decreasing at the 4th under exposure to ozone, and Phoenix exhibiting the exact opposite. The highest MDA levels in Click were observed at the 2nd leaf position, wherein MDA levels were 40% higher in ozone-exposed leaves.

4.4.4 Leaf area and shoot mass

The morphologies of the two cultivars also responded differently to ozone. While leaf area was 30% smaller in Click than Phoenix at all nodal positions in the control plants, it was maintained under high ozone treatment (Figure 4.5a). However, in Phoenix, leaf area was 60% smaller under ozone at the 2nd and 4th nodal positions, but unchanged in the 6th leaf. Moreover, there was an acropetal gradient in leaf area in both varieties, wherein area increased by 88% (2nd to 4th) and 30% (4th to 6th) in Click and 70% and 10%, respectively, in Phoenix under control conditions, and similarly, although to a lesser extent, in ozone-fumigated plants. Leaf biomass tended to decline by 27-38% in the presence of ozone at all nodal positions in Phoenix, while remaining unchanged in Click (Figure 4.5b). Total shoot biomass significantly decreased by 21% in Phoenix in response to high ozone but was maintained in Click between the two treatments (Table 8.3). Overall, leaf area and biomass were maintained in Click under elevated ozone exposure, whereas both declined in Phoenix.

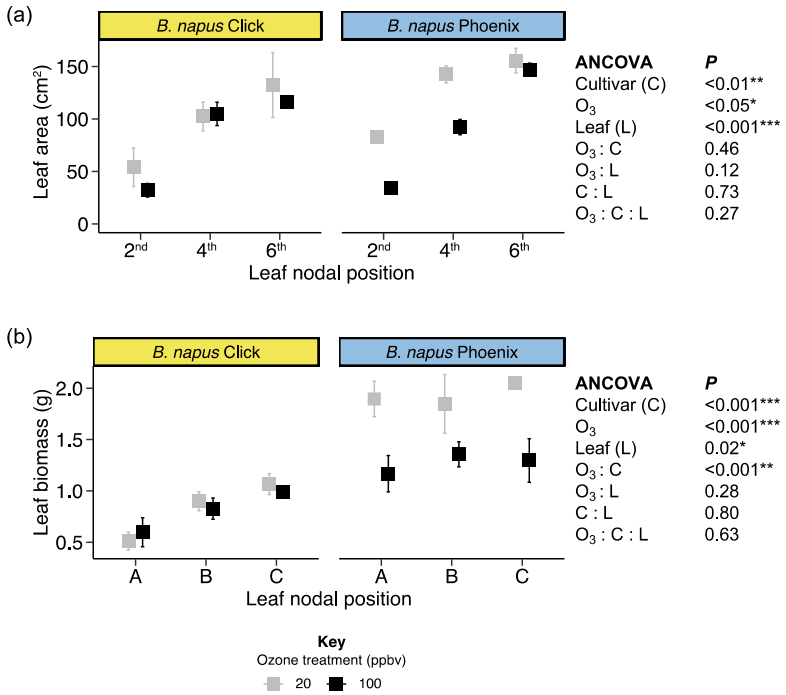

Figure 4.5. Error plots (left) showing a) Leaf area at three nodal positions, and b) Dried above in OSR cv. Click (yellow) and Phoenix (blue) under control conditions (ambient ozone at 20 ppbv) and 100 ppbv ozone exposure after 12 days' treatment (n = 3); ±SEM.

4.5 Discussion

This study is novel in comparing the non-enzymatic antioxidant ascorbic acid (AsA) content in a biennial winter-sown OSR cultivar, *B. napus* cv. Phoenix, and an annual spring-sown cultivar, *B. napus* cv. Click under exposure to ozone levels representative of high Northern Hemisphere summertime concentrations (Archibald et al., 2020; Morgan et al, 2006). Multiple studies show high levels of AsA are associated with ozone tolerance, and we postulated they may be a relevant marker for differences in tolerance between cultivars (Chen and Gallie, 2005; Frei et al., 2012; Gillespie et al., 2012; Zhang et al., 2013). We primarily hypothesised that Phoenix would have higher AsA levels due to diverting more photosynthate to synthesis of this ubiquitous antioxidant as a growth strategy under stress. Total foliar AsA was indeed higher in Phoenix than Click across all nodal positions (Figure 4a), confirming our first hypothesis.

We also hypothesised that OSR with higher AsA content will be better able to maintain physiological (g_s; P_{net}; F_v/F_m; Performance Index) and morphological (leaf area, total mass) productivity under ozone exposure. Indeed, Phoenix did maintain gas exchange (Figure 1a and 1b), chlorophyll content (Figure 3a) and F_v/F_m under elevated ozone (Figure 3b). However, Phoenix presented substantial declines in leaf area, and

Leaf biomass (Figure 5). Conversely, although g_s (Figure 1a) and chlorophyll content (Figure 3a) declined in Click under high ozone, leaf area and leaf biomass were maintained (Figure 5). It is likely the decline in both leaf area and dried mass in Phoenix, which proved contrary to our second hypothesis, reflected the higher CUO_3 (Figure 2) of this cultivar. The fact that productivity was not maintained despite higher AsA levels in Phoenix, supports the optimal growth theory, that Phoenix diverted photosynthate to defence rather than growth under ozone stress; however this defence was overwhelmed. Conversely, Click's decline in g_s with elevated ozone suggests that the faster-growing cultivar avoided stress and damage by limiting ozone uptake via stomatal closure. Such an avoidance mechanism may be due to increased stomatal sensitivity to exogenous stress (Mansfield & Freer-Smith, 1984; Price et al, 2002) which could potentially be exploited in future cultivar development programmes (Faralli et al, 2019).

We lastly hypothesised that AsA would increase in an acropetal gradient and under exposure to ozone but found no clear evidence of this in either cultivar. Instead AsA was highest at the middle nodal position (Figure 4a) meaning that our third hypothesis was not accepted. This suggests that, in the case of AsA, Phoenix did not fully conform to the optimal defence theory, wherein defensive compounds are diverted to the most 'productive' organs when under abiotic stress. Such productive parts are thought to be young, expanding leaf tissues in biennial plants (as in Phoenix), and reproductive sites in annual plants (as in Click) (McKey, 1974; Ohnmeiss and Baldwin, 2000). Alternatively, AsA synthesis may be upregulated in fully expanded leaves due to cumulative ozone damage, i.e. as part of an acceleration of senescence (indicated by declines in chlorophyll content at lower nodal positions), rather than for prioritisation of young tissue protection (McCall & Fordyce, 2010). Moreover, Phoenix's acropetal AsA pattern was seemingly disrupted by ozone (Figure 4a), most likely caused by the loss of AsA for directly quenching ozone in the apoplast (Yeoh et al., 2014). Our measured declines in AsA at the 6th nodal positions in ozone-treated plants are consistent with some previous studies, wherein total endogenous AsA declined with ozone exposure in white stonecrop (Castillo & Greppin, 1988), soybean (Guri, 1983), and papaya (Yeoh et al., 2014). The small ozone-induced declines measured in this study may reflect the net effect of the simultaneous dynamic responses of both AsA synthesis and loss via ozone quenching (Akram et al., 2017). Overall, AsA responses appear conflicting, with small net responses being measured between leaf nodal positions and treatments, and therefore warrant future investigation by taking leaf samples during or immediately after fumigaiton.

Of note was the difference in acropetal chlorophyll gradient between the two cultivars, coupled with a pronounced ozone effect (Figure 3a). While foliar chlorophyll decline is a marker of endogenous senescence, it is also known to increase as a hormesis effect in response to stress (Agathokleous et al., 2019; 2020). Moreover, increased H_2O_2 levels (as in Figure 4b) has been shown to stimulate chlorophyll under water deficit conditions (Ashraf et al., 2015), and may act similarly in other abiotic stress, thus playing a key role as a protective compound/stress conditioning response in the hormesis effect (Agathokleous et al., 2020). This is evident here as although ozone-

induced senescence occurred at the lower nodal positions, there was no decrease in chlorophyll content at the 6th nodal position in Click and a marked increase in Phoenix. The difference in response between leaf nodal positions, suggest that traditional leaf sampling methods (i.e. selecting the youngest fully expanded leaf; as in Roberts et al., 2022, etc) mask physiological sensitivity to abiotic stress. Specifically, in this study, the youngest fully expanded leaf in Phoenix may have been stimulated by ozone at the time of sampling, presenting an apparent physiological ozone tolerance that is not observed in other leaves.

The high H_2O_2 levels in Phoenix were likely driven by high levels of gas exchange (Figures 4.4 and 4.1). Increased H_2O_2 production is a known by-product of photosynthesis (Hüve et al., 2015), and the measurements in this study may solely reflect this. Moreover, it has been observed that plants may exhibit ozone injury caused by increased ROS before lipid peroxidation thus MDA formation (Scandalios, 1997) and that appeared to be the case here. High levels of AsA did not prevent oxidative damage (MDA) caused by exposure to high real-world ozone levels. The apparent lack of relationship between H_2O_2 and MDA in both cultivars presents H_2O_2 as a local signal in an acropetal gradient, possibly functioning as a signal for preventing oxidative damage (Rhee, 2006), or aiding cellular expansion enzymes at higher nodal positions (Foyer, 1997; Smirnoff, Nicholas & Arnaud, 2019). Overall, H_2O_2 is key in leaf responses to external factors, blurring the lines between ageing, cell signalling, and senescence.

The high variability shown in some of our observations is most likely due to the (lack of) representativeness of using a 6 cm^2 portion of a leaf for measurements given potential microclimate effects, and this study therefore raises several avenues for further research - not only to identify and exploit biochemical and/or physiological ozone tolerance but also to improve leaf-level sampling and measurement techniques. Extending the duration of similar experiments may produce more pronounced and significant results, and importantly show whether final yield would be similarly maintained in this laboratory-based study compared to larger glasshouse studies (De Bock et al., 2012; Roberts et al., 2022) and under field conditions. Furthermore, measuring additional markers of oxidative stress and tolerance, e.g. ascorbate-glutathione cycle during (rather than after) fumigation may provide further insight into OSR's defence response to real-world ozone exposure and identify a more suitable and applicable marker for ozone tolerance than AsA (Örvar and Ellis, 1997; Pasqualini et al., 2001; Wu et al., 2017).

4.6 Conclusions

We quantified the effect of realistic ozone conditions on acropetal gradients in physiology and biochemistry in a shorter-lived oilseed rape (OSR) cultivar (spring OSR, cv. Click) and longer-lived cultivar (winter OSR, cv. Phoenix) and provide further insight into multi-leaf ozone responses. Our results provide evidence that Click is more ozone tolerant, i.e. better able to maintain productivity, despite having lower total

ascorbic acid (AsA) levels than Phoenix, primarily due to a decline in stomatal conductance and therefore lower ozone uptake in Click. Our results indicate that Click avoids ozone uptake thus limiting stress and damage whereas Phoenix limits damage by diverting photosynthate from growth to defence. We also found AsA to be a constituent molecule independent of nodal position in pre-senescent and senescent OSR leaves. Although total AsA is not a simple predictor for physiological and morphological ozone tolerance in OSR, this study provides a more detailed understanding of constituent and leaf-level responses. Furthermore, selection of multiple leaves at different nodal positions on the same plant presented findings which are contrary to previous studies. Essentially, we find that multiple leaf-level measurements are required to understand and identify physiological tolerance which may be otherwise masked through hormesis effects. Overall, there is a greater need for multiple leaf-level measurements along with the identification and development of easily applied ozone tolerance markers to enable growers and breeders to select and breed ozone tolerant OSR.

5. Canola *Brassica* oilseed species are more ozone-tolerant than non-canola counterparts

Author contributions

Hattie R. Roberts: Initiated experimental planning and design, carried out plant propagation and care, carried out practical experimental work, performed biochemical assays, compiled, and analysed statistical data, developed relative oxidative stress index, visualised data, prepared manuscript, and submitted manuscript.

Felicity Hayes: Participated in interpretation of results, manuscript preparation.

Ian C. Dodd: Advised experimental planning and design, participated in interpretation of results, participated in manuscript preparation.

Kirsti Ashworth: Principal Investigator. Experimental planning and design, participated in interpretation of results, participated in manuscript preparation.

Submission to journal

This chapter was submitted to *Plant, Cell, and Environment* as a primary research article in April 2023.

A summary of this chapter can be found in section 2.2

Graphical Abstract

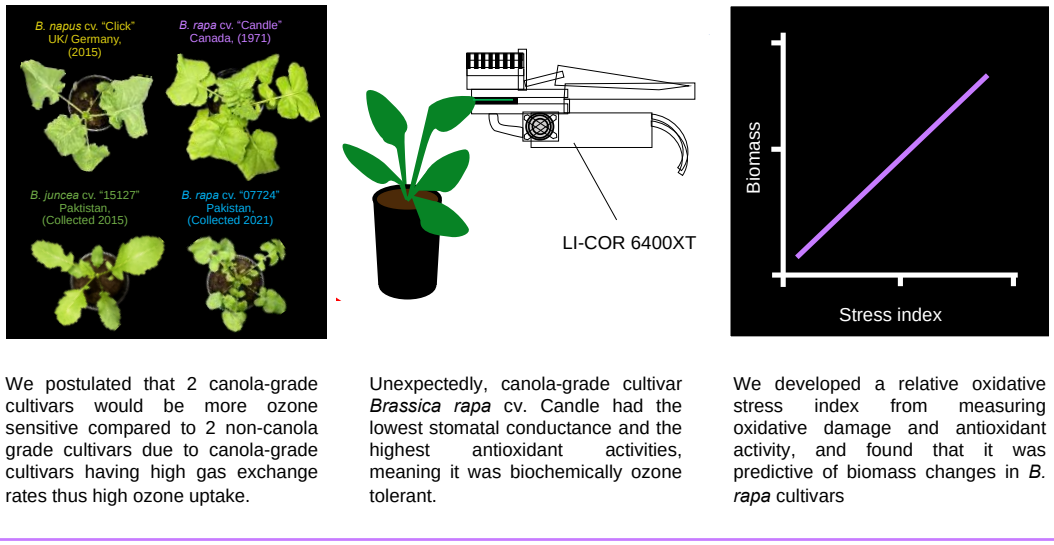

We postulated that 2 canola-grade cultivars would be more ozone sensitive compared to 2 non-canola grade cultivars due to canola-grade cultivars having high gas exchange rates thus high ozone uptake.

Unexpectedly, canola-grade cultivar *Brassica rapa* cv. Candle had the lowest stomatal conductance and the highest antioxidant activities, meaning it was biochemically ozone tolerant.

We developed a relative oxidative stress index from measuring oxidative damage and antioxidant activity, and found that it was predictive of biomass changes in *B. rapa* cultivars

5.1 Abstract

Ozone tolerance is associated with low gas exchange and hence low ozone uptake and/or high activity levels of enzymatic antioxidants such as superoxide dismutase and ascorbate peroxidase. However, intensive breeding programmes generally select for high carbon assimilation and thus high gas exchange rates, suggesting they may inadvertently select ozone sensitive cultivars. Here, *Brassica* cultivars of contrasting breeding pedigrees were exposed to typical European ozone levels (20, 50, 75, 100 ppbv) for 26 days. We measured the impacts on gas exchange, biochemical oxidative stress, and the activities of key antioxidant enzymes in two canola (*B. napus* Click and *B. rapa* Candle) and two non-canola (*B. rapa* 07224 and *B. juncea* 15127) cultivars. *B. rapa* 07224 was the most sensitive cultivar, with higher oxidative stress and damage, and lower gas exchange and shoot biomass. Its canola-grade progeny, *B. rapa* Candle accumulated less reactive oxygen species, maintained gas exchange rates, and even increased its biomass under ozone exposure. To quantify ozone tolerance, we developed a relative oxidative stress index using normalised levels of antioxidant and oxidative stress markers. Our index correlated strongly with observed changes in biomass. Applying this index should enable breeders to identify ozone-tolerant varieties and maximise tolerance without forfeiting yield.

5.2 Introduction

Brassica oilseed species are a globally important crop, used to produce food, animal feed and fuel. There are currently three dominant rapeseed species under cultivation in different global regions: *B. rapa*, *B. napus*, and *B. juncea*, with *B. rapa* considered the 'parent' species of both *B. juncea* and *B. napus*, as demonstrated in The Triangle of U (as in Xue et al., 2020 and adapted in Figure 1.1, Chapter 1). The three *Brassica* species. Can be readily interbred to produce hybrid species (Lefol et al., 1997; Choudhary et al., 2000). *B. napus* is the major oilseed crop globally, with 30 million tonnes cultivated in Europe, North America, and Australia in 2021. Both *B. juncea* and *B. rapa* are widely cultivated in India and Pakistan, while *B. napus* and *B. rapa* are grown in China and Scandinavia (USDA, 2023). The combined global yield of these *Brassica* oilseeds is ~86 million tonnes annually, only 23% of soybean yields but providing the same calorific content (USDA, 2023).

Extensive crop breeding programmes have traditionally selected for commercially important rapeseed traits, including high seed yield, oil content and quality, to meet strict market regulations (FOFSA, 2016). Moreover, meeting canola-quality guidelines requires tight control of sowing time, and nutrient, pesticide, and fungicide applications, to ensure in-field seed quality. These guidelines further stipulate that seeds must reach >40% oil, <2% erucic acid, and <20 ppm chlorophyll content to maintain canola-grade status (Bommarco et al., 2012; FOFSA, 2016). However, climate change-related abiotic stresses including exposure to ozone (Tripathi and Agrawal, 2012; Huang et al., 2019; Roberts et al., 2022) can increase the content of undesirable compounds such as chlorophyll, erucic acid, and Glucosinolates in seeds. Breeding programmes usually select crops with high productivity, and therefore high gas exchange, stomatal conductance, and photosynthetic rates (Long et al., 2006; Roche, 2015), which may also increase their sensitivity to abiotic stresses by increasing water loss and uptake of phytotoxic pollutants such as ozone.

High levels of the secondary pollutant ozone decrease crop yield and quality (Mills et al., 2018). *Brassica* oilseeds are considered moderately sensitive to ozone (Mills et al., 2007), with exposure to ozone concentrations of ~100 ppbv over a growing season shown to decrease thousand seed weight by 20-40% (Roberts et al. 2022). Once taken up via stomata, ozone rapidly dissolves in the apoplastic space, damaging lipid membranes and primary metabolic pathways (Grulke and Heath, 2020). These oxidation reactions produce reactive oxygen species (ROS), such as superoxide ($O_2^{\bullet-}$) and hydrogen peroxide (H_2O_2) (Sharma et al., 2012). Oxidative stress occurs when ROS production exceeds defensive mechanisms, thereby disrupting gas exchange, and decreasing biomass accumulation (Choudhury et al., 2013). Photosynthate may be diverted from primary metabolism to secondary metabolism (enzymatic antioxidant synthesis), which is encompassed in the optimal defence theory (McKey, 1974). This theory states that the most productive plant parts, i.e., young leaf tissue, will have high constitutive antioxidant levels, thus conferring biochemical (ozone) tolerance (Fagerstrom et al., 1987; McCall and Fordyce, 2010). To prevent oxidative stress, enzymatic and non-enzymatic antioxidants produced by the plant decrease ROS, either

directly by quenching or indirectly by donating electrons to enzymatic antioxidants (Farooq et al., 2019).

Enzymatic antioxidants, in particular superoxide dismutase (SOD) and ascorbate peroxidase (APX), have long been associated with abiotic stress tolerance (Giannopolitis and Ries, 1977). SOD is considered a primary enzymatic antioxidant in *Brassica* oilseed crops, initiating a series of reactions by reducing superoxide to H_2O_2 (Lee et al., 2003; Jalali-e-Emam et al., 2011). In turn, H_2O_2 is quenched to water and oxygen by other enzymatic antioxidants, of which APX is key. Many abiotic stresses such as salinity, cold (Verma et al., 2019), waterlogging, and drought (Su et al., 2021) upregulate SOD genes in all three *Brassica* oilseed lines. Increased SOD and APX activity have been associated with decreases in ozone-induced programmed cell death (PCD) and promotion of plant growth in Brassicaceae (Lee and Bennett, 1982; Shafi et al., 2015; Gill et al., 2015). However, biochemical synthesis of these secondary compounds is metabolically costly, as photosynthate may be diverted from biomass allocation, reducing yield (Barto and Cipollini, 2005; Wolinska and Berens, 2019). While studies have used enzymatic antioxidants as markers of abiotic stress tolerance (Fiscus et al., 2005), results are often presented in isolation and are rarely suitable to inform crop breeding. Developing and applying a parsimonious numeric scale, a "relative oxidative stress index" to directly compare oxidant and antioxidant levels in different lines would provide a quantitative measure of ozone tolerance. This would enable future breeding programmes to select varieties with greater ozone-tolerance thus ensuring growers are able to maximise their profits by cultivating oilseeds that reliably provide high-quality edible food products, regardless of environmental conditions.

Two *B. napus* cultivars with differing growth rates had contrasting ozone sensitivities (Roberts et al., 2022). The cultivar with the shorter lifecycle better maintained oilseed yield than the slower-growing cultivar, despite more substantial declines in gas exchange and chlorophyll content. However, it was unclear whether this difference in physiological sensitivity was due to differences in gas exchange rates and hence ozone uptake, or activities of key antioxidants. In the present study, we directly compare the physiological, biochemical, and morphological responses across all three key *Brassica* oilseed lines when exposed to agronomically-relevant ozone levels. We surmised that the more intensively bred lines likely show increased ozone sensitivity due to: (1) higher ozone uptake via the stomata, and (2) lower antioxidative (SOD and APX) activity. Our specific hypotheses are that:

i. Canola-grade cultivars, the result of intensive breeding programmes, will have higher stomatal conductance, and therefore ozone uptake, than non-canola-grade lines.
ii. Cultivars with higher enzymatic antioxidant (SOD and APX) activity will accumulate less ROS due to scavenging and therefore exhibit less oxidative damage.

To test our hypotheses, we measured the impacts of real-world ozone levels on gas exchange, oxidative stress and tissue damage, and the activities of key antioxidant enzymes SOD and APX in four lines differing in crop improvement pedigree (improved

B. napus Click and *B. rapa* Candle *versus* non-improved *B. juncea* 15127 and *B. rapa* 07224).

5.3 Methodology

5.3.1 Cultivar selection and plant care

Seeds were donated by Centre for Genetic Resources, The Netherlands (CGN) and Deutsche Saatveredelung AG (DSV). Four lines of *Brassica* oilseeds were sown: two advanced canola-grade lines, *B. napus* Click (developed 2011, Germany; DSV) and *B. rapa* Candle (developed 1973; Canada; CGN); and two traditional cultivar/landrace rapeseed lines, *B. rapa* 07224 and *B. juncea* 15127 (CGN; both originally collected from arable farm stores in Pakistan in 2015 and 2021).

The four *Brassica* lines were sown in bedding packs of John Innes no. 2 soil in a naturally lit glasshouse on May 8th, 2022. All lines germinated 3 to 6 days later. Single plants of uniform size and growth stage (GS12) were transplanted into John Innes no. 2 soil in 2 L pots (ø = 14 cm (top), 9.5 cm (base), d = 18.2 cm) on May 21st. On June 6th, at GS14-15, 9 plants of each line were transferred to each of four 1 m^3 independently lit and fumigated growth chambers (Figure 8.4) to allow acclimation to the chamber light regime of 14-hr light at 321.2±23.2 μmol photons m^{-2} s^{-1} (Powerstar HQI-BT, 600 W/D daylight, OSRAM, Munich, Germany) and temperature (21.2±1.01°C). The 36 pots per chamber at the start of the experiment were reduced to 32 on June 19th, and then to 16 on July 3rd, as plants were harvested for biochemical analyses of leaf tissue. Plants were kept well-watered by 100% daily replacement of evapotranspiration losses based on pot weight and were rotated within chambers every two days to limit chamber effects. Chamber relative humidity, temperature (RH 2nl-02 Humidity Sensors; Fenwal UUA32J2 2K Thermistors) and leaf-level PAR (QS2 Quantum Sensors) were continuously monitored and recorded using data GP2 loggers (sensors and loggers from Delta-T, Cambridge, UK).

5.3.2 Ozone fumigation system

Plants were exposed to one of 4 ozone levels for 8 hours per day (09:00-17:00): ambient (~20 ppbv), 50 ppbv, 75 ppbv, and 100 ppbv over 26 days. A high-voltage ozone generator (Opti Sciences, New Hampshire, USA) was supplied with compressed air, filtered using a scrubber containing glass wool, carbon, and a desiccant, at a flow rate of 400 cm^3 s^{-1}. From the generator, ¼-inch PTFE tubing delivered ozone at the required rate to each chamber via needle valves (Swagelok, Ohio, USA). Ozone was mixed with external ambient air at the top of each chamber using perforated PTFE tubing and circulated at 100 cm^3 s^{-1}. Ozone levels were logged at canopy height (30 cm) every 20 minutes using a PTFE tubing line from each chamber connected to two ozone monitors (Model T400 and Enviro 600 ozone analyser, Enviro Technology Services, Gloucestershire, UK). Fumigation ceased overnight, reflecting a real-world diurnal profile. Fumigation was suspended on days 13 and 26 to allow measurements to be conducted safely.

5.3.3 Leaf gas exchange measurements

Leaf gas exchange was measured on experimental days 0, 13, and 26 from an area 2 cm from the main vein on the youngest fully expanded leaf using an automated photosynthesis system (LI-COR 6400XT) with a 6-cm^2 LED chamber head (LI-COR biosciences, Nebraska, USA). LI-COR chamber conditions closely matched growth conditions at average canopy height: RH 55%, leaf temperature 23°C, CO_2 400 ppm, PAR 400 µmol photons m^{-2} s^{-1}. The flow rate through the chamber head was 300 mmol sec^{-1}. Instantaneous measurements were logged once chamber conditions had stabilised (5-10 minutes). Chlorophyll fluorescence F_v/F_m and non-photochemical quenching, NPQt, were then collected using a MultiSpeQ 2.0 (PhotosynQ, Minnesota, USA) from the same location on the leaf. Leaf area of the sampled leaf, and total leaf area were measured using a leaf area meter (LI-COR biosciences, Nebraska, USA). The number of leaves per plant, and fresh and dried masses were also recorded.

5.3.4 Biochemical assay: Leaf tissue sampling and reagent preparation

Leaf tissue samples were collected following measurements (n = 4 per treatment and timepoint) for subsequent analyses of hydrogen peroxide (H_2O_2; a measure of ROS) and malondialdehyde (MDA; a measure of lipid peroxidation) content, and SOD and APX activities to monitor changes in oxidative stress, damage, and antioxidant activity. At each time, 1g leaf tissue was taken using a 1-cm^2 corkborer from an area 2 cm from the main vein in the youngest fully expanded leaf on the opposite side of the vein to that used for physiological sampling. Tissue samples were placed into punctured 2 ml Eppendorf tubes and immediately frozen in liquid nitrogen. Samples were stored at -80 ˚C until analysed, a period of ~8 weeks.

Each solution required for the biochemical assays detailed below was made in autoclaved volumetric flasks with deionised water less than 24 hours before assays were performed. Reagents were agitated using a stirrer (Apex Digital Pro hotplate stirrer, Apex Scientific, Kwazulu-Natal, South Africa). pH was checked using a pH meter (Milwaukee Mi 151, Milwaukee Electronics Kft., Szeged, Hungary), and adjusted using 1M NaOH or 1M HCl as needed. Reagents and stock solutions were sourced from Sigma-Aldrich (Dorset, UK), unless otherwise stated.

5.3.5 Oxidative stress: Hydrogen peroxide and malondialdehyde

Thioacetal acid (TCA) at 4°C was added at 1 ml 0.1% to 100 mg frozen leaf tissue in 1.5 ml Eppendorf tubes. Two sterilised Tungsten carbide beads were added to each Eppendorf tube and lids were secured. The samples were ground in batches of 10 for three minutes at 30 Hz using an ice-cooled Tungsten carbide bead mill (MM400 mixer mill; Retsch, Germany). After grinding, samples were checked for uniform consistency, kept at 4 ˚C and centrifuged at 15000 RPM for 30 mins (Jouan CR3i multifunction, Thermo Fisher Scientific, MA, USA). Samples were placed on ice in a polystyrene box and 400 µl supernatant was aliquoted for each assay.

Hydrogen peroxide (H_2O_2) assays were determined using a spectrophotometer (Ultrospec 2100 pro, Biochrom Ltd., Cambridge, UK) following the methods initially

detailed in Ovenston and Rees (1950) and refined by Junglee et al. (2014). Initially, eight standards (each with a technical replicate) ranging from 0 to 400 µmol H_2O_2 were made from a 10 mM H_2O_2 stock solution. 400 µl supernatant was added to 400 µl 10 mM potassium phosphate buffer (PPB; pH 7.0; K_2HPO_4 and KH_2PO_4) in 1.5 ml opaque centrifuge tubes. 800 µl 1 M KI solution was then added to each sample to initiate the reaction. Samples and standards were pipetted into separate disposable cuvettes and placed in an eight-sample carousel in a UV-spectrophotometer (Ultrospec 2100 pro, Biochrom Ltd., Cambridge, UK). A reference sample comprising 400 µl PPB, 400 µl TCA, and 800 µl KI was used to zero the spectrophotometer at 360 nm before measuring the absorption of standards and samples. Concentrations of H_2O_2 in the sample solutions were calculated by comparing absorbance against a calibration curve derived from known standards.

Lipid peroxidation was deduced from malondialdehyde (MDA) levels, which were determined using the thiobarbituric acid (TBA) reactive substances assay methodology first described by Buege and Aust (1978) and outlined by Senthilkumar et al. (2021). 400 µl supernatant was added to 1 ml 0.5% TBA in 1.5 ml Eppendorf tubes with perforated lids. A reference sample was also made with 400 µl TCA and 1 ml TBA. After closing the Eppendorf tubes, reference and sample tubes were incubated for 30 minutes at 80°C in a water bath (Thermo Scientific, MA, USA). After incubation, the tubes were immediately put into ice for 5 minutes to stop the heat-initiated reaction. The tubes were centrifuged for a further 5 minutes at 15000 rpm at 4°C to form pellets of precipitate. The samples were then transferred to disposable cuvettes, as above. The reference sample was used to zero the spectrophotometer at 532 nm and at 600 nm. Absorbances of samples were then also measured at both wavelengths.

MDA concentration was calculated using its millimolar extinction coefficient, ε, such that the MDA equivalents are:

$$nmol\ MDA\ g^{-1}FW = \frac{\Delta A \cdot 3.5 \cdot x \cdot 1000}{\varepsilon \cdot \beta \cdot \gamma}$$

[Equation 1]

where: ΔA is the difference between absorptions at 532 and 600 nm ($A_{532} - A_{600}$), corrected by subtracting ΔA of the blank; β is the light path length (0.56 cm); ε is TBA extinction coefficient (155 mM^{-1} cm^{-1}); 3.5 represents the dilution factor from 400 µl extract + 1 ml TBA/TCA solution; x is the volume of TCA 0.1 % used for extraction (1 ml); γ is the frozen weight used for extraction (0.1 g); 1000 is the conversion factor of µmol to nmol (as in Du et al., 1989).

5.3.6 Antioxidant enzyme activity

Extraction buffer (1 ml 50 mM PPB and 0.1 mM EDTA) was added to 100 mg leaf tissue samples in 1.5 ml Eppendorf tubes. Two technical replicates of each sample were taken: 1 ml PPB with pH 7.8 was added to one technical set and used for Bradford and SOD assays, and 1 ml PPB at pH 7.0 was added to replicates used in APX assay. The

samples were ground, centrifuged and put on ice, as described for H_2O_2 and MDA samples (*section 5.3.5)*.

Total protein content, needed to quantify SOD and APX activity of samples, was determined using the Bradford Assay (1976), which was prepared by mixing 100 mg Coomassie Blue G250 (Merck Group, 64293, Germany) with 50 ml 95% ethanol and 850 ml de-ionised water, before adding 100 ml 85% v.v. phosphoric acid. The solution was filtered using Whatman filter paper no. 1 to remove any undissolved Coomassie Blue G250. A reference sample of 400 µl 50 mM PPB (pH 7.8) and Bradford Reagent was used to zero the spectrophotometer at 595 nm. Samples consisted of 10 µl leaf extract, 90 µl extraction buffer, and 900 µl of Bradford reagent, which were combined in 1.5 ml Eppendorf tubes and incubated in the dark at 25˚C for 30 minutes, after which samples were pipetted into disposable cuvettes. Absorbance was measured at 595 nm. Standards were made by replacing supernatant with 7 known concentrations of bovine serum albumen (BSA; Merck Group, 64293, Germany) ranging from 0 to 200 µg/ml. Total protein content in sample solutions was determined by comparing absorbance values against a calibration curve of the BSA standards.

SOD activity was measured using the inhibition of nitroblue tetrazolium (NBT) reduction by superoxide (Giannopolitis and Ries; 1977) with methodology outlined by Elavarthi and Martin (2010). A reaction mixture consisting of 2 mM EDTA, 9.9 mM L-methionine, 0.025% Triton-X100, and 55 µM NBT was added to 100 µl supernatant in each of a translucent (Thermo Fisher Scientific, MA, USA) ('light' sample), and an opaque 2 ml microcentrifuge tube ('dark' sample). Reference samples, referred to as 'control' and 'blank' respectively, were made by replacing the supernatant with 100 µl PPB (50 mM, pH 7.8). The reaction was initiated by adding 20 µl of 1 mM riboflavin. The 'light' and 'control' samples were placed in a polystyrene box illuminated with a fluorescent lamp for 10 minutes, while the 'dark' and 'blank' sample tubes were placed in an identical but unlit box. After this, references and samples were immediately transferred to the spectrophotometer and absorbance of 'dark' and 'light' samples measured at 560 nm, with the 'blank' used to zero the spectrophotometer. SOD activity, with one SOD unit representing the amount of SOD inhibiting NBT photoreduction, was calculated using the following:

$$\mathrm{SOD} = \frac{(A_{control} - \Delta A_{sample})}{A_{control} \cdot \mathrm{P}}$$

[Equation 2]

where: SOD is SOD activity in U mg^{-1} protein; $A_{control}$ is absorbance of 'control' sample; ΔA_{sample} is the absorbance of the 'dark' sample subtracted from the corresponding 'light' sample; P is protein content of each sample in mg.

Ascorbate peroxidase (APX) activity was determined by measuring the rate of consumption of ascorbic acid (AsA), as APX uses AsA as a specific electron donor to catalyse the decomposition of H_2O_2 into H_2O and O_2 (Nakano and Asada 1981; Caverzan et al., 2012). A reaction mixture was made containing 100 µl supernatant, 600 µl 50 mM potassium phosphate buffer (pH 7.0), 100 µl of 5 mM ascorbate and 100

µl of 1 mM EDTA in 1.5 Eppendorf tubes and was pipetted into disposable cuvettes. 100 µl 20 mM H_2O_2 was added to initiate the reaction and the sample agitated using a mechanical pipette. Absorbances were measured at 290 nm immediately after agitation, and again 2 minutes later. A reference sample with the supernatant and H_2O_2 replaced by the extraction buffer was used to zero the spectrophotometer. APX activity of samples was calculated as:

$$\mathrm{APX} = \frac{(A_0 - A_2)}{\varepsilon \cdot \mathrm{t} \cdot \mathrm{P}}$$

[Equation 3]

where: APX is APX activity in U mg^{-1} protein; A_0 is the absorbance of the sample immediately after adding H_2O_2; A_2 is absorbance of the same sample 2 minutes later; ε is the ascorbate molar extinction coefficient (2.8 mM^{-1} cm^{-1}); t is the incubation time; P is the protein content in the test sample in mg.

5.3.7 Biochemical stress intensity index

We defined a Relative Oxidative Stress Index (rOSI) by adapting phenotypic indices used in crop breeding, as described by Fischer and Maurer (1978), and a human-health oxidative stress index, after Škrha and Hilgertová (1999). rOSI was calculated using values of H_2O_2, MDA, SOD and APX for each sample normalised against those under control conditions., such that:

$$\mathrm{rOSI} = \sum \bar{x}\left(1 - \frac{\chi s\mathrm{APX} + \chi s\mathrm{SOD}}{\chi a\mathrm{APX} + \chi a\mathrm{SOD}}\right) + \left(1 - \left(\frac{\chi s\mathrm{MDA} + \chi s\mathrm{H_2O_2}}{\chi a\mathrm{MDA} + \chi a\mathrm{H_2O_2}}\right)(\cdot -1)\right)$$

[Equation 4]

where: $\chi a\mathrm{APX}$ and $\chi a\mathrm{SOD}$ are the average APX and SOD activity for each genotype under ambient conditions (i.e. at an ozone concentration of 20 ppbv); $\chi s\mathrm{APX}$ and $\chi s\mathrm{SOD}$ are the observed activities under each stress treatment (50, 70, 100 ppbv); $\chi a\mathrm{MDA}$, $\chi a\mathrm{H_2O_2}$, $\chi s\mathrm{H_2O_2}$, and $\chi s\mathrm{MDA}$ are the equivalent for MDA and H_2O_2 content. The resulting values lay between -1.0 (low oxidative stress, i.e. highly ozone tolerant) and 1.0 (high oxidative stress, i.e. highly ozone sensitive). To account for stress intensity and duration these were plotted against cumulative ozone exposure such that:

$$CEO_3\ (mmol\ mol^{-1}\,\mathrm{h}) = [O_3] \cdot H \cdot D \cdot 10^{-3}$$

[Equation 5]

where: $[O_3]$ is ozone concentration in mol, H is number of hours, and D number of days (Lombardozzi et al., 2013).

5.3.8 Statistical analysis

Data was compiled in Microsoft Excel (Microsoft Corporation, USA) and analysed/visualised in R Studio (R Foundation for Statistical Computing, Vienna, Austria). After testing data for normality (Bartlett test) and homogeneity of variances

(Levene's test), analyses of covariance (ANCOVA) and regression analyses (linear and curvilinear models) were used where appropriate to deduce the effects of ozone, time point and *Brassica* line on gas exchange, physiology, morphology, and biochemistry. Where regression analyses were used, models with the lowest Akaike's Information Criterion (AIC) value determined model choice. R Package *ggplot2* was used to produce scatter and faceted bar plots.

5.4 Results

5.4.1 Leaf gas exchange

Gas exchange declined over time and with increasing ozone concentration in all lines, but the effect was more pronounced in the non-canola lines, *B. rapa* 07224 and *B. juncea* 15127. For these lines, stomatal conductance (g_s) decreased by 90% (Figure 5.1a) and net photosynthetic rate (P_{net}) by 63% in *B. rapa* 07224 and 73% in *B. juncea* 15127 (Figure 5.1b) under the highest ozone concentration (100 ppbv). Although gas exchange also generally declined, though to a lesser extent, in the canola-grade lines, *B. napus* Click and *B. rapa* Candle, there were notable exceptions at the highest concentration. While g_s declined by 90% relative to ambient under 75 ppbv, g_s was three times higher at 100 than 75 ppbv on Day 26 in both lines, suggesting incomplete stomatal closure under the highest cumulative exposure (Figure 5.1a and 5.1b). Despite these differences, all lines showed a statistically similar relationship between P_{net} and g_s, indicating similar intrinsic water use efficiency ($_i$WUE, the slope of Figure 5.1c).

Overall, the canola-grade *B. rapa* Candle had significantly lower average g_s and P_{net} than the non-canola *B. rapa* 07224 across all timepoints and ozone treatments ($P <$ 0.01**). Despite its low gas exchange and therefore ozone uptake, maximum quantum use efficiency of PSII (F_v/F_m) declined by 17%, and non-photochemical quenching (NPQ_t) increased by three-fold between ambient and 100 ppbv (Table 8.4). By contrast, *B. rapa* 07224 which showed the highest leaf gas exchange, and therefore the highest ozone uptake, appeared less physiologically affected than any other line.

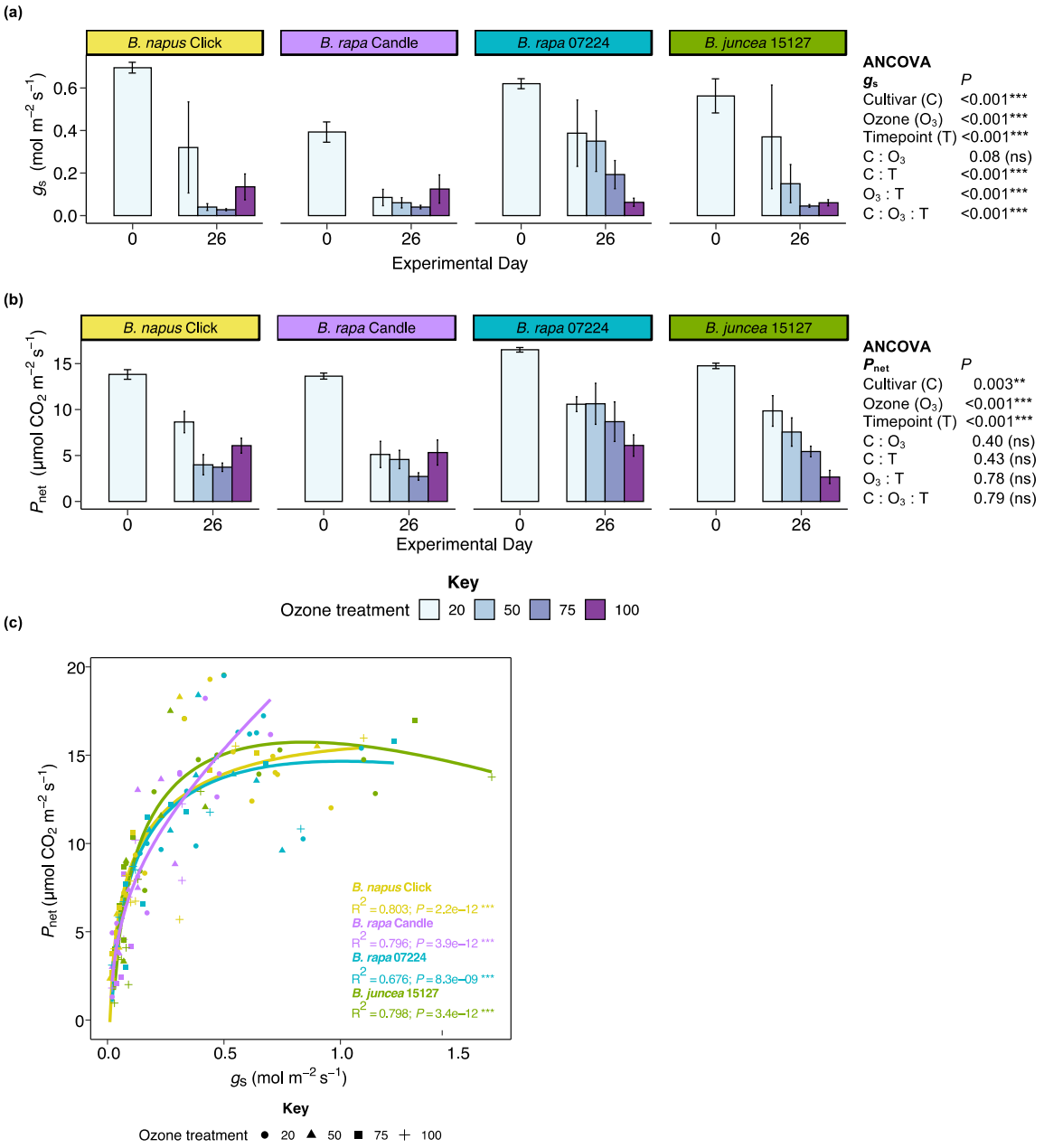

Figure 5.1 Average (a) stomatal conductance (g_s) and (b) net photosynthetic rate (P_{net}) of canola (*B. napus* Click and *B. rapa* Candle) and non-canola-grade *Brassica* cultivars (*B. rapa* 07224 and *B. juncea* 15127) after 0, 13 (shown in Table 8.4) and 26 days of ozone fumigation; n = 4, ±SEM. (c) Relationship between P_{net} plotted against g_s. Symbols represent individual plants and shapes of points show ozone treatment, with lines representing intrinsic water use efficiency ($_i$WUE), R^2 and *P* values present linear model outputs showing significant relationships. Statistical significance indicated by asterisks such that *P* <0.05 *, *P* <0.01 **, *P* <0.001 ***.

5.4.2 ROS and lipid peroxidation

Greater ozone exposure significantly increased H_2O_2 concentrations (a marker of oxidative stress) in all lines, with higher values in the non-canola-grade cultivars. *B. rapa* 07224 presented significantly higher H_2O_2 levels, with a 30-fold increase by day 26 under 100 ppbv ozone relative to ambient and a five-fold increase in *B. juncea* 15127 but only a three-fold increase in *B. rapa* Candle (Figure 5.2a). Similar increases were observed in *B. napus* Click across all treatments, whereas 50 ppbv ozone only increased H_2O_2 by 4-fold on day 26 in *B. rapa* Candle. Overall, ozone treatment significantly increased H_2O_2, with the most substantial increases in *B. rapa* 07224.

Similarly, MDA concentration, a marker of oxidative damage, was significantly higher in *B. rapa* 07224 than other lines (P <0.01** for all lines; Figure 5.2b) with a 25-fold increase at an exposure of 100 ppbv relative to ambient. The canola-grade cultivars presented the lowest MDA levels, with no significant change with either time or ozone treatment (Figure 5.2b). MDA levels had a strong positive linear relationship with H_2O_2 in *B. rapa* 07224, with relatively weaker relationships in *B. juncea* and *B. rapa* Candle, and no significant relationship in *B. napus* Click (Figure 5.2c). Overall, *B. rapa* 07224 presented the highest levels of both MDA and H_2O_2 at the highest ozone treatment, indicating that *B. rapa* 07224 suffered the highest oxidative stress and damage levels, caused by increasing ROS levels with increasing ozone exposure.

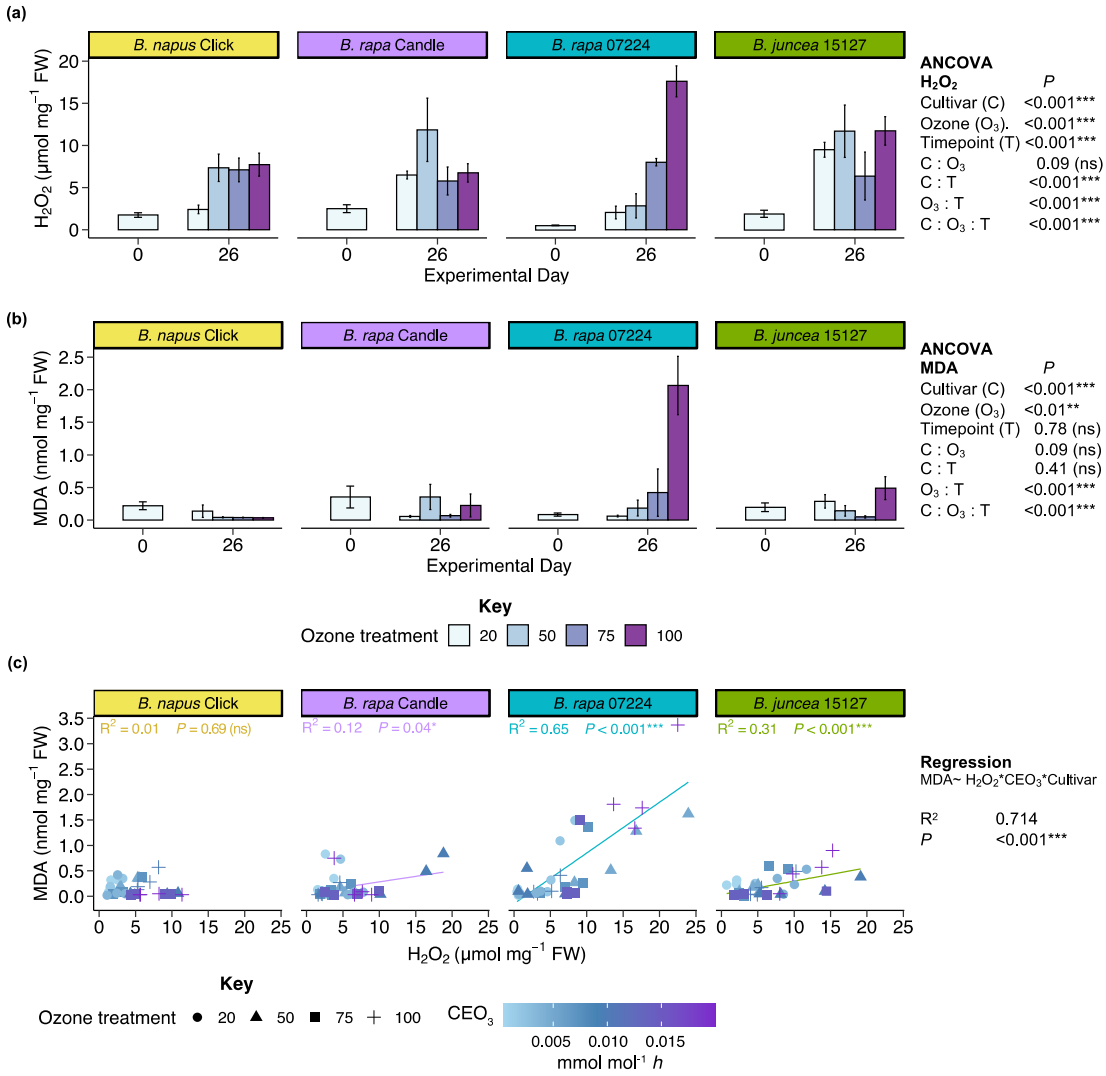

Figure 5.2. Average (a) hydrogen peroxide (H_2O_2) and (b) malondialdehyde (MDA) concentrations of two canola (*B. napus* Click and *B. rapa* Candle) and non-canola-grade *Brassica* cultivars (*B. rapa* 07224 and *B. juncea* 15127) at experimental days 0, 13 (shown in Table 8.4) and 26; n = 4, ±SEM. (c) Relationship between H_2O_2 and MDA, Symbols represent individual plants and shapes of points show ozone treatment. R^2 and *P* values present linear model outputs. Statistical significance indicated by asterisks such that *P* <0.05 *, *P* <0.01 **, *P* <0.001 ***.

5.4.3 Antioxidant enzyme activity

SOD activity, indicating the rate of formation of H_2O_2, generally increased in canola-grade lines with increasing ozone treatment and time. The highest absolute activities, however, were observed under 75 ppbv with SOD activity doubling in *B. napus* Click and increasing four-fold in *B. rapa* Candle relative to ambient (Figure 5.3a). By contrast, the non-canola grade lines presented non-linear changes in SOD activity with increasing ozone treatment and time. *B. rapa* 07224 had the highest SOD activity under 100 ppbv halfway through the experiment (Day 13; Figure 8.), after which activity declined by 73%. While SOD activity did not change by Day 13 in *B. juncea* 15127, there was a similar relative decline, of 64%, between Days 13 and 26 under 100 ppbv ozone.

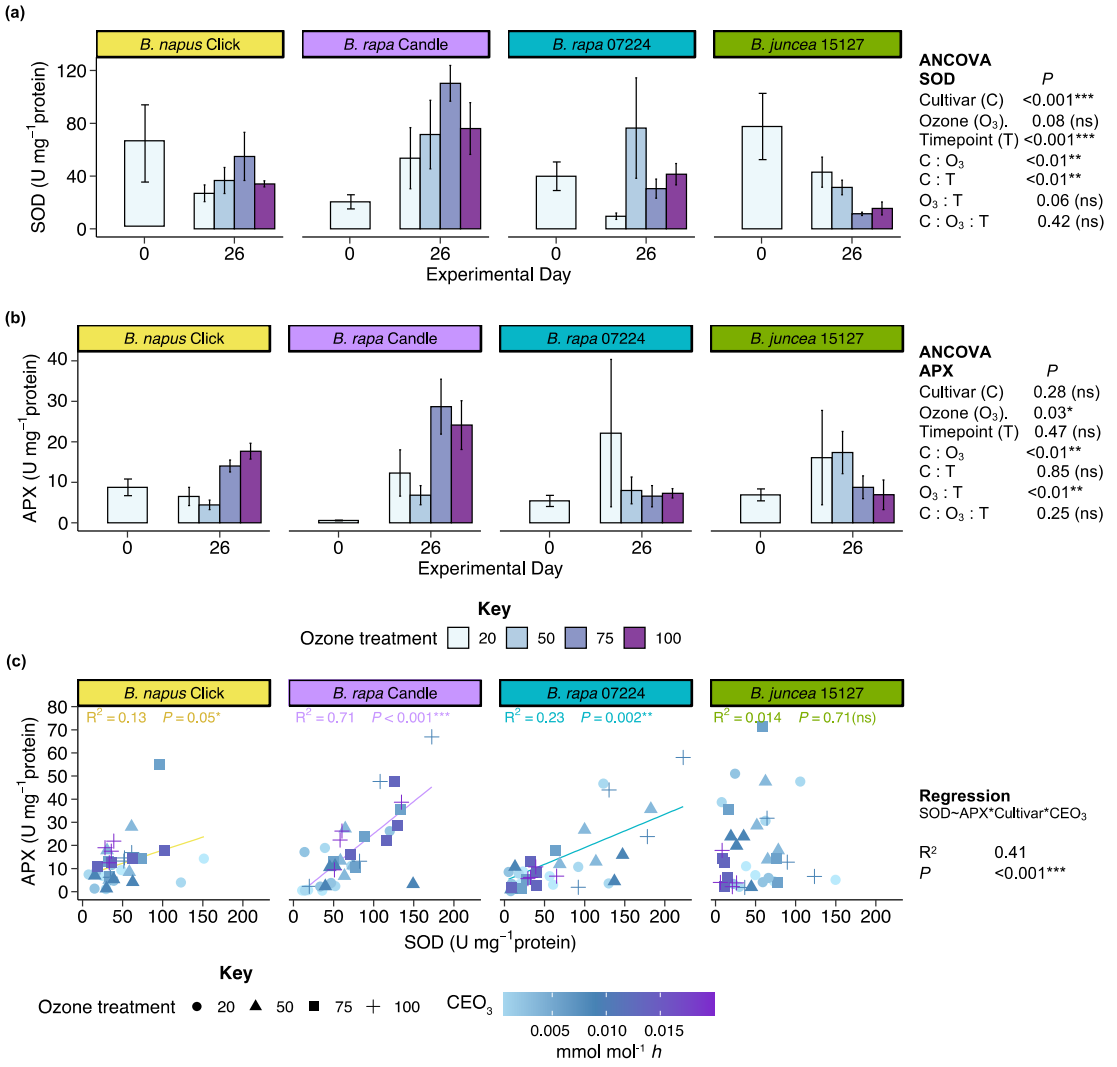

Figure 5.3. Average (a) superoxide dismutase (SOD) and (b) ascorbate peroxidase (APX) activities in tissue samples taken from two canola (*B. napus* Click and *B. rapa* Candle) and non-canola-grade *Brassica* cultivars (*B. rapa* 07224 and *B. juncea* 15127) at experimental days 0, 13 (shown in Table 8.4) and 26; n = 4, ±SEM. (c) Relationship of APX against SOD activities. Symbols represent individual plants and shapes of points show ozone treatment. R^2 and *P* values present linear model outputs. Statistical significance indicated by asterisks such that *P* <0.05 *, *P* <0.01 **, *P* <0.001 ***.

APX activity, a measure of the rate at which H_2O_2 is reduced to water, tended to be higher in canola-grade lines, with APX activity doubling by Day 26 in *B. rapa* Candle under both 75 and 100 ppbv compared to ambient. The relationship was similar for *B. napus* Click but, as with SOD activity, APX activity was a third lower than in *B. rapa* Candle. APX activity also tracked that of SOD activity in the non-canola cultivars, with strong increases by Day 13 followed by large relative declines by Day 26. This was most evident in *B. rapa* 07224, in which APX activity increased three-fold at 100 ppbv relative to ambient at the mid-point (Table 8.4) before declining by as much as two-thirds in all treatments by day 26. APX and SOD activities were significantly positively correlated for all lines except *B. juncea* 15127.

5.4.4 Relative oxidative stress index (rOSI)

Despite apparent similarities in physiological and biochemical responses, the relative oxidative stress index (rOSI) markedly differed between the four cultivars. Small positive increases occurred in both *B. juncea* 15127 and *B. napus* Click with rOSI reaching 0.04 for *B. napus* Click and 0.09 for *B. juncea* 15127 at the highest cumulative exposures (~0.020 mmol mol^{-1} h ozone). However, the two *B. rapa* cultivars showed more extreme and contrasting responses (Figure 5.4), with a strong positive increase of 0.49 in the non-canola grade *B. rapa* 07224 at a CEO_3 of 0.020 mmol mol^{-1} h and a similar decrease, to −0.31 at ~0.014 mmol mol^{-1} *h*, in the canola-grade *B. rapa* Candle. This negative value indicates that antioxidant activity increased in *B. rapa* Candle with increasing CEO_3 resulting in less damage from ROS. By contrast, *B. rapa* 07224 appears highly ozone sensitive with substantially higher levels of oxidative damage with

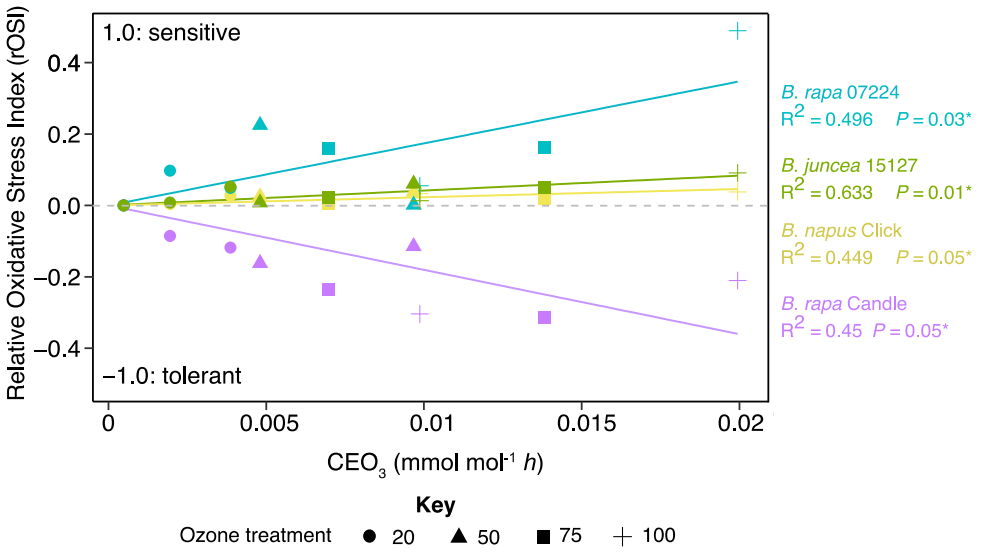

Figure 5.4. Oxidative Stress Index in two canola (*B. napus* Click and *B. rapa* Candle) and non-canola-grade *Brassica* cultivars (*B. rapa* 07224 and *B. juncea* 15127) with increasing cumulative ozone exposure under four ozone treatments. Shapes of points show ozone treatment. R^2 and *P* values present linear model outputs; statistical significance indicated by asterisks such that $P < 0.05$ *, $P < 0.01$ **, $P < 0.001$ ***.

increasing CEO_3. Overall, the lowest absolute rOSI was seen in the canola-grade cultivars, *B. rapa* Candle and *B. napus* Click.

Shoot biomass and chlorophyll content

The different ozone sensitivities identified using rOSI were reflected in plant morphology. By Day 26, the non-canola grade cultivars accumulated less shoot mass as ozone exposure increased. *B. juncea* 15127 and *B. rapa* 07224 plants exposed to 100 ppbv ozone had 31% and 48% lower dried masses than ambient (Figure 5.5a). Foliar chlorophyll content also declined (by 20%) in both non-canola grade lines, suggesting foliar chlorosis, a classic ozone injury symptom (Table 8.4). Although shoot biomass of the canola-grade *B. napus* Click also decreased (by 10%) at 100 ppbv ozone relative to ambient ozone levels, it increased by 44% in *B. rapa* Candle. The differences in shoot biomass relative to ambient strongly correlated with rOSI, particularly in *B. rapa* cultivars (Figure 5.5b).

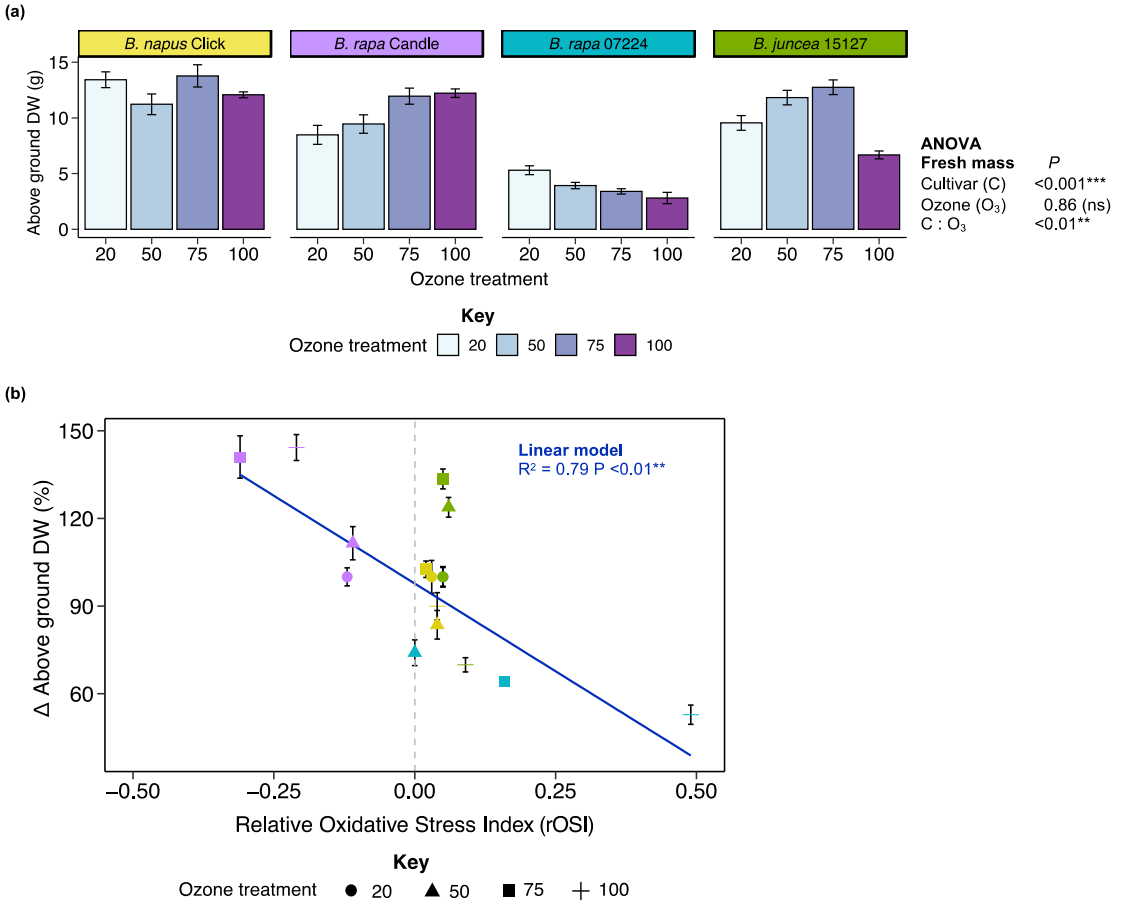

Figure 5.5. a) Average shoot biomass in two canola (*B. napus* Click and *B. rapa* Candle) and non-canola-grade *Brassica* cultivars (*B. rapa* 07224 and *B. juncea* 15127). b) Changes in dried mass relative to 20 ppbv vs rOSI. Symbols represent four plants, and shapes of points show ozone treatment. Error bars indicate ±SEM, some of which are smaller than the symbols. Regression lines shown for statistically significant (P <0.05) linear relationship between dried weight changes and rOSI.

5.5 Discussion

Ozone sensitivity has long been assessed quantitatively, by determining visible injury (Melhorn et al., 1991; Paoletti et al., 2022) or final shoot biomass (Reich, 1987; Chaudhary, and Rathore, 2021). Here, we develop and demonstrate the relevance of a novel parsimonious oxidative stress index (rOSI) that can be used as a quantitative indicator of ozone sensitivity. Across canola *vs.* non-canola cultivars of *Brassica* oilseeds, this biochemical index was correlated with decreased gas exchange, chlorophyll content, and shoot biomass of *B. rapa* 07224 (Figure 5.5; Table 8.4) and increased shoot dried mass of *B. rapa* Candle. Key enzymatic antioxidants prevent oxidative damage, with SOD reducing superoxide radical to hydrogen peroxide (H_2O_2), and ascorbate peroxidase (APX) reducing H_2O_2 to water (Hossain and Asada, 1984). These processes act independently of ozone uptake rates, which are dictated by stomatal conductance (Brosché et al., 2010).

In contrast to our first hypothesis, the least selectively bred of the four lines (the non-canola grade *B. rapa* 07224) had the highest stomatal conductance, which resulted in the highest ozone uptake into the apoplast of the four cultivars. However, high uptake may not fully account for high oxidative damage in *B. rapa* 07224 – it also had the lowest APX and SOD activities at highest ozone treatments (Figure 5.3). By contrast, the canola-grade *B. rapa* (Candle) accumulated the least ROS due to scavenging from APX and SOD (Figure 5.3) and therefore had the lowest oxidative damage (Figure 5.2), meaning that our second hypothesis, that cultivars with higher enzymatic antioxidant activity will accumulate less ROS due to scavenging and therefore exhibit less oxidative damage, was partially accepted. This line also best maintained photosynthetic rate relative to ambient due to a combination of low stomatal conductance and high enzymatic antioxidant (APX and SOD) activity (Figure 5.1b). This supports the optimal defence theory that defensive compounds are highest in the most productive tissues which increases plant fitness when under stress (Fagerstrom et al., 1987; McKey, 1974). However, the optimal defence theory does not explicitly consider stress avoidance.

Crops generally avoid (via stomatal closure) or tolerate (via biochemical defences) abiotic stresses (Tausz et al., 2007; Wang et al., 2023). By limiting ozone uptake via low stomatal conductance (avoidance) and increasing enzymatic antioxidant (here APX and SOD) activity (defence), *B. rapa* Candle effectively combines both mechanisms and hence shows least oxidative stress and damage under exposure to real-world levels of ozone. Indeed, all markers indicate the canola-grade *B. rapa* Candle was the most tolerant cultivar, with a strong negative relative oxidative stress index (rOSI; Figure 5. 4) and exposure to ozone stimulating biomass accumulation (Figure 5.5). Thus increasing ozone exposure decreased levels of damage by stimulating APX and SOD activities, similarly to ozone-tolerant soybean exposed to 65 ppbv ozone for ~60 days over two seasons (Chernikova et al., 2000), and spinach under 80 ppbv ozone for 60 days (Calatayud et al., 2003. *B. rapa* Candle therefore presented a possible hormesis effect to ozone, with low stress levels (50 ppbv ozone) stimulating antioxidant responses and increasing shoot biomass. Similarly ozone levels of 40-70 ppbv, two to three times that of ambient, stimulated antioxidant and chlorophyll levels and biomass

accumulation in herbaceous annual and perennial plants (Agathokleous et al., 2019a, 2019b; Agathokleous et al., 2020, Li et al., 2021).

The lower gas exchange of older cultivars relative to modern cultivars has long been thought to increase their tolerance to abiotic stress (Pleijel et al., 2006; Brewster et al., 2019; Yadav et al., 2020). This is evident here with the high ozone tolerance of *B. rapa* Candle (developed in 1971) compared to the other canola-grade cultivar *B. napus* Click (developed in 2011). Nevertheless, although rOSI and the increased shoot mass of *B. rapa* Candle indicate tolerance, its absolute shoot biomass and gas exchange were less than the other canola-grade cultivar *B. napus* Click.

Although ozone stimulated enzyme activity in both non-canola lines, *B. rapa* 07224 and *B. juncea* 15127, at Day 13, further increases in cumulative ozone exposure decreased enzyme activity by the end of the experiment (Day 26), suggesting a possible toxicity threshold effect. Antioxidant activity decreased in *B. rapa* 07224 under 75 and 100 ppbv ozone, corresponding to cumulative ozone exposures >0.014 mmol mol^{-1} *h* CEO_3, suggesting either damage to antioxidation processes most likely due to denatured enzymes (Lee et al., 2003), or that high ozone uptake downregulated biosynthesis pathways (Booker et al., 2012). Moreover, APX and SOD activities were not correlated in *B. juncea* 15127, suggesting a lower threshold to ozone stress for SOD and APX activities. Similarly, Lee et al. (2003) demonstrated SOD was a primary target of ozone *in vitro*, meaning it was more susceptible to inactivation than ascorbate-glutathione cycle enzymes unless severe oxidative stress occurred in plant tissues. Similarly, Booker and Fiscus (2005) found that 80 ppbv ozone tended to decrease soybean SOD activity, while peroxidases were maintained, with a response like that of APX activity in *B. juncea* in this study. Overall, SOD and APX activities present threshold effects, indicating enzymatic sensitivity to ozone in the non-canola lines through possible denaturing of enzymes.

Interestingly, the highest cumulative ozone exposures increased P_{net} and g_s in both canola-grade lines, suggesting incomplete stomatal closure (Figure 5.1a and 5.1b), possibly due to "stomatal sluggishness" (Hoshika et al., 2015). Despite lower gas exchange and therefore ozone uptake, maximum efficiency of Photosystem II (F_v/F_m) declined in *B. rapa* Candle and non-photochemical quenching (NPQ_t) increased (Table 8.4). While this line dissipated excess energy via NPQ_t compared to other lines, the apparent contradiction between performance of Photosystem II and increased shoot biomass mass show that observations of the photosystem may not be suitable or appropriate indicators of oxidative stress in *Brassica* species in short-term experiments.

Currently, *B. napus* breeding programmes take approximately six years for new cultivars to reach recommended lists (Barnes et al., 2016). Routine leaf biochemical assays such as those employed in this study could be applied to rapidly identify and develop ozone-tolerant canola cultivars, with a standardised oxidative stress index allowing high throughput biochemical screening of *Brassica* oilseed species over shorter experimental periods than traditional seasonal yield metrics. Including other antioxidants such as catalase, and other enzymes involved in the ascorbate-glutathione cycle (Sharma and Davis, 1997), in our oxidative stress index may boost its explanatory power but likely at the expense of throughput. Our parsimonious formulation

adequately predicted (R^2=0.79) shoot biomass accumulation (Figure 5.5b) similarly to other stress vs yield predictive models, such as water stress index models used to predict yield in wheat (R^2<0.84) (Rizza et al., 2004). While multiple studies show that realistic ozone concentrations impair modern crop yield and quality (Pleijel et al., 2018; Yadav et al., 2020; Tisdale et al., 2021), canola breeding programmes in the Northern Hemisphere seldom explicitly account for ozone as a potential stress (Frei, 2015). Without any easily applied selection method for ozone tolerance, growers currently risk both yield and quality losses from this hidden threat.

5.6 Conclusions

Contrary to our hypotheses, a selectively bred canola-grade cultivar, *B. rapa* Candle, had lower gas exchange, and therefore lower ozone uptake, than non-canola-grade lines. *B. rapa* Candle also had higher enzymatic antioxidant (SOD and APX) activity and therefore accumulated less ROS due to scavenging and exhibited less oxidative damage. Generally, cultivated *Brassica* varieties were more ozone tolerant than their non-canola counterparts to 'real-world' ozone conditions. Differences in shoot growth were strongly correlated with a novel relative oxidative stress index, developed here by adapting similar measures used in human health and crop phenotypic studies. This index accurately predicted differences in biomass accumulation in *B. rapa*, but further testing on other stresses, and species is needed before its possible inclusion in breeding programmes. However, the greater tolerance of canola-grade cultivars, particularly older cultivars, represents an opportunity for breeders and agronomists to exploit the diversity of oilseed *Brassica* biochemical tolerance to safeguard the economic viability of this important crop.

6. General Discussion and Conclusions

This thesis was motivated by the hidden threat that tropospheric ozone poses to globally important *Brassica* oilseed crops. As with many crops, such as soya, the increased productivity of modern crop varieties has meant that the currently recommended *Brassica* oilseed cultivars are prone to displaying symptoms of abiotic stress, such as accelerated senescence and declines in gas exchange leading to reduced productivity (Kalaji et al., 2016). This is because breeders have tended to favour increased stomatal conductance, carbon assimilation, and uniformity in advanced cultivars to achieve high yields (Digrado et al., 2020; FOFSA, 2016; Lu and Zeiger, 1994). This has led inexorably to greater sensitivity to abiotic stresses such as drought, illustrated in chlorosis and biomass declines in *B. napus*, (Ghosh et al., 2001) and relatives, such as *B. campestris* (Tripathi and Agrawal, 2012). However, little attention had been given to the effects of tropospheric ozone, although moderate-high levels (>60 ppbv) are known to impede yields in other oilseed crops such as soya (McGrath et al., 2015). The main aim of this research was to determine how *Brassica napus* (oilseed rape; OSR) and other agriculturally relevant *Brassica* oilseed species (*B. rapa* and *B. juncea*) respond to ozone concentrations representative of Northern Hemisphere conditions. To achieve this, I combined measurements of gas exchange, chlorophyll content, seed yield and quality, biochemical markers of stress, and antioxidant levels and activities in *Brassica* plants (as in Paoletti et al., 2022 and Chaudhary, and Rathore, 2021) exposed to levels of ozone between 20 and 110 ppbv, for part or most of their life cycles. This concluding chapter summarises the key findings and main achievements of each data chapter and discusses the questions which arose from these primary research studies. Avenues of further research are also identified.

6.1 Summary of chapters and key findings

After identifying key knowledge gaps in the literature, I first decided to investigate how ‘real-world’ seasonal ozone concentrations impacted two European OSR cultivars of differing life cycle lengths. I hypothesised that increasing ozone exposure would decrease both seed yield and quality in both cultivars, reflecting biomass loss caused by photosynthetic limitation throughout the lifecycle of each cultivar. I also hypothesised that these declines would be more pronounced in the short-lived cultivar and would occur at lower cumulative exposure due to higher gas exchange. One annual (spring-sown; cv. Click) and one biennial (winter-sown; cv. Phoenix) were exposed to four ozone levels comparable to European summertime concentrations over most of their life cycles. I measured physiological changes (stomatal conductance and photosynthetic rate) and chlorophyll content during the vegetative and reproductive stages, and seed yield (thousand seed weight, TSW) and quality (macro- and micro-nutrients, fatty acid

proportions) when plants had fully senesced. With this information, I developed an economic model to determine how yield and quality losses may impact growers' profits. Overall, while both cv. Click and Phoenix did indeed present declines in seed yield at highest ozone treatments (80 and 110 ppbv), Gas exchange and chlorophyll declined in Click at a lower cumulative ozone exposure. Seed quality also decreased in Click: seed oil content declined from 49% to 41% with increased cumulative ozone, which translates to a substantial economic decline for growers as they are a paid a premium for oil content over 41%. However, Click seemingly better maintained seed yield: TSW declined twice as much at highest ozone treatments in Phoenix than Click, at 40% and 20%. Importantly, however, Phoenix conserved gas exchange and chlorophyll content even in high ozone treatments, meaning that the impact of ozone was hidden until harvest. Overall, I calculated that the losses of yield and quality at the highest ozone treatments could lead to sizeable economic declines, at 175–325 USD ha^{-1} (Click) and 500–665 USD ha^{-1}, potentially jeopardising OSR production. However, the different cultivar responses may allow breeders to identify ozone tolerance traits for physiology and yield in spring and winter OSR, which can be used to produce more ozone-tolerant varieties.

In Chapter 4, I explored why there were more substantial declines in yield in the longer-lived OSR cultivar, Phoenix, despite maintenance of gas exchange and chlorophyll content. I postulated that Phoenix diverted more of its photosynthate to the synthesis of defensive compounds, antioxidants, to protect the most 'productive' tissues i.e., leaves in longer-lived varieties, as stated in the optimal defence theory. I focussed on a key antioxidant, ascorbic acid (AsA), high levels of which are associated with ozone tolerance. I postulated that AsA content would be higher in Phoenix than Click, and that this increased ascorbic acid would confer physiological tolerance, such as maintained gas exchange and chlorophyll content, and morphology (e.g., leaf area and shoot biomass). I therefore exposed both Click and Phoenix to background (~20 ppbv) and high (100 ppbv) ozone levels for 12 days in sealed semi-controlled environment chambers, to investigate the relationship between AsA, physiology, morphology, and markers of oxidative stress and damage at three nodal positions, i.e. at three different leaf ages, on the plant.

The key findings from this experiment were that, in contrast to previous studies (Chameides, 1989; Frei et al., 2012; Bellini and De Tullio, 2019), AsA does not appear to be directly involved in prevention of ozone-induced damage in OSR but does likely play a role in the different responses of the two cultivars. My hypothesis was correct that AsA was indeed higher in Phoenix than Click, and that Phoenix maintained physiology such as gas exchange in younger leaf tissue. However, shoot biomass was substantially reduced in Phoenix after 12 days of exposure to 100 ppbv of ozone. Therefore, Phoenix partially conformed to the optimal defence theory: it seemingly constitutively diverted its photosynthate to AsA in most productive tissues, the leaves, which came at a metabolic cost - in this case the loss of leaf area and shoot biomass. By contrast, stomatal conductance declined substantially in Click, while it maintained biomass, suggesting that Click employed an avoidance strategy which limited ozone

uptake, therefore avoiding internal ozone damage, and maintaining physiology and therefore biomass.

High gas exchange (thus high ozone uptake) and high productivity (biomass allocation) is favoured in advanced breeding programmes so based on my findings in Chapter 4, I hypothesised that intensively-bred canola cultivars would be less tolerant to high ozone levels than non-canola (landrace) counterparts. In the experiment presented in Chapter 5, I made biochemical, physiological, and morphological measurements in two canola-grade cultivars and two non-canola grade cultivars over 26 days under four ozone levels. I was able to use the biochemical responses I observed to develop a novel relative oxidative stress index (rOSI), which encompassed markers of stress and defence.

The key finding from Chapter 5 was that rOSI, my novel metric, correlated with changes in productivity, thus providing a biochemical measure of each cultivar's sensitivity to ozone exposure. Unexpectedly, however, the most ozone tolerant cultivar, which was best able to maintain biomass, proved to be a canola-grade *B. rapa* line (Candle), indicated by high enzymatic antioxidant activity, while its non-canola-grade counterpart *B. rapa* (07224) was the most ozone sensitive. This was clearly reflected in the calculated values of rOSI for the two cultivars, with *B. rapa Candle* returning a strongly negative value and *B. rapa 07224* an almost identical positive one. The comparative differences in tolerance were caused by a combination of lower stomatal conductance (stress avoidance) and high enzymatic antioxidant activity (defence) in *B. rapa* Candle, in contrast to *B. rapa 07224* which exhibited, and maintained, the highest gas exchange of all the cultivars. rOSI was significantly related to cumulative ozone exposure and shoot biomass in all lines and could therefore provide an important addition to the assessment of ozone tolerance in high throughput trials during breeding programmes.

6.2 Opportunities for further research

6.2.1 Agronomic practices

Findings from Chapter 3 prompted key questions regarding agronomic practices, such as in-field canopy management. However, as all the experiments used throughout this thesis were pot-based, the relevance of my results to in-field effects are not entirely clear due to pot constraints (Poorter et al., 2012a). Some consider the natural experimental progression from chamber and glasshouse studies to be the use of a free-air enrichment facility due to the larger scale and closer representation of in-field conditions. However, discerning ozone effects can, and particularly dose-response relationships, can be more challenging in such environments due to the limited control possible over ozone generation and distribution within the cropping area (Watanabe et al., 2013; Paoletti et al., 2017). Despite such challenges, applying the methodologies of this Solardome study to a free-air environment would allow comparison of potential ozone-induced yield losses and their combinatorial interactions with other key stressors,

such as drought, pathogens, e.g. turnip mosaic virus, and pests, e.g. cabbage stem flea beetle (Pullens, 2019). Such stresses are already considered imminent risks to OSR productivity by growers, agronomists, and breeders (AHDB, 2023; Pullens, 2019) and are the subject of on-going research. Ozone, however, remains a hidden threat, one that is seldom considered during breeding programmes.

As I investigated how moderately high ozone exposure affects OSR yield and quality over shorter growing periods, it became apparent that another key knowledge gap is the ozone sensitivity of specific OSR growth stages (GS). GS10 (emergence of fully expanded leaves) through to GS59 (flower bud emergence) are generally considered the most ozone sensitive stages, but this comprises four or nine months of growth, depending on whether a spring- or winter-sown cultivar (AHDB, 2023). Moreover, these growth stages usually coincide with incidences of high ozone during the late spring and summer months in rural Northern Hemisphere agricultural regions (Fowler, 2008). *Brassica* oilseeds are sown in 'low ozone' seasons – either late autumn (August to October) or early spring (February to March) in the Northern Hemisphere (AHDB, 2023; Charters et al., 1996). Based on my observations, I postulate that shifting sowing times to ensure later growth stages coincide with low ozone periods may limit ozone-induced yield declines. It may be easier to move the sowing time of spring cultivars e.g., to January, in projected future, warmer climates, due to the lack of a vernalisation requirement to flower, a requirement that may fix the growing times of winter OSR. However, photosensitivity, wherein onset growth transitions are triggered by daylight exposure and photoperiod, may limit spring OSR sowing to early February (AHDB, 2020). Establishing differences in ozone sensitivity between conventional and restored hybrids which exploit cytoplasmic male sterility to combine desirable traits from a single line, as well as in early- vs. late-sown varieties warrants further study (Aksouh et al., 2001).

6.2.2 Biomass allocation changes in response to ozone

The primary research study in Chapter 3 gave rise to new research questions, particularly why longer-lived OSR Phoenix appeared to have conflicting physiological and morphological responses to ozone at highest cumulative exposures, i.e. that Phoenix seemingly maintained foliar gas exchange and chlorophyll content, but its yield parameters declined, whereas Click showed pronounced reductions in foliar gas exchange and chlorophyll but better maintained yield. While the precise cause was unclear, I postulated that Phoenix conforms to the optimal defence theory, wherein photosynthate is diverted away from biomass accumulation to synthesis of defensive compounds, such as antioxidants (Fagerstrom et al., 1987; McKey, 1974). Multiple studies have demonstrated that plants respond to stress by protecting the most 'productive' tissues, usually considered the youngest fully expanding or expanding leaves in longer-lived (perennial or biannual) plants, and reproductive sites in shorter-lived annual plants (McCall and Fordyce, 2010; Van Dam et al., 1996). By contrast, Click appears to employ and alternative strategy: one of avoidance. By reducing gas

exchange by reducing stomatal conductance Click was able to avoid uptake of ozone into the apoplast thereby limiting damage and avoiding the need to divert photosynthate. The findings of this study also prompt the question of exactly where the carbon produced from photosynthesis is allocated, sequestered, or lost. I hypothesise that in addition to the production of antioxidants, there may also be carbon "loss" via biogenic volatile organic carbon (BVOC) synthesis and emission. This is because BVOCs, particularly those associated with peroxidation such as green leaf volatiles, are observed to increase in response to abiotic stresses such as high temperature. For example, fatty acid- and glucosinolate-derived emissions increased by an order of magnitude at >40°C in *B. nigra* (Kask et al., 2016). Similarly I found in preliminary experiments not presented elsewhere that foliar biogenic emissions of monoterpenes and aldehydes were a third higher in B. napus Click after 4 weeks' exposure to 110 ppbv ozone compared to 30 ppbv (Figure 6.1). Taken in conjunction with the findings of the diversion of photosynthate to defensive compounds by Phoenix presented in Chapter 4, this suggests further investigation of carbon allocation and of assimilation is required. Quantifying the proportion of carbon diverted from primary to secondary metabolism using methods such as stable carbon isotope tracing is needed to improve understanding of whether cultivars conform to the optimal defence theory under stress, which may further compound yield loss. Such quantification of carbon loss and transitions between metabolic processes may aid breeders in identifying individuals or lines that maintain yield under high ozone levels.

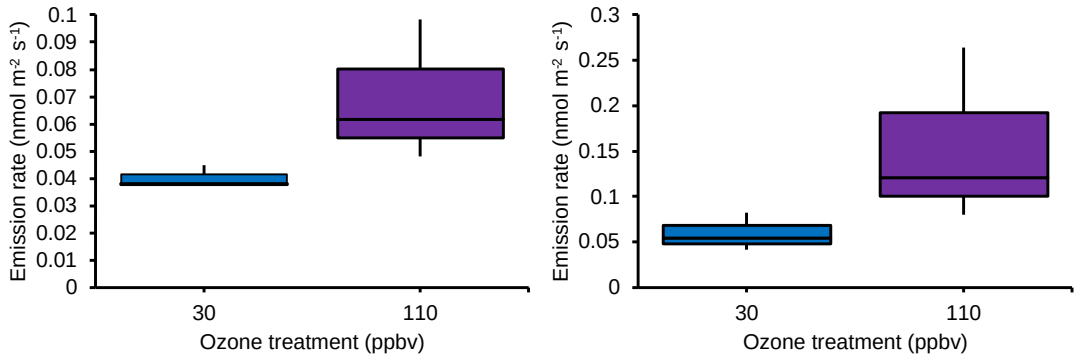

Figure 6.1.Emission rate of foliar BVOC from spring oilseed rape cv. Click under 21 days ozone exposure 30 ppbv and 110 ppbv a) monoterpenes and b) aldehydes collected over 20 minute intervals.

In my final research study, described in Chapter 5, I found that the non-canola landrace *B. rapa* 07224 was the most ozone sensitive of the four cultivars considered, exhibiting the most substantial declines in biomass under increased ozone exposure. This resulted in the biggest increase in my novel quantitative measure of ozone sensitivity, rOSI, for this cultivar. Conversely, the canola-grade cultivar *B. rapa* Candle was most tolerant, even exhibiting increases in biomass in response to exposure, which was evident in the large negative value returned for rOSI. The results provide evidence of *B. rapa* 07224 and *B. rapa* Candle employing different defence strategies: *B. rapa* 07224 appears to allocate photosynthate to the "productive" tissues of seed, therefore attempting to improve genetic fitness by securing future generations (McKey, 1974). Conversely, *B. rapa* Candle appeared to identify leaves with high photosynthetic rates

as the most productive tissues, thus conferring tolerance and improving fitness via maintaining physiology, i.e. *B. rapa* Candle diverts its photosynthate to leaf biomass accumulation rather than reproductive sites. However, as this was a short-term experiment the lines did not produce seed, meaning uncertainty remains regarding whether the yield and seed quality of these cultivars are also opposingly impacted by ozone, and therefore further study is warranted to quantify biomass partitioning throughout the lifecycle of these important oilseed crops. Furthermore, genetic, and biochemical control, and indeed respirational cost of transitioning photosynthate from primary metabolism (growth) to secondary metabolism (defence) warrants further investigation, as the mechanism behind this is poorly understood, and known to be further complicated by abiotic stress (Poorter et al., 2012b).

6.2.3 Physiological and gas exchange responses

As demonstrated in Chapters 4 and 5, avoiding ozone uptake can be achieved through decreasing stomatal conductance. Therefore, a key question arising from the findings of Chapters 4 and 5 was how the perception, the physiological control, and the uptake of ozone influenced a cultivar's sensitivity to ozone. A major future avenue of research should focus on the stomata, as they are the primary entry point of ozone into the apoplast. Despite stomata being one of the most-widely studied plant systems, substantial knowledge gaps remain regarding perception and responses to ozone, such as whether there are different closure thresholds and whether closure strategy is species- or cultivar-specific. It is understood that high stomatal conductance, especially if maintained in moderately high (>60 ppbv) ozone levels, increases ozone uptake (Bailey et al., 2019), and hence the actual dose of this powerful phytotoxin received by plant cells and structures. I postulate that stomatal sensitivity/responsiveness, and heritable stomatal traits contribute to observed ozone tolerance in some crops (Brosché et al., 2010). Therefore, identification of the genes involved in the regulation of stomatal responses and sensitivity are required to understand the control of ozone flux.

There is no standard accepted definition of physiological ozone tolerance, although various tolerance indicators have been proposed, including the maintained performance of Photosystem II (Hoshika et al., 2020) and net photosynthetic rate (Frei et al., 2008) under elevated ozone levels. Key photosynthetic components have been identified as sensitive to ozone, e.g., Calvin cycle, namely carboxylation of ribulose bisphosphate to glycerate-3-phospate via Rubisco (Pell et al., 1992). However, elucidating exactly how the photosynthetic components of *Brassica* oilseed species are impeded requires further interrogation, as efficiency of Photosystem II measurements showed high variability during all my experiments. I propose that further leaf-level measurements of gas exchange across multiple ozone-exposed *Brassica* oilseed lines should be taken in the future to quantify maximum rate of carboxylation (V_{cmax}), maximum electron transport rate (J_{max}), and respiration. Focussing attention on gas exchange components will inform dose-response models and may aid in calculating a physiologically-relevant phytotoxic ozone dose (as in Emberson et al., 2001).

Moreover, direct comparison of inter- and intraspecific responses to ozone would facilitate identification of desirable traits, contributing towards breeding ozone tolerant crops.

Other components of *Brassica* oilseed gas exchange may be ozone-limited, such as mesophyll conductance, which is the rate of carbon dioxide diffusion from spongy mesophyll layer to inside cell (Evans, 2020). Indeed, ozone has been shown to decrease mesophyll conductance in Sebold's beech (Hoshika et al., 2020) and poplar (Xu et al., 2019), but not yet in agricultural crops. Decreased mesophyll conductance limits carbon dioxide (CO_2) movement in the mesophyll, and therefore the fixation rate of ribulose bisphosphate via Rubisco declines, which decreases carbon and nitrogen use efficiencies. Such declines are critical to *Brassica* oilseeds, as these crops are already considered to have a low nitrogen use efficiency relative to global agricultural crops such as wheat and soya, and this is further compounded by ozone-accelerated senescence (Avice and Etienne, 2014). Despite this, mesophyll conductance is given little attention in studies investigating crop responses to ozone. Therefore, I suggest that quantifying key components of mesophyll conductance e.g., CO_2 membrane permeability (Evans, 2020) would allow quantification of how ozone may limit CO_2 uptake into cells and would further elucidate shifts in carbon and nitrogen balance and allocation.

6.2.4 Biochemical responses and conferring ozone tolerance

As demonstrated in Chapters 4 and 5, further research is required to quantify the degree of ozone and subsequent ROS detoxification by apoplastic antioxidants in different species and cultivars (Dai et al., 2018). In the case of AsA, there is added complexity as it is an important component of much more extensive constituent enzymatic antioxidant systems, such as ascorbate peroxidase regeneration in the ascorbate-glutathione cycle (Örvar and Ellis, 1997; Pasqualini et al., 2001). Each of these enzymatic and non-enzymatic components may play a more important role in defence, depending on species, phenology, and ontology. For example, quantifying AsA in various redox states (dehydroascorbic acid and monodehydroascorbate, respectively), and the reactions with ROS (namely singlet oxygen), and enzymatic activity involved in AsA regeneration, may provide further insight into differences in OSR cultivars' ozone tolerance (Akram et al., 2017). This is because there may be shifts or disruptions in antioxidant enzyme/substrate efficiencies that also play important roles in this cycle (Conklin et al., 2004). Furthermore, as the primary interface of internal ozone is the apoplast, further study is also warranted to investigate localised sub-cellular antioxidant concentrations (as in Dai et al., 2022). A limitation to the chamber experiments in Chapters 4 and 5 were that antioxidant activity could not be determined during ozone fumigation for safety reasons; this may be mitigated by fumigating for a short period directly before sampling.

Similarly to biochemical ozone tolerance, the biochemical mechanism of ozone-induced senescence has not been fully identified, due to its extensive genetic orchestration and complexity, and knowledge gaps remain (Yendrek et al., 2017). For

example, exactly how changes in both extracellular and intracellular redox homeostasis may cause ozone-induced accelerated senescence, both at the leaf-level, and whole-plant level, is unknown (Wang et al., 2013). Primarily, research is also needed regarding reactive oxygen species (ROS) perception and transfer between cellular and organelle membranes in ozone-stressed or pre-senescent tissues. For example, reduced nicotinamide adenine dinucleotide phosphate (NADPH) oxidases (or respiratory burst oxidase homologues; Rboh) which are bound to cell membranes, also catalyse the formation of apoplastic superoxide and play a key role in signal transduction within cells. This leads to a similar upregulation of auxins, ethylene, and therefore stress perception (Quartacci et al., 2001). Moreover, there are Arabidopsis mutants such as RbohF and RbohD knockout lines are available, to probe NADPH oxidases' functions in ozone tolerance (Morales et al., 2016).

A further area of future study includes identifying the role of hydrogen peroxide (H_2O_2) which I observed to increase in an acropetal gradient (Chapter 4) and with elevated ozone (Chapter 5), therefore acting as both a molecular signal and ROS. Therefore, the question is posed regarding what exactly H_2O_2 is signalling. I postulate that H_2O_2 is a signal transducer for senescence-associated genes (SAG). Such genes may include *SAG18*, a gene specifically upregulated in the presence of ozone, which is one of many genes that promotes anthocyanin production (Agrawal et al., 2021). While many previous studies have suggested that AsA conveys ozone tolerance in plants, anthocyanins have been seldom investigated in crops in response to ozone but may provide a more suitable marker of biochemical stress tolerance (Naing and Kim, 2021). This is because foliar anthocyanins act as an antioxidant when plants are under abiotic stress (Smirnoff, 2008), and anthocyanin concentrations are known to increase in *Brassica* species under elevated ozone (Naing et al., 2017) and seemingly maintains the efficiency of Photosystem II based on correlative evidence (Zhang et al., 2017). Additionally, *B rapa* genes encoding anthocyanin synthesis have been identified, and found to be highly conserved, and therefore heritable (Agrawal et al., 2021). Although anthocyanins are synthesised and located inside cell vacuoles (rather than the apoplast; as shown in Small and Pecket, 1982), they may be considered a suitable intracellular marker of ozone stress/tolerance. Thus, further research is warranted to fully understand the function of anthocyanins in ozone responses in Brassicaceae and its promise as a biochemical marker of tolerance.

Another major research avenue is the further interrogation of the relative oxidative stress index (rOSI) proposed in Chapter 5. Testing efficacy by a) establishing common biochemical markers of ozone tolerance in crops, and b) incorporating these markers into rOSI is required to explore whether its predictiveness of crop responses could be improved with the inclusion of additional factors. Moreover, applying the index to other stresses such as drought, or key pests and diseases, and to other species as described in Section 6.2.1 is also urgently needed to determine whether rOSI is predictive in other contexts, and could therefore provide a universal marker of oxidative stress and damage. Additionally, applying rOSI to other *Brassica* oilseed cultivars/species presents an opportunity to compare ozone tolerance directly and efficiently across numerous lines and to increase throughput in screening investigations.

6.3 Identifying and exploiting ozone tolerance traits

Based on my research presented throughout this thesis, I strongly recommend that ozone be explicitly included as a stress to be considered in breeding programmes to allow identification of ozone-tolerant individuals/lines and heritable tolerance traits. Current programmes rarely consider tropospheric ozone a stress of priority compared to disease and drought (Frei, 2015), despite the substantial yield losses and declines outlined in this thesis. Identifying markers of tolerance remains challenging, as traits may be controlled by myriad genes which may not be heritable, or expressed (Mathew et al., 2019). It has been suggested that breeders may turn to older cultivars, which are considered more ozone tolerant, due to lower gas exchange rates and thus limited ozone uptake, to breed modern varieties (Frenck et al., 2011; Brewster et al., 2019; Yadav et al., 2020), but further research is warranted here as there may be productivity penalties. Although our findings from the species intercomparison experiment presented in Chapter 5, appear to support this, it should be borne in mind that the two canola-grade cultivars differed in progenitor species and not just age.

Interrogation of morphology at different orders of organisation, such as from biomass partitioning and yield, to leaf anatomy (e.g., cellular organisation, stomatal density, and size), and/or ultrastructure (e.g., arrangement of organelles, size of apoplast), under a range of ozone levels, may aid identification of shared morphological characteristics in ozone-tolerant plants and facilitate high-throughput phenotyping. Such investigation, alongside the measurement of gas exchange and identification of the primary and secondary metabolites and antioxidants that respond to ozone-induced oxidative stress is required. It is only by an integrated interdisciplinary approach such as this that tolerance biomarkers can be determined/developed to enable identification of resilient phenotypes that can biochemically/physiologically tolerate moderate-high ozone levels. However, as demonstrated in this thesis, such physiological and biochemical ozone tolerance may not correlate to maintained yield due to conflicts with the optimal defence theory, namely discerning which tissues are prioritised by the different cultivars.

Importantly, a systematic approach to identifying genetic ozone tolerance traits (‘genotype’) which translate to observable species traits (‘phenotype’) is required. Desirable genotypic traits are rarely simply detectable or describable, with multiple genes making small and cumulative contributions to a phenotype (termed ‘quantitative traits’) (Holland et al., 2004). This is important because it suggests the genetic upregulation of a combination of genes may be required to confer maintained or increased yield under high ozone levels (Mickelbart et al., 2015). Genome-wide association studies (GWAS), which may offer an opportunity for crop breeders to identify myriad genes that control biomass allocation (Mathew et al., 2019), may therefore be required. GWAS would allow identification and exploitation of quantitative trait loci which are associated with ozone tolerance in *Brassica* and facilitate linkage mapping (presenting relative locations of genetic markers to each

other) between the phenotypic and genetic/biochemical markers, which will aid identification and exploitation of cumulative ozone tolerance traits in *Brassica* oilseeds, as previously demonstrated in rice cultivars (Wang et al., 2014). Once tolerance traits have been identified, the diversity of OSR and *Brassica* oilseed breeding methods, such as restored hybridisation and introgression offer a promising opportunity to exploit ozone tolerance and enable breeders and growers to minimise ozone-induced losses of yield or crop quality without forfeiting productivity.

6.4 Conclusions

This thesis has demonstrated that ozone is a real, substantive, but still hidden, threat to *Brassica* oilseed yield and quality. I provided evidence that ozone-induced losses can be substantial, and therefore this abiotic stress needs to be considered in breeding programmes. The results from these primary research studies alongside the current body of literature led me to conclude that a combination of diversion of photosynthate to the synthesis of enzymatic antioxidants (defence), stomatal closure (avoidance), and prioritisation of biomass allocation to productive tissues, are required to confer ozone tolerance in *Brassica* oilseeds. Further identification and exploitation of these traits may lead to enhanced ozone tolerance in canola cultivars, with an opportunity to exploit introgression to transfer tolerance to important *Brassica* oilseed cultivars. However, the biggest challenge will be ensuring biomass allocation to reproductive sites is not sacrificed for biochemical defence, to conserve seed yield and quality.

The most important next steps include determining whether the rOSI presented in this thesis is widely applicable and/or whether further variables need to be included to enable it to be predictive of final yield across a range of species and stressors. Moreover, identifying ozone tolerance traits by determining and aligning biochemical, genotypic, and phenotypic data in tolerant lines is needed. Such traits include stomatal control, maintaining allocation to reproductive sites, and biochemical defence. Incorporating agronomic practices in future experiments, such as altering sowing times may allow growers to optimise ozone tolerance of current cultivars in field conditions. Overall, this thesis has demonstrated that ozone is a hidden threat to *Brassica* oilseed yield and quality, but the diverse physiological, biochemical, and morphological responses in this crop provide an opportunity to safeguard its productivity in high ozone climates.

7. References

Adaros, G., Weigel, H.J., Jäger, H.J., 1991. Single and interactive effects of low levels of O_3, SO_2 and NO2 on the growth and yield of spring rape. Environmental Pollution 72, 269–286. https://doi.org/10.1016/0269-7491(91)90002-E

Agathokleous, E., Araminiene, V., Belz, R.G., Calatayud, V., De Marco, A., Domingos, M., Feng, Z., Hoshika, Y., Kitao, M., Koike, T., Paoletti, E., Saitanis, C.J., Sicard, P., Calabrese, E.J., 2019a. A quantitative assessment of hormetic responses of plants to ozone. Environmental Research 176, 108527. https://doi.org/10.1016/j.envres.2019.108527

Agathokleous, E., Belz, R.G., Calatayud, V., De Marco, A., Hoshika, Y., Kitao, M., Saitanis, C.J., Sicard, P., Paoletti, E., Calabrese, E.J., 2019b. Predicting the effect of ozone on vegetation via linear non-threshold (LNT), threshold and hormetic dose-response models. Science of The Total Environment 649, 61–74. https://doi.org/10.1016/j.scitotenv.2018.08.264

Agathokleous, E., Feng, Z., Oksanen, E., Sicard, P., Wang, Q., Saitanis, C.J., Araminiene, V., Blande, J.D., Hayes, F., Calatayud, V., Domingos, M., Veresoglou, S.D., Peñuelas, J., Wardle, D.A., De Marco, A., Li, Z., Harmens, H., Yuan, X., Vitale, M., Paoletti, E., 2020. Ozone affects plant, insect, and soil microbial communities: A threat to terrestrial ecosystems and biodiversity. Science Advances 6, eabc1176. https://doi.org/10.1126/sciadv.abc1176

Agathokleous, E., Feng, Z., Peñuelas, J., 2020. Chlorophyll hormesis: Are chlorophylls major components of stress biology in higher plants? Science of The Total Environment 726, 138637. https://doi.org/10.1016/j.scitotenv.2020.138637

Agrawal, G.K., Jwa, N.-S., Iwahashi, H., Rakwal, R., 2003. Importance of ascorbate peroxidases OsAPX1 and OsAPX2 in the rice pathogen response pathways and growth and reproduction revealed by their transcriptional profiling. Gene 322, 93–103. https://doi.org/10.1016/j.gene.2003.08.017

Agrawal, S.B., Agrawal, M., Singh, A., 2021. Tropospheric Ozone: A Hazard for Vegetation and Human Health. Cambridge Scholars Publishing.

AHDB. (2020). Oilseed Rape Growth Guide. https://ahdb.org.uk/osrgg. (Last accessed 31/03/2021)

AHDB. (2023). Oilseed Rape Growth Guide. https://ahdb.org.uk/osrgg. (Last accessed 12/04/2023)

Ainsworth, E.A., Yendrek, C.R., Sitch, S., Collins, W.J., Emberson, L.D., 2012b. The Effects of Tropospheric Ozone on Net Primary Productivity and Implications for Climate Change. Annual Review of Plant Biology 63, 637–661. https://doi.org/10.1146/annurev-arplant-042110-103829

Akram, N.A., Shafiq, F., Ashraf, M., 2017. Ascorbic Acid-A Potential Oxidant Scavenger and Its Role in Plant Development and Abiotic Stress Tolerance. Frontiers in Plant Science 8. https://doi.org/10.3389/fpls.2017.00613

Alexieva, V., Sergiev, I., Mapelli, S., Karanov, E., 2001. The effect of drought and ultraviolet radiation on growth and stress markers in pea and wheat. Plant, Cell & Environment 24, 1337–1344. https://doi.org/10.1046/j.1365-3040.2001.00778.x

Allender, C.J., King, G.J., 2010a. Origins of the amphiploid species *Brassica napus* L. investigated by chloroplast and nuclear molecular markers. BMC Plant Biology 10, 54. https://doi.org/10.1186/1471-2229-10-54

Alscher, R.G., 1989. Biosynthesis and antioxidant function of glutathione in plants. Physiologia Plantarum 77, 457–464. https://doi.org/10.1111/j.1399-3054.1989.tb05667.x

Archibald, A.T., Neu, J.L., Elshorbany, Y.F., Cooper, O.R., Young, P.J., Akiyoshi, H., Cox, R.A., Coyle, M., Derwent, R.G., Deushi, M., Finco, A., Frost, G.J., Galbally, I.E., Gerosa, G., Granier, C., Griffiths, P.T., Hossaini, R., Hu, L., Jöckel, P., Josse, B., Lin, M.Y., Mertens, M., Morgenstern, O., Naja, M., Naik, V., Oltmans, S., Plummer, D.A., Revell, L.E., Saiz-Lopez, A., Saxena, P., Shin, Y.M., Shahid, I., Shallcross, D., Tilmes, S., Trickl, T., Wallington, T.J., Wang, T., Worden, H.M., Zeng, G., 2020. Tropospheric Ozone Assessment Report: A critical review of changes in the tropospheric ozone burden and budget from 1850 to 2100. Elementa: Science of the Anthropocene 8, 034. https://doi.org/10.1525/elementa.2020.034

Archibald, A.T., Turnock, S.T., Griffiths, P.T., Cox, T., Derwent, R.G., Knote, C., Shin, M., 2020. On the changes in surface ozone over the twenty-first century: sensitivity to changes in surface temperature and chemical mechanisms. Philosophical Transactions of the Royal Society A: Mathematical, Physical and Engineering Sciences 378, 20190329. https://doi.org/10.1098/rsta.2019.0329

Arrutia, F., Binner, E., Williams, P., Waldron, K.W., 2020. Oilseeds beyond oil: Press cakes and meals supplying global protein requirements. Trends in Food Science & Technology 100, 88–102. https://doi.org/10.1016/j.tifs.2020.03.044

Ashmore, M.R., Ainsworth, N., 1995. The Effects of Ozone and Cutting on the Species Composition of Artificial Grassland Communities. Functional Ecology 9, 708–712. https://doi.org/10.2307/2390242

Ashraf, M.A., Rasheed, R., Hussain, I., Iqbal, M., Haider, M.Z., Parveen, S., Sajid, M.A., 2015. Hydrogen peroxide modulates antioxidant system and nutrient relation in maize (Zea mays L.) under water-deficit conditions. Archives of Agronomy and Soil Science 61, 507–523. https://doi.org/10.1080/03650340.2014.938644

Avice, J.-C., Etienne, P., 2014. Leaf senescence and nitrogen remobilization efficiency in oilseed rape (*Brassica napus* L.). Journal of Experimental Botany 65, 3813–3824. https://doi.org/10.1093/jxb/eru177

Bailey, A., Burkey, K., Taggart, M., Rufty, T., 2019. Leaf Traits That Contribute to Differential Ozone Response in Ozone-Tolerant and Sensitive Soybean Genotypes. Plants 8, 235. https://doi.org/10.3390/plants8070235

Barnes, A.P., Ferreira, J., Revoredo-Giha, C.R.G, Hoad, S., Hoebe, P., Burnett. F. (2016). The UK Plant Breeding Sector and Innovation (CT-RES-042). Report for the Intellectual Property Office. HMSO, London. URL https://assets.publishing.service.gov.uk/government/uploads/system/uploads/attachment_data/file/552498/Plant-breeders.pdf (20/04/2023)

Barnes, J., Zheng, Y., Lyons, T., 2002. Plant Resistance to Ozone: the Role of Ascorbate, in: Omasa, K., Saji, H., Youssefian, S., Kondo, N. (Eds.), Air Pollution and Plant Biotechnology: Prospects for Phytomonitoring and Phytoremediation. Springer Japan, Tokyo, 235–252. https://doi.org/10.1007/978-4-431-68388-9_12

Barth, C., De Tullio, M., Conklin, P.L., 2006. The role of ascorbic acid in the control of flowering time and the onset of senescence. Journal of Experimental Botany 57, 1657–1665. https://doi.org/10.1093/jxb/erj198

Barto, E.K., Cipollini, D., 2005. Testing the optimal defense theory and the growth-differentiation balance hypothesis in *Arabidopsis thaliana*. Oecologia 146, 169–178. https://doi.org/10.1007/s00442-005-0207-0

Bayer Crop Science. (2020). Weather much more important than CSFB in OSR performance.

Bellini, E., De Tullio, M.C., 2019. Ascorbic Acid and Ozone: Novel Perspectives to Explain an Elusive Relationship. Plants 8, 122. https://doi.org/10.3390/plants8050122

Berens, M.L., Wolinska, K.W., Spaepen, S., Ziegler, J., Nobori, T., Nair, A., Krüler, V., Winkelmüller, T.M., Wang, Y., Mine, A., Becker, D., Garrido-Oter, R., Schulze-Lefert, P., Tsuda, K., 2019. Balancing trade-offs between biotic and abiotic stress responses through leaf age-dependent variation in stress hormone cross-talk. Proceedings of the National Academy of Sciences 116, 2364–2373. https://doi.org/10.1073/pnas.1817233116

Berners-Lee, M., Kennelly, C., Watson, R., Hewitt, C.N., 2018. Current global food production is sufficient to meet human nutritional needs in 2050 provided there is radical societal adaptation. Elementa: Science of the Anthropocene 6, 52. https://doi.org/10.1525/elementa.310

Bieker, S., Riester, L., Stahl, M., Franzaring, J., Zentgraf, U., 2012. Senescence-specific Alteration of Hydrogen Peroxide Levels in Arabidopsis thaliana and Oilseed Rape Spring Variety Brassica napus L. cv. MozartF. Journal of Integrative Plant Biology 54, 540–554. https://doi.org/10.1111/j.1744-7909.2012.01147.x

Bienert, G.P., Chaumont, F., 2014. Aquaporin-facilitated transmembrane diffusion of hydrogen peroxide. Biochimica et Biophysica Acta (BBA) - General Subjects, Aquaporins 1840, 1596–1604. https://doi.org/10.1016/j.bbagen.2013.09.017

Bingham, I.J., Kightley, S.P.J., Walker, K., n.d. Identifying the factors determining the chlorophyll content of UK rapeseed.

Black, V.J., Black, C.R., Roberts, J.A., Stewart, C.A., 2000. Tansley Review No. 115 Impact of ozone on the reproductive development of plants. New Phytologist 147, 421–447. https://doi.org/10.1046/j.1469-8137.2000.00721.x

Black, V.J., Stewart, C.A., Roberts, J.A., Black, C.R., 2010. Direct effects of ozone on reproductive development in Plantago major L. populations differing in sensitivity. Environmental and Experimental Botany 69, 121–128. https://doi.org/10.1016/j.envexpbot.2010.04.006

Bohler, S., Bagard, M., Oufir, M., Planchon, S., Hoffmann, L., Jolivet, Y., Hausman, J.-F., Dizengremel, P., Renaut, J., 2007. A DIGE analysis of developing poplar leaves subjected to ozone reveals major changes in carbon metabolism. Proteomics 7, 1584–1599. https://doi.org/10.1002/pmic.200600822

Boleti, E., Hueglin, C., Grange, S.K., Prévôt, A.S.H., Takahama, S., 2020. Temporal and spatial analysis of ozone concentrations in Europe based on timescale decomposition and a multi-clustering approach. Atmospheric Chemistry and Physics 20, 9051–9066. https://doi.org/10.5194/acp-20-9051-2020

Bommarco, R., Marini, L., Vaissière, B.E., 2012. Insect pollination enhances seed yield, quality, and market value in oilseed rape. Oecologia 169, 1025–1032. https://doi.org/10.1007/s00442-012-2271-6

Booker, F., Burkey, K., Morgan, P., Fiscus, E., Jones, A., 2012. Minimal influence of G-protein null mutations on ozone-induced changes in gene expression, foliar injury, gas exchange and peroxidase activity in *Arabidopsis thaliana* L. Plant, Cell & Environment 35, 668–681. https://doi.org/10.1111/j.1365-3040.2011.02443.x

Booker, F.L., Fiscus, E.L., 2005. The role of ozone flux and antioxidants in the suppression of ozone injury by elevated CO_2 in soybean. Journal of Experimental Botany 56, 2139–2151. https://doi.org/10.1093/jxb/eri214

Bosac, C., Black, V.J., Roberts, J.A., Black, C.R., 1998. Impact of ozone on seed yield and quality and seedling vigour in oilseed rape (*Brassica napus* L.). Journal of Plant Physiology 153, 127–134. https://doi.org/10.1016/S0176-1617(98)80055-2

Bouchet, A.-S., Laperche, A., Bissuel-Belaygue, C., Snowdon, R., Nesi, N., Stahl, A., 2016. Nitrogen use efficiency in rapeseed. A review. Agronomic Sustainable Development. 36, 38. https://doi.org/10.1007/s13593-016-0371-0

Bradford, M.M., 1976. A rapid and sensitive method for the quantitation of microgram quantities of protein utilizing the principle of protein-dye binding. Analytical Biochemistry 72, 248–254. https://doi.org/10.1016/0003-2697(76)90527-3

Brewster, C., Hayes, F., Fenner, N., 2019. Ozone Tolerance Found in Aegilops tauschii and Primary Synthetic Hexaploid Wheat. Plants 8, 195. https://doi.org/10.3390/plants8070195

Broberg, M.C., Daun, S., Pleijel, H., 2020. Ozone Induced Loss of Seed Protein Accumulation Is Larger in Soybean than in Wheat and Rice. Agronomy 10, 357. https://doi.org/10.3390/agronomy10030357

Brosché, M., Merilo, E., Mayer, F., Pechter, P., Puzõrjova, I., Brader, G., Kangasjärvi, J., Kollist, H., 2010. Natural variation in ozone sensitivity among *Arabidopsis thaliana* accessions and its relation to stomatal conductance. Plant, Cell & Environment 33, 914–925. https://doi.org/10.1111/j.1365-3040.2010.02116.x

Buege, J.A., Aust, S.D., 1978. [30] Microsomal lipid peroxidation, in: Fleischer, S., Packer, L. (Eds.), Methods in Enzymology, Biomembranes - Part C: Biological Oxidations. Academic Press, 302–310. https://doi.org/10.1016/S0076-6879(78)52032-6

Butruille, D. v., Guries, R. p., Osborn, T. c., 1999. Increasing Yield of Spring Oilseed Rape Hybrids through Introgression of Winter Germplasm. Crop Science 39, 1491–1496. https://doi.org/10.2135/cropsci1999.3951491x

Calatayud, A., Iglesias, D.J., Talón, M., Barreno, E., 2003. Effects of 2-month ozone exposure in spinach leaves on photosynthesis, antioxidant systems and lipid peroxidation. Plant Physiology and Biochemistry 41, 839–845. https://doi.org/10.1016/S0981-9428(03)00123-2

Calatayud, A., Iglesias, D.J., Talón, M., Barreno, E., 2004. Response of Spinach Leaves (*Spinacia oleracea* L.) to Ozone Measured by Gas Exchange, Chlorophyll a Fluorescence, Antioxidant Systems, and Lipid Peroxidation. Photosynthetica 42, 23–29. https://doi.org/10.1023/B:PHOT.0000040565.53844.c6

Calatayud, V., Cerveró, J., Calvo, E., García-Breijo, F.-J., Reig-Armiñana, J., Sanz, M.J., 2011. Responses of evergreen and deciduous Quercus species to enhanced ozone levels. Environmental Pollution 159, 55–63. https://doi.org/10.1016/j.envpol.2010.09.024

Calvo, E., Martin, C., Sanz, M.J., 2007. Ozone Sensitivity Differences in Five Tomato Cultivars: Visible Injury and Effects on Biomass and Fruits. Water Air Soil Pollution 186, 167–181. https://doi.org/10.1007/s11270-007-9475-0

Camp, W.V., Willekens, H., Bowler, C., Montagu, M.V., Inzé, D., Reupold-Popp, P., Sandermann, H., Langebartels, C., 1994. Elevated Levels of Superoxide Dismutase Protect Transgenic Plants Against Ozone Damage. Nature Biotechnology 12, 165–168. https://doi.org/10.1038/nbt0294-165

Castagna, A., Ranieri, A., 2009. Detoxification and repair process of ozone injury: From O_3 uptake to gene expression adjustment. Environmental Pollution, Special Issue Section: Ozone and Mediterranean Ecology: Plants, People, Problems 157, 1461–1469. https://doi.org/10.1016/j.envpol.2008.09.029

Castillo, F.J., Greppin, H., 1988. Extracellular ascorbic acid and enzyme activities related to ascorbic acid metabolism in *Sedum album* L. leaves after ozone exposure. Environmental and Experimental Botany 28, 231–238. https://doi.org/10.1016/0098-8472(88)90033-0

Caverzan, A., Jardim-Messeder, D., Paiva, A.L., Margis-Pinheiro, M., 2019. Ascorbate Peroxidases: Scavengers or Sensors of Hydrogen Peroxide Signaling? in: Panda, S.K., Yamamoto, Y.Y. (Eds.), Redox Homeostasis in Plants: From Signalling to Stress Tolerance, Signaling and Communication in Plants. Springer International Publishing, Cham, 85–115. https://doi.org/10.1007/978-3-319-95315-1_5

Caverzan, A., Passaia, G., Rosa, S.B., Ribeiro, C.W., Lazzarotto, F., Margis-Pinheiro, M., 2012. Plant responses to stresses: role of ascorbate peroxidase in the antioxidant protection. Genetic and Molecular Biology 35, 1011–1019. https://doi.org/10.1590/S1415-47572012000600016

Chameides, W.L., 1989. The chemistry of ozone deposition to plant leaves: role of ascorbic acid. Environmental Science Technology 23, 595–600. https://doi.org/10.1021/es00063a013

Charters, Y.M., Robertson, A., Wilkinson, M.J., Ramsay, G., 1996. PCR analysis of oilseed rape cultivars (*Brassica napus* L. ssp. oleifera) using 5′ -anchored simple sequence repeat (SSR) primers. Theoretical and Applied Genetics 92, 442–447. https://doi.org/10.1007/BF00223691

Chaudhary, I.J., Rathore, D., 2021. Assessment of dose–response relationship between ozone dose and groundnut (Arachis hypogaea L) cultivars using Open Top Chamber (OTC) and Ethylenediurea (EDU). Environmental Technology & Innovation 22, 101494. https://doi.org/10.1016/j.eti.2021.101494

Chen, C.P., Frank, T.D., Long, S.P., 2009. Is a short, sharp shock equivalent to long-term punishment? Contrasting the spatial pattern of acute and chronic ozone damage to soybean leaves via chlorophyll fluorescence imaging. Plant, Cell & Environment 32, 327–335. https://doi.org/10.1111/j.1365-3040.2008.01923.x

Chen, F., Liu, C.-J., Tschaplinski, T.J., Zhao, N., 2009. Genomics of Secondary Metabolism in Populus: Interactions with Biotic and Abiotic Environments. Critical Reviews in Plant Sciences 28, 375–392. https://doi.org/10.1080/07352680903241279

Chen, Z., Gallie, D.R., 2005. Increasing Tolerance to Ozone by Elevating Foliar Ascorbic Acid Confers Greater Protection against Ozone Than Increasing Avoidance. Plant Physiology 138, 1673–1689. https://doi.org/10.1104/pp.105.062000

Chen, Z., Gallie, D.R., 2006. Dehydroascorbate Reductase Affects Leaf Growth, Development, and Function. Plant Physiology 142, 775–787. https://doi.org/10.1104/pp.106.085506

Chernikova, T., Robinson, J.M., Lee, E.H., Mulchi, C.L., 2000. Ozone tolerance and antioxidant enzyme activity in soybean cultivars. Photosynthesis Research 64, 15–26. https://doi.org/10.1023/A:1026500911237

Chou, P.-T., Khan, A.U., 1983. L-ascorbic acid quenching of singlet delta molecular oxygen in aqueous media: Generalized antioxidant property of vitamin C. Biochemical and Biophysical Research Communications 115, 932–937. https://doi.org/10.1016/S0006-291X(83)80024-2

Choudhary, B.R., Joshi, P., Ramarao, S., 2000. Interspecific hybridization between *Brassica carinata* and *Brassica rapa*. Plant Breeding 119, 417–420. https://doi.org/10.1046/j.1439-0523.2000.00503.x

Christiansen, A., Mickley, L.J., Liu, J., Oman, L.D., Hu, L., 2022. Multidecadal increases in global tropospheric ozone derived from ozonesonde and surface site observations: can models reproduce ozone trends? Atmospheric Chemistry and Physics 22, 14751–14782. https://doi.org/10.5194/acp-22-14751-2022

Clausen, S.K., Frenck, G., Linden, L.G., Mikkelsen, T.N., Lunde, C., Jørgensen, R.B., 2011. Effects of Single and Multifactor Treatments with Elevated Temperature, CO_2 and Ozone on Oilseed Rape and Barley. Journal of Agronomy and Crop Science 197, 442–453. https://doi.org/10.1111/j.1439-037X.2011.00478.x

Coates, J., Mar, K.A., Ojha, N., Butler, T.M., 2016. The influence of temperature on ozone production under varying NO_x conditions – a modelling study. Atmospheric Chemistry and Physics 16, 11601–11615. https://doi.org/10.5194/acp-16-11601-2016

Conesa, A., Beck, S., 2019. Making multi-omics data accessible to researchers. Sci Data 6, 251. https://doi.org/10.1038/s41597-019-0258-4

D'Odorico, P., Carr, J.A., Laio, F., Ridolfi, L., Vandoni, S., 2014. Feeding humanity through global food trade. Earth's Future 2, 458–469. https://doi.org/10.1002/2014EF000250

Dai, L., Kobayashi, K., Nouchi, I., Masutomi, Y., Feng, Z., 2020. Quantifying determinants of ozone detoxification by apoplastic ascorbate in peach (Prunus persica) leaves using a model of ozone transport and reaction. Global Change Biology 26, 3147–3162. https://doi.org/10.1111/gcb.15049

Das, K., Roychoudhury, A., 2014. Reactive oxygen species (ROS) and response of antioxidants as ROS-scavengers during environmental stress in plants. Frontiers in Environmental Science 2.

Dat, J.F., Pellinen, R., Beeckman, T., Van De Cotte, B., Langebartels, C., Kangasjärvi, J., Inzé, D., Van Breusegem, F., 2003. Changes in hydrogen peroxide homeostasis trigger an active cell death process in tobacco. The Plant Journal 33, 621–632. https://doi.org/10.1046/j.1365-313X.2003.01655.x

De Bock, M., Ceulemans, R., Horemans, N., Guisez, Y., Vandermeiren, K., 2012. Photosynthesis and crop growth of spring oilseed rape and broccoli under elevated tropospheric ozone. Environmental and Experimental Botany 82, 28–36. https://doi.org/10.1016/j.envexpbot.2012.03.008

De Bock, M., Op de Beeck, M., De Temmerman, L., Guisez, Y., Ceulemans, R., Vandermeiren, K., 2011. Ozone dose–response relationships for spring oilseed rape and broccoli. Atmospheric Environment 45, 1759–1765. https://doi.org/10.1016/j.atmosenv.2010.12.027

De La Torre, D., 2008. Quantification of Mesophyll Resistance and Apoplastic Ascorbic Acid as an Antioxidant for Tropospheric Ozone in Durum Wheat (*Triticum durum* Desf. cv. Camacho). The Scientific World Journal 8, 1197–1209. https://doi.org/10.1100/tsw.2008.149

De Pinto, M.C., Locato, V., De Gara, L., 2012. Redox regulation in plant programmed cell death. Plant, Cell & Environment 35, 234–244. https://doi.org/10.1111/j.1365-3040.2011.02387.x

De Temmerman, L., Karlsson, G.P., Donnelly, A., Ojanperä, K., Jäger, H.-J., Finnan, J., Ball, G., 2002. Factors influencing visible ozone injury on potato including the interaction with carbon dioxide. European Journal of Agronomy 17, 291–302. https://doi.org/10.1016/S1161-0301(02)00067-9

De Zoysa, H.K.S., Waisundara, V.Y., 2021. Mustard (*Brassica nigra*) Seed, in: Tanwar, B., Goyal, A. (Eds.), Oilseeds: Health Attributes and Food Applications. Springer, Singapore, 191–210. https://doi.org/10.1007/978-981-15-4194-0_8

DEFRA. (2020). UK Farming Statistics. https://assets.publishing.service.gov.uk/government/uploads/system/uploads/attachment_data/file/910585/structure-jun2020provcrops-eng-20aug20.pdf. Last accessed 24/03/2021.

Demidchik, V., 2015. Mechanisms of oxidative stress in plants: From classical chemistry to cell biology. Environmental and Experimental Botany 109, 212–228. https://doi.org/10.1016/j.envexpbot.2014.06.021

Derwent, R.G., Utembe, S.R., Jenkin, M.E., Shallcross, D.E., 2015. Tropospheric ozone production regions and the intercontinental origins of surface ozone over Europe. Atmospheric Environment 112, 216–224. https://doi.org/10.1016/j.atmosenv.2015.04.049

Desikan, R., Hancock, J.T., Bright, J., Harrison, J., Weir, I., Hooley, R., Neill, S.J., 2005. A Role for ETR1 in Hydrogen Peroxide Signaling in Stomatal Guard Cells. Plant Physiology 137, 831–834. https://doi.org/10.1104/pp.104.056994

Desotgiu, R., Pollastrini, M., Cascio, C., Gerosa, G., Marzuoli, R., Bussotti, F., 2013. Responses to ozone on Populus "Oxford" clone in an open top chamber experiment assessed before sunrise and in full sunlight. Photosynthetica 51, 267–280. https://doi.org/10.1007/s11099-012-0074-y

Digrado, A., Mitchell, N.G., Montes, C.M., Dirvanskyte, P., Ainsworth, E.A., 2020. Assessing diversity in canopy architecture, photosynthesis, and water-use efficiency in a cowpea magic population. Food and Energy Security 9, e236. https://doi.org/10.1002/fes3.236

Doğru, A., Çakırlar, H., 2020. Is leaf age a predictor for cold tolerance in winter oilseed rape plants? Functional Plant Biology 47, 250–262. https://doi.org/10.1071/FP19200

Dolatabadian, A., Sanavy, S. a. M.M., Chashmi, N.A., 2008. The Effects of Foliar Application of Ascorbic Acid (Vitamin C) on Antioxidant Enzymes Activities, Lipid Peroxidation and Proline Accumulation of Canola (*Brassica napus* L.) under Conditions of Salt Stress. Journal of Agronomy and Crop Science 194, 206–213. https://doi.org/10.1111/j.1439-037X.2008.00301.x

Du, Zhanyuan., Bramlage, W.J., 1992. Modified thiobarbituric acid assay for measuring lipid oxidation in sugar-rich plant tissue extracts. Journal of Agricultural Food Chemistry 40, 1566–1570. https://doi.org/10.1021/jf00021a018

Duckham, M. (DEFRA), 2022. Farming Statistics - provisional arable crop areas at 1 June 2020 England.

Dueñas, C., Fernández, M.C., Cañete, S., Carretero, J., Liger, E., 2004. Analyses of ozone in urban and rural sites in Málaga (Spain). Chemosphere 56, 631–639. https://doi.org/10.1016/j.chemosphere.2004.04.013

Dumanović, J., Nepovimova, E., Natić, M., Kuča, K., Jaćević, V., 2021. The Significance of Reactive Oxygen Species and Antioxidant Defense System in Plants: A Concise Overview. Frontiers in Plant Science 11.

Elavarthi, S., Martin, B., 2010. Spectrophotometric Assays for Antioxidant Enzymes in Plants, in: Sunkar, R. (Ed.), Plant Stress Tolerance: Methods and Protocols, Methods in Molecular Biology. Humana Press, Totowa, NJ, 273–280. https://doi.org/10.1007/978-1-60761-702-0_16

Emberson, L.D., Ashmore, M.R., Simpson, D., Tuovinen, J.-P., Cambridge, H.M., 2001. Modelling and Mapping Ozone Deposition in Europe. Water, Air, & Soil Pollution 130, 577–582. https://doi.org/10.1023/A:1013851116524

Emberson, L.D., Pleijel, H., Ainsworth, E.A., van den Berg, M., Ren, W., Osborne, S., Mills, G., Pandey, D., Dentener, F., Büker, P., Ewert, F., Koeble, R., Van Dingenen, R., 2018. Ozone effects on crops and consideration in crop models. European Journal of Agronomy, Recent advances in crop modelling to support sustainable agricultural production and food security under global change 100, 19–34. https://doi.org/10.1016/j.eja.2018.06.002

Etienne, P., Diquelou, S., Prudent, M., Salon, C., Maillard, A., Ourry, A., 2018. Macro and Micronutrient Storage in Plants and Their Remobilization When Facing Scarcity: The Case of Drought. Agriculture 8, 14. https://doi.org/10.3390/agriculture8010014

European Commission (2020). Oilseed rape Dashboard. URL: https://circabc.europa.eu/sd/a/2c8378ab-c686-449d-9dd1-65371ab30889/Oilseeds-dashboard_en.pdf. (Last accessed 10/02/2021)

European Environment Agency (2018) Air quality in Europe — 2018 report. EEA Report No 12/2018. URL: https://www.eea.europa.eu/publications/air-quality-in-europe-2018 (Last accessed 21/04/23)

Evans, J.R., 2021. Mesophyll conductance: walls, membranes and spatial complexity. New Phytologist 229, 1864–1876. https://doi.org/10.1111/nph.16968

Fagerstrom, T., Larsson, S., Tenow, O., 1987. On Optimal Defence in Plants. Functional Ecology 1, 73–81. https://doi.org/10.2307/2389708

Farooq, M.A., Niazi, A.K., Akhtar, J., Saifullah, Farooq, M., Souri, Z., Karimi, N., Rengel, Z., 2019. Acquiring control: The evolution of ROS-Induced oxidative stress and redox signaling pathways in plant stress responses. Plant Physiology and Biochemistry 141, 353–369. https://doi.org/10.1016/j.plaphy.2019.04.039

Farvardin, A., González-Hernández, A.I., Llorens, E., García-Agustín, P., Scalschi, L., Vicedo, B., 2020. The Apoplast: A Key Player in Plant Survival. Antioxidants 9, 604. https://doi.org/10.3390/antiox9070604

Fatima, A., Singh, A.A., Mukherjee, A., Agrawal, M., Agrawal, S.B., 2019. Ascorbic acid and thiols as potential biomarkers of ozone tolerance in tropical wheat cultivars. Ecotoxicology and Environmental Safety 171, 701–708. https://doi.org/10.1016/j.ecoenv.2019.01.030

Federation of Oils, Seeds and Fats Associations Ltd (FOSFA). 2016. Document 26A: Contract for UK rapeseed in bulk suitable for oil extraction. URL https://www.fosfa.org/document-library/contract-no-26a/ (Last accessed 14/03/2023).

Felzer, B.S., Cronin, T., Reilly, J.M., Melillo, J.M., Wang, X., 2007. Impacts of ozone on trees and crops. Comptes Rendus Geoscience, Impact du changement climatique global sur la qualité de l'air à l'échelle régionale 339, 784–798. https://doi.org/10.1016/j.crte.2007.08.008

Feng, Y., Nguyen, T.H., Alam, M.S., Emberson, L., Gaiser, T., Ewert, F., Frei, M., 2022. Identifying and modelling key physiological traits that confer tolerance or sensitivity to ozone in winter wheat. Environmental Pollution 304, 119251. https://doi.org/10.1016/j.envpol.2022.119251

Feng, Z., Paoletti, E., Bytnerowicz, A., Harmens, H., 2015. Ozone and plants. Environmental Pollution 202, 215–216. https://doi.org/10.1016/j.envpol.2015.02.004

Feng, Z., Uddling, J., Tang, H., Zhu, J., Kobayashi, K., 2018. Comparison of crop yield sensitivity to ozone between open-top chamber and free-air experiments. Global Change Biology 24, 2231–2238. https://doi.org/10.1111/gcb.14077

Fiala, J., Černikovský, L., de Leeuw, F., Kurfürst, P., 2003. Air pollution by ozone in Europe in summer 2003. Overview of exceedances of EC ozone threshold values during the summer season April-August 2003 and comparisons with previous years. URL: https://www.researchgate.net/profile/Frank-De-Leeuw/publication/235961536_Air_pollution_by_ozone_in_Europe_in_summer_2003_Overview_of_exceedances_of_EC_ozone_threshold_values_during_the_summer_season_April-August_2003_and_comparisons_with_previous_years/links/5a538d11a6fdccf3e2df79d3/Air-pollution-by-ozone-in-Europe-in-summer-2003-Overview-of-exceedances-of-EC-ozone-threshold-values-during-the-summer-season-April-August-2003-and-comparisons-with-previous-years.pdf

Finnan, J.M., Jones, M.B., Burke, J.I., 1996. A time-concentration study on the effects of ozone on spring wheat (*Triticum aestivum* L.). 2. A comparison of indices. Agriculture, Ecosystems & Environment 57, 169–177. https://doi.org/10.1016/0167-8809(95)01004-1

Fischer, R.A., Maurer, R., 1978. Drought resistance in spring wheat cultivars. I. Grain yield responses. Australian Journal of Agricultural Research 29, 897–912. https://doi.org/10.1071/ar9780897

Fiscus, E.L., Booker, F.L., Burkey, K.O., 2005. Crop responses to ozone: uptake, modes of action, carbon assimilation and partitioning. Plant, Cell & Environment 28, 997–1011. https://doi.org/10.1111/j.1365-3040.2005.01349.x

Fowler, D., Amann, M., Anderson, R., Ashmore, M., Cox, P., Depledge, M., Derwent, D., Grennfelt, P., Hewitt, N., Hov, O., Jenkin, M., Kelly, F., Liss, P.S., Pilling, M., Pyle, J., Slingo, J., Stevenson, D., 2008. Ground-level ozone in the 21st century: Future trends, impacts and policy implications, Royal Society Science Policy Report.

Franzaring, J., Tonneijck, A.E.G., Kooijman, A.W.N., Dueck, Th.A., 2000. Growth responses to ozone in plant species from wetlands. Environmental and Experimental Botany 44, 39–48. https://doi.org/10.1016/S0098-8472(00)00052-6

Frei, E.R., Schnell, L., Vitasse, Y., Wohlgemuth, T., Moser, B., 2020. Assessing the Effectiveness of in-situ Active Warming Combined With Open Top Chambers to Study Plant Responses to Climate Change. Frontiers in Plant Science 11. 539-584. https://doi.org/10.3389/fpls.2020.539584

Frei, M., 2015. Breeding of ozone resistant rice: Relevance, approaches and challenges. Environmental Pollution 197, 144–155. https://doi.org/10.1016/j.envpol.2014.12.011

Frei, M., Tanaka, J.P., Wissuwa, M., 2008. Genotypic variation in tolerance to elevated ozone in rice: dissection of distinct genetic factors linked to tolerance mechanisms. Journal of Experimental Botany 59, 3741–3752. https://doi.org/10.1093/jxb/ern222

Frei, M., Wissuwa, M., Pariasca-Tanaka, J., Chen, C.P., Südekum, K.-H., Kohno, Y., 2012. Leaf ascorbic acid level – Is it really important for ozone tolerance in rice? Plant Physiology and Biochemistry, Reactive Oxygen, Nitrogen, Carbonyl and Sulfur Species in Plants 59, 63–70. https://doi.org/10.1016/j.plaphy.2012.02.015

Frenck, G., van der Linden, L., Mikkelsen, T.N., Brix, H., Jørgensen, R.B., 2011. Increased [CO_2] does not compensate for negative effects on yield caused by higher temperature and [O_3] in *Brassica napus* L. European Journal of Agronomy 35, 127–134. https://doi.org/10.1016/j.eja.2011.05.004

Fu, Y.B., Gugel, R.K., 2009. Genetic variability of Canadian elite cultivars of summer turnip rape (*Brassica rapa* L.) revealed by simple sequence repeat markers. Canadian Journal of Plant Science. 89, 865–874. https://doi.org/10.4141/CJPS09021

Fuhrer, J., 1994. Effects of ozone on managed pasture: I. Effects of open-top chambers on microclimate, ozone flux, and plant growth. Environmental Pollution 86, 297–305. https://doi.org/10.1016/0269-7491(94)90170-8

Fuhrer, J., Acherman, B., 1994. Critical levels for ozone, an UN-ECE workshop report.

Fuhrer, J., Booker, F., 2003. Ecological issues related to ozone: agricultural issues. Environment International, Future Directions in Air Quality Research: Ecological, Atmospheric, Regulatory/Policy/Economic, and Educational Issues 29, 141–154. https://doi.org/10.1016/S0160-4120(02)00157-5

Fujita, E.M., Campbell, D.E., Zielinska, B., Sagebiel, J.C., Bowen, J.L., Goliff, W.S., Stockwell, W.R., Lawson, D.R., 2003. Diurnal and Weekday Variations in the Source Contributions of Ozone Precursors in California's South Coast Air Basin. Journal of the Air & Waste Management Association 53, 844–863. https://doi.org/10.1080/10473289.2003.10466226

Gan, S., Amasino, R.M., 1997. Making Sense of Senescence (Molecular Genetic Regulation and Manipulation of Leaf Senescence). Plant Physiology 113, 313–319. https://doi.org/10.1104/pp.113.2.313

Gandin, A., Dizengremel, P., Jolivet, Y., 2021. Integrative role of plant mitochondria facing oxidative stress: The case of ozone. Plant Physiology and Biochemistry 159, 202–210. https://doi.org/10.1016/j.plaphy.2020.12.019

Gaudel, A., Cooper, O.R., Ancellet, G., Barret, B., Boynard, A., Burrows, J.P., Clerbaux, C., Coheur, P.-F., Cuesta, J., Cuevas, E., Doniki, S., Dufour, G., Ebojie, F., Foret, G., Garcia, O., Granados-Muñoz, M.J., Hannigan, J.W., Hase, F., Hassler, B., Huang, G., Hurtmans, D., Jaffe, D., Jones, N., Kalabokas, P., Kerridge, B., Kulawik, S., Latter, B., Leblanc, T., Le Flochmoën, E., Lin, W., Liu, J., Liu, X., Mahieu, E., McClure-Begley, A., Neu, J.L., Osman, M., Palm, M., Petetin, H., Petropavlovskikh, I., Querel, R., Rahpoe, N., Rozanov, A., Schultz, M.G., Schwab, J., Siddans, R., Smale, D., Steinbacher, M., Tanimoto, H., Tarasick, D.W., Thouret, V., Thompson, A.M., Trickl, T., Weatherhead, E., Wespes, C., Worden, H.M., Vigouroux, C., Xu, X., Zeng, G., Ziemke, J., 2018. Tropospheric Ozone Assessment Report: Present-day distribution and trends of tropospheric ozone relevant to climate and global atmospheric chemistry model evaluation. Elementa: Science of the Anthropocene 6, 39. https://doi.org/10.1525/elementa.291

Gaudel, A., Cooper, O.R., Chang, K.-L., Bourgeois, I., Ziemke, J.R., Strode, S.A., Oman, L.D., Sellitto, P., Nédélec, P., Blot, R., Thouret, V., Granier, C., 2020. Aircraft observations since the 1990s reveal increases of tropospheric ozone at multiple locations across the Northern Hemisphere. Science Advances 6, eaba8272. https://doi.org/10.1126/sciadv.aba8272

Ghosh, S., Mahoney, S.R., Penterman, J.N., Peirson, D., Dumbroff, E.B., 2001. Ultrastructural and biochemical changes in chloroplasts during Brassica napus senescence. Plant Physiology and Biochemistry 39, 777–784. https://doi.org/10.1016/S0981-9428(01)01296-7

Giannopolitis, C.N., Ries, S.K., 1977. Superoxide Dismutases: I. Occurrence in Higher Plants 1 2. Plant Physiology 59, 309–314. https://doi.org/10.1104/pp.59.2.309

Gill, S.S., Anjum, N.A., Gill, R., Yadav, S., Hasanuzzaman, M., Fujita, M., Mishra, P., Sabat, S.C., Tuteja, N., 2015. Superoxide dismutase—mentor of abiotic stress tolerance in crop plants. Environmenal Science Pollution Research 22, 10375–10394. https://doi.org/10.1007/s11356-015-4532-5

Gill, S.S., Tuteja, N., 2010. Reactive oxygen species and antioxidant machinery in abiotic stress tolerance in crop plants. Plant Physiology and Biochemistry 48, 909–930. https://doi.org/10.1016/j.plaphy.2010.08.016

Gillespie, K.M., Xu, F., Richter, K.T., Mcgrath, J.M., Markelz, R.J.C., Ort, D.R., Leakey, A.D.B., Ainsworth, E.A., 2012. Greater antioxidant and respiratory metabolism in field-grown soybean exposed to elevated O_3 under both ambient and elevated CO_2. Plant, Cell & Environment 35, 169–184. https://doi.org/10.1111/j.1365-3040.2011.02427.x

Girondé, A., Etienne, P., Trouverie, J., Bouchereau, A., Le Cahérec, F., Leport, L., Orsel, M., Niogret, M.-F., Nesi, N., Carole, D., Soulay, F., Masclaux-Daubresse, C., Avice, J.-C., 2015. The contrasting N management of two oilseed rape genotypes reveals the mechanisms of proteolysis associated with leaf N remobilization and the respective contributions of leaves and stems to N storage and remobilization during seed filling. Biomed Central Plant Biology 15, 59. https://doi.org/10.1186/s12870-015-0437-1

Grace, S.C., n.d. The role of photosynthetic electron transport in production and scavenging of reactive oxygen species in chloroplasts of *Pisum sativum*. PhD Thesis. Duke University, United States -- North Carolina.

Grantz, D.A., Gunn, S., Vu, H.-B., 2006. O_3 impacts on plant development: a meta-analysis of root/shoot allocation and growth. Plant, Cell & Environment 29, 1193–1209. https://doi.org/10.1111/j.1365-3040.2006.01521.x

Grbić, V., Bleecker, A.B., 1995. Ethylene regulates the timing of leaf senescence in Arabidopsis. The Plant Journal 8, 595–602. https://doi.org/10.1046/j.1365-313X.1995.8040595.x

Green, S., Kiener, T., 1989. Digestibilities of nitrogen and amino acids in soya-bean, sunflower, meat and rapeseed meals measured with pigs and poultry. Animal Production 48, 157–179. https://doi.org/10.1017/S0003356100003895

Grulke, N.E., Heath, R.L., 2020. Ozone effects on plants in natural ecosystems. Plant Biology 22, 12–37. https://doi.org/10.1111/plb.12971

Guiboileau, A., Sormani, R., Meyer, C., Masclaux-Daubresse, C., 2010. Senescence and death of plant organs: Nutrient recycling and developmental regulation. Comptes Rendus Biologies, Développement végétatif des plantes 333, 382–391. https://doi.org/10.1016/j.crvi.2010.01.016

Guiboileau, A., Sormani, R., Meyer, C., Masclaux-Daubresse, C., 2010. Senescence and death of plant organs: Nutrient recycling and developmental regulation. Comptes Rendus Biologies, Développement végétatif des plantes 333, 382–391. https://doi.org/10.1016/j.crvi.2010.01.016

Gulden, R.H., Warwick, S.I., Thomas, A.G., 2008. The Biology of Canadian Weeds. 137. *Brassica napus* L. and *B. rapa* L. Canadian Journal of Plant Science 88, 951–996. https://doi.org/10.4141/CJPS07203

Guo, J., Li, X.F., Qi, D.M., Chen, S.Y., Li, Z.Q., Nijs, I., Li, Y.G., Liu, G.S., 2009. Effects of ozone on wild type and transgenic tobacco. Biol Plant 53, 670–676. https://doi.org/10.1007/s10535-009-0121-0

Guri, A., 1983. Variation on glutathione and ascorbic acid content among selected cultivars of *Phaseolus vulgaris* prior to and after exposure to ozone. Canadian Journal of Plant Science 63, 733–737. https://doi.org/10.4141/cjps83-090

Hajiboland, R., 2014. Chapter 1 - Reactive Oxygen Species and Photosynthesis, in: Ahmad, P. (Ed.), Oxidative Damage to Plants. Academic Press, San Diego, 1–63. https://doi.org/10.1016/B978-0-12-799963-0.00001-0

Halliwell, B., 2006. Reactive Species and Antioxidants. Redox Biology Is a Fundamental Theme of Aerobic Life. Plant Physiology 141, 312–322. https://doi.org/10.1104/pp.106.077073

Han, H., Liu, J., Yuan, H., Zhuang, B., Zhu, Y., Wu, Y., Yan, Y., Ding, A., 2018. Characteristics of intercontinental transport of tropospheric ozone from Africa to Asia. Atmospheric Chemistry and Physics 18, 4251–4276. https://doi.org/10.5194/acp-18-4251-2018

Han, Y.J., Gharibeshghi, A., Mewis, I., Förster, N., Beck, W., Ulrichs, C., 2020. Plant responses to ozone: Effects of different ozone exposure durations on plant growth and biochemical quality of *Brassica campestris* L. ssp. *chinensis*. Scientia Horticulturae 262, 108921. https://doi.org/10.1016/j.scienta.2019.108921

Harmens, H., Hayes, F., Sharps, K., Mills, G., Calatayud, V., 2017. Leaf traits and photosynthetic responses of Betula pendula saplings to a range of ground-level ozone concentrations at a range of nitrogen loads. Journal of Plant Physiology 211, 42–52. https://doi.org/10.1016/j.jplph.2017.01.002

Hauglustaine, D.A., Brasseur, G.P., 2001. Evolution of tropospheric ozone under anthropogenic activities and associated radiative forcing of climate. Journal of Geophysical Research: Atmospheres 106, 32337–32360. https://doi.org/10.1029/2001JD900175

Hayes, F., Bangor, C., 2017. III. Mapping Critical Levels for Vegetation. URL: https://unece.org/fileadmin/DAM/env/documents/2017/AIR/EMEP/Final_new_Chapter_3_v2_August_2017_.pdf (Last accessed 12/03/2023).

Hayes, F., Mills, G., Williams, P., Harmens, H., Büker, P., 2006. Impacts of summer ozone exposure on the growth and overwintering of UK upland vegetation. Atmospheric Environment 40, 4088–4097. https://doi.org/10.1016/j.atmosenv.2006.03.012

Heggestad, H.E., Middleton, J.T., 1959. Ozone in High Concentrations as Cause of Tobacco Leaf Injury. Science 129, 208–210. https://doi.org/10.1126/science.129.3343.208

Hegglin, M.I., Shepherd, T.G., 2009. Large climate-induced changes in ultraviolet index and stratosphere-to-troposphere ozone flux. Nature Geosci 2, 687–691. https://doi.org/10.1038/ngeo604

Herbinger, K., Tausz, M., Wonisch, A., Soja, G., Sorger, A., Grill, D., 2002. Complex interactive effects of drought and ozone stress on the antioxidant defence systems of two wheat cultivars. Plant Physiology and Biochemistry, Free radicals and oxidative stress in plants: A new insight 40, 691–696. https://doi.org/10.1016/S0981-9428(02)01410-9

Heuzé V., Tran G., Kaushik S. (2020). Soybean meal. Feedipedia, a programme by INRAE, CIRAD, AFZ and FAO. https://www.feedipedia.org/node/674. (Last accessed 10/01/2021)

HGCA., 2006. Identifying the factors determining the chlorophyll content of UK rapeseed. Topic Report OS61. URL: https://projectblue.blob.core.windows.net/media/Default/Research%20Papers/Cereals%20and%20Oilseed/os61_complete_final_report.pdf (Last accessed 10/04/2023)

HGCA., 2006. Improving oil content and minimising green seeds in oilseed rape. Topic Sheet No. 93, Topic Report 397. URL

Holland, J.B., 2004. Implementation of molecular markers for quantitative traits in breeding programs - challenges and opportunities.

Hoshika, Y., Haworth, M., Watanabe, M., Koike, T., 2020. Interactive effect of leaf age and ozone on mesophyll conductance in Siebold's beech. Physiologia Plantarum 170, 172–186. https://doi.org/10.1111/ppl.13121

Hoshika, Y., Katata, G., Deushi, M., Watanabe, M., Koike, T., Paoletti, E., 2015. Ozone-induced stomatal sluggishness changes carbon and water balance of temperate deciduous forests. Sci Rep 5, 9871. https://doi.org/10.1038/srep09871

Hossain, M.A., Asada, K., 1984. Inactivation of Ascorbate Peroxidase in Spinach Chloroplasts on Dark Addition of Hydrogen Peroxide: Its Protection by Ascorbate. Plant and Cell Physiology 25, 1285–1295. https://doi.org/10.1093/oxfordjournals.pcp.a076837

https://cropscience.bayer.co.uk/blog/articles/2020/12/importance-of-weather-in-oilseed-rape-performance/ (Last accessed 07/03/2021).

Hu, C., Kang, P., Jaffe, D.A., Li, C., Zhang, X., Wu, K., Zhou, M., 2021. Understanding the impact of meteorology on ozone in 334 cities of China. Atmospheric Environment 248, 118221. https://doi.org/10.1016/j.atmosenv.2021.118221

Hu, Q., Hua, W., Yin, Y., Zhang, X., Liu, L., Shi, J., Zhao, Y., Qin, L., Chen, C., Wang, H., 2017. Rapeseed research and production in China. The Crop Journal, Advances in Crop Science: Innovation and Sustainability 5, 127–135. https://doi.org/10.1016/j.cj.2016.06.005

Huang, R., Liu, Z., Xing, M., Yang, Y., Wu, X., Liu, H., Liang, W., 2019. Heat Stress Suppresses *Brassica napus* Seed Oil Accumulation by Inhibition of Photosynthesis and BnWRI1 Pathway. Plant and Cell Physiology 60, 1457–1470. https://doi.org/10.1093/pcp/pcz052

Hüve, K., Bichele, I., Rasulov, B., Niinemets, Ü., 2011. When it is too hot for photosynthesis: heat-induced instability of photosynthesis in relation to respiratory burst, cell permeability changes and H_2O_2 formation. Plant, Cell & Environment 34, 113–126. https://doi.org/10.1111/j.1365-3040.2010.02229.x

Iqbal Qureshi, A.M., Sofi, M.U., Dar, N.A., Khan, M.H., Mahdi, S.S., Dar, Z.A., Bangroo, S., El-Serehy, H.A., Hefft, D.I., Popescu, S.M., 2021. Insilco identification and characterization of superoxide dismutase gene family in *Brassica rapa*. Saudi Journal of Biological Sciences 28, 5526–5537. https://doi.org/10.1016/j.sjbs.2021.08.009

Ishikawa, T., Shigeoka, S., 2008. Recent Advances in Ascorbate Biosynthesis and the Physiological Significance of Ascorbate Peroxidase in Photosynthesizing Organisms. Bioscience, Biotechnology, and Biochemistry 72, 1143–1154. https://doi.org/10.1271/bbb.80062

Jenkin, M.E., 2008. Trends in ozone concentration distributions in the UK since 1990: Local, regional and global influences. Atmospheric Environment 42, 5434–5445. https://doi.org/10.1016/j.atmosenv.2008.02.036

Jones, D.K., Dalton, D.A., Rosell, F.I., Raven, E.L., 1998. Class I Heme Peroxidases: Characterization of Soybean Ascorbate Peroxidase. Archives of Biochemistry and Biophysics 360, 173–178. https://doi.org/10.1006/abbi.1998.0941

Junglee, S., Urban, L., Sallanon, H., Lopez-Lauri, F., 2014. Optimized Assay for Hydrogen Peroxide Determination in Plant Tissue Using Potassium Iodide. American Journal of Analytical Chemistry 05, 730. https://doi.org/10.4236/ajac.2014.511081

Kalaji, H.M., Jajoo, A., Oukarroum, A., Brestic, M., Zivcak, M., Samborska, I.A., Cetner, M.D., Łukasik, I., Goltsev, V., Ladle, R.J., 2016. Chlorophyll a fluorescence as a tool to monitor physiological status of plants under abiotic stress conditions. Acta Physiol Plant 38, 102. https://doi.org/10.1007/s11738-016-2113-y

Kant, M.R., Jonckheere, W., Knegt, B., Lemos, F., Liu, J., Schimmel, B.C.J., Villarroel, C.A., Ataide, L.M.S., Dermauw, W., Glas, J.J., Egas, M., Janssen, A., Van Leeuwen, T., Schuurink, R.C., Sabelis, M.W., Alba, J.M., 2015. Mechanisms and ecological consequences of plant defence induction and suppression in herbivore communities. Annals of Botany 115, 1015–1051. https://doi.org/10.1093/aob/mcv054

Karuppanapandian, T., Moon, J.-C., Kim, C., Manoharan, K., Kim, W., 2011. Reactive Oxygen Species in Plants: Their Generation, Signal Transduction, and Scavenging Mechanisms. Australian Journal of Crop Science 5, 709–725. https://doi.org/10.3316/informit.282079847301776

Kask, K., Kännaste, A., Talts, E., Copolovici, L., Niinemets, Ü., 2016. How specialized volatiles respond to chronic and short-term physiological and shock heat stress in *Brassica nigra*. Plant, Cell & Environment 39, 2027–2042. https://doi.org/10.1111/pce.12775

Kessel, B., Schierholt, A., Becker, H.C., 2012. Nitrogen Use Efficiency in a Genetically Diverse Set of Winter Oilseed Rape (*Brassica napus* L.). Crop Science 52, 2546–2554. https://doi.org/10.2135/cropsci2012.02.0134

Kiddle, G., Pastori, G.M., Bernard, S., Pignocchi, C., Antoniw, J., Verrier, P.J., Foyer, C.H., 2003. Effects of Leaf Ascorbate Content on Defense and Photosynthesis Gene Expression in *Arabidopsis thaliana*. Antioxidants & Redox Signaling 5, 23–32. https://doi.org/10.1089/152308603321223513

Kim, J., Woo, H.R., Nam, H.G., 2016. Toward Systems Understanding of Leaf Senescence: An Integrated Multi-Omics Perspective on Leaf Senescence Research. Molecular Plant 9, 813–825. https://doi.org/10.1016/j.molp.2016.04.017

Knutsen, H.K., Alexander, J., Barregård, L., Bignami, M., Brüschweiler, B., Ceccatelli, S., Dinovi, M., Edler, L., Grasl-Kraupp, B., Hogstrand, C., Hoogenboom, L. (Ron), Nebbia, C.S., Oswald, I., Petersen, A., Rose, M., Roudot, A.-C., Schwerdtle, T., Vollmer, G., Wallace, H., Cottrill, B., Dogliotti, E., Laakso, J., Metzler, M., Velasco, L., Baert, K., Ruiz, J.A.G., Varga, E., Dörr, B., Sousa, R., Vleminckx, C., 2016. Erucic acid in feed and food. EFSA Journal 14, e04593. https://doi.org/10.2903/j.efsa.2016.4593

Koester, R.P., Nohl, B.M., Diers, B.W., Ainsworth, E.A., 2016. Has photosynthetic capacity increased with 80 years of soybean breeding? An examination of historical soybean cultivars. Plant, Cell & Environment 39, 1058–1067. https://doi.org/10.1111/pce.12675

Kotchoni, S.O., Larrimore, K.E., Mukherjee, M., Kempinski, C.F., Barth, C., 2009. Alterations in the Endogenous Ascorbic Acid Content Affect Flowering Time in Arabidopsis. Plant Physiology 149, 803–815. https://doi.org/10.1104/pp.108.132324

Kozioł, M.J., Whatley, F.R., 2016. Gaseous Air Pollutants and Plant Metabolism. Butterworth-Heinemann. PDF: https://shop.elsevier.com/books/gaseous-air-pollutants-and-plant-metabolism/koziol/978-0-408-11152-2 (last accessed 21/06/2023).

Kumar, S., Trivedi, P.K., 2018. Glutathione S-Transferases: Role in Combating Abiotic Stresses Including Arsenic Detoxification in Plants. Frontiers in Plant Science 9. https://doi.org/10.3389/fpls.2018.00751

Kusaba, M., Tanaka, A., Tanaka, R., 2013. Stay-green plants: what do they tell us about the molecular mechanism of leaf senescence. Photosynthesis Research 117, 221–234. https://doi.org/10.1007/s11120-013-9862-x

Larson, R.A., 1988. The antioxidants of higher plants. Phytochemistry 27, 969–978. https://doi.org/10.1016/0031-9422(88)80254-1

Lawlor, D.W., 2013. Genetic engineering to improve plant performance under drought: physiological evaluation of achievements, limitations, and possibilities. Journal of Experimental Botany 64, 83–108. https://doi.org/10.1093/jxb/ers326

Lee, E.H., Bennett, J.H., 1982. Superoxide Dismutase: A possible protective enzyme against ozone injury in snap beans (*phaseolus vulgaris* L.). Plant Physiology 69, 1444–1449. https://doi.org/10.1104/pp.69.6.1444

Lee, Y.K., Mok Kim, S., Han, S., 2003. Ozone-induced inactivation of antioxidant enzymes. Biochimie 85, 947–952. https://doi.org/10.1016/j.biochi.2003.09.012

Lefohn, A.S., Runeckles, V.C., 1987. Establishing standards to protect vegetation—ozone exposure/dose considerations. Atmospheric Environment (1967) 21, 561–568. https://doi.org/10.1016/0004-6981(87)90038-2

Lefol, E., Séguin-Swartz, G., Downey, R.K., 1997. Sexual hybridisation in crosses of cultivated *Brassica* species with the crucifers *Erucastrum gallicum* and *Raphanus raphanistrum*: Potential for gene introgression. Euphytica 95, 127–139. https://doi.org/10.1023/A:1002940009104

Lei, H., Wuebbles, D.J., Liang, X.-Z., 2012. Projected risk of high ozone episodes in 2050. Atmospheric Environment 59, 567–577. https://doi.org/10.1016/j.atmosenv.2012.05.051

Lelieveld, J., Roelofs, G. –J., Ganzeveld, L., Feichter, J., Rodhe, H., 1997. Terrestrial sources and distribution of atmospheric sulphur. Philosophical Transactions of the Royal Society of London. Series B: Biological Sciences 352, 149–158. https://doi.org/10.1098/rstb.1997.0010

Li, Z., Peng, J., Wen, X., Guo, H., 2013. *ETHYLENE-INSENSITIVE3* is a senescence-associated gene that accelerates age-dependent leaf senescence by directly repressing miR164 transcription in Arabidopsis. The Plant Cell 25, 3311–3328. https://doi.org/10.1105/tpc.113.113340

Li, Z., Yang, J., Shang, B., Agathokleous, E., Rubert-Nason, K.F., Xu, Y., Feng, Z., 2021. Nonlinear responses of foliar phenylpropanoids to increasing O_3 exposure: Ecological implications in a Populus model system. Science of The Total Environment 767, 144358. https://doi.org/10.1016/j.scitotenv.2020.144358

Lin, M., Horowitz, L.W., Xie, Y., Paulot, F., Malyshev, S., Shevliakova, E., Finco, A., Gerosa, G., Kubistin, D., Pilegaard, K., 2020. Vegetation feedbacks during drought exacerbate ozone air pollution extremes in Europe. Nature Climate Change 10, 444–451. https://doi.org/10.1038/s41558-020-0743-y

Liyong, H., Hao, C., Guangsheng, Z., Tingdong, F., n.d. Effect of different nitrogen nutrition on the quality of rapeseed (*Brassica napus* L.) stressed by drought. Crop Physiology. https://doi.org/10.1631/jzus.2007.B0731

Lombardozzi, D., Sparks, J.P., Bonan, G., 2013. Integrating O_3 influences on terrestrial processes: photosynthetic and stomatal response data available for regional and global modeling. Biogeosciences 10, 6815–6831. https://doi.org/10.5194/bg-10-6815-2013

Lombardozzi, D., Sparks, J.P., Bonan, G., 2013. Integrating O_3 influences on terrestrial processes: photosynthetic and stomatal response data available for regional and global modeling. Biogeosciences 10, 6815–6831. https://doi.org/10.5194/bg-10-6815-2013

Lombardozzi, D., Sparks, J.P., Bonan, G., Levis, S., 2012. Ozone exposure causes a decoupling of conductance and photosynthesis: implications for the Ball-Berry stomatal conductance model. Oecologia 169, 651–659. https://doi.org/10.1007/s00442-011-2242-3

Long, S.P., Zhu, X.-G., Naidu, S.L., Ort, D.R., 2006. Can improvement in photosynthesis increase crop yields? Plant, Cell & Environment 29, 315–330. https://doi.org/10.1111/j.1365-3040.2005.01493.x

Lu, S., Aziz, M., Sturtevant, D., Chapman, K.D., Guo, L., 2020. Heterogeneous Distribution of Erucic Acid in *Brassica napus* Seeds. Frontiers in Plant Science 10. https://doi.org/10.3389/fpls.2019.01744

Lu, X., Zhang, L., Shen, L., 2019. Meteorology and Climate Influences on Tropospheric Ozone: a Review of Natural Sources, Chemistry, and Transport Patterns. Current Pollution Reports 5, 238–260. https://doi.org/10.1007/s40726-019-00118-3

Lu, Z., Percy, R.G., Qualset, C.O., Zeiger, E., 1998. Stomatal conductance predicts yields in irrigated Pima cotton and bread wheat grown at high temperatures. Journal of Experimental Botany 49, 453–460. https://doi.org/10.1093/jxb/49.Special_Issue.453

Lu, Z., Zeiger, E., 1994. Selection for higher yields and heat resistance in Pima cotton has caused genetically determined changes in stomatal conductances. Physiologia Plantarum 92, 273–278. https://doi.org/10.1111/j.1399-3054.1994.tb05337.x

Luwe, MWF., Takahama, U., Heber, U., 1993. Role of Ascorbate in Detoxifying Ozone in the Apoplast of Spinach (Spinacia oleracea L.) Leaves. Plant Physiology 101, 969–976. https://doi.org/10.1104/pp.101.3.969

Ma, L., Qi, W., Bai, J., Li, H., Fang, Y., Xu, J., Xu, Y., Zeng, X., Pu, Y., Wang, W., Liu, L., Li, X., Sun, W., Wu, J., 2022. Genome-Wide Identification and Analysis of the Ascorbate Peroxidase (APX) Gene Family of Winter Rapeseed (*Brassica rapa* L.) Under Abiotic Stress. Frontiers in Genetics 12. https://doi.org/10.3389/fgene.2021.753624

Masclaux-Daubresse, C., Daniel-Vedele, F., Dechorgnat, J., Chardon, F., Gaufichon, L., Suzuki, A., 2010. Nitrogen uptake, assimilation and remobilization in plants: challenges for sustainable and productive agriculture. Annals of Botany 105, 1141–1157. https://doi.org/10.1093/aob/mcq028

Masiol, M., Squizzato, S., Chalupa, D., Rich, D.Q., Hopke, P.K., 2019. Spatial-temporal variations of summertime ozone concentrations across a metropolitan area using a network of low-cost monitors to develop 24 hourly land-use regression models. Science of The Total Environment 654, 1167–1178. https://doi.org/10.1016/j.scitotenv.2018.11.111

Mathew, I., Shimelis, H., Shayanowako, A.I.T., Laing, M., Chaplot, V., 2019. Genome-wide association study of drought tolerance and biomass allocation in wheat. Plos One 14, e0225383. https://doi.org/10.1371/journal.pone.0225383

Mattila, P., Mäkinen, S., Eurola, M., Jalava, T., Pihlava, J.-M., Hellström, J., Pihlanto, A., 2018. Nutritional Value of Commercial Protein-Rich Plant Products. Plant Foods and Human Nutrition 73, 108–115. https://doi.org/10.1007/s11130-018-0660-7

Matyssek, R., Bytnerowicz, A., Karlsson, P.-E., Paoletti, E., Sanz, M., Schaub, M., Wieser, G., 2007. Promoting the O_3 flux concept for European forest trees. Environmental Pollution, Critcial Levels for Ozone Effects

on Vegetation: Further Applying and Developing the Flux Concept 146, 587–607. https://doi.org/10.1016/j.envpol.2006.11.011

McAdam, E.L., Brodribb, T.J., McAdam, S.A.M., 2017. Does ozone increase ABA levels by non-enzymatic synthesis causing stomata to close? Plant, Cell & Environment 40, 741–747. https://doi.org/10.1111/pce.12893

McAinsh, M.R., Evans, N.H., Montgomery, L.T., North, K.A., 2002. Calcium signalling in stomatal responses to pollutants. New Phytologist 153, 441–447. https://doi.org/10.1046/j.0028-646X.2001.00336.x

McCall, A.C., Fordyce, J.A., 2010. Can optimal defence theory be used to predict the distribution of plant chemical defences? Journal of Ecology 98, 985–992. https://doi.org/10.1111/j.1365-2745.2010.01693.x

McCord, J.M., Fridovich, I., 1969. Superoxide Dismutase: an enzymic function for erythrocuprein (hemocuprein). Journal of Biological Chemistry 244, 6049–6055. https://doi.org/10.1016/S0021-9258(18)63504-5

McGrath, J.M., Betzelberger, A.M., Wang, S., Shook, E., Zhu, X.-G., Long, S.P., Ainsworth, E.A., 2015. An analysis of ozone damage to historical maize and soybean yields in the United States. Proceedings of the National Academy of Sciences 112, 14390–14395. https://doi.org/10.1073/pnas.1509777112

McKey, D., 1974. Adaptive Patterns in Alkaloid Physiology. The American Naturalist 108, 305–320. https://doi.org/10.1086/282909

Mehlhorn, H., Cottam, D.A., Lucas, P.W., Wellburn, A.R., 1987. Induction of Ascorbate Peroxidase and Glutathione Reductase Activities by Interactions of Mixtures of Air Pollutants. Free Radical Research Communications 3, 193–197. https://doi.org/10.3109/10715768709069784

Mehlhorn, H., O'Shea, J.M., Wellburn, A.R., 1991. Atmospheric Ozone Interacts with Stress Ethylene Formation by Plants to Cause Visible Plant Injury. Journal of Experimental Botany 42, 17–24. https://doi.org/10.1093/jxb/42.1.17

Mickelbart, M.V., Hasegawa, P.M., Bailey-Serres, J., 2015. Genetic mechanisms of abiotic stress tolerance that translate to crop yield stability. Nature Reviews Genetics 16, 237–251. https://doi.org/10.1038/nrg3901

Mikkelsen, T.N., Heide-Jørgensen, H.S., 1996. Acceleration of leaf senescence inFagus sylvatica L. by low levels of tropospheric ozone demonstrated by leaf colour, chlorophyll fluorescence and chloroplast ultrastructure. Trees 10, 145–156. https://doi.org/10.1007/BF02340766

Miller, J.D., Arteca, R.N., Pell, E.J., 1999. Senescence-Associated Gene Expression during Ozone-Induced Leaf Senescence in *Arabidopsis*. Plant Physiology 120, 1015–1024. https://doi.org/10.1104/pp.120.4.1015

Mills, G., Buse, A., Gimeno, B., Bermejo, V., Holland, M., Emberson, L., Pleijel, H., 2007. A synthesis of AOT40-based response functions and critical levels of ozone for agricultural and horticultural crops. Atmospheric Environment 41, 2630–2643. https://doi.org/10.1016/j.atmosenv.2006.11.016

Mills, G., Hayes, F., Simpson, D., Emberson, L., Norris, D., Harmens, H., Büker, P., 2011. Evidence of widespread effects of ozone on crops and (semi-)natural vegetation in Europe (1990–2006) in relation to AOT40- and flux-based risk maps. Global Change Biology 17, 592–613. https://doi.org/10.1111/j.1365-2486.2010.02217.x

Mills, G., Hayes, F., Wilkinson, S., Davies, W.J., 2009. Chronic exposure to increasing background ozone impairs stomatal functioning in grassland species. Global Change Biology 15, 1522–1533. https://doi.org/10.1111/j.1365-2486.2008.01798.x

Mills, G., Pleijel, H., Malley, C.S., Sinha, B., Cooper, O.R., Schultz, M.G., Neufeld, H.S., Simpson, D., Sharps, K., Feng, Z., Gerosa, G., Harmens, H., Kobayashi, K., Saxena, P., Paoletti, E., Sinha, V., Xu, X., 2018a. Tropospheric Ozone Assessment Report: Present-day tropospheric ozone distribution and trends relevant to vegetation. Elementa: Science of the Anthropocene 6, 47. https://doi.org/10.1525/elementa.302

Mills, G., Sharps, K., Simpson, D., Pleijel, H., Broberg, M., Uddling, J., Jaramillo, F., Davies, W.J., Dentener, F., Van den Berg, M., Agrawal, M., Agrawal, S.B., Ainsworth, E.A., Büker, P., Emberson, L., Feng, Z., Harmens, H., Hayes, F., Kobayashi, K., Paoletti, E., Van Dingenen, R., 2018b. Ozone pollution will compromise efforts to increase global wheat production. Global Change Biology 24, 3560–3574. https://doi.org/10.1111/gcb.14157

Mills, G., Sharps, K., Simpson, D., Pleijel, H., Frei, M., Burkey, K., Emberson, L., Uddling, J., Broberg, M., Feng, Z., Kobayashi, K., Agrawal, M., 2018c. Closing the global ozone yield gap: Quantification and cobenefits for multistress tolerance. Global Change Biology 24, 4869–4893. https://doi.org/10.1111/gcb.14381

Mishra, A.K., Agrawal, S.B., 2015. Biochemical and physiological characteristics of tropical mung bean (*Vigna radiata* L.) cultivars against chronic ozone stress: an insight to cultivar-specific response. Protoplasma 252, 797–811. https://doi.org/10.1007/s00709-014-0717-x

Miyazaki, K., Bowman, K., Sekiya, T., Takigawa, M., Neu, J.L., Sudo, K., Osterman, G., Eskes, H., 2021. Global tropospheric ozone responses to reduced NO_x emissions linked to the COVID-19 worldwide lockdowns. Science Advances 7, eabf7460. https://doi.org/10.1126/sciadv.abf7460

Mizuno, M., Kamei, M., Tsuchida, H., 1998. Ascorbate peroxidase and catalase cooperate for protection against hydrogen peroxide generated in potato tubers during low-temperature storage. IUBMB Life 44, 717–726. https://doi.org/10.1080/15216549800201762

Morgan, P.B., Mies, T.A., Bollero, G.A., Nelson, R.L., Long, S.P., 2006. Season-long elevation of ozone concentration to projected 2050 levels under fully open-air conditions substantially decreases the growth and production of soybean. New Phytologist 170, 333–343. https://doi.org/10.1111/j.1469-8137.2006.01679.x

Musselman, R.C., McCool, P.M., Lefohn, A.S., 1994. Ozone Descriptors for an Air Quality Standard to Protect Vegetation. Air & Waste 44, 1383–1390. https://doi.org/10.1080/10473289.1994.10467330

Naing, A.H., Kim, C.K., 2021. Abiotic stress-induced anthocyanins in plants: Their role in tolerance to abiotic stresses. Physiologia Plantarum 172, 1711–1723. https://doi.org/10.1111/ppl.13373

Naing, A.H., Park, K.I., Ai, T.N., Chung, M.Y., Han, J.S., Kang, Y.-W., Lim, K.B., Kim, C.K., 2017. Overexpression of snapdragon Delila (Del) gene in tobacco enhances anthocyanin accumulation and abiotic stress tolerance. Biomed Central Plant Biology 17, 65. https://doi.org/10.1186/s12870-017-1015-5

Nakano, Y., Asada, K., 1981. Hydrogen Peroxide is Scavenged by Ascorbate-specific Peroxidase in Spinach Chloroplasts. Plant and Cell Physiology 22, 867–880. https://doi.org/10.1093/oxfordjournals.pcp.a076232

Nali, C., Pucciariello, C., Mills, G., Lorenzini, G., 2005. On the Different Sensitivity of White Clover Clones to Ozone: Physiological and Biochemical Parameters in a Multivariate Approach. Water Air Soil Pollution 164, 137–153. https://doi.org/10.1007/s11270-005-2717-0

Namazkar, S., Stockmarr, A., Frenck, G., Egsgaard, H., Terkelsen, T., Mikkelsen, T., Ingvordsen, C.H., Jørgensen, R.B., 2016. Concurrent elevation of CO_2, O_3 and temperature severely affects oil quality and quantity in rapeseed. Journal of Experimental Botany 67, 4117–4125. https://doi.org/10.1093/jxb/erw180

Nicácio, A.E., Rodrigues, C.A., Visentainer, J.V., Maldaner, L., 2021. Evaluation of the QuEChERS method for the determination of phenolic compounds in yellow (*Brassica alba*), brown (*Brassica juncea),* and black (*Brassica nigra)* mustard seeds. Food Chemistry 340, 128162. https://doi.org/10.1016/j.foodchem.2020.128162

Nievola, C.C., Carvalho, C.P., Carvalho, V., Rodrigues, E., 2017. Rapid responses of plants to temperature changes. Temperature 4, 371–405. https://doi.org/10.1080/23328940.2017.1377812

Noctor, G., Arisi, A.-C.M., Jouanin, L., Kunert, K.J., Rennenberg, H., Foyer, C.H., 1998. Glutathione: biosynthesis, metabolism and relationship to stress tolerance explored in transformed plants. Journal of Experimental Botany 49, 623–647. https://doi.org/10.1093/jxb/49.321.623

Noodén, L.D. ed., 2003. *Plant cell death processes*. Elsevier. 114-159

Ogunkunle, A.O., Beckett, P.H.T., 1988. The efficiency of pot trials, or trials on undisturbed soil cores, as predictors of crop behaviour in the field. Plant Soil 107, 85–93. https://doi.org/10.1007/BF02371548

Ollerenshaw, J.H., Lyons, T., Barnes, J.D., 1999. Impacts of ozone on the growth and yield of field-grown winter oilseed rape. Environmental Pollution 104, 53–59. https://doi.org/10.1016/S0269-7491(98)00155-9

Orlovius, K., 2003. Oilseed rape. Fertilizing for high yield and quality, Bulletin, 16. URL: https://www.ipipotash.org/uploads/udocs/No%2016%20Oilseed%20rape.pdf (Last accessed 23/04/23)

Örvar, B.L., Ellis, B.E., 1997. Transgenic tobacco plants expressing antisense RNA for cytosolic ascorbate peroxidase show increased susceptibility to ozone injury. The Plant Journal 11, 1297–1305. https://doi.org/10.1046/j.1365-313X.1997.11061297.x

Osborne, S., Pandey, D., Mills, G., Hayes, F., Harmens, H., Gillies, D., Büker, P., Emberson, L., 2019. New Insights into Leaf Physiological Responses to Ozone for Use in Crop Modelling. Plants 8, 84. https://doi.org/10.3390/plants8040084

Osborne, S.A., Mills, G., Hayes, F., Ainsworth, E.A., Büker, P., Emberson, L., 2016. Has the sensitivity of soybean cultivars to ozone pollution increased with time? An analysis of published dose–response data. Global Change Biology 22, 3097–3111. https://doi.org/10.1111/gcb.13318

Ovenston, T.C.J., Rees, W.T., 1950. The spectrophotometric determination of small amounts of hydrogen peroxide in aqueous solutions. Analyst 75, 204. https://doi.org/10.1039/an9507500204

Pan, J., Zhang, L., Chen, M., Ruan, Yuxuan, Li, P., Guo, Z., Liu, B., Ruan, Ying, Xiao, M., Huang, Y., 2022. Identification and charactering of APX genes provide new insights in abiotic stresses response in *Brassica napus*. PeerJ 10, e13166. https://doi.org/10.7717/peerj.13166

Pandey, A.K., Ghosh, A., Agrawal, M., Agrawal, S.B., 2018. Effect of elevated ozone and varying levels of soil nitrogen in two wheat (*Triticum aestivum* L.) cultivars: Growth, gas-exchange, antioxidant status, grain yield and quality. Ecotoxicology and Environmental Safety 158, 59–68. https://doi.org/10.1016/j.ecoenv.2018.04.014

Pandey, A.K., Majumder, B., Keski-Saari, S., Kontunen-Soppela, S., Pandey, V., Oksanen, E., 2019. High Variation in Resource Allocation Strategies among 11 Indian Wheat (*Triticum aestivum*) Cultivars Growing in High Ozone Environment. Climate 7, 23. https://doi.org/10.3390/cli7020023

Pandey, S., Fartyal, D., Agarwal, A., Shukla, T., James, D., Kaul, T., Negi, Y.K., Arora, S., Reddy, M.K., 2017. Abiotic Stress Tolerance in Plants: Myriad Roles of Ascorbate Peroxidase. Frontiers in Plant Science 8. https://doi.org/10.3389/fpls.2017.00581

Panjabi, P., Yadava, S.K., Kumar, N., Bangkim, R., Ramchiary, N., 2019. Breeding *Brassica juncea* and *B. rapa* for Sustainable Oilseed Production in the Changing Climate: Progress and Prospects, in: Kole, C. (Ed.), Genomic Designing of Climate-Smart Oilseed Crops. Springer International Publishing, Cham, 275–369. https://doi.org/10.1007/978-3-319-93536-2_6

Paoletti, E., Grulke, N.E., 2010. Ozone exposure and stomatal sluggishness in different plant physiognomic classes. Environmental Pollution 158, 2664–2671. https://doi.org/10.1016/j.envpol.2010.04.024

Paoletti, E., Materassi, A., Fasano, G., Hoshika, Y., Carriero, G., Silaghi, D., Badea, O., 2017. A new-generation 3D ozone FACE (Free Air Controlled Exposure). Science of The Total Environment 575, 1407–1414. https://doi.org/10.1016/j.scitotenv.2016.09.217

Paoletti, E., Sicard, P., Hoshika, Y., Fares, S., Badea, O., Pitar, D., Popa, I., Anav, A., Moura, B.B., De Marco, A., 2022. Towards long-term sustainability of stomatal ozone flux monitoring at forest sites. Sustainable Horizons 2, 100018. https://doi.org/10.1016/j.horiz.2022.100018

Parrish, D.D., Derwent, R.G., Steinbrecht, W., Stübi, R., Van Malderen, R., Steinbacher, M., Trickl, T., Ries, L., Xu, X., 2020. Zonal Similarity of Long-Term Changes and Seasonal Cycles of Baseline Ozone at Northern Midlatitudes. Journal of Geophysical Research: Atmospheres 125, e2019JD031908. https://doi.org/10.1029/2019JD031908

Pasqualini, S., Batini, P., Ederli, L., Porceddu, A., Piccioni, C., De Marchis, F., Antonielli, M., 2001. Effects of short-term ozone fumigation on tobacco plants: response of the scavenging system and expression of the glutathione reductase. Plant, Cell & Environment 24, 245–252. https://doi.org/10.1111/j.1365-3040.2001.00671.x

Paul-Victor, C., Züst, T., Rees, M., Kliebenstein, D.J., Turnbull, L.A., 2010. A new method for measuring relative growth rate can uncover the costs of defensive compounds in *Arabidopsis thaliana*. New Phytologist 187, 1102–1111. https://doi.org/10.1111/j.1469-8137.2010.03325.x

Pavet, V., Olmos, E., Kiddle, G., Mowla, S., Kumar, S., Antoniw, J., Alvarez, M.E., Foyer, C.H., 2005. Ascorbic Acid Deficiency Activates Cell Death and Disease Resistance Responses in Arabidopsis. Plant Physiology 139, 1291–1303. https://doi.org/10.1104/pp.105.067686

Pay, M.T., Gangoiti, G., Guevara, M., Napelenok, S., Querol, X., Jorba, O., Pérez García-Pando, C., 2019. Ozone source apportionment during peak summer events over southwestern Europe. Atmospheric Chemistry and Physics 19, 5467–5494. https://doi.org/10.5194/acp-19-5467-2019

Pell, E. J., Schlagnhaufer, C.D., Arteca, R.N., 1997. Ozone-induced oxidative stress: Mechanisms of action and reaction. Physiologia Plantarum 100, 264–273. https://doi.org/10.1111/j.1399-3054.1997.tb04782.x

Pell, E.J., Eckardt, N., Enyedi, A.J., 1992. Timing of ozone stress and resulting status of ribulose bisphosphate carboxylase/oxygenase and associated net photosynthesis. New Phytologist 120, 397–405. https://doi.org/10.1111/j.1469-8137.1992.tb01080.x

Pellegrini, E., Francini, A., Lorenzini, G., Nali, C., 2015. Ecophysiological and antioxidant traits of Salvia officinalis under ozone stress. Environmental Science Pollution Research 22, 13083–13093. https://doi.org/10.1007/s11356-015-4569-5

Petetin, H., Thouret, V., Athier, G., Blot, R., Boulanger, D., Cousin, J.-M., Gaudel, A., Nédélec, P., Cooper, O., 2016. Diurnal cycle of ozone throughout the troposphere over Frankfurt as measured by MOZAIC-IAGOS commercial aircraft. Elementa: Science of the Anthropocene 4, 000129. https://doi.org/10.12952/journal.elementa.000129

Phua, S.Y., De Smet, B., Remacle, C., Chan, K.X., Van Breusegem, F., 2021. Reactive oxygen species and organellar signaling. Journal of Experimental Botany 72, 5807–5824. https://doi.org/10.1093/jxb/erab218

Pignocchi, C., Foyer, C.H., 2003. Apoplastic ascorbate metabolism and its role in the regulation of cell signalling. Current Opinion in Plant Biology 6, 379–389. https://doi.org/10.1016/S1369-5266(03)00069-4

Pisoschi, A.M., Pop, A., 2015. The role of antioxidants in the chemistry of oxidative stress: A review. European Journal of Medicinal Chemistry 97, 55–74. https://doi.org/10.1016/j.ejmech.2015.04.040

Pleijel, H., Broberg, M.C., Uddling, J., Mills, G., 2018. Current surface ozone concentrations significantly decrease wheat growth, yield and quality. Science of The Total Environment 613–614, 687–692. https://doi.org/10.1016/j.scitotenv.2017.09.111

Pleijel, H., Danielsson, H., Broberg, M.C., 2022. Benefits of the Phytotoxic Ozone Dose (POD) index in dose-response functions for wheat yield loss. Atmospheric Environment 268, 118797. https://doi.org/10.1016/j.atmosenv.2021.118797

Pleijel, H., Danielsson, H., Gelang, J., Sild, E., Selldén, G., 1998. Growth stage dependence of the grain yield response to ozone in spring wheat (*Triticum aestivum* L.). Agriculture, Ecosystems, & Environment 70, 61–68. https://doi.org/10.1016/S0167-8809(97)00167-9

Pleijel, H., Eriksen, A.B., Danielsson, H., Bondesson, N., Selldén, G., 2006. Differential ozone sensitivity in an old and a modern Swedish wheat cultivar—grain yield and quality, leaf chlorophyll and stomatal conductance. Environmental and Experimental Botany 56, 63–71. https://doi.org/10.1016/j.envexpbot.2005.01.004

Pleijel, H., Skärby, L., Wallin, G., Selldén, G., 1991. Yield and grain quality of spring wheat (*Triticum aestivum* L., cv. Drabant) exposed to different concentrations of ozone in open-top chambers. Environmental Pollution 69, 151–168. https://doi.org/10.1016/0269-7491(91)90140-R

Plöchl, M., Lyons, T., Ollerenshaw, J., Barnes, J., 2000. Simulating ozone detoxification in the leaf apoplast through the direct reaction with ascorbate. Planta 210, 454–467. https://doi.org/10.1007/PL00008153

Poorter, H., Bühler, J., Dusschoten, D. van, Climent, J., Postma, J.A., Poorter, H., Bühler, J., Dusschoten, D. van, Climent, J., Postma, J.A., 2012a. Pot size matters: a meta-analysis of the effects of rooting volume on plant growth. Functional Plant Biology 39, 839–850. https://doi.org/10.1071/FP12049

Poorter, H., Niklas, K.J., Reich, P.B., Oleksyn, J., Poot, P., Mommer, L., 2012b. Biomass allocation to leaves, stems and roots: meta-analyses of interspecific variation and environmental control. New Phytologist 193, 30–50. https://doi.org/10.1111/j.1469-8137.2011.03952.x

Potter, L., Foot, J.P., Caporn, S.J.M., Lee, J.A., 1996. The effects of long-term elevated ozone concentrations on the growth and photosynthesis of Sphagnum recurvum and Polytrichum commune. New Phytologist 134, 649–656. https://doi.org/10.1111/j.1469-8137.1996.tb04930.x

Price, A.H., Cairns, J.E., Horton, P., Jones, H.G., Griffiths, H., 2002. Linking drought-resistance mechanisms to drought avoidance in upland rice using a QTL approach: progress and new opportunities to integrate stomatal and mesophyll responses. Journal of Experimental Botany 53, 989–1004. https://doi.org/10.1093/jexbot/53.371.989

Pullens, J.W.M., Sharif, B., Trnka, M., Balek, J., Semenov, M.A., Olesen, J.E., 2019. Risk factors for European winter oilseed rape production under climate change. Agricultural and Forest Meteorology 272–273, 30–39. https://doi.org/10.1016/j.agrformet.2019.03.023

Pusede, S.E., Steiner, A.L., Cohen, R.C., 2015. Temperature and Recent Trends in the Chemistry of Continental Surface Ozone. Chemical Reviews. 115, 3898–3918. https://doi.org/10.1021/cr5006815

Qi, J., Wang, J., Gong, Z., Zhou, J.-M., 2017. Apoplastic ROS signaling in plant immunity. Current Opinion in Plant Biology 38: Biotic interactions, 92–100. https://doi.org/10.1016/j.pbi.2017.04.022

Quartacci, M.F., Cosi, E., Navari-Izzo, F., 2001. Lipids and NADPH-dependent superoxide production in plasma membrane vesicles from roots of wheat grown under copper deficiency or excess. Journal of Experimental Botany 52, 77–84. https://doi.org/10.1093/jxb/52.354.77

Rai, R., Agrawal, M., 2012. Impact of Tropospheric Ozone on Crop Plants. Proceedings of the National Academy of Sciences, India Section B: Biological Sciences 82, 241–257. https://doi.org/10.1007/s40011-012-0032-2

Raseetha, S., Leong, S.Y., Burritt, D.J., Oey, I., 2013. Understanding the degradation of ascorbic acid and glutathione in relation to the levels of oxidative stress biomarkers in broccoli (*Brassica oleracea* L. *italica* cv. Bellstar) during storage and mechanical processing. Food Chemistry 138, 1360–1369. https://doi.org/10.1016/j.foodchem.2012.09.126

Raven, E.L., 2003. Understanding functional diversity and substrate specificity in haem peroxidases: what can we learn from ascorbate peroxidase? Natural Product Reports 20, 367–381. https://doi.org/10.1039/B210426C

Raymer, P.L., 20002. Canola: An Emerging Oilseed Crop. Trends in new crops and new uses. J. Janick and A. Whipkey (eds.). ASHS Press, Alexandria, VA.

Reich, P.B., 1987. Quantifying plant response to ozone: a unifying theory. Tree Physiology 3, 63–91. https://doi.org/10.1093/treephys/3.1.63

Rhee, S.G., 2006. H_2O_2, a Necessary Evil for Cell Signaling. Science 312, 1882–1883. https://doi.org/10.1126/science.1130481

Rizza, F., Badeck, F.W., Cattivelli, L., Lidestri, O., Di Fonzo, N., Stanca, A.M., 2004. Use of a Water Stress Index to Identify Barley Genotypes Adapted to Rainfed and Irrigated Conditions. Crop Science 44, 2127–2137. https://doi.org/10.2135/cropsci2004.2127

Roberts, H.R., Dodd, I.C., Hayes, F., Ashworth, K., 2022. Chronic tropospheric ozone exposure reduces seed yield and quality in spring and winter oilseed rape. Agricultural and Forest Meteorology 316, 108859. https://doi.org/10.1016/j.agrformet.2022.108859

Roberts, H.R., Hayes, F., Dodd, I., Ashworth, K., 2023. Canola *Brassica* oilseed species are more ozone-tolerant than non-canola counterparts (Under review at Plant, Cell, Environment).

Roche, D., 2015. Stomatal Conductance Is Essential for Higher Yield Potential of C3 Crops. Critical Reviews in Plant Sciences 34, 429–453. https://doi.org/10.1080/07352689.2015.1023677

Roslinsky, V., Falk, K.C., Gaebelein, R., Mason, A.S., Eynck, C., 2021. Development of B. carinata with super-high erucic acid content through interspecific hybridization. Theoretical and Applied Genetics 134, 3167–3181. https://doi.org/10.1007/s00122-021-03883-2

Ruser, R., Fuß, R., Andres, M., Hegewald, H., Kesenheimer, K., Köbke, S., Räbiger, T., Quinones, T.S., Augustin, J., Christen, O., Dittert, K., Kage, H., Lewandowski, I., Prochnow, A., Stichnothe, H., Flessa, H., 2017. Nitrous oxide emissions from winter oilseed rape cultivation. Agriculture, Ecosystems & Environment 249, 57–69. https://doi.org/10.1016/j.agee.2017.07.039

Ryan, A., Cojocariu, C., Possell, M., Davies, W.J., Hewitt, C.N., 2009. Defining hybrid poplar (*Populus deltoides* × *Populus trichocarpa)* tolerance to ozone: identifying key parameters. Plant, Cell & Environment 32, 31–45. https://doi.org/10.1111/j.1365-3040.2008.01897.x

Sarkar, A., Singh, A.A., Agrawal, S.B., Ahmad, A., Rai, S.P., 2015. Cultivar specific variations in antioxidative defense system, genome and proteome of two tropical rice cultivars against ambient and elevated ozone. Ecotoxicology and Environmental Safety 115, 101–111. https://doi.org/10.1016/j.ecoenv.2015.02.010

Sawada, H., Komatsu, S., Nanjo, Y., Khan, N.A., Kohno, Y., 2012. Proteomic analysis of rice response involved in reduction of grain yield under elevated ozone stress. Environmental and Experimental Botany 77, 108–116. https://doi.org/10.1016/j.envexpbot.2011.11.009

Schjoerring, J.K., Bock, J.G.H., Gammelvind, L., Jensen, C.R., Mogensen, V.O., 1995. Nitrogen incorporation and remobilization in different shoot components of field-grown winter oilseed rape (*Brassica napus* L.) as affected by rate of nitrogen application and irrigation. Plant Soil 177, 255–264. https://doi.org/10.1007/BF00010132

Sen Raychaudhuri, S., Deng, X.W., 2000. The role of superoxide dismutase in combating oxidative stress in higher plants. Botanical Review 66, 89–98. https://doi.org/10.1007/BF02857783

Senior, I.J., Dale, P.J., 2002. Herbicide-tolerant crops in agriculture: oilseed rape as a case study. Plant Breeding 121, 97–107. https://doi.org/10.1046/j.1439-0523.2002.00688.x

Senthilkumar, M., Amaresan, N., Sankaranarayanan, A., 2021. Estimation of Malondialdehyde (MDA) by Thiobarbituric Acid (TBA) Assay, in: Senthilkumar, M., Amaresan, N., Sankaranarayanan, A. (Eds.), Plant-Microbe Interactions: Laboratory Techniques, Springer Protocols Handbooks. Springer US, New York, NY,

2 103–105. https://doi.org/10.1007/978-1-0716-1080-0_25

Sgarbi, E., Medeghini Bonatti, P., Baroni Fornasiero, R., Lins, A., 1999. Differential Sensitivity to Ozone in Two Selected Cell Lines from Grape Leaf. Journal of Plant Physiology 154, 119–126. https://doi.org/10.1016/S0176-1617(99)80327-7

Shafi, A., Chauhan, R., Gill, T., Swarnkar, M.K., Sreenivasulu, Y., Kumar, S., Kumar, N., Shankar, R., Ahuja, P.S., Singh, A.K., 2015. Expression of SOD and APX genes positively regulates secondary cell wall biosynthesis and promotes plant growth and yield in Arabidopsis under salt stress. Plant Molecular Biology 87, 615–631. https://doi.org/10.1007/s11103-015-0301-6

Sharma, P., Jha, A.B., Dubey, R.S., Pessarakli, M., 2012. Reactive Oxygen Species, Oxidative Damage, and Antioxidative Defense Mechanism in Plants under Stressful Conditions. Journal of Botany 2012, 1–26. https://doi.org/10.1155/2012/217037

Sharma, Y.K., Davis, K.R., 1997. The Effects of Ozone on Antioxidant Responses in Plants. Free Radical Biology and Medicine 23, 480–488. https://doi.org/10.1016/S0891-5849(97)00108-1

Sharps, K., Hayes, F., Harmens, H., Mills, G., 2021. Ozone-induced effects on leaves in African crop species. Environmental Pollution 268, 115789. https://doi.org/10.1016/j.envpol.2020.115789

Shekhawat, K., Rathore, S.S., Premi, O.P., Kandpal, B.K., Chauhan, J.S., 2012. Advances in Agronomic Management of Indian Mustard (*Brassica juncea* (L.) Czernj. Cosson): An Overview. International Journal of Agronomy 2012, 1–14. https://doi.org/10.1155/2012/408284

Short, E.F., North, K.A., Roberts, M.R., Hetherington, A.M., Shirras, A.D., McAinsh, M.R., 2012. A stress-specific calcium signature regulating an ozone-responsive gene expression network in Arabidopsis. The Plant Journal 71, 948–961. https://doi.org/10.1111/j.1365-313X.2012.05043.x

Shulaev, V., Oliver, D.J., 2006. Metabolic and Proteomic Markers for Oxidative Stress. New Tools for Reactive Oxygen Species Research. Plant Physiology 141, 367–372. https://doi.org/10.1104/pp.106.077925

Sicard, P., 2021. Ground-level ozone over time: An observation-based global overview. Current Opinion in Environmental Science & Health 19, 100226. https://doi.org/10.1016/j.coesh.2020.100226

Siemens, D.H., Keck, A.G., Ziegenbein, S., 2010. Optimal defense in plants: assessment of resource allocation costs. Evolution Ecology 24, 1291–1305. https://doi.org/10.1007/s10682-010-9374-5

Singh, S., Bhatia, A., Tomer, R., Kumar, V., Singh, B., Singh, S.D., 2013. Synergistic action of tropospheric ozone and carbon dioxide on yield and nutritional quality of Indian mustard (*Brassica juncea* (L.) Czern.). Environmental Monitoring Assessment 185, 6517–6529. https://doi.org/10.1007/s10661-012-3043-9

Sirko, A., De Kok, L., Haneklaus, S., Hawkesford, M., Rennenberg, H., Saito, K., Schnug, E., Stulen, I., 2009. Sulfur Metabolism in Plants - Regulatory Aspects, Significance of Sulfur in the Food Chain, Agriculture and the Environment. URL: (Last accessed 21/04/2023)

Škrha, J., Hilgertová, J., 1999. Relationship of serum N-acetyl-β-glucosaminidase activity to oxidative stress in diabetes mellitus. Clinica Chimica Acta 282, 167–174. https://doi.org/10.1016/S0009-8981(99)00025-X

Small, C.J., Pecket, R.C., 1982. The ultrastructure of anthocyanoplasts in red-cabbage. Planta 154, 97–99. https://doi.org/10.1007/BF00387900

Smirnoff, N., 2000. Ascorbic acid: metabolism and functions of a multi-facetted molecule. Current Opinion in Plant Biology 3, 229–235. https://doi.org/10.1016/S1369-5266(00)80070-9

Smirnoff, N., 2008. Antioxidants and Reactive Oxygen Species in Plants. John Wiley & Sons.

Smirnoff, N., Arnaud, D., 2019. Hydrogen peroxide metabolism and functions in plants. New Phytologist 221, 1197–1214. https://doi.org/10.1111/nph.15488

Smith, G.C., 2008. Ozone Bioindicators and Forest Health: A Guide to the Evaluation Analysis, and Interpretation of the Ozone Injury Data in the Forest Inventory and Analysis Program. United States Department of Agriculture, Forest Service, Northern Research Station. https://doi.org/10.2737/NRS-GTR-34

Snowdon, R.J., Friedt, W., 2004. Molecular markers in *Brassica* oilseed breeding: current status and future possibilities. Plant Breeding 123, 1–8. https://doi.org/10.1111/j.1439-0523.2003.00968.x

Soengas, P., Cartea, M.E., Francisco, M., Sotelo, T., Velasco, P., 2012. New insights into antioxidant activity of *Brassica* crops. Food Chemistry 134, 725–733. https://doi.org/10.1016/j.foodchem.2012.02.169

Song, Y.J., Joo, J.H., Ryu, H.Y., Lee, J.S., Bae, Y.S., Nam, K.H., 2007. Reactive oxygen species mediate IAA-lnduced ethylene production in mungbean (*Vigna radiata* L.) hypocotyls. Journal of Plant Biology. 50, 18–23. https://doi.org/10.1007/BF03030595

Souza, S.R., Pagliuso, J.D., 2009. Design and assembly of an experimental laboratory for the study of atmosphere–plant interactions in the system of fumigation chambers. Environmental Monitoring Assessment 158, 243–249. https://doi.org/10.1007/s10661-008-0578-x

Steinbrecht, W., Kubistin, D., Plass-Dülmer, C., Davies, J., Tarasick, D.W., von der Gathen, P., Deckelmann, H., Jepsen, N., Kivi, R., Lyall, N., Palm, M., Notholt, J., Kois, B., Oelsner, P., Allaart, M., Piters, A., Gill, M., Van Malderen, R., Delcloo, A.W., Sussmann, R., Mahieu, E., Servais, C., Romanens, G., Stübi, R., Ancellet, G., Godin-Beekmann, S., Yamanouchi, S., Strong, K., Johnson, B., Cullis, P., Petropavlovskikh, I., Hannigan, J.W., Hernandez, J.-L., Diaz Rodriguez, A., Nakano, T., Chouza, F., Leblanc, T., Torres, C., Garcia, O., Röhling, A.N., Schneider, M., Blumenstock, T., Tully, M., Paton-Walsh, C., Jones, N., Querel, R., Strahan, S., Stauffer, R.M., Thompson, A.M., Inness, A., Engelen, R., Chang, K.-L., Cooper, O.R., 2021. COVID-19 Crisis Reduces Free Tropospheric Ozone Across the Northern Hemisphere. Geophysical Research Letters 48, e2020GL091987. https://doi.org/10.1029/2020GL091987

Stevens, M., McGrann, G., Clark, B., 2008. Turnip yellows virus (syn. Beet western yellows virus): an emerging threat to European oilseed rape production? PDF: https://ahdb.org.uk/turnip-yellows-virus-syn-beet-western-yellows-virus-an-emerging-threat-to-european-oilseed-rape-production (Last accessed 21/06/2023).

Stokes, N.J., Lucas, P.W., Nicholas Hewitt, C., 1993. Controlled environment fumigation chambers for the study of reactive air pollutant effects on plants. Atmospheric Environment. Part A. General Topics 27, 679–683. https://doi.org/10.1016/0960-1686(93)90186-3

Strauss, S.Y., Irwin, R.E., Lambrix, V.M., 2004. Optimal Defence Theory and Flower Petal Colour Predict Variation in the Secondary Chemistry of Wild Radish. Journal of Ecology 92, 132–141.

Su, W., Raza, A., Gao, A., Jia, Z., Zhang, Y., Hussain, M.A., Mehmood, S.S., Cheng, Y., Lv, Y., Zou, X., 2021. Genome-Wide Analysis and Expression Profile of Superoxide Dismutase (SOD) Gene Family in Rapeseed (*Brassica napus* L.) under Different Hormones and Abiotic Stress Conditions. Antioxidants 10, 1182. https://doi.org/10.3390/antiox10081182

Tammam, A., Badr, R., Abou-Zeid, H., Hassan, Y., Bader, A., 2019. Nickel and ozone stresses induce differential growth, antioxidant activity and mRNA transcription in *Oryza sativa* cultivars. Journal of Plant Interactions 14, 87–101. https://doi.org/10.1080/17429145.2018.1556356

Tarasick, D., Galbally, I.E., Cooper, O.R., Schultz, M.G., Ancellet, G., Leblanc, T., Wallington, T.J., Ziemke, J., Liu, X., Steinbacher, M., Staehelin, J., Vigouroux, C., Hannigan, J.W., García, O., Foret, G., Zanis, P., Weatherhead, E., Petropavlovskikh, I., Worden, H., Osman, M., Liu, J., Chang, K.-L., Gaudel, A., Lin, M., Granados-Muñoz, M., Thompson, A.M., Oltmans, S.J., Cuesta, J., Dufour, G., Thouret, V., Hassler, B., Trickl, T., Neu, J.L., 2019. Tropospheric Ozone Assessment Report: Tropospheric ozone from 1877 to 2016, observed levels, trends and uncertainties. Elementa: Science of the Anthropocene 7, 39. https://doi.org/10.1525/elementa.376

Tausz, M., Grulke, N.E., Wieser, G., 2007. Defense and avoidance of ozone under global change. Environmental Pollution, Air Pollution and Climate Change: A Global Overview of the Effects on Forest Vegetation 147, 525–531. https://doi.org/10.1016/j.envpol.2006.08.042

Teixeira, E., Fischer, G., van Velthuizen, H., van Dingenen, R., Dentener, F., Mills, G., Walter, C., Ewert, F., 2011. Limited potential of crop management for mitigating surface ozone impacts on global food supply. Atmospheric Environment 45, 2569–2576. https://doi.org/10.1016/j.atmosenv.2011.02.002

Tewari, R.K., Hadacek, F., Sassmann, S., Lang, I., 2013. Iron deprivation-induced reactive oxygen species generation leads to non-autolytic PCD in *Brassica napus* leaves. Environmental and Experimental Botany 91, 74–83. https://doi.org/10.1016/j.envexpbot.2013.03.006

Tisdale, R.H., Zentella, R., Burkey, K.O., 2021. Impact of elevated ozone on yield and carbon-nitrogen content in soybean cultivar 'Jake.' Plant Science 306, 110855. https://doi.org/10.1016/j.plantsci.2021.110855

Torsethaugen, G., Pitcher, L.H., Zilinskas, B.A., Pell, E.J., 1997. Overproduction of Ascorbate Peroxidase in the Tobacco Chloroplast Does Not Provide Protection against Ozone. Plant Physiology 114, 529–537. https://doi.org/10.1104/pp.114.2.529

Treshow, M., 1970. Ozone damage to plants. Environmental Pollution 1, 155–161. https://doi.org/10.1016/0013-9327(70)90016-9

Tripathi, R., Agrawal, S.B., 2012. Effects of ambient and elevated level of ozone on *Brassica campestris* L. with special reference to yield and oil quality parameters. Ecotoxicology and Environmental Safety 85, 1–12. https://doi.org/10.1016/j.ecoenv.2012.08.012

USDA (2021) Oilseeds: World Markets and Trade. https://downloads.usda.library.cornell.edu/usda-esmis/files/tx31qh68h/2n49tt94d/76537t17x/oilseeds.pdf. (Last accessed 03/02/2021)

USDA (2023) Oilseeds: World Markets and Trade. https://apps.fas.usda.gov/psdonline/circulars/oilseeds.pdf (Last accessed 15/03/2023).

Vahisalu, T., Puzõrjova, I., Brosché, M., Valk, E., Lepiku, M., Moldau, H., Pechter, P., Wang, Y.-S., Lindgren, O., Salojärvi, J., Loog, M., Kangasjärvi, J., Kollist, H., 2010. Ozone-triggered rapid stomatal response involves the production of reactive oxygen species, and is controlled by SLAC1 and OST1. The Plant Journal 62, 442–453. https://doi.org/10.1111/j.1365-313X.2010.04159.x

Van Dam, N.M., De Jong, T.J., Iwasa, Y., Kubo, T., 1996. Optimal Distribution of Defences: Are Plants Smart Investors? Functional Ecology 10, 128–136. https://doi.org/10.2307/2390271

Van Oijen, M., Büker, P., Coyle, M., Fowler, D., Hargreaves, K., Hayes, F., Levy, P., Mills, G., Murray, M., 2003. a CEH-Integrating Fund Project 2001-2003.

Vandermeiren, K., De Bock, M., Horemans, N., Guisez, Y., Ceulemans, R., De Temmerman, L., 2012. Ozone effects on yield quality of spring oilseed rape and broccoli. Atmospheric Environment 47, 76–83. https://doi.org/10.1016/j.atmosenv.2011.11.035

Vaultier, M.-N., Jolivet, Y., 2015. Ozone sensing and early signaling in plants: An outline from the cloud. Environmental and Experimental Botany, Plant signalling mechanisms in response to the environment 114, 144–152. https://doi.org/10.1016/j.envexpbot.2014.11.012

Verma, D., Lakhanpal, N., Singh, K., 2019. Genome-wide identification and characterization of abiotic-stress responsive SOD (superoxide dismutase) gene family in *Brassica juncea* and *B. rapa*. BMC Genomics 20, 227. https://doi.org/10.1186/s12864-019-5593-5

Wan, J., Griffiths, R., Ying, J., McCourt, P., Huang, Y., 2009. Development of Drought-Tolerant Canola (*Brassica napus* L.) through Genetic Modulation of ABA-mediated Stomatal Responses. Crop Science 49, 1539–1554. https://doi.org/10.2135/cropsci2008.09.0568

Wang, H., Lu, X., Jacob, D.J., Cooper, O.R., Chang, K.-L., Li, K., Gao, M., Liu, Y., Sheng, B., Wu, K., Wu, T., Zhang, J., Sauvage, B., Nédélec, P., Blot, R., Fan, S., 2022. Global tropospheric ozone trends, attributions, and radiative impacts in 1995–2017: an integrated analysis using aircraft (IAGOS) observations, ozonesonde, and multi-decadal chemical model simulations. Atmospheric Chemistry and Physics 22, 13753–13782. https://doi.org/10.5194/acp-22-13753-2022

Wang, J., Zeng, Q., Zhu, J., Chen, C., Liu, G., Tang, H., 2014. Apoplastic antioxidant enzyme responses to chronic free-air ozone exposure in two different ozone-sensitive wheat cultivars. Plant Physiology and Biochemistry 82, 183–193. https://doi.org/10.1016/j.plaphy.2014.06.004

Wang, J., Zeng, Q., Zhu, J., Liu, G., Tang, H., 2013. Dissimilarity of ascorbate–glutathione (AsA–GSH) cycle mechanism in two rice (Oryza sativa L.) cultivars under experimental free-air ozone exposure. Agriculture, Ecosystems & Environment 165, 39–49. https://doi.org/10.1016/j.agee.2012.12.006

Wang, M., Li, G., Feng, Z., Liu, Y., Yuan, X., Uscola, M., 2023. A wider spectrum of avoidance and tolerance mechanisms explained ozone sensitivity of two white poplar ploidy levels. Annals of Botany 019. https://doi.org/10.1093/aob/mcad019

Wang, Y., Yang, L., Höller, M., Zaisheng, S., Pariasca-Tanaka, J., Wissuwa, M., Frei, M., 2014. Pyramiding of ozone tolerance QTLs OzT8 and OzT9 confers improved tolerance to season-long ozone exposure in rice. Environmental and Experimental Botany 104, 26–33. https://doi.org/10.1016/j.envexpbot.2014.03.005

Wang, Y., Ying, Y., Chen, J., Wang, X., 2004. Transgenic Arabidopsis overexpressing Mn-SOD enhanced salt-tolerance. Plant Science 167, 671–677. https://doi.org/10.1016/j.plantsci.2004.03.032

Watanabe, M., Balazadeh, S., Tohge, T., Erban, A., Giavalisco, P., Kopka, J., Mueller-Roeber, B., Fernie, A.R., Hoefgen, R., 2013. Comprehensive Dissection of Spatiotemporal Metabolic Shifts in Primary, Secondary, and Lipid Metabolism during Developmental Senescence in Arabidopsis. Plant Physiology 162, 1290–1310. https://doi.org/10.1104/pp.113.217380

Watanabe, M., Hoshika, Y., Inada, N., Wang, X., Mao, Q., Koike, T., 2013. Photosynthetic traits of Siebold's beech and oak saplings grown under free air ozone exposure in northern Japan. Environmental Pollution 174, 50–56. https://doi.org/10.1016/j.envpol.2012.11.006

Wedow, J.M., Burroughs, C.H., Rios Acosta, L., Leakey, A.D.B., Ainsworth, E.A., 2021. Age-dependent increase in α-tocopherol and phytosterols in maize leaves exposed to elevated ozone pollution. Plant Direct 5, e00307. https://doi.org/10.1002/pld3.307

Wefers, H., Sies, H., 1983. Oxidation of glutathione by the superoxide radical to the disulfide and the sulfonate yielding singlet oxygen. European Journal of Biochemistry 137, 29–36. https://doi.org/10.1111/j.1432-1033.1983.tb07791.x

Westhoek, H., Rood, T., Berg, M. van den, Janse, J., Nijdam, D., Reudink, M., Stehfest, E., Lesschen, J.P., Oenema, O., Woltjer, G.B., 2011. The protein puzzle : the consumption and production of meat, dairy and fish in the European Union (No. 500166001). Netherlands Environmental Assessment Agency, The Hague. URL: https://edepot.wur.nl/167520 (Last accessed 23/04/2023).

Wheeler, G.L., Jones, M.A., Smirnoff, N., 1998. The biosynthetic pathway of vitamin C in higher plants. Nature 393, 365–369. https://doi.org/10.1038/30728

Whitfield, C.P., Davison, A.W., Ashenden, T.W., 1996. Interactive effects of ozone and soil volume on Plantago major. New Phytologist 134, 287–294. https://doi.org/10.1111/j.1469-8137.1996.tb04633.x

Wilkinson, S., Davies, W.J., 2009. Ozone suppresses soil drying- and abscisic acid (ABA)-induced stomatal closure via an ethylene-dependent mechanism. Plant, Cell & Environment 32, 949–959. https://doi.org/10.1111/j.1365-3040.2009.01970.x

Williams, R.S., Hegglin, M.I., Kerridge, B.J., Jöckel, P., Latter, B.G., Plummer, D.A., 2019. Characterising the seasonal and geographical variability in tropospheric ozone, stratospheric influence and recent changes. Atmospheric Chemistry and Physics 19, 3589–3620. https://doi.org/10.5194/acp-19-3589-2019

Wittkop, B., Snowdon, R.J., Friedt, W., 2009. Status and perspectives of breeding for enhanced yield and quality of oilseed crops for Europe. Euphytica 170, 131–140. https://doi.org/10.1007/s10681-009-9940-5

Wolinska, K.W., Berens, M.L., 2019. Optimal Defense Theory 2.0: tissue-specific stress defense prioritization as an extra layer of complexity. Communicative & Integrative Biology 12, 91–95. https://doi.org/10.1080/19420889.2019.1625661

Wu, H., Guo, J., Wang, C., Li, K., Zhang, X., Yang, Z., Li, M., Wang, B., 2019a. An Effective Screening Method and a Reliable Screening Trait for Salt Tolerance of *Brassica napus* at the Germination Stage. Frontiers in Plant Science 10. https://doi.org/10.3389/fpls.2019.00530

Wu, Z., Liu, S., Zhao, J., Wang, F., Du, Y., Zou, S., Li, H., Wen, D., Huang, Y., 2017. Comparative responses to silicon and selenium in relation to antioxidant enzyme system and the glutathione-ascorbate cycle in flowering Chinese cabbage (*Brassica campestris* L. ssp. *chinensis* var. utilis) under cadmium stress. Environmental and Experimental Botany 133, 1–11. https://doi.org/10.1016/j.envexpbot.2016.09.005

Wynn, S., Ecclestone, E. & Carter, R. (2017). Cabbage stem flea beetle live incidence and severity monitoring autumn 2016 and spring 2017. AHDB Cereals & Oilseeds Project Report No. 571.

Xiao, M., Li, Z., Zhu, L., Wang, J., Zhang, B., Zheng, F., Zhao, B., Zhang, H., Wang, Y., Zhang, Z., 2021. The Multiple Roles of Ascorbate in the Abiotic Stress Response of Plants: Antioxidant, Cofactor, and Regulator. Frontiers in Plant Science 12. https://doi.org/10.3389/fpls.2021.598173

Xu, J., Huang, X., Wang, N., Li, Y., Ding, A., 2021. Understanding ozone pollution in the Yangtze River Delta of eastern China from the perspective of diurnal cycles. Science of The Total Environment 752, 141928. https://doi.org/10.1016/j.scitotenv.2020.141928

Xu, X., Zhang, T., Su, Y., 2019. Temporal variations and trend of ground-level ozone based on long-term measurements in Windsor, Canada. Atmospheric Chemistry and Physics 19, 7335–7345. https://doi.org/10.5194/acp-19-7335-2019

Xu, Y., Feng, Z., Shang, B., Dai, L., Uddling, J., Tarvainen, L., 2019. Mesophyll conductance limitation of photosynthesis in poplar under elevated ozone. Science of The Total Environment 657, 136–145. https://doi.org/10.1016/j.scitotenv.2018.11.466

Xue, J.Y., Wang, Y., Chen, M., Dong, S., Shao, Z.-Q., Liu, Y., 2020. Maternal Inheritance of U's Triangle and Evolutionary Process of *Brassica* Mitochondrial Genomes. Frontiers in Plant Science 11. https://doi.org/10.3389/fpls.2020.00805

Yadav, D.S., Mishra, A.K., Rai, R., Chaudhary, N., Mukherjee, A., Agrawal, S.B., Agrawal, M., 2020. Responses of an old and a modern Indian wheat cultivar to future O_3 level: Physiological, yield and grain quality parameters. Environmental Pollution 259, 113939. https://doi.org/10.1016/j.envpol.2020.113939

Yendrek, C.R., Erice, G., Montes, C.M., Tomaz, T., Sorgini, C.A., Brown, P.J., McIntyre, L.M., Leakey, A.D.B., Ainsworth, E.A., 2017. Elevated ozone reduces photosynthetic carbon gain by accelerating leaf senescence of inbred and hybrid maize in a genotype-specific manner. Plant, Cell & Environment 40, 3088–3100. https://doi.org/10.1111/pce.13075

Yendrek, C.R., Koester, R.P., Ainsworth, E.A., 2015. A comparative analysis of transcriptomic, biochemical, and physiological responses to elevated ozone identifies species-specific mechanisms of resilience in legume crops. Journal of Experimental Botany 66, 7101–7112. https://doi.org/10.1093/jxb/erv404

Yeoh, W.K., Ali, A., Forney, C.F., 2014. Effects of ozone on major antioxidants and microbial populations of fresh-cut papaya. Postharvest Biology and Technology 89, 56–58. https://doi.org/10.1016/j.postharvbio.2013.11.006

Young, P.J., Archibald, A.T., Bowman, K.W., Lamarque, J.-F., Naik, V., Stevenson, D.S., Tilmes, S., Voulgarakis, A., Wild, O., Bergmann, D., Cameron-Smith, P., Cionni, I., Collins, W.J., Dalsøren, S.B., Doherty, R.M., Eyring, V., Faluvegi, G., Horowitz, L.W., Josse, B., Lee, Y.H., MacKenzie, I.A., Nagashima, T., Plummer, D.A., Righi, M., Rumbold, S.T., Skeie, R.B., Shindell, D.T., Strode, S.A., Sudo, K., Szopa, S., Zeng, G., 2013. Pre-industrial to end 21st century projections of tropospheric ozone from the Atmospheric Chemistry and Climate Model Intercomparison Project (ACCMIP). Atmospheric Chemistry and Physics 13, 2063–2090. https://doi.org/10.5194/acp-13-2063-2013

Yu, Y., Wang, J., Li, S., Kakan, X., Zhou, Y., Miao, Y., Wang, F., Qin, H., Huang, R., 2019. Ascorbic Acid Integrates the Antagonistic Modulation of Ethylene and Abscisic Acid in the Accumulation of Reactive Oxygen Species. Plant Physiology 179, 1861–1875. https://doi.org/10.1104/pp.18.01250

Zentgraf, U., Andrade-Galan, A.G., Bieker, S., 2022. Specificity of H_2O_2 signaling in leaf senescence: is the ratio of H_2O_2 contents in different cellular compartments sensed in Arabidopsis plants? Cellular & Molecular Biology Letters 27, 4. https://doi.org/10.1186/s11658-021-00300-w

Zhanassova, K., Kurmanbayeva, A., Gadilgereyeva, B., Yermukhambetova, R., Iksat, N., Amanbayeva, U., Bekturova, A., Tleukulova, Z., Omarov, R., Masalimov, Z., 2021. ROS status and antioxidant enzyme activities in response to combined temperature and drought stresses in barley. Acta Physiol Plant 43, 114. https://doi.org/10.1007/s11738-021-03281-7

Zhang, C., Ouyang, B., Yang, C., Zhang, X., Liu, H., Zhang, Y., Zhang, J., Li, H., Ye, Z., 2013. Reducing AsA Leads to Leaf Lesion and Defence Response in Knock-Down of the AsA Biosynthetic Enzyme GDP-D-Mannose Pyrophosphorylase Gene in Tomato Plant. Plos One 8, e61987. https://doi.org/10.1371/journal.pone.0061987

Zhang, H., Zhang, G., Lü, X., Zhou, D., Han, X., 2015. Salt tolerance during seed germination and early seedling stages of 12 halophytes. Plant Soil 388, 229–241. https://doi.org/10.1007/s11104-014-2322-3

Zhang, H., Zhu, J., Gong, Z., Zhu, J.-K., 2022. Abiotic stress responses in plants. Nat Rev Genet 23, 104–119. https://doi.org/10.1038/s41576-021-00413-0

Zhou, B., Guo, Z., 2009. Calcium is involved in the abscisic acid-induced ascorbate peroxidase, superoxide dismutase and chilling resistance in *Stylosanthes guianensis*. Biologia Plantarum 53, 63–68. https://doi.org/10.1007/s10535-009-0009-z

Zhu, J.K., 2002. Salt and Drought Stress Signal Transduction in Plants. Annual Review of Plant Biology 53, 247–273. https://doi.org/10.1146/annurev.arplant.53.091401.143329

Ziemke, J.R., Oman, L.D., Strode, S.A., Douglass, A.R., Olsen, M.A., McPeters, R.D., Bhartia, P.K., Froidevaux, L., Labow, G.J., Witte, J.C., Thompson, A.M., Haffner, D.P., Kramarova, N.A., Frith, S.M., Huang, L.-K., Jaross, G.R., Seftor, C.J., Deland, M.T., Taylor, S.L., 2019. Trends in global tropospheric ozone inferred from a composite record of TOMS/OMI/MLS/OMPS satellite measurements and the MERRA-2 GMI simulation. Atmospheric Chemistry and Physics 19, 3257–3269. https://doi.org/10.5194/acp-19-3257-2019

Zilberman, D., Kaplan, S., Kim, E., Hochman, G., Graff, G., 2013. Continents divided. GM Crops & Food 4, 202–208. https://doi.org/10.4161/gmcr.26981

Züst, T., Joseph, B., Shimizu, K.K., Kliebenstein, D.J., Turnbull, L.A., 2011. Using knockout mutants to reveal the growth costs of defensive traits. Proceedings of the Royal Society B: Biological Sciences 278, 2598–2603. https://doi.org/10.1098/rspb.2010.2475

8. Appendices

8.1 Appendix 1. Chronic ozone exposure reduces seed yield and quality in spring and winter oilseed rape

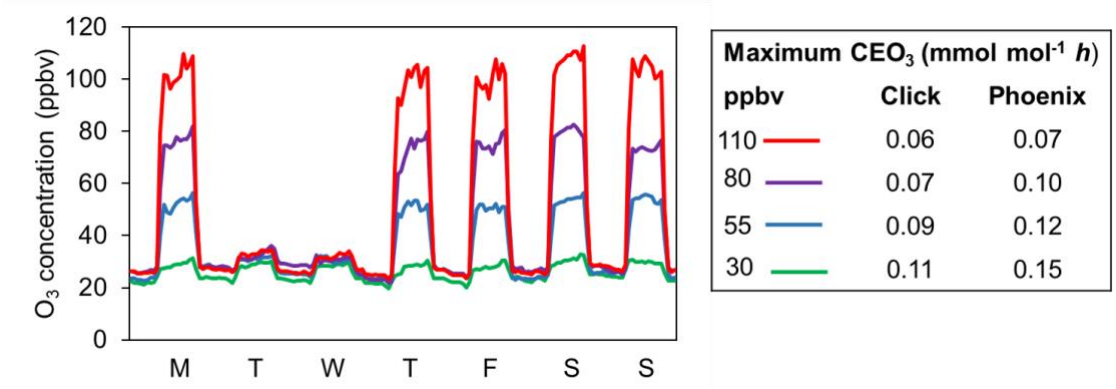

Figure 8.1. Left: Mean hourly ozone levels over the entire experimental period (7th June to 9th October 2019). Right: CEO_3 (cumulative ozone exposure) calculated as: CEO_3 (mmol mol^{-1} *h*) = $[O_3] \times H \times D \times 10^{-3}$ where $[O_3]$ is ozone concentration in ppbv, *H* is number of hours, and *D* number of days. Maximum CEO_3 of each variety and treatment at point of harvest (5th September for Click and 9th October 2019 for Phoenix).

Table 8.1. Linear model outputs for oilseed rape quantity, quality, and physiological parameters.

Variety	Parameter		R^2	*P*
Click	Physiology	P_{net}	0.51	< 0.001 ***
		g_s	0.22	< 0.01 **
		SPAD	0.73	< 0.001 ***
	Quantity	TSW	0.78	< 0.01 **
		Total seed mass	0.42	ns
		Raceme number	0.58	< 0.01 **
		Siliques per raceme	-0.36	ns
		Seeds per silique	0.34	ns
	Quality	Total oil content	0.65	< 0.001 ***
		Total protein content	0.67	< 0.01 **
		Total chlorophyll content	0.57	< 0.01 **
		Moisture	0.58	< 0.01 **
		Ash	0.61	< 0.01 **
		Glucosinolate content	0.01	ns
		Erucic acid content	0.23	ns
		Sulphur	0.35	< 0.01 **
		N:S Ratio	-0.03	ns
		Manganese	0.31	< 0.05 *
		Zinc	0.21	< 0.05 *
		Iron	0.18	< 0.05 *
Phoenix	Physiology	P_{net}	0.24	< 0.001 ***
		g_s	0.01	ns
		SPAD	0.08	< 0.05 *
	Quantity	TSW	0.85	< 0.001 ***
		Total seed mass	0.42	< 0.05 *
		Raceme number	0.85	< 0.001 ***
		Siliques per raceme	-0.37	ns
		Seeds per silique	-0.11	ns
	Quality	Total oil content	-0.08	ns
		Total protein content	-0.1	ns
		Total chlorophyll content	-0.08	ns
		Moisture	-0.09	ns
		Ash	-0.06	ns
		Glucosinolate content	-0.04	ns
		Erucic acid content	-0.01	ns
		Sulphur	-0.05	ns
		N:S Ratio	-0.071	ns
		Manganese	0.2	< 0.05 *
		Zinc	-0.07	ns
		Iron	-0.07	ns

±SEM of 4 replicates. Asterisks indicate *P*<0.05 *, *P* <0.01 **, P<0.001 ***, *P* > 0.05 ns (not significant).

Plant physiology and seed quantity presented significant interactions with CEO_3 for both varieties, with the exceptions of stomatal conductance (g_s) in Phoenix and total seed mass in Click. The latter can likely be ascribed to a substantial increase in raceme number compensating the significant decrease in TSW. Click's oil content significantly dropped with increasing CEO_3, while other quality parameters significantly rose, while there was no significant change in Phoenix's quality parameters, apart from Manganese. Erucic acid, saturated fatty acid content, and glucosinolate contents did not significantly change with increasing CEO_3 in either variety. N:S ratio along with other micronutrients remained consistent and were above grain suite analysis limits, indicating that plants used in this study were not nutrient deficient.

Table 8.2. Absolute values of seed quality parameters in 30ppv and 110 ppbv in Click (spring oilseed rape) and Phoenix (winter OSR)

Seed quality parameter	variety	moisture	oil	protein	ash	erucic acid	saturated FA	GSL	sulphur	N:S ratio	manganese	zinc	iron
Units		(%)	(%)	(%)	(%)	(%)	(%)	(µmol g^{-1})	%		(mg kg^{-1})	(mg kg^{-1})	(mg kg^{-1})
30 ppbv	Click	6.3±0.4 a	48.1±3.0 a	18.0±1.5 a	3.1±0.3 a	1.9±0.07 a	6.0±0.04 a	3.6±2.7 a	0.2±0.01 a	6.2±0.4 a	123.3±12.2 a	30.4±2.1 a	0.6±0.05 a
110 ppbv	Click	7.3 ±0.04b	40.9 ±0.4 c	24.1 ±0.5 c	3.8 ±0.1 c	1.6 ±0.3 a	5.9 ±0.04 a	9.3±4.2 a	0.3±0.1 b	6.8±0.2 a	155.7±5.0 b	34.5±1.4 b	0.7±0.02 b
P		< 0.05*	< 0.05*	< 0.05*	< 0.05*	ns	ns	ns	< 0.01 **	ns	< 0.05*	< 0.05*	< 0.05*
30 ppbv	Phoenix	6.7 ±0.39ab	44.0 ±3.5 ab	21.7 ±3.1 ab	3.2 ±0.3 ab	1.7 ±0.2 a	5.9 ±0.1 a	30.4±4.1 b	0.6±0.2 c	12.5±0.3 b	88.7±3.2 c	36.1±4.6 b	0.6±0.04 ab
110 ppbv	Phoenix	6.6 ±0.08ab	43.9 ±0.9 b	22.1 ±1.0 b	3.3 ±0.1 ab	1.8 ±0.3 a	5.8 ±0.04 a	34.6±3.1 b	0.5±0.05 c	11.7 ±0.1 b	76.6±3.6 c	36.1±4.2 b	0.5±0.05 a
P		ns	ns	ns	ns	ns	ns	ns	ns	ns	ns	ns	ns

±SEM of 4 replicates. Asterisks indicate $P<0.05$ *, $P<0.01$ **, $P<0.001$ ***, $P>0.05$ ns (not significant). Differing letters indicate differences between and within treatments. Letters denote mean discrimination. GSL = Glucosinolates.

Click's oil content was significantly lower in 110 ppb, while other quality parameters were significantly higher at 110 ppb (Table 8.2). Seed quality did not significantly change between lowest and highest ozone treatments in Phoenix. Glucosinolates were higher in Phoenix than Click across all treatments, but further study is warranted to establish a true effect as glucosinolate variation was high between individual plants. Moreover, as Phoenix was sown out of season, therefore may have increased Glucosinolates content due to accelerated phenology.

8.2 Appendix 2. Cultivar and leaf-specific biochemical responses to short-term ozone exposure in spring and winter oilseed rape

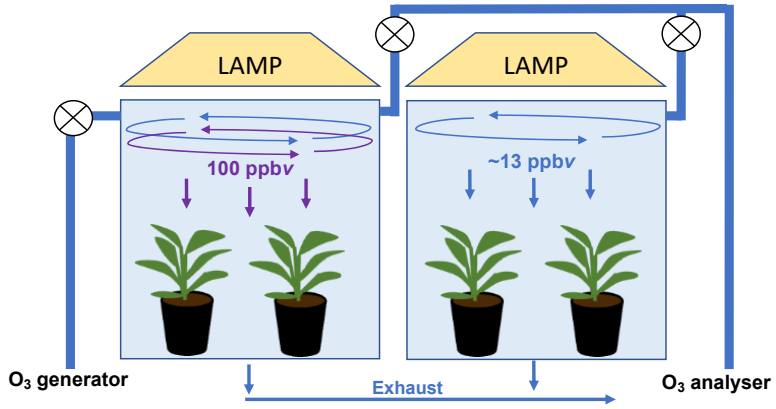

Environmental parameters in each chamber (±STD)

Chamber	RH (%)	Temperature (°C)	Light (PAR)
100 ppbv	29.5±1.3	25.7±0.7	291.2±11.8
~20 ppbv	27.7±1.7	24.8±0.5	296.2±15.5
T-test output	0.10 (ns)	0.10 (ns)	(0.88) ns

Figure 8.2. Two 1-m^3 sealed chambers used to fumigate plants ~20 ppbv and 100 ppb ozone for 12 days. OSR leaves on the basal rosette were tagged: the 2^{nd} , 4^{th} , and 6^{th} leaves numbering from the base of the plant were selected for measurements. Environmental parameters: relative humidity (RH), temperature, and light monitored throughout experiment ±STD= standard deviation.

Table 8.3. Means of physiological, morphological, and biochemical data of two oilseed rape cultivars exposed to ozone at experimental days 0, 6, and 12.

Day	Variety	Ozone	Leaf nodal position	g_s	P_{net}	Chlorophyll content	PI	Fv/Fm	AsA	H_2O_2	MDA	Leaf length	Leaf area	Total dried mass
N/A	N/A	ppbv		mol m^{-2} s^{-1}	µmol CO_2 m^{-2} s^{-1}	(CCI)	N/A	N/A	µg mg^{-1} FW	µmol mg^{-1} FW	nmol mg^{-1} FW	cm	cm^2	g
0	Click	control	2	0.37±0.01	9.69±0.49	212.8±7.6	4.10±1.61	0.79 ±0.02	0.67±0.23	0.26±0.04	0.05±0.03	3.93±0.41	18.5±2.2	
0	Click	control	4	0.56±0.17	13.66±0.70	251.8±21.5	2.74±0.56	0.80 ±0.01	0.46±0.09	0.39±0.09	0.03±0.01	4.03±0.53	29.4±7.0	
0	Click	control	6	0.43±0.14	12.07±1.16	246.4±16.3	3.03±1.23	0.80 ±0.01	1.10±0.28	0.91±0.20	0.03±0.01	4.23±0.39	22.2±4.5	
0	Phoenix	control	2	0.25±0.03	8.19±1.80	219.8±11.6	3.36±0.47	0.82 ±0.01	0.96±0.43	0.20±0.05	0.05±0.01	4.17±0.33	27.6±0.4	
0	Phoenix	control	4	0.38±0.07	12.80±0.85	249.6±21.9	4.94±1.19	0.82 ±0.00	0.64±0.26	0.52±0.10	0.08±0.01	5.30±1.04	35.1±11.6	
0	Phoenix	control	6	0.48±0.11	13.08±1.19	244.1±13.6	5.09±1.12	0.82 ±0.01	1.37±0.17	0.56±0.31	0.05±0.01	4.50±0.76	23.2±7.0	
6	Click	20	2	0.33±0.02	9.27±0.55	191.2±17.5	2.16±0.40	0.61 ±0.09				5.71±0.33	23.7±3.3	
6	Click	20	4	0.67±0.06	15.20±0.79	282.6±21.4	2.81±0.89	0.79 ±0.02				8.73±0.39	49.4±8.2	
6	Click	20	6	0.70±0.07	14.27±0.82	281.2±28.5	2.47±0.92	0.80 ±0.01				8.17±1.31	40.2±3.8	
6	Click	100	2	0.30±0.07	7.69±1.81	173.9±6.7	0.67±0.19	0.67 ±0.03				4.73±0.15	19.8±5.8	
6	Click	100	4	0.34±0.09	10.51±1.20	222.6±14.4	4.03±0.52	0.79 ±0.01				5.63±0.57	36.1±10.6	
6	Click	100	6	0.49±0.14	11.68±1.28	271.6±16.9	3.28±0.39	0.80 ±0.01				7.63±0.98	45.5±7.1	
6	Phoenix	20	2	0.19±0.02	5.38±1.51	174.0±7.8	1.30±1.10	0.40 ±0.23				6.70±0.96	34.0±4.0	
6	Phoenix	20	4	0.39±0.08	11.11±0.21	246.6±3.1	2.42±0.92	0.78 ±0.02				7.70±0.64	60.0±5.7	
6	Phoenix	20	6	0.62±0.07	13.40±0.46	282.3±8.5	2.15±0.89	0.76 ±0.03				8.87±0.42	58.5±12.8	
6	Phoenix	100	2	0.30±0.03	6.26±1.25	181.3±7.2	1.77±0.12	0.74 ±0.01				5.13±0.23	21.7±3.5	
6	Phoenix	100	4	0.48±0.16	11.43±1.11	237.4±12.3	2.84±0.19	0.78 ±0.01				7.30±0.25	37.5±3.1	
6	Phoenix	100	6	0.51±0.01	11.95±0.97	276.2±16.6	3.08±0.08	0.78 ±0.01				8.23±0.93	63.7±9.0	
12	Click	20	2	0.20±0.06	5.71±0.74	223.6±15.3	1.61±0.87	0.59 ±0.11	0.38±0.03	0.22±0.04	0.03±0.01	6.30±0.67	54.0±18.3	15.57 ±0.60
12	Click	20	4	0.41±0.08	8.00±0.94	330.5±23.1	3.22±0.77	0.80 ±0.01	0.84±0.11	0.59±0.25	0.03±0.01	9.37±0.35	102.4±13.7	15.57 ±0.60
12	Click	20	6	0.69±0.07	13.65±0.69	340.7±18.7	4.16±0.46	0.80 ±0.02	0.68±0.17	0.67±0.13	0.03±0.01	11.13±1.46	132.3±30.9	15.57 ±0.60
12	Click	100	2	0.17±0.05	6.26±0.30	172.2±12.4	1.87±1.11	0.82 ±0.03	0.39±0.09	0.24±0.13	0.06±0.02	5.50±0.12	32.1±6.4	15.1 ±0.96
12	Click	100	4	0.22±0.08	9.6±1.56	236.7±18.2	3.58±1.43	0.80 ±0.01	0.76±0.13	0.65±0.13	0.02±0.01	7.80±0.70	104.8±11.1	15.1 ±0.96
12	Click	100	6	0.33±0.13	11.6±1.31	344.8±12.6	5.89±1.31	0.81 ±0.01	0.57±0.10	0.90±0.21	0.05±0.01	10.57±0.35	116.0±2.5	15.1 ±0.96
12	Phoenix	20	2	0.14±0.01	5.88±0.88	202.1±11.2	0.63±0.24	0.66 ±0.06	1.00±0.15	0.47±0.06	0.04±0.01	8.33±0.73	83.0±5.8	18.33 ±0.73
12	Phoenix	20	4	0.53±0.07	11.78±0.98	276.1±6.9	3.89±1.39	0.78 ±0.02	1.15±0.26	0.94±0.55	0.05±0.01	10.50±0.93	142.5±8.2	18.33 ±0.73
12	Phoenix	20	6	0.40±0.13	11.57±0.30	259.7±30.5	3.83±0.84	0.81 ±0.02	1.70±0.14	1.31±0.14	0.04±0.01	12.00±0.29	155.6±11.7	18.33 ±0.73
12	Phoenix	100	2	0.17±0.05	6.66±0.33	169.8±10.5	2.24±0.59	0.77 ±0.02	0.75±0.20	0.57±0.18	0.03±0.01	5.73±0.19	33.9±2.9	14.4 ±1.39
12	Phoenix	100	4	0.37±0.17	10.93±1.33	220.4±6.7	3.36±0.46	0.76 ±0.02	1.31±0.28	0.92±0.14	0.05±0.01	8.83±0.18	92.3±7.3	14.4 ±1.39
12	Phoenix	100	6	0.51±0.03	13.09±0.14	321.6±4.5	3.43±0.84	0.79 ±0.01	1.09±0.26	1.38±0.18	0.04±0.01	12.47±0.48	147.1±6.1	14.4 ±1.39

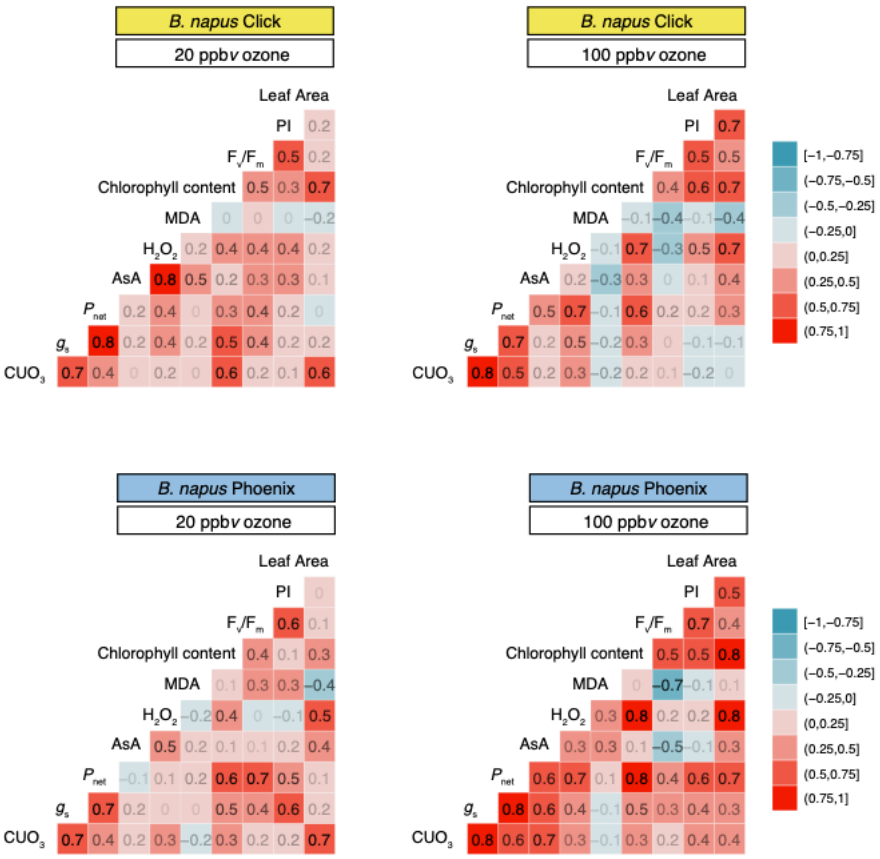

Figure 8.3. Heat maps showing Pearson's correlation between biochemical, physiological, and morphological data in response to cumulative ozone uptake.

8.3 Appendix 3. Canola-grade cultivars are more ozone-tolerant than non-canola counterparts

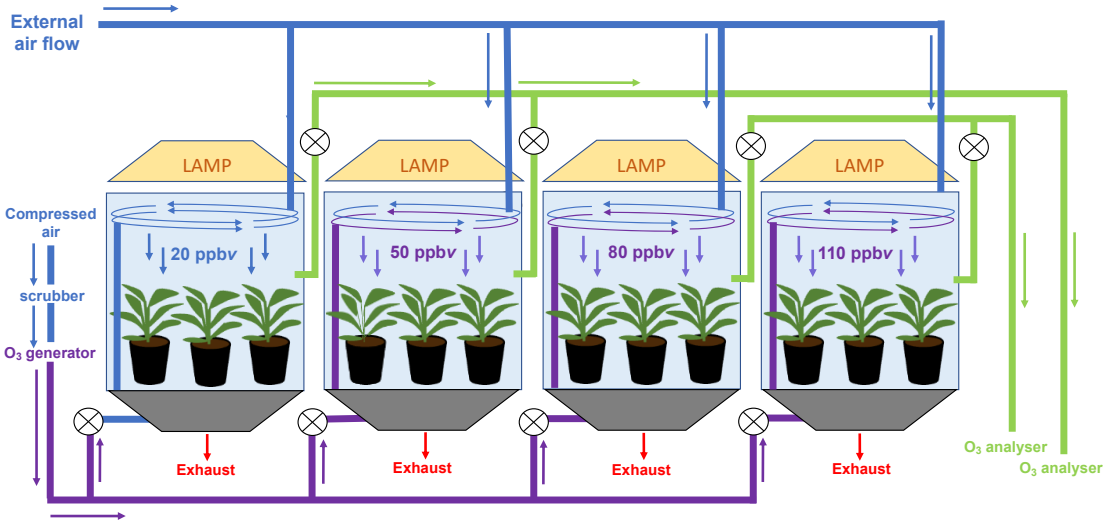

Target (ppb*v*)	20	50	75	100
Ozone (ppb*v*)	17.08 ±0.82	47.21 ±0.75	70.42 ±1.30	103.90 ±1.25

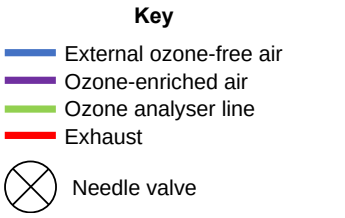

Figure 8.4. Experimental fumigation setup and mean ozone concentrations (ppbv) over 26 days. Arrows represent direction of flow in lines.

Table 8.4. Physiological, biochemical, and morphological absolute values for four *Brassica* oilseed lines

Line	O_3	Day	CEO_3	P_{net}	g_s	F_v/F_m	NPQt	SOD	APX	MDA	H_2O_2	Protein	Chlorophyll	Leaf area	Fresh Mass	Dried Mass
Units	ppbv	days	mmol mol *h*	µmol CO_2 m^{-2} s^{-1}	mol m^{-2} s^{-1}	N/A	N/A	U mg^{-1} protein	U mg^{-1} protein	nmol mg^{-1} FW	µmol mg^{-1} FW	mg g^{-1} FW	SPAD	cm^2	g	g
	20	0	0.00	13.82±0.53	0.69±0.03	0.79±0.01	0.34±0.04	64.71±29.29	8.78±2.05	0.22±0.06	1.74±0.27	0.11±0.04	18.10±1.02	59.73±5.42	4.17±0.78	
	20	13	0.00	15.23±2.13	0.36±0.09	0.77±0.01	0.48±0.06	57.56±25.35	6.70±2.83	0.15±0.07	2.13±0.38	0.32±0.14	23.53±0.85	219.67±14.02		
	50	13	0.00	10.53±3.79	0.32±0.21	0.77±0.01	0.42±0.04	45.86±8.06	14.88±5.15	0.26±0.05	4.14±0.73	0.17±0.05	28.13±3.30	224.99±8.30		
B.	75	13	0.01	11.57±1.99	0.31±0.14	0.78±<0.01	0.38±0.02	58.79±15.77	22.17±11.05	0.14±0.08	3.52±0.84	0.31±0.11	28.77±4.73	206.76±9.03		
napus	100	13	0.01	11.60±2.41	0.46±0.24	0.78±<0.01	0.36±0.01	50.02±5.55	12.74±2.29	0.29±0.10	6.43±0.70	0.28±0.04	27.33±2.92	188.21±18.76		
Click	20	26	0.00	8.64±1.16	0.32±0.21	0.76±0.01	0.54±0.10	26.93±6.36	6.52±2.24	0.14±0.09	2.41±0.51	0.61±0.14	32.10±2.05	112.71±4.83	99.13±5.63	13.42±0.71
	50	26	0.01	3.99±1.10	0.04±0.01	0.78±<0.01	0.37±0.04	36.66±9.91	4.45±1.18	0.04±0.01	7.35±1.62	0.56±0.18	32.30±5.18	150.18±18.90	85.68±4.91	11.22±0.92
	75	26	0.01	3.72±0.46	0.03±<0.01	0.76 ±0.01	0.51±0.12	54.86±18.25	14.04±1.46	0.04±0.01	7.10±1.41	0.47±0.19	24.05±4.78	143.13±11.69	91.63±2.83	13.78±0.99
	100	26	0.02	6.07±0.81	0.13±0.06	0.76 ±0.01	0.54±0.10	34.09±2.29	17.70±5.15	0.04±<0.01	7.72±1.37	0.48±0.05	24.73±1.13	113.38±13.18	90.50±4.66	12.08±0.26
	20	0	0.00	13.63±0.33	0.39±0.05	0.77 ±0.01	0.46±0.06	20.46±5.37	0.60±1.96	0.35±0.17	2.50±0.47	0.50±0.08	9.60±0.72	51.05±7.30	3.01±0.67	
	20	13	0.00	14.84±3.20	0.41±0.14	0.77 ±0.01	0.49±0.05	44.45±12.09	8.24±4.24	0.25±0.16	3.29±0.47	0.33±0.13	15.30±1.03	141.12±9.19		
	50	13	0.00	10.72±1.55	0.18±0.05	0.77 ±0.01	0.47±0.05	65.18±3.33	14.72±4.41	0.09±0.03	3.73±0.74	0.19±0.02	16.58±1.35	154.5±24.24		
B.	75	13	0.01	5.81±0.95	0.07±0.01	0.68 ±0.07	0.70±0.07	87.06±17.62	20.72±5.78	0.11±0.05	3.66±0.90	0.17±0.03	15.23±0.93	186.75±14.96		
rapa	100	13	0.01	8.75±1.64	0.16±0.06	0.77 ±0.01	0.45±0.04	95.65±31.62	32.51±15.00	0.10±0.06	2.58±0.67	0.34±0.20	16.04±1.74	167.67±13.44		
Candle	20	26	0.00	5.11±1.43	0.09±0.04	0.75 ±0.02	0.65±0.14	53.53±23.20	12.32±5.71	0.06±0.01	6.49±0.47	0.55±0.23	14.45±1.06	130.38±6.23	59.48±3.09	8.48±0.85
	50	26	0.01	4.56±1.00	0.06±0.02	0.66 ±0.05	1.67±0.64	71.49±26.01	6.84±2.35	0.36±0.19	11.85±3.76	0.31±0.08	12.85±1.89	100.35±12.86	62.55±5.67	9.45±0.82
	75	26	0.01	2.71±0.40	0.04±0.01	0.64 ±0.08	2.34±1.40	110.31±13.61	28.69±6.79	0.07±0.02	5.78±1.66	0.12±0.05	9.43±2.38	91.95±26.68	76.43±7.24	11.95±0.72
	100	26	0.02	5.32±1.36	0.12±0.07	0.64 ±0.04	1.83±0.55	76.08±19.63	24.15±6.03	0.23±0.18	6.74±1.09	0.15±0.01	11.65±3.06	105.15±9.03	79.83±4.44	12.23±0.37
	20	0	0.00	16.50±0.24	0.62±0.02	0.78±<0.01	0.37±0.03	39.86±10.83	5.43±1.38	0.08±0.02	0.51±0.03	0.32±0.10	13.75±0.96	26.25±6.08	1.72±0.53	
	20	13	0.00	13.69±2.33	0.54±0.20	0.77±0.01	0.45±0.07	90.78±25.71	17.20±9.94	0.75±0.33	6.09±0.84	0.30±0.19	21.30±4.02	151.78±22.36		
	50	13	0.00	13.15±1.97	0.45±0.10	0.78±0.01	0.40±0.04	116.36±23.98	21.85±5.73	0.92±0.32	15.59±3.29	0.12±0.04	17.18±2.18	102.75±13.57		
B.	75	13	0.01	12.10±2.05	0.56±0.26	0.77±0.01	0.48±0.08	31.39±11.05	6.42±5.78	0.47±0.30	7.53±1.48	0.64±0.24	17.39±1.25	93.88±13.21		
rapa	100	13	0.01	11.48±1.30	0.46±0.14	0.77±<0.01	0.49±0.03	155.94±28.43	31.92±12.23	0.16±0.08	4.36±0.85	0.12±0.03	20.02±1.67	85.93±7.75		
07224	20	26	0.00	10.58±0.81	0.39±0.16	0.77 ±0.01	0.48±0.06	9.55±2.42	22.16±18.20	0.06±0.01	2.04±0.76	0.66±0.33	31.75±5.60	85.63±7.35	48.13±3.20	5.30±0.40
	50	26	0.01	10.62±2.24	0.35±0.14	0.77±<0.01	0.44±0.03	76.40±38.05	8.01±3.30	0.18±0.12	2.83±1.44	0.61±0.33	24.65±5.00	87.75±9.40	44.03±4.39	3.93±0.28
	75	26	0.01	8.68±2.15	0.19±0.07	0.74 ±0.02	0.69±0.16	30.48±7.26	6.59±2.60	0.42±0.36	8.01±0.45	0.67±0.32	20.05±4.08	62.33±11.06	32.15±0.90	3.40±0.23
	100	26	0.02	6.08±1.16	0.06±0.02	0.74 ±0.01	0.72±0.11	41.39±8.12	7.29±1.16	2.06±0.45	17.60±1.83	0.31±0.07	9.68±1.51	59.35±8.29	31.35±3.28	2.80±0.51
	20	0	0.00	14.75±0.29	0.56±0.08	0.79±<0.01	0.30±0.03	77.62±25.11	6.92±1.47	0.20±0.07	1.90±0.42	0.14±0.02	14.18±1.50	33.54±2.73	1.90±0.06	
	20	13	0.00	15.59±1.64	0.54±0.21	0.76 ±0.01	0.55±0.08	51.38±21.32	29.75±9.86	0.09±0.05	3.14±0.50	0.39±0.22	18.94±0.88	159.94±15.94		
	50	13	0.00	10.36±2.94	0.16±0.05	0.76±<0.01	0.52±0.01	64.36±5.48	26.98±7.54	0.14±0.03	4.26±0.63	0.14±0.03	19.51±1.27	96.34±12.43		
B.	75	13	0.01	10.13±2.59	0.39±0.31	0.78±<0.01	0.42±0.04	56.82±14.27	31.36±14.90	0.30±0.15	5.29±1.58	0.30±0.17	18.28±1.95	147.13±13.12		
juncea	100	13	0.01	9.53±2.40	0.56±0.37	0.72 ±0.02	0.68±0.04	78.46±18.50	13.21±6.57	0.18±0.11	6.17±1.39	0.20±0.10	14.87±0.89	92.88±10.97		
15127	20	26	0.00	9.85±1.67	0.37±0.24	0.78 ±0.01	0.37±0.06	42.93±11.42	16.11±11.64	0.29±0.10	9.49±0.88	0.24±0.05	15.28±0.47	101.10±20.86	60.05±3.51	9.55±0.67
	50	26	0.01	7.56±1.54	0.15±0.09	0.77 ±0.01	0.44±0.05	31.38±5.50	17.36±5.21	0.14±0.08	11.68±3.10	0.39±0.06	18.90±2.14	107.45±8.88	65.08±3.37	11.82±0.66
	75	26	0.01	5.43±0.58	0.04±0.01	0.74 ±0.01	0.71±0.07	11.39±1.23	8.78±2.81	0.05±0.02	6.36±2.85	1.22±0.15	14.15±1.18	94.93±5.65	65.43±3.40	12.75±0.66
	100	26	0.02	2.65±0.72	0.06±0.02	0.72 ±0.02	0.94±0.20	15.44±4.89	6.94±3.66	0.49±0.17	11.72±1.69	0.72±0.14	11.00±2.45	76.73±15.93	41.38±2.44	6.68±0.35

TABLE 1. Mean data over 3 timepoints (before exposure i.e., day 0, mid-exposure, day 13, and after exposure, day 26); n=4; ±SEM.